Synthesis of multidentate PNE ligands and their late transition metal coordination chemistry

Anderson, Carly Elizabeth

Synthesis of Multidentate PNE Ligands and their Late Transition Metal Coordination Chemistry

Thesis submitted for the degree of Doctor of Philosophy

By

Carly Elizabeth Anderson B.Sc., M.Phil. (Leicester)

Department of Chemistry
Durham University

February 2007

Statement of originality

This thesis is based on work conducted in the Department of Chemistry at Durham University between May 2004 and February 2007. All work was performed by the author, unless stated to the contrary, and has not been submitted for another degree at this or at any other University.

Carly Elizabeth Anderson
24th February 2007

Abstract

Title: Synthesis of Multidentate PNE Ligands and their Late Transition Metal Coordination Chemistry

Author: Carly Elizabeth Anderson

This thesis describes the synthesis of a family of potentially tridentate PNE (E = NMe, O, S, CH_2, NPh) ligands comprising a six-membered diheteroatomic saturated ring system bearing a pendent phosphine donor arm and studies on their coordination chemistry with a selection of late transition metals.

Chapter 1 comprises an overview of the nature of the bonding of phosphine, amine, ether and thioether donors to metals and reviews the dynamic behaviour of saturated heteroatom-containing ring systems in solution. Selected examples of the coordination chemistry and catalytic applications of complexes of Pd, Pt and Rh are given.

Chapter 2 details the concise synthesis of variously-substituted diphenylphosphine-bearing PNE ligands, $Ph_2PCH_2CH_2N(CH_2CH_2)_2E$ (E = NMe, **2.4-1**; E = O, **2.4-2**; E = S, **2.4-3**; E = CH_2, **2.4-4**; E = NPh, **2.4-5**; E = $NCH_2CH_2PPh_2$, **2.4-7**), by reaction of diphenylvinylphosphine with a cyclic secondary amine. The synthesis of both hydrochloride and chalcogen derivatives are also reported. Attempts to synthesise a related family of PNE ligands with amino-substituents at P were unsuccessful. Similar reactions of allyldiphenylphosphine with *N*-methylpiperazine led to the formation of $Ph_2PCH_2CH(Me)N(CH_2CH_2)_2NMe$ as a result of base-catalysed isomerisation of the allyl phosphine.

The complexation of the PNE ligands with a variety of Pd(II) fragments is detailed in Chapter 3. Reaction with $[PdCl_2(MeCN)_2]$ affords the $[PdCl\{\kappa^3\text{-PNE}\}]^+$ Cl^- salts when E = NMe, O, S and CH_2, although when E = NPh and $NCH_2CH_2PPh_2$, the expected products were not obtained. A bidentate $[PdCl_2\{\kappa^2\text{-PN(NMe)}\}]$ isomer of **3.1-1** was characterised crystallographically although this was indicated not to be representative of the bulk sample, which consisted mainly of the tridentate $[PdCl\{\kappa^3\text{-PNE}\}]^+$ Cl^- isomer. Treatment of **3.1-1** with $MgSO_4$ affords the unusual $[PdCl\{\kappa^3\text{-PNE}\}]^+$ $.½[Mg(SO_4)_2.4H_2O]$ complex which was characterised crystallographically. Reaction of **2.4-1 – 2.4-4** with [PdCl(Me)(cod)] and $[PdMe_2(tmeda)]$ affords the $[PdCl(Me)\{\kappa^2\text{-PN(E)}\}]$ and $[PdMe_2\{\kappa^2\text{-PN(E)}\}]$ complexes, respectively.

Chapter 4 describes the coordination chemistry of the PNE ligands with Pt(II) metal fragments. The reaction of **2.4-1 – 2.4-3** with $[PtCl_2(cod)]$ affords the doubly ligated $[PtCl\{\kappa^2\text{-PN(E)}\}\{\kappa^1\text{-P(NE)}\}]^+$ Cl^- complexes with both stoichiometric and half molar equivalents of the platinum precursor. Reaction of the PNE ligands with $[PtCl\{\mu\text{-Cl}\}(PEt_3)]_2$ gives $[PtCl(PEt_3)\{\kappa^2\text{-PN(E)}\}]$ complexes in all cases.

The coordination of the PNE ligands with Rh(I) metal centres is detailed in Chapter 5. Reaction of **2.4-1 – 2.4-4** with $[Rh_2\{\mu\text{-Cl}\}_2(CO)_4]$ affords the $[RhCl(CO)\{PNE\}]$ complexes in all cases, although when E = NMe and S, dynamic interconversion between $[RhCl(CO)\{\kappa^2\text{-PN(E)}\}]$ and $[Rh(CO)\{\kappa^3\text{-PNE}\}]^+$ Cl^- complexes is observed by low temperature NMR spectroscopy. By contrast, no isomerisation is noted when E = O. When E = NPh and $NCH_2CH_2PPh_2$, the expected products were not obtained. Abstraction of the metal-bound chloride from $[RhCl(CO)\{PNE\}]$ proved successful when E = NMe and S but this reaction failed to afford the expected product when E = O, even in MeCN solution.

Full experimental data and methods of preparation for the compounds in this thesis are listed in Chapter 6 with supplementary crystallographic data available in the Appendices.

Acknowledgements

Firstly I would like to thank Dr. Philip Dyer for all his help, guidance and assistance over the course of my Ph.D. Thanks must also go to Prof. Todd Marder, Dr. Keith Dillon and Dr. Paul Low for guidance and helpful discussions. Dr. Elizabeth Grayson is also thanked for advice and providing numerous chemicals. Thanks also to Prof. Judith Howard.

I must thank the NMR service, Dr. Alan Kenwright, Catherine Heffernan and Ian McKeag, for hours and hours of NMR time and their patience with VT studies. Thanks also to Dr. Andrei Batsanov for running all my X-ray structures, Dr. Mike Jones and Dr. David Parker for mass spectrometric analyses and Jaroslava Dostal for CHN elemental analyses. I must also extend my gratitude to Dr. David Apperley and Fraser Markwell for running solid state NMR experiments. Peter Coyne and Malcolm Richardson are gratefully acknowledged for glassware repairs.

Thanks to my friends and to my colleagues (both past and present) for all your support. From my group, I must thank Lise, Sam, Alice, Will, Daniel, Seb B. and Sophia for all their help and support over the last couple of years. Thanks also to Pippa, Khairul, Georg, Seb S. and Sara Jane for their friendship. I must also thank my friends from outside the department, Shona, Oat, Andrew, Chris, Stuart and Dominic, your support has been much appreciated.

Durham University and the EPSRC are gratefully acknowledged for financial support.

Finally I must thank all my family, especially my parents and my brother. Your support has been truly invaluable over the past years – I couldn't have finished this without you. At last it's all over!

Contents

Chapter 3: Complexation of PNE ligands with Pd

Chapter 4: Complexation of PNE ligands with Pt

Chapter 5: Complexation of PNE ligands with Rh

Abbreviations in the text

B^-	generic base
br	broad
^{t}Bu	^{t}butyl
^{n}Bu	n-butyl
CHN	carbon, hydrogen and nitrogen elemental analyses
cod	cycloocta-1,5-diene
COSY	correlation spectroscopy
Cy	cyclohexyl
DEPT	distortionless enhancement by polarisation transfer
DBU	1,8-diazabicyclo[5.4.0]undec-7-ene
EI	electron impact
ES	electrospray mass spectrometry
e.s.d.	estimated standard deviation
Et	ethyl
HETCOR	heteronuclear (^{1}H–^{13}C {^{1}H}) correlation spectroscopy
HOMO	highest occupied molecular orbital
Hz	Hertz
i-	*ipso-*
IR	infrared spectroscopy
L	generic $2e^-$ donor ligand
LUMO	lowest unoccupied molecular orbital
m-	*meta-*
MALDI	matrix-assisted laser desorption ionisation
Me	methyl
MS	mass spectrometry
m/z	mass-to-charge ratio
NMR	nuclear magnetic resonance
nOe	nuclear Overhauser effect
nOeSY	correlation nuclear Overhauser effect spectroscopy
o-	*ortho-*
p-	*para-*
Ph	phenyl

ppm	parts per million
ppz	piperazine
^{i}Pr	isopropyl
pyrr	pyrrole
R	generic alkyl/aryl group
RT	room temperature
Tf	triflate (CF_3SO_3–)
THF	tetrahydrofuran
tmeda	*N*,*N*,*N*′,*N*′-tetramethylethylenediamine
ToF	time of flight
X	generic 1 e^- ligand

NMR Abbreviations

δ	chemical shift (in ppm)
s	singlet
d	doublet
dd	doublet of doublet
t	triplet
dt	doublet of triplets
quat	quartet
d quat	doublet of quartets
quin	quintet
sept	septet
d sept	doublet of septets
m	complex multiplet

Chapter 1:

Introduction

1.1 Introduction

There is a continuing drive towards the development of new and innovative ligand systems from industrial, pharmaceutical and academic laboratories for use in a wide range of catalytic and coordination applications. Indeed, it is widely acknowledged that the auxiliary ligands coordinated to a metal centre play a number of crucial roles, namely exerting control over the metal's coordination number and coordination geometry and formal oxidation state and are capable of providing steric protection to the metal site in question.[1] Specifically, there is a particular interest in polydentate chelating ligands due, in part, to the enhanced stability that these species confer onto the metal site to which they are bound. Frequently the resulting metal-chelate complexes show an enhanced tolerance towards conditions that is not demonstrated with monodentate ligands of an analogous nature.[2]

Whilst a vast combination of donor moieties are possible, the development of unsymmetrical multidentate ligands that contain a number of electronically different donor fragments is particularly desirable as these present a given metal centre with a variety of possible coordination environments.[3] The combination of significantly differing functionalities, such as hard and soft donor moieties, may give rise to interesting behaviour as the ligand may be able to partially dissociate thereby generating a vacant coordination site at the metal that is 'masked' in the ground state,[4] Scheme 1.1. This phenomenon has great potential to be exploited in catalytic applications as the ligand is not lost completely from the metal's coordination sphere over the course of the catalytic cycles.

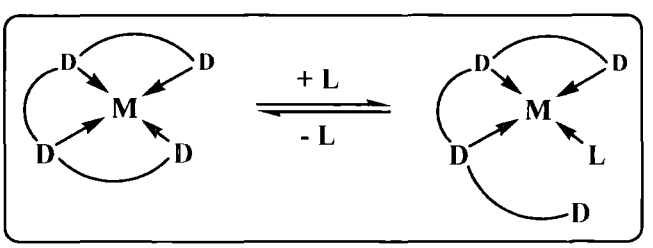

Scheme 1.1: Partial ligand dissociation in a square planar metal complex

By 'tailoring' the structure of a ligand and the nature of its donor fragments, the coordination at a given metal centre may be controlled in a responsive manner.

Therefore, the presence of electronically differing donor fragments within the same metal scaffold should significantly influence the reactivity of the metal complex as a whole.

It is expected, on the basis of Pearson's "hard-soft-acid-base" (HSAB) theorem, that soft late transition metals will bind more strongly to softer, more polarisable donor moieties and conversely harder less polarisable donor fragments will preferentially bind to the earlier metals.[5] For this reason, it is desirable to introduce a number of electronically differing donors into a single ligand framework, *e.g.* a range of soft donors such as thiols and phosphines to contrast with harder oxygen and amine donors. By incorporating a variety of donor atoms, the differences in their *trans* effects has the potential to be exploited in their resulting complexes as organochalcogen ligands generally show greater *trans* influences than nitrogen donors which, in turn, show smaller *trans* influences than tertiary phosphines.[6] Moreover, the systematic variation of one donor functionality, with the creation of a family of closely related ligands, allows the full coordination abilities of the resulting multidentate ligand family to be extensively probed with metal centres.

1.2 Phosphine/amine donors

The ubiquitous presence of phosphine and amine donors in coordination chemistry can be attributed to their excellent ability to ligate metals throughout the *d*-block. Indeed, a large number of industrially relevant homogeneously-catalysed processes rely on metal centres coordinated with phosphine and amine ligands, something due in part, to their high donor strengths, which in turn gives rise to very stable complexes.[7] Moreover, the versatile, readily available and structurally diverse PR_3 and NR_3 donors allow for facile fine tuning of the steric and electronic properties of these ligands by systematic modulation of the R substituents. A wide variety of phosphines and amines are available commercially and well-developed synthetic methodologies exist which assist the synthesis of novel varieties.

The principal difference between amine and phosphine donor moieties, other than the difference in the size of the central atom, is the nature of the bonds that they form with metal centres, Figure 1.1. Theoretical studies of $Mo(CO)_5(R_3E)$ complexes (where E = N, P) have determined that phosphine donors consistently form stronger

bonds with the metal centre than their analogous aliphatic amines as the M–P bond has a higher degree of covalent character in comparison to the M–N bond (essentially an effect of the differing electronegativities of the two donor atoms). These studies have further clarified the differing levels of back-acceptance experienced by the ER_3 moiety from the metal centre as the P–Mo bond contains a significantly higher degree of π character than the N–Mo bond, regardless of the nature of the R substituent. Indeed this effect becomes particularly important when phosphorus is substituted with electronegative substituents that yield low-lying vacant π^* orbitals (such as an amino-substituent).[8] Additionally, it has been noted that the strength of M–N bonds are more significantly affected by steric effects than their corresponding M–P bonds.[9]

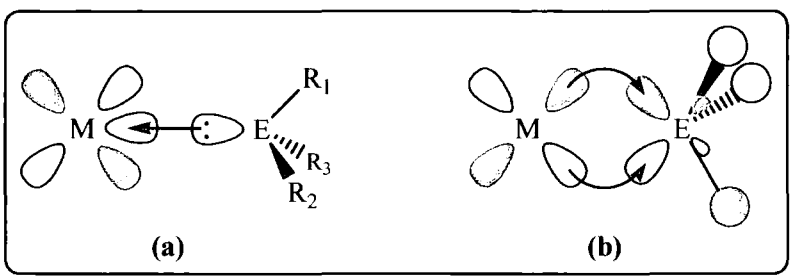

Figure 1.1: Bonding in metal-pnictogen complexes:

(a) σ-donation of an E lone pair into a vacant σ-symmetry M-based orbital;

(b) π-acceptance from a filled metal *d*-orbital into a P_π LUMO on E

1.3 Oxygen/sulphur donors

There are numerous examples of sulphur- and oxygen-based ligands and their applications are widespread in the literature. As would be expected on the basis of the HSAB principle, sulphur donors, especially thioethers, show a tendency towards forming stronger bonds with the softer later transition metals.[10,11] In contrast, the harder oxygen donors, in particular oxo-ethers, display stronger interactions with *s*-block and the earlier metals, with perhaps the best example of these donor ligands being those of crown ethers.[12]

In contrast to phosphine and amine donors, thioether and ether ligands are relatively weak σ-donors and poor π-acceptors, something that has been established by

theoretical studies on the $Cr(CO)_5(R_2E)$ (E = O, S) systems.[13] In both the ether and thioether Cr complexes, the chalcogen ligand orbital responsible for donation to the metal is mainly a chalcogen *p*-hybrid lone pair. In order to accommodate the remaining lone pair, the chalcogen adopts a coordination tilt with respect to the metal, Figure 1.2 (a). This deviation from linearity leads to a poor overlap of the $1A'_M$ orbitals and the filled $1A'_L$ bonding orbital, but at the same time allows for a compensatory overlap between the $1A'_M$ and the σ-bonding orbital, Figure 1.2 (b).[13] This σ-bonding orbital is of lower energy than $1A'_M$ lone pair orbital, and thus less readily available for donation.

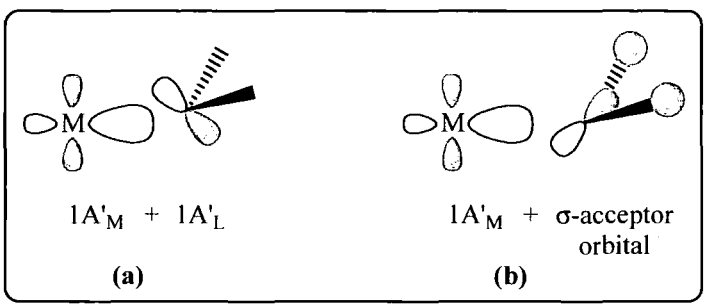

Figure 1.2: σ-bonding in metal-chalcogen complexes[13]

Whilst both ether and thioether donors are capable of σ-donation to metal centres, only thioethers have a capacity for π-back acceptance. Indeed, this π-back acceptance component of the metal-sulphur bond has two major metal-ligand interactions; firstly back donation from the metal d_{xy}-orbital to the $2A'_L$ orbital of the ligand, Figure 1.3 (a), with the second being a back-bonding interaction between the metal's d_{xy}-orbital and the second σ^*-orbital ($1A''_L$) orbital, Figure 1.3 (b). In order to minimise the antibonding interaction between the orbitals of the substituent at E and the *d*-polarised *p*-orbital of the chalcogen, there is a concomitant reduction in the R–S–R bond angle (along with an associated lengthening of the S–R bond). Calculations on the $Cr(CO)_5(R_2E)$ system have shown that this back-donation component to the overall Cr–S bond is small but increases with increasing electronegativity of the substituents. It follows that the π-acceptor character of SR_2 ligands will be further reduced when the geometry about sulphur is constrained, such as with heterocyclic sulphur donors. In contrast, no back acceptor character is observed for ether moieties due to the

unsuitability (as a consequence of their high energy) of the σ^* bonds to accept electron density.[13]

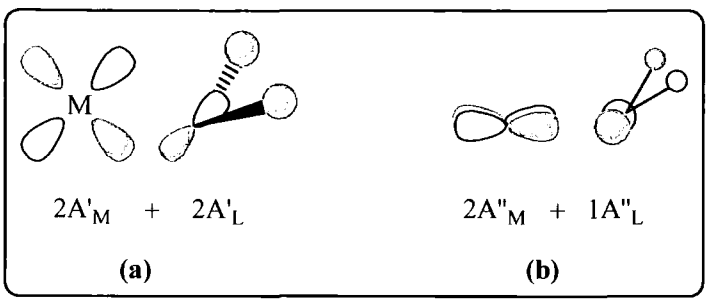

Figure 1.3: π-back donation in metal-thioether complexes[13]

In summary, comparative studies of the σ-donor strength of P-, N-, S- and O-based donor fragments have afforded the following series:[13]

$OMe_2 < NH_3 < SMe_2 < PH_3$

Furthermore, the ligand's relative capacity for π-acceptance has been determined as:[13]

$OMe_2 < NH_3 < SMe_2 < PH_3$

1.4 Saturated heterocyclic ligands

One particularly interesting aspect of the extensive coordination chemistry of heteroatom donor ligands is the use of *bis*-heterocyclic ring systems as metal scaffolds, *e.g.* the introduction of *trans* ditopic species such as piperazine (N^N), morpholine (O^N) and thiomorpholine (S^N) units, which have the potential to doubly-bridge a given metal centre. In contrast to their hetero-acyclic counterparts, the *bis*-chelated ring has the potential to offer the metal an enhanced degree of steric protection due to the presence of the cyclic backbone, thereby potentially hindering the approach of substrate molecules from this direction. Additionally, the incorporation of these bidentate ring systems into larger ligand frameworks increases the stability of their resulting coordination compounds, with these complexes (in some cases) exhibiting enhanced resistance towards demetallation when both heteroatoms are bound to the metal site in question.[14,15]

Saturated heterocycles are of interest not only due to their potential bidentate coordination, but also due to the dynamic behaviour that these ring systems demonstrate in solution, which could then be transmitted to the system as a whole. This is particularly the case when nitrogen atoms are incorporated into the ring framework. For example, the presence of one (*e.g.* piperidine) or two nitrogen (*e.g.* piperazine) heteroatoms in a saturated ring system has a profound effect on the solution behaviour of the ring framework as a whole.[16] Whilst pyramidal inversion in simple acyclic amines is well understood and tends to generally have a low energy barrier (*ca.* 6 kcal mol^{-1}),[17] by contrast, nitrogen inversion in saturated heterocyclic systems is significantly different since the system must surmount a higher energy barrier as a result of the necessary conformational changes within the ring during the inversion process.[16] In these types of heterocycles there are also ring inversion (R) processes that can take place in addition to nitrogen inversion (N), and therefore the overall motion of the molecule is in essence a two-state equilibrium between these two processes, as shown for piperidine in Scheme 1.2.

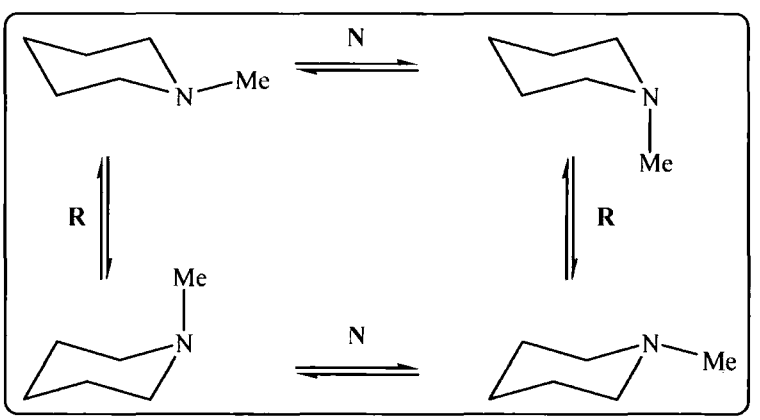

Scheme 1.2: Ring (R) and Nitrogen (N) inversion processes in *N*-methylpiperidine

The existence of these two discrete processes makes study of the system as a whole significantly more difficult, as it is complicated to differentiate between them without resorting to in-depth quantum and molecular modelling. Hence most studies report Gibbs' free energies for the overall dynamic process (N and R inversion), with most being generated with the use of low temperature NMR studies. However these studies do not take account of energy contribution resulting form torsional strain and

non-bonding interactions (such as hydrogen bonding), which may play a significant role in the overall inversion process.[18]

From a coordination chemistry viewpoint, incorporating such heteroatomic ring systems into ligand frameworks could allow this dynamic behaviour to be transmitted to the bound metal. This could potentially be used to create a vacant coordination site at the metal, thereby taking advantage of facile chair-boat interconversion of the doubly-bridged chelate, as illustrated in Scheme 1.3.

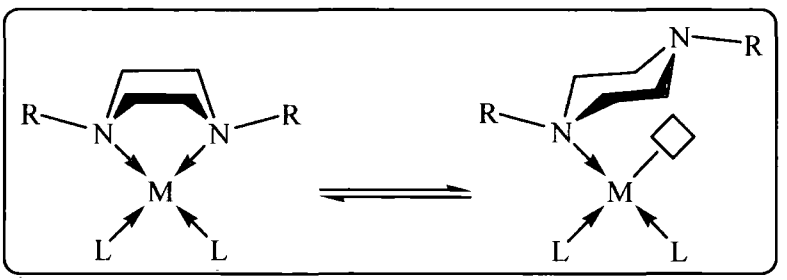

Scheme 1.3: Reversible partial dissociation of a piperazine ligand to a metal site

The introduction of further heteroatoms into the piperidine skeleton has been demonstrated to further complicate the nature of the dynamic deformation of the ring as a whole, as would be expected. The *trans* di-nitrogen moiety piperazine has been extensively studied with varying conclusions about the nature and the energy barrier of its inversion processes. It was originally thought that the energy maximum for this process was the twist-boat conformer,[18] however a more recent theoretical analysis of piperazine rings has demonstrated that the energy maximum for this inversion process is reached on the ring passing through the half-boat conformer with an overall energy of 6.33 kcal mol^{-1} relative to the lowest energy chair conformer. These calculations have revealed that the boat conformation is 5.34 kcal mol^{-1} higher in energy than the thermodynamically more favourable chair conformer, Figure 1.4.[15] This motion in solution is reflected in the ^{1}H NMR spectra of heterocycles of this nature, as at room temperature, broadened signals are typically observed that denote rapid exchange processes, which result in magnetic equivalence of all piperazine protons.

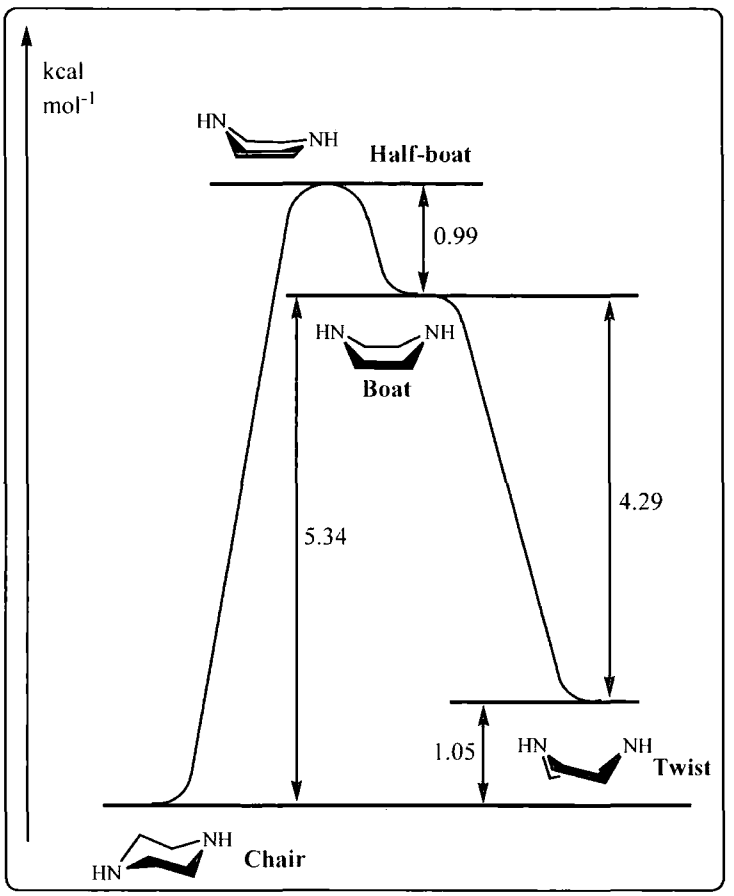

Figure 1.4: Energy profile for the interconversion of the conformers of piperazine[15]

The introduction of a second heteroatom into the ring, *e.g.* a second nitrogen atom (*i.e.* piperazine), an oxygen (*i.e.* morpholine) or a sulphur (*i.e.* thiomorpholine) has a significant impact on the nature of the inversion of the ring. Indeed it has been demonstrated that sulphur and oxygen heteroatoms in saturated six-membered ring systems also undergo pyramidal inversion processes in a similar manner to that of amine nitrogen centres.[19,20]

Substituted piperazine- and morpholine-containing moieties have been subject to considerable attention, which can be partly attributed to their frequent incorporation in pharmaceutical species.[21,22,23] In contrast, their analogous thiomorpholine counterparts have received comparatively little attention and thus relatively few systems have been developed that contain this ring fragment.[24,25] In particular, few unsymmetrical ligand systems comprising these heterocycles with a pendant phosphine donor exist. Piperazine systems bearing two phosphines at the nitrogen atoms[26] and *N*-substituted morpholines

bearing pendent phosphine donors[27,28,29,30] have been reported, but no thiomorpholine-based examples exist to date.

Several in-depth studies on the coordination chemistry of piperazine fragments bearing pendant donor arms have been reported,[15,31] with one of the most interesting being that reported by Chadhuary and co-workers,[32] Scheme 1.4. In this case, an N–O Schiff-base ligand has been modified by the incorporation of a piperazine moiety, providing a metal scaffold that can behave either as a tri- or tetra-dentate ligand in response to changes in solution pH. Here, boat-to-chair conformational changes occur, dissociating one piperazine donor fragment. Consequently, the lower denticity of the ONN framework permits the Ni(II) centre to expand its coordination sphere from 4 to 6, as a result of the decrease in ligand field strength. The presence of a potentially doubly-chelating piperazine means that, upon addition of base, there is a considerable driving force towards recoordination of the pendant piperazine amine.

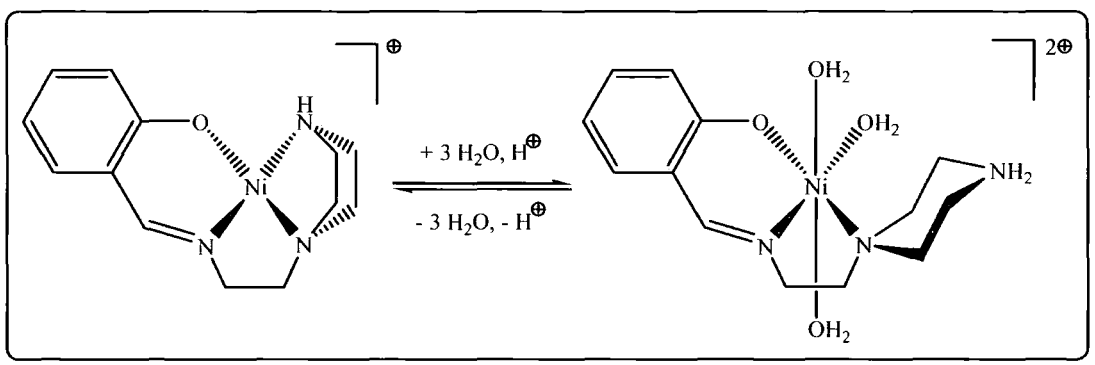

Scheme 1.4: pH-responsive 'flexidentate' coordination of piperazine about a Ni centre[32]

1.5 Phosphine Inversion

Unlike their related amine, ether and thioether counterparts, pyramidal inversion in phosphines is a less facile process as the inversion barriers for phosphines are frequently much higher than those of their analogous amines and this is therefore a disfavoured process. The origins of this higher energy barrier have been a source of much debate, with many different theories being invoked in order to provide satisfactory explanations.[33]

While many arguments focus on the relative size of the central atom, it is now widely accepted that the origin of the higher inversion barrier for phosphines is to be found at the electronic level, in particular, in the differing electronegativities of nitrogen and phosphorus. It has been demonstrated that the energy gap between the HOMO and LUMO of a given ER_3 molecule is of critical importance in governing the preferred geometry of that molecule. Specifically, the molecule will adopt the geometry that best stabilises the HOMO, while the occupied orbital lying closest to the HOMO, unless perturbed, will govern the molecule's geometric preference.[34]

It has been demonstrated that there is an inverse relationship between the difference in energy of the HOMO and LUMO states (δE) and the stabilisation energy (E) in the planar forms of eight electron EH_3 species, Figure 1.5. Whilst values for δE are found to be large for amines, resulting in small values of E and hence facile inversion, the opposite is found for the less electronegative phosphorus-containing species, which give rise to small values of δE and, in turn, large values of E, thus disfavouring inversion of the lone pair as a direct result of the higher stabilisation of the pyramidal geometry.[33,35]

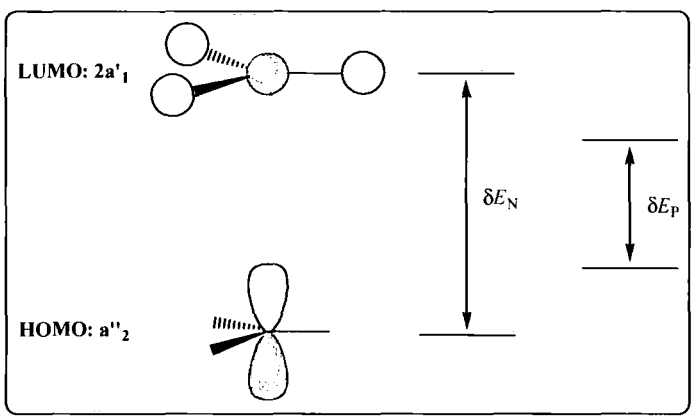

Figure 1.5: Relative HOMO–LUMO energy separations (δE) in planar EH_3 for nitrogen compared to phosphorus[35]

As for amines, the nature of the substituents in phosphines plays a role in governing the inversion barrier at the phosphorus centre. In phosphines containing highly electronegative substituents, the existence of near-degenerate energy levels for the planar conformation substantially lowers the inversion barrier although it remains high with respect to the equivalent amine species.[36]

	$\Delta G^{\ddagger *}$ Inversion barrier		$\Delta G^{\ddagger *}$ Inversion barrier
PH_3	36.1 [37]	NH_3	5.4 [38]
PMe_3	47.5 [37]	NMe_3	8.2 [39]
PPh_3	35.1 [37]		

*kcal mol^{-1}

Table 1.1: Gibbs' free energy inversion barriers for representative phosphines and amines

It is evident that heteroatom-based ligands provide enormous diversity in the number of possible multidentate ligand structures. The relative ease with which such donor fragments may be incorporated into complex ligand frameworks provides opportunities to design metal scaffolds with precise characteristics. This is significant since it allows metal complexes to be 'tuned' at the molecular level to have specific behaviour, which is crucial for their application in catalysis, something that is illustrated in the following overview.

1.6 Homogeneous catalysis with late transition metals

There is a continuing demand for the development of single-site homogeneous pre-catalysts for applications in both industrial and preparative organic chemistry. These homogeneous systems have many advantages over their multi-sited heterogeneous counterparts, in particular, these soluble systems frequently display higher regio- and stereo-selectivities in the resulting products (as a result of their well-defined active sites) whilst operating under milder conditions.[7] A further advantage of homogenous systems lies in their soluble nature as this can facilitate scrutiny of the catalytic process in operation, with the use of specialised equipment (such as high pressure NMR and IR spectroscopies) potentially allowing a greater insight into the nature and mechanism of the catalytic process in question.[40]

Of the wide range of transition metal systems known, late metal catalysts are frequently preferred over earlier metal systems as later metals show a greater propensity for tolerance towards oxygen-containing substrates.[41] Moreover, late metal systems tend

to show wide-ranging activity of functionalised substrates which potentially limit the need for protection/deprotection strategies, which may be a necessity in organometallic transformations.[42] Whilst there may be a loss of expensive metal catalysts over the course of a homogeneously catalysed process, there exist well-defined methodologies for the recovery and 'recycling' of these expensive metals.[43,44]

Today, a vast number of different transition metal-based catalysts are both known and used, which provides huge scope for the range of catalytic transformations possible. Consequently, it is impossible to give a comprehensive overview of homogeneous transition metal catalysis in a manuscript of this type. Hence, only a number of selected examples are given, which indicate possible applications of the complexes prepared during this study.

1.7 Palladium complexes in homogeneous catalysis

Applications of organometallic palladium complexes in the area of homogeneous catalysis are numerous, with a vast array of Pd-mediated transformations being found throughout the literature. Indeed palladium remains perhaps the most versatile metal in terms of application in catalytic processes due to both its wide-ranging applicability and its ability to effect high rates of both stereo- and regio-selectivities in the products of these reactions.[44]

Palladium derivatives are of great use in preparative laboratory reactions. Pd complexes have been shown to be efficient catalysts for reactions such as molecular rearrangement (*e.g.* Cope,[45] Claisen[46]) and hydrogenation,[47] however, one of the most industrially significant Pd-mediated processes is the oxidation of olefins to carbonyl compounds (the Wacker oxidation).[48] Indeed, the Wacker oxidation is widely recognised to have opened the field of palladium catalytic chemistry.

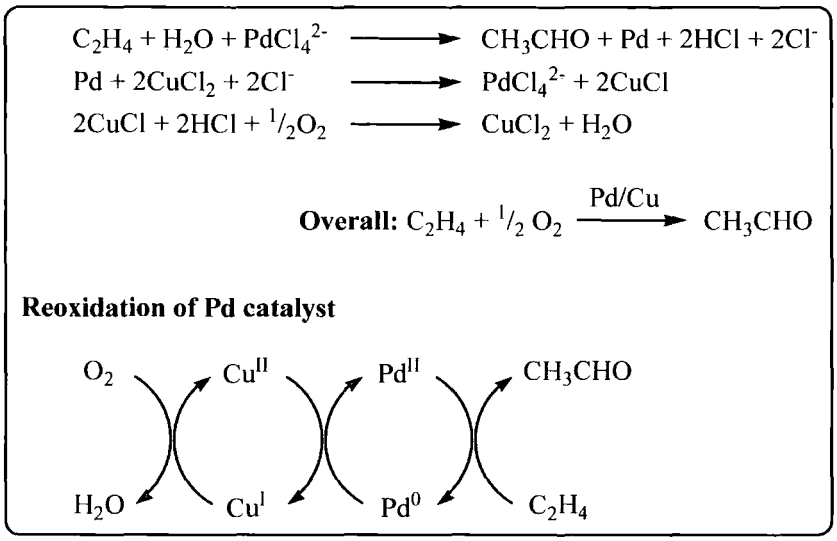

Scheme 1.5: Mechanism of the Wacker Process

Until the introduction of the Monsanto process in 1968, the Wacker oxidation was the principle commercial method for the production of acetaldehyde, an important basic chemical feedstock.[49] As shown in Scheme 1.5, this process comprises three steps, the overall process being the simple Pd-catalysed air oxidation of ethylene to acetaldehyde in the presence of a copper co-catalyst. The presence of copper chloride is essential in this catalytic cycle as this regenerates the active palladium (II) catalyst. This reaction is performed in the presence of air or oxygen, the purpose of this being to oxidise the Cu(I) to Cu(II), thus completing the catalytic cycle.

1.7.1 Group 10 catalysts for olefin homopolymerisation

The controlled catalytic production of polyolefin products is a key area of commercial interest with much activity being directed towards the development of new homogeneous single-site catalysts for the preparation of polymeric materials with ever-increasing degrees of control of the resulting polymer architectures. There is continued industrial demand for the development of new homogeneous catalysts that efficiently and economically produce the required polymeric materials with well-defined microstructures and more uniform incorporation of α-olefins and co-monomers.

The trend towards homogeneous initiators for application in polymer production can be attributed to the development of the Group 4 metallocenes (along with their

related *ansa*-metallocenes and half-sandwich complexes) which, in conjunction with alkyl aluminium-based co-initiators such as methylaluminiumoxane,[50] provide highly active initiators for the polymerisation of ethylene and other related polyolefins.[51]

In contrast to these early transition metal systems, late transition metal initiators for olefin polymerisation were largely overlooked until the mid-1990's, a situation that can be attributed to the misconception that these late metal systems were only suitable for the production of low molecular weight oligomeric products. This inaccurate perception largely arose as late metals generally display higher rates of chain termination over chain propagation processes as a result of facile β-hydride elimination in these systems.[52] Indeed, the propensity of these late metal systems to generate low molecular weight products was utilised in systems such as the Ni-based SHOP (Shell Higher Olefin Process) system, Figure 1.6 (a), used for the production of oligomeric materials.[53] Whilst principally employed in oligomerisation, the SHOP system is capable of the polymerisation of ethylene under certain conditions.[54,55]

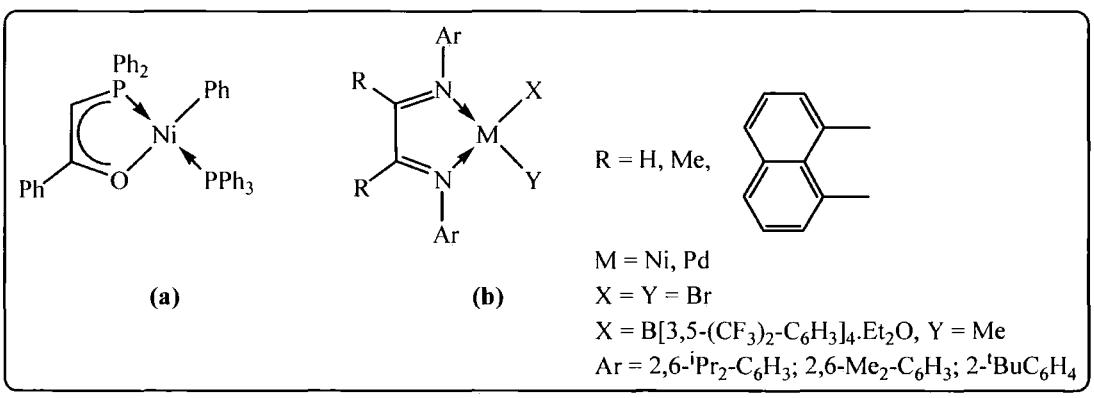

Figure 1.6: Keim's SHOP **(a)**[53] and Brookhart's α-diimine **(b)**[52] oligo-/poly-merisation catalysts

The Ni(II) and Pd(II) systems introduced by Brookhart and co-workers in 1995 based on square planar cationic alkyl complexes represent the first examples of late transition metal initiators capable of polymerising higher alpha-olefins and ethylene to high molecular weight materials, Figure 1.6 (b).[52] The key feature of the α-diimine ligand systems used was the incorporation of sterically demanding organic substituents in the axial positions, which greatly limited rates of β-hydride elimination/associative

chain displacement, thus promoting chain growth, whilst blocking the approach of substrates from this direction, a feature that has been verified by theoretical studies.[56]

As the Brookhart systems illustrate, ligand design remains one of the important considerations in the development of active initiators for the polymerisation of polyethylene. By judicious alteration of the ancillary ligands about the metal site, high levels of control over the chain length and degree of polymer chain branching can be attained. Indeed, by careful variation of the steric and electronic properties of the coordinated ligands, the formation of unwanted by-products formed by associative displacement and 'chain-walking' processes can be limited. The mechanistic rationale for these observations is shown in Scheme 1.6, below.

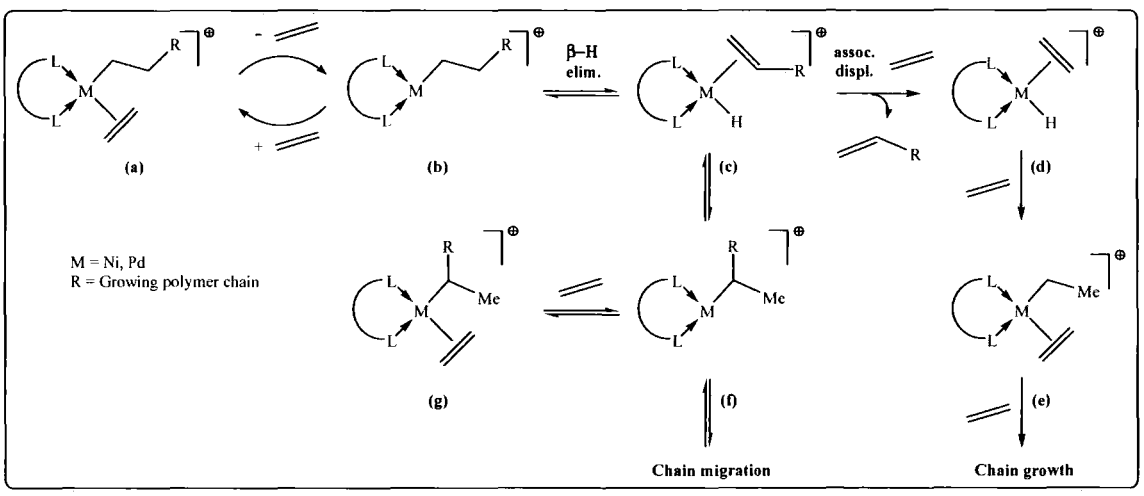

Scheme 1.6: Mechanism of chain-walking in olefin polymerisation[52]

Upon formation of an active catalyst, the insertion of ethylene gives rise to the so-called 'catalyst resting state' (**a**), which, *via* loss of the coordinated ethylene, generates the coordinatively unsaturated cation (**b**). Complex (**b**) then undergoes β-hydride elimination to afford an olefin hydride species (**c**),[57] which can either release the olefin through a chain transfer process *via* associative displacement {thus initiating the formation of a new chain, complexes (**d**)/(**e**)}, or the coordinated α-olefin of complex (**c**) can reinsert with a different regiochemistry, forming a methyl branch {complex (**f**)}. With the use of sterically demanding ligands, particularly those with bulky groups occupying the axial sites about the metal, the rates of these associative displacement and

α-olefin reinsertion processes can be slowed relative to the rate of chain growth, thereby promoting the formation of long chain polymers.[58]

The introduction of homoditopic diimine Pd and Ni polymerisation catalysts initiated the development of numerous late transition systems with the most common based on Brookhart-type systems.[1,41,59] While many homoditopic N–N and P–P systems have found application in the area of polymerisation, there has been a significant increase in activity in the development of hybrid systems comprising P–N ligands. Owing to the ease of both steric and electronic variation possible for these nitrogen and phosphorus donors, it is unsurprising that a great number of complexes containing ligands of this nature have been reported.[60] This interest can be attributed to the realisation that replacement of one of the imine donors in Brookhart-type systems afforded complexes with increased thermal stability, something that is presumed to be a result of stronger binding of the phosphine to the late metal centre.[61] Indeed, palladium complexes comprising P–N ligands have been shown to be highly active catalysts for the oligomerisation of ethylene.[62,63,64]

1.7.2 Palladium-catalysed copolymerisation

The copolymerisation of carbon monoxide with strained cyclic or terminal olefins has attracted much attention due to the interesting physical and chemical properties of the resulting copolymers. Specifically, the production of polyketones (alternating co-polymer of CO and olefin) has been the subject of industrial interest as these represent a class of low-cost processable thermoplastics with potential widespread commercial application.[65] For example, the presence of the carbonyl functionality potentially permits further functionalisation, thus making these polymers desirable starting materials for other functionalised polymers.

The discovery of efficient catalysts for CO/olefin copolymerisation originated from the study of the alkoxycarbonylation of ethylene to methylpropionate, Scheme 1.7. Upon variation of the reaction conditions, this system was found to produce perfectly alternating CO/ethylene copolymer with near-perfect selectivity.[66]

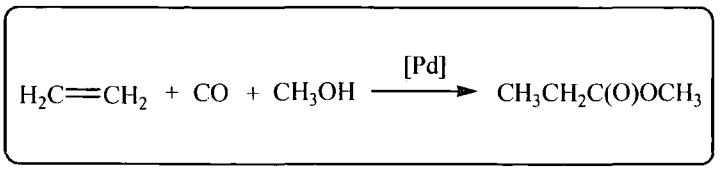

Scheme 1.7: The Pd-catalysed alkoxycarbonylation of ethylene to methylpropionate[55]

The use of Pd-based systems in the area of copolymerisation is widespread, with the schematic pathway for this process being shown in Scheme 1.8. Indeed, whilst Ni systems demonstrate faster rates for the production of polyketones, Pd systems typically show more uniform incorporation of ethylene into the resulting polymers.[67] The high regio-regularity of the polyketone is kinetic in origin, as the rate of CO insertion into the Pd–Me bond is greater than the rate of insertion of a second ethylene unit into the growing chain. Furthermore, the rate of decarbonylation is slow due to the high energy barriers for this process.[68] The double insertion of ethylene is possible, however, and promoted by interaction of the ketone oxygen with the Pd centre which leads to an irregularity in the chain.[69] By contrast, the double insertion of CO into the chain is a strongly disfavoured process on thermodynamic grounds.[58]

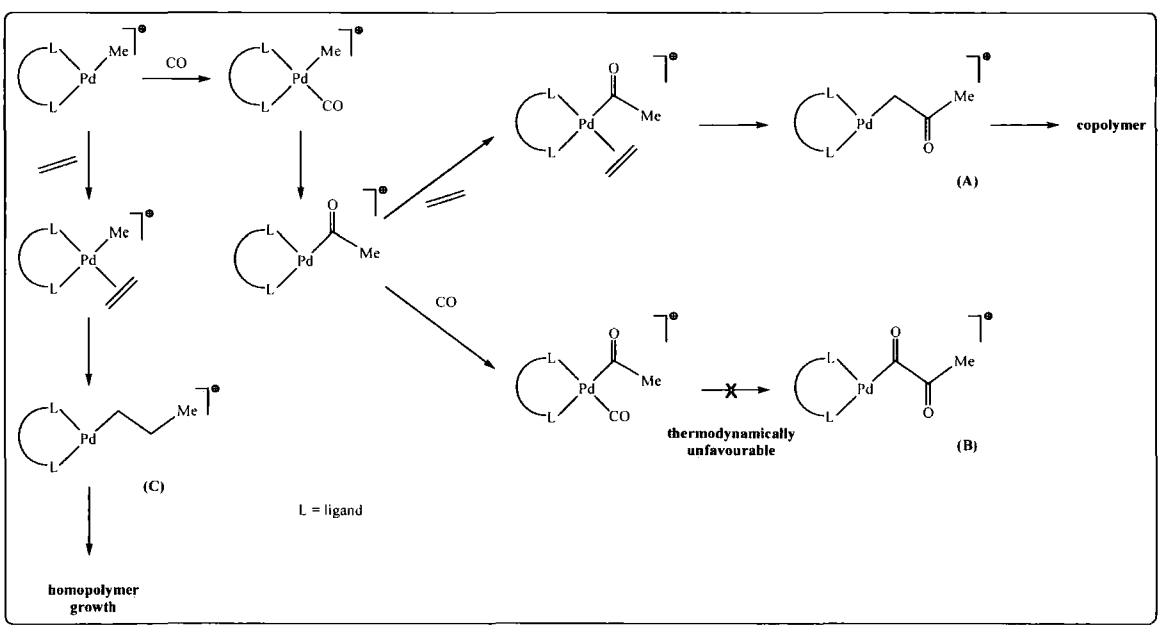

Scheme 1.8: A schematic pathway for CO/ethylene copolymerisation with a Pd catalyst[57]

As with any homogeneously-catalysed process, ligand design plays a crucial role in the synthesis of active copolymerisation initiators. As growth of the polyketone chain is dependent on the migration of the alkyl chain to the metal-bound CO group,[70] the mutual *cis* orientation of these fragments is essential.[71] Chelating ligands are thus ideal ligands for the promotion of polyketone polymers as these impose the required *cis*-geometry about the metal centre.

The copolymerisation of ethylene and CO tends to be favoured with the use of chelating P–P ligands,[72] while Pd-centres bound with N–N ligands, in general, show activity towards other olefinic co-monomers such as styrene.[73] The use of organopalladium complexes bearing hybrid P–N ligands affords an interesting middle-ground as these complexes have been shown to display activity towards both the simple copolymerisation of ethylene with CO[74,75] and copolymerisation of styrene and CO.[76,77] Moreover, electronic disparity between the nitrogen and phosphorus donors, combined with sterically demanding ligands, promote the formation of stereoregular polymers as a result of site selective coordination of the olefinic substrate.[75]

1.7.3 Palladium-catalysed cross coupling

One of the most important applications of palladium catalysis is Pd^0-catalysed cross-coupling reactions. These processes have found numerous uses in synthetic organic preparations as they provide facile, atom economic routes to carbon-carbon coupled products that may be difficult to obtain by other synthetic means. The realisation of the synthetic utility of these reactions has stimulated great interest in the development of new systems that exhibit greater tolerance towards substrate functionality under ever milder conditions (including reactions in the presence of air and/or water), whilst increasing catalyst activity and maintaining chemo- and stereo-selectivity in reaction products.[44]

Many different categories and subcategories of Pd-catalysed C–C bond formation have found utility in preparative organic chemistry, with variations of the Heck,[78] Suzuki-Miyara,[42] Stille,[79] Sonogashira[80] and Hartwig-Buchwald[81] cross-coupling reactions perhaps receiving the most attention due their general versatility. Although the catalytic cycles for these processes may differ in several aspects, it is

however generally agreed that there are three principal steps in operation as depicted in Scheme 1.9 for a generalised alkyl-aryl cross-coupling reaction.

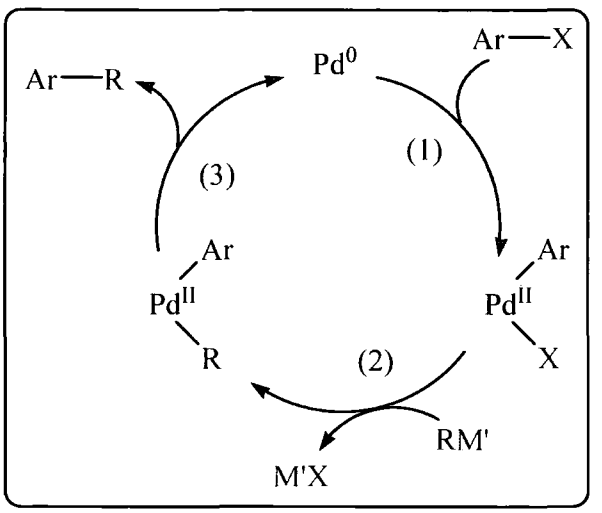

Scheme 1.9: A generalised mechanistic cycle for palladium-mediated cross-coupling reactions[82]

As shown in the above generalised mechanism, the first step in the catalytic cycle is the oxidative addition of Ar–X to the active Pd(0) species, Scheme 1.9 (1). This oxidative addition reaction is frequently the rate limiting step in the catalytic cycle and, as expected, the rate of substrate reactivity decreases in the order of increasing bond strength, *i.e.*

I > OTf > Br >> Cl

The second key catalytic intermediate is formed by an organo group transfer reaction (sometimes termed *transmetallation*) to afford two organic substituents at the Pd(II) centre, Scheme 1.9 (2). The final step is the regeneration of the active Pd(0) catalyst by the reductive elimination of the two organic groups to form the coupled product with the associated production of the active Pd(0) catalyst, Scheme 1.9 (3). Whilst a number of other processes may be operative in addition to these three principal steps, there remains little doubt that these species are key intermediates in catalytic cycles of this nature.[83,84]

Central to the operation of these catalytic systems is the formation of the active Pd(0) species either by employing a Pd(0) complex directly or by the *in situ* generation of Pd(0) (usually from a Pd(II) precursor). A wide variety of Pd(0) species have been found to be active in cross-coupling reactions with $[Pd(PPh_3)_4]$ being one of the most

frequently used, although $[PdCl_2(PPh_3)_2]$ and $[Pd(OAc)_2]$, the latter with *in situ* addition of PPh_3 or other phosphine ligands, are also efficient and widely employed, since they are stable to air and readily reduced to the active Pd(0) complexes.[42] When a Pd(II) precursor is employed in cross-coupling reactions, the *in situ* formation of the active Pd(0) species is generally achieved by one of two methods. Elimination of two organic moieties from a $[PdR_2(L)_2]$ complex produces the required zerovalent palladium species with stoichiometric loss of the organic by-product. The order of reactivity lies in the order:[42]

diaryl- > (alkyl)aryl- > dipropyl- > diethyl- > dimethyl-palladium (II)

In an alternative thermolytic synthesis of Pd(0), *cis*-(dialkyl)palladium(II) systems chelated with phosphine ligands have proved to be an effective starting point. As this process is inhibited by excess phosphine, the presence of excess PR_3 ligands is undesirable. The rate of thermolysis is proportional to the ease of dissociation of the phosphine co-ligand, with an approximate order of reactivity being:[42]

dppe << PEt_3 < PEt_2Ph < $PMePh_2$ < $PEtPh_2$ < PPh_3

It is interesting to note that phosphine ligands are central for the stabilisation of the zerovalent palladium complex due to the softer nature of these donors.[85] Indeed, harder donors, such as nitrogen-based systems, do not coordinate well to low valent transition metals,[86] due to their reduced ability to stabilise the increased Lewis basicity of the metal site.[5] This situation is reflected in the structure of $Pd[N(CH_2CH_2PPh_2)_3]$, as only phosphine coordination is noted to the zerovalent palladium, whereas upon reaction with an alkyl iodide, coordination of the pendant amine donor is observed, Scheme 1.10.[87]

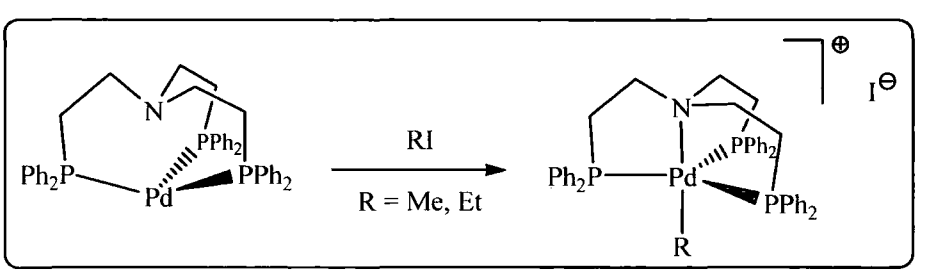

Scheme 1.10: Unusual trigonal planar coordination of a tripodal NP_3 ligand to Pd^0 [87]

1.8 Platinum complexes in homogeneous catalysis

Whereas nickel- and palladium-based systems have widespread uses in homogenously-catalysed processes, their platinum counterparts have found comparatively fewer applications due to the propensity of Pt-based systems to exhibit higher kinetic stability.[88] The generally stable nature of platinum complexes, however, can be used to great advantage, especially in the elucidation of mechanistic processes, as species that are transient intermediates in catalytic cycles with related metals (such as Ni and Pd) may be isolated and characterised in the analogous platinum systems.[89] This is particularly the case in palladium-catalysed reactions given the similarities between these 2nd and 3rd row transition metals.[90] Indeed Pt complexes may even be used to 'model' catalytic intermediates and even permit evaluation of kinetic and thermodynamic data for a wide range of reactions.[91]

Platinum complexes have however found limited application in homogeneously catalysed processes such as hydrosilylation[92] and hydroformylation (in conjunction with an $SnCl_2$ co-catalyst)[93,94] processes, in some cases with high enantioselectivities. Two representative complexes are shown in Figure 1.7.

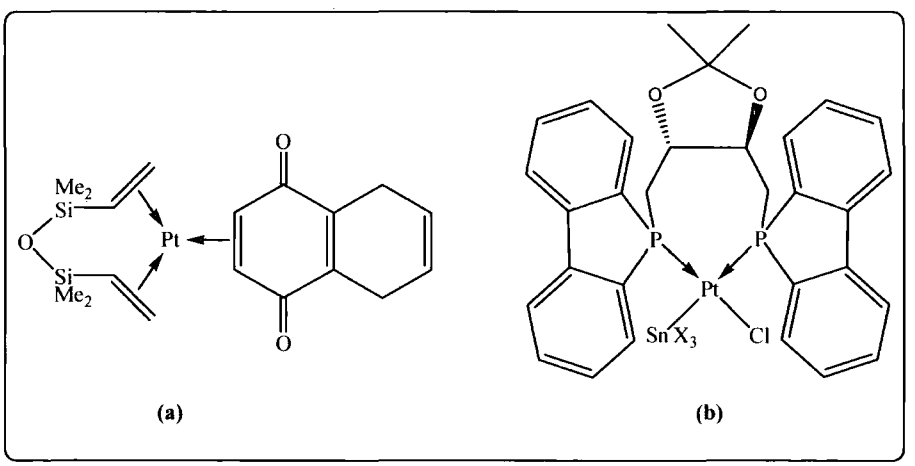

Figure 1.7: Active Pt pre-catalysts for hydrosilylation **(a)**[92] and hydroformylation **(b)**[93] processes

Whilst platinum complexes have applications in preparative laboratory processes, the slow rates of reductive elimination and ligand substitution reactions at Pt centres have disfavoured their use in cross-coupling reactions such as Heck,[95] Suzuki[96]

and Stille[97] transformations, Figure 1.8. To date, Pd catalysts continue to take precedence over these Pt-based systems for these applications. However, the study of the coordination chemistry of Pt still remains an active area of research. The predictable chemistry combined with its ease of manipulation and study make it a valuable tool in the mechanistic understanding of related Ni- and Pd-based systems that are used in wide variety of catalytic applications.

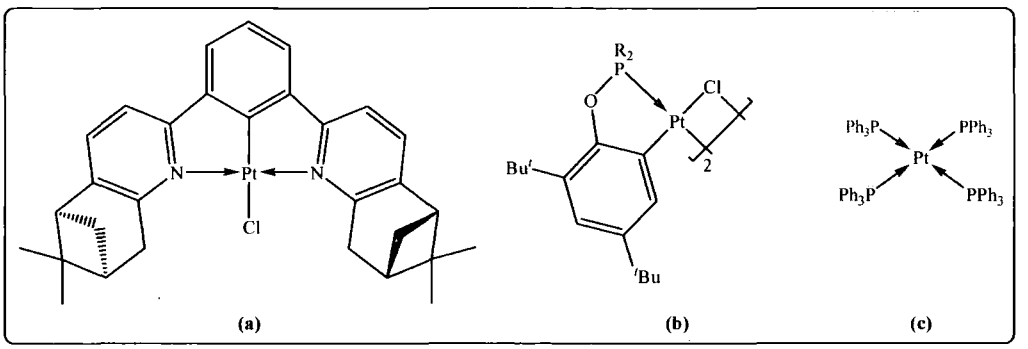

Figure 1.8: Pt-based pre-catalysts showing activity in Heck **(a)**[95], Suzuki **(b)**[96] and Stille **(c)**[97] cross-coupling reactions

1.9 Rhodium complexes in homogeneous catalysis

Rhodium has proven to be an extremely useful metal in the area of homogeneous catalysis due to the ability of its organometallic complexes to catalyse a wide range of synthetic transformations, often with high levels of selectivity.[98] Rhodium is most commonly found in two oxidation states; Rh(I) and Rh(III). Rh(I) complexes have a d^8 electron configuration and are usually four-coordinate square planar or five-coordinate trigonal bipyramidal structures, whereas Rh(III) complexes form d^6 complexes with octahedral geometry. The two-electron oxidation between these principal oxidation states is usually a facile process and, in many cases, occurs in a reversible manner. The reversible nature of such oxidative addition-reductive elimination reactions is an essential element of many of the organic transformations that are encountered in organorhodium chemistry.[99]

Rhodium-{especially Rh(I)} based catalysts have found wide-ranging utility in numerous synthetically relevant processes including hydrogenolysis, hydrosilylation,

hydroboration and hydroamination, to name but a few, but perhaps the most industrially relevant and widely employed are those of hydrogenation, carbonylation and hydroformylation.[100] It is for this reason that the development of new rhodium-based systems and the exploration of their coordination chemistry and potential in homogeneous catalysis is a continued area of research.

1.9.1 Rhodium-catalysed homogeneous hydrogenation

For many years the catalytic hydrogenation of unsaturated organic substrates has been of major interest from both academic and industrial viewpoints. Whilst traditionally the majority of hydrogenation catalysts have been based on heterogeneous systems, there has been considerable interest in the development of soluble alternatives. Homogeneous systems present a number of advantageous features over their heterogeneous counterparts, not least that these soluble systems have the potential to offer high levels of both chemo- and stereo-selectivities as a direct result of the well-defined active sites in these systems. Moreover, through systematic variation of the metal's co-ligands, specific levels of control over these processes can be attained. Thus asymmetric hydrogenation is an important methodology for the preparation of chiral building blocks for use in a variety of synthetic applications.[101,102]

The potential of Rh complexes to behave as efficient homogeneous catalysts for the hydrogenation of olefins and the partial hydrogenation of acetylenes was realised in 1965 with the introduction of $[RhCl(PPh_3)_3]$ by Wilkinson and co-workers,[103,104] which inspired world-wide interest in the development of Rh-based catalysts for these types of hydrogenation. While a number of transition metals show activity for homogeneous hydrogenation, rhodium is now widely acknowledged to show among the highest rates of reactivity and selectivity for this process.[105]

The addition of dihydrogen to unsaturated olefins is formally a symmetry-forbidden process,[106] however the participation of a transition metal catalyst breaks this addition down into a number of successive steps that do not suffer from these restrictions. The mechanism of catalytic hydrogenation of olefins with Wilkinson's catalyst has been widely studied and has been shown to comprise four key steps as shown in Scheme 1.11.[107]

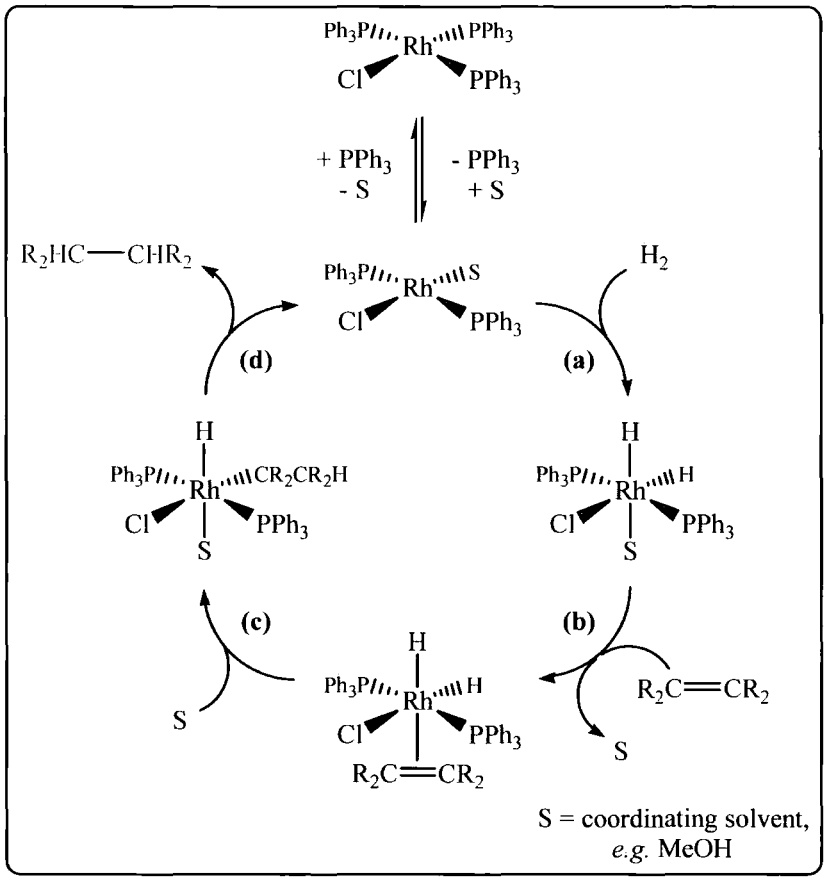

Scheme 1.11: Mechanism of hydrogenation of olefins with Wilkinson's Catalyst[108]

As shown in Scheme 1.11, the initial step in the catalytic hydrogenation of olefins with Wilkinson's catalyst involves the dissociation of a phosphine donor which creates a vacant coordination site at the metal centre and facilitates the oxidative addition of dihydrogen to the metal centre **(a)**. Following insertion of the unsaturated substrate **(b)**, the olefin undergoes a migratory insertion reaction **(c)** to generate a metal hydrido alkyl species. Upon reductive elimination of the hydrogenated product **(d)**, the active catalyst is regenerated, thus completing the catalytic cycle.

In the development of initiators for asymmetric hydrogenation, many factors (such as substrate structure[109] and solvent[110]) have to be taken into account, however the foremost consideration remains the choice of metal precursor for the process in question. Indeed, the nature of the auxiliary co-ligands present at the metal site impact greatly on the chemo- and stereo-selectivities observed in the resulting products.[102]

While numerous Rh-based hydrogenation catalysts exist, some of the largest advances have been made with the use of bidentate ligands, and in particular with

diphosphines. These systems exhibit greater control over coordination number and the mode of substrate binding than their monodentate counterparts, which are important features of asymmetric hydrogenation where rigidly chelating bidentate ligands give best transfer of chirality.

While numerous reports of chelating bisphosphine ligands for asymmetric hydrogenation have been reported, by contrast relatively few active rhodium compounds comprising bifunctional heteroditopic ligands have been reported. While it is acknowledged that the incorporation of a combination of hard and soft donor fragments can afford high levels of control over consequent catalytic activity,[111] only a small number of rhodium-containing bidentating chelating P–N,[111,112,113,114] N–S[115] and P–S[116,117] complexes have been reported. Furthermore, the use of tridentate ligands, such as P–N–N, for asymmetric hydrogenation are even more scarce.[118] However, it is noteworthy that the introduction of phosphite donor fragments appears to increase the rate of catalytic activity[101,109] and the combination of aminophosphine-phosphite donor fragments within the same ligand scaffold can prove an effective strategy for the development of highly active and selective catalysts.[119]

1.9.2 Rhodium-catalysed homogeneous carbonylation

The carbonylation of methanol to give acetic acid is one of the most important commercial homogeneous-catalysed reactions. Since the introduction of a rhodium-catalysed carbonylation procedure in 1968 by the Monsanto company, over 90 % of all acetic acid capacity worldwide is produced by this process.[120] Acetic acid remains one of the most important industrial feedstocks as this basic chemical is used in the manufacture of vinyl acetate and acetate ester and cellulose acetate to name but a few.[121] The widespread use of the Monsanto process can be attributed to the excellent product selectivity and the moderate pressures and temperatures of this commercial process. Indeed, under correct operating conditions, product selectivities of 99 % can be obtained with minimal formation of by-products.[120]

The basic Monsanto rhodium-catalysed process features six basic stoichiometric reactions, which link together to form the cycle shown in Scheme 1.12. Detailed experimental and theoretical studies have determined that the Rh catalyst partakes in only four of these six reactions with the first and last step being purely organic.[122]

Studies of the Monsanto process by Forster using high pressure infrared spectroscopy [123] have determined the active carbonylation catalyst to be that of $[Rh(CO)_2I_2]^-$, with the rate-limiting step for this cycle being the oxidative addition of methyl iodide to Rh.

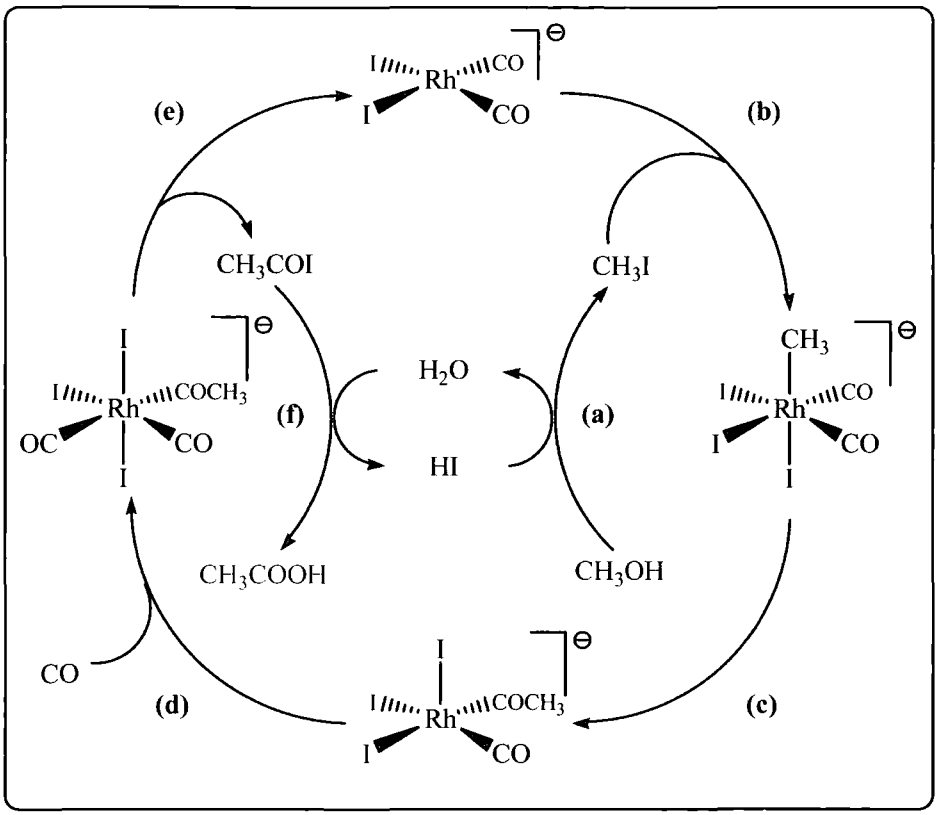

Scheme 1.12: The Rh-catalysed carbonylation of methanol with $[Rh(CO)_2I_2]^-$ (Monsanto process)[122]

The first step of this catalytic cycle is the conversion of methanol to methyl iodide by reaction with hydroiodic acid **(a)**. The methyl iodide then oxidatively adds to the active carbonylation catalyst, $[Rh(CO)_2I_2]^-$, to afford a *cis*-$[(CH_3)Rh(CO)_2I_3]^-$ anion **(b)**.[124] Due to the kinetic instability of this *cis*-$[(CH_3)Rh(CO)_2I_3]^-$ species, isomerisation to the more stable acetyl anion occurs **(c)**, which has been characterised crystallographically as both its dimeric[125] and pyridine[126] derivatives. The $[(CH_3CO)Rh(CO)I_3]^-$ reacts rapidly to form the six-coordinate dicarbonyl $[(CH_3CO)Rh(CO)_2I_3]^-$ complex,[126] **(d)**. The acetyl iodide is then released from the Rh centre, **(e)**, thus regenerating the active $[Rh(CO)_2I_2]^-$ catalyst, whilst acetyl iodide hydrolysis affords the final acetic acid product, **(f)**. Kinetic experiments on this catalytic

cycle have determined the rate limiting step to be (**b**), the oxidative addition of MeI to the Rh(I) centre.[122]

The Monsanto process is unusual as a considerable quantity of water (14 – 15%) is required to achieve high catalytic rates and prolong the lifetime of the catalyst.[124] If the volume of water in the reactor vessel is allowed to fall lower than these levels (approx. 8%), the $[Rh(CO)_2I_2]^-$ catalyses the alternative water-gas shift reaction (WGSR), which results in the generation of H_2 and CO_2 gases, Scheme 1.13, due to an increase of the catalyst concentration in the reaction mixture. It is therefore of critical importance that the concentration of $[Rh(CO)_2I_2]^-$ remains constant in the reaction solution to promote methanol carbonylation over the alternative WGSR process.[127] Indeed, the presence of the WGSR side reaction is the major inefficiency of the carbonylation process.

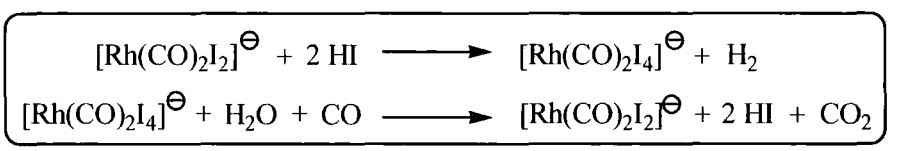

Scheme 1.13: $[Rh(CO)_2I_2]^-$ catalysed water-gas shift reaction (WGSR)[121]

In an effort to improve the efficiency of methanol carbonylation, considerable attention has been directed towards the development of catalysts that promote the required transformation under milder, more economic conditions whilst suppressing the secondary WGSR process.[121] Studies on a variety of ligand systems have determined that the use of *cis*-chelating ligands promotes the oxidative addition of methyl iodide to the Rh(I) centre and results in faster product conversion rates,[128] although interestingly, the employment of '*trans*-spanning' ligands shows no carbonylation activity due to inhibition of MeI addition.[129]

It has been demonstrated that the incorporation of basic ligands, such as alkyl phosphines,[130] promotes carbonylation processes, although the use of homoditopic chelating ligands generally results in catalysts with activities that are broadly comparable to that of the original Monsanto system.[131,132] Unusually, there have been reports of an active O–O chelated Rh initiator.[133]

There is growing interest however in the development of hybrid ligands for carbonylation activities. Indeed, theoretical studies on complexes containing these

heteroditopic ligands indicate that the enhanced electronic disparity between the donor atoms has a profound effect on the CO migratory insertion step of this process and the incorporation of strong π-donating ligands, such as thiols, promotes this step.[131] Active Rh-based carbonylation catalysts ligated with P–S[134,135,136] and P–O[137,138,139] ligands have also been reported.

1.9.3 Rhodium-catalysed homogeneous hydroformylation

Hydroformylation is a useful and atom-efficient reaction that combines three simple reactants, an olefin, H_2 and CO, to create a new carbon-carbon bond and a new carbon-hydrogen bond. As a result, this process introduces a synthetically versatile aldehyde functionality thus enabling subsequent functionalisation of the products.[140] A further attractive feature of this process is that, depending on the nature of the catalyst and the substitution pattern of the olefin, a number of stereocentres may be introduced into the aldehyde products. Through this asymmetric hydroformylation, a wide variety of chiral molecules are accessible which are important building blocks for the production of fine chemicals, pharmaceuticals and agrochemicals.[141] Indeed, gaining control over the regioselective formation of linear aldehydes from terminal or internal olefins and the enantioselectivity of the resulting products remains an important challenge in this process, Scheme 1.14.

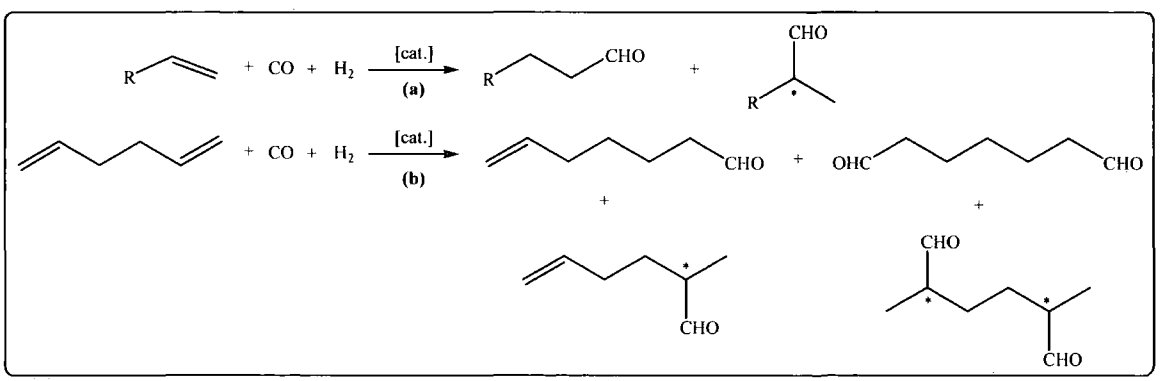

Scheme 1.14: Representative hydroformylation of olefins

While the first hydroformylation catalysts were based on Co systems,[140] the high toxicity and poor selectivity that these systems exhibited led to the development of

highly active Rh-based hydroformylation catalysts, the first efficient and well-defined systems being reported by Wilkinson and co-workers in 1968.[142,143,144] Compared to the older cobalt hydroformylation systems, rhodium initiators offer the advantages of enhanced rates, lower operating temperatures and pressures and higher regio- and stereo-selectivities of the resulting aldehydes.[140] Furthermore, these Rh-based systems eliminated the problems of olefin isomerisation and hydrogenation, which were typical side-reactions of the original Co systems whilst demonstrating enhanced tolerance towards substrate functionalities.[145] The basic catalytic cycle for the hydrogenation of a terminal olefin with Wilkinson's $[H(CO)Rh(PPh_3)_3]$ catalyst is shown below in Scheme 1.15.

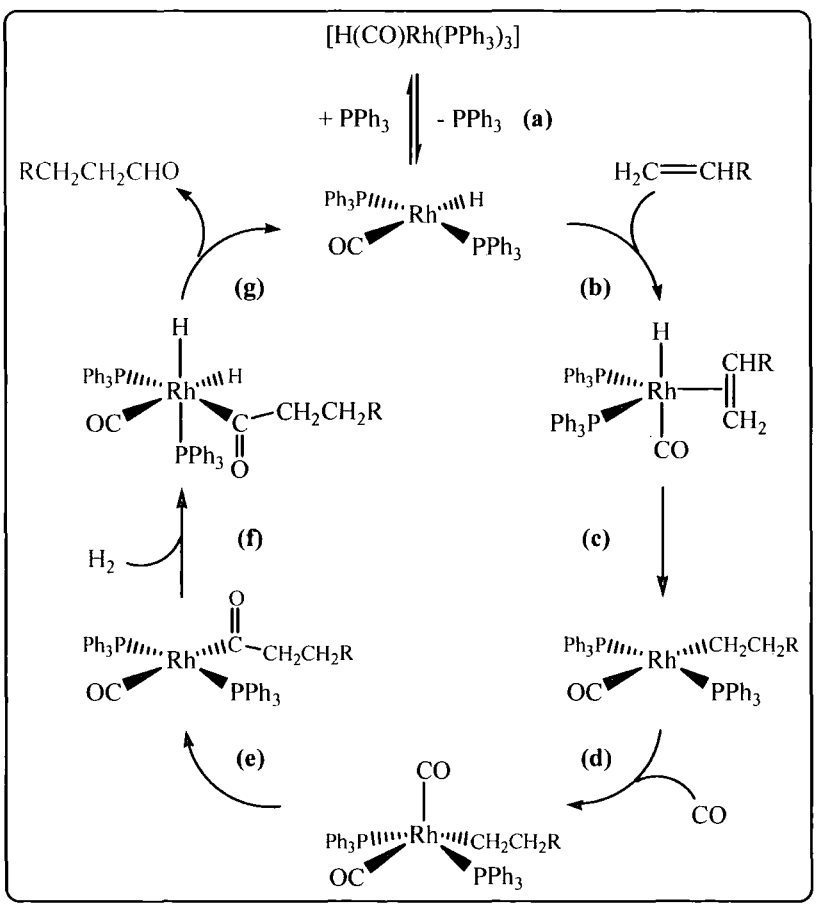

Scheme 1.15: Hydroformylation catalytic cycle with Wilkinson's $[H(CO)Rh(PPh_3)_3]$ initiator

The first step in this hydroformylation catalytic cycle is the generation of the active catalyst *via* dissociation of a phosphine, which generates a vacant coordination

site at the metal centre **(a)**. Following insertion of the unsaturated substrate, **(b)**, the olefin undergoes a migratory insertion process, **(c)**, to afford the corresponding metal-alkyl complex. Upon binding of CO, **(d)**, this carbonyl inserts into the metal-alkyl bond, **(e)**, to generate a metal alkyl carbonyl complex. The final steps involves oxidative addition of dihydrogen to rhodium, **(f),** followed by subsequent reductive elimination of the aldehyde, (**g**), which regenerates the active catalyst.[140]

Kinetic investigations on this cycle have indicated that the oxidative addition of dihydrogen to Rh {Scheme 1.15, (**f**)} and the reductive elimination of the aldehyde product {Scheme 1.15, (**g**)} are the rate limiting processes in this cycle.[146] By contrast, insertion of the olefin is a fast process and, in the case of unsymmetrical olefins, can occur with different regiochemistries, which results in the formation of linear (*n*-alkyl) and branched (*iso*-) aldehydes.[146] Thus, in asymmetric hydroformylation it is vital to control the olefin insertion process for the specific production of aldehydes with desired stereochemistries.

Many ligands and their resulting Rh complexes have been evaluated to examine the levels of enantio- and regio-selectivity that they impart on this process. Theoretical ligand design studies for hydroformylation applications have indicated that bidentate chelating ligands lead to better control over *n*:*iso* product ratios and favour the formation of linear aldehydes.[146]

Due to the facile variation of the steric and electronic properties of phosphines,[147] these ligands frequently find employment in hydroformylation catalysis although the prevalence of phosphite ligands in this process is almost as widespread.[145] Mixed phosphine-phosphite-ligated Rh complexes have also been shown to exhibit high levels of control over the *n*/*iso* product ratio,[148,149] as have bidentate aminophosphine rhodium species.[150] Additionally, homoditopic N–N complexes have also showed activity for this process.[151] Polydentate hybrid ligands have received comparably less attention although there are examples of P–N,[152,153,154,155] P–O,[155] P–S[156,157] as well as P – olefin[158] chelated rhodium complexes showing activity in the hydroformylation of a variety of unsaturated substrates. Interestingly, the potential of hemilabile N–P–N rhodium complexes has also been explored with promising results being observed for these unusual systems.[159,160]

1.10 Aims of this work

This thesis presents the synthesis of a number of diheteroatomic ring systems bearing a pendant phosphine donor arm and the exploration of the coordination chemistry of these ligands with a variety of Pd(II), Pt(II) and Rh(I) metal centres.

The versatile dynamic behaviour of these diheteroatomic rings has been combined with the significant electronic and steric control provided by heteroditopic P–N ligands to provide a novel set of potentially tridentate ligands, Figure 1.9 (**L**). These potentially multidentate systems have the effect of enforcing *meridional* coordination {Figure 1.9, (**b**)} of the ligand over the alternative *facial* geometry {Figure 1.9, (**c**)}, as a result of the rigid, pre-defined geometry of the double-chelate rings, thereby simplifying the number of potential coordination modes available to the ligand in question.[161]

In particular, the ability of various E donor fragments of **L** will be expanded to establish the factors that control the mode of ligand binding to a given metal centre (*i.e.* $\kappa^1/\kappa^2/\kappa^3$). Emphasis will be placed upon understanding the factors that control how the ligand (**L**) may bind and how this subsequently affects the remainder of the metal's coordination sphere.

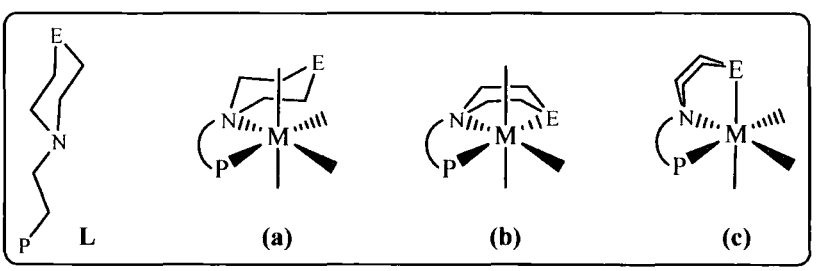

Figure 1.9: Some potential coordination modes of a N^E 'double-chelate' ring bearing a pendant phosphorus donor

1.11 References

[1] G. J. P. Britovsek, V. C. Gibson and D. F. Wass, *Angew. Chem. Int. Ed. Engl.*, 1999, **38**, 428 – 447.

[2] "*Inorganic Chemistry*", P. Atkins, T. Overton, J. Rourke, M. Weller and F. Armstrong, 4th Ed. OUP, Oxford, 2006, pg. 494.

[3] See for example, J. R. Dilworth and N. Wheatly, *Coord. Chem. Rev.*, 2000, **199**, 89 – 158 and references therein.

[4] P. Braunstein and F. Naud, *Angew. Chem. Int. Ed.*, 2001, **40**, 680 – 699.

[5] R. G. Pearson, *J. Am. Chem. Soc.*, 1963, **85**, 3533 – 3539.

[6] T. G. Appleton, H. C. Clark, L. E. Manzer, *Coord. Chem. Rev.*, 1973, **10**, 335 – 422.

[7] "*Applied Homogeneous Catalysis with Organometallic Compounds*", B. Cornils and W. A. Herrmann, (Eds.), VCH, Weinheim, Germany, 1996.

[8] F. Bessac and G. Frenking, *Inorg. Chem.*, 2006, **45**, 6956 – 6964.

[9] A. Togni and L. M. Venanzi, *Angew. Chem. Int. Ed.*, 1994, **33**, 497 – 526.

[10] See for example: S. G. Murray and F. R. Hartley, *Chem. Rev.*, 1981, **81**, 365 – 414.

[11] M. Akbar Ali and S. E. Livingstone, *Coord. Chem. Rev.*, 1974, **13**, 101 – 132.

[12] See for examples: G. W. Gokel, W. M. Leevy and M. E. Weber, *Chem. Rev.*, 2004, **104**, 2723 – 2750.

[13] H.-B. Kraatz, H. Jacobsen, T. Ziegler and P. M. Boorman, *Organometallics*, 1993, **12**, 76 – 80.

[14] J. A. Aguilar, E. Garcìa-España, J. A. Guerrero, J. M. Llinares, J. A. Ramìrez, C. Soriano, S. V. Luis, A. Bianchi, L. Ferrini and V. Fusi, *J. Chem. Soc., Dalton Trans.*, 1996, 239 – 246.

[15] M. Boiocchi, M. Bonizzoni, L. Fabbrizzi, F. Foti, M. Licchelli and A. Taglietti, *Dalton Trans.*, 2004, 653 – 658.

[16] "*Conformational Analysis*", E.L. Eliel, N.L. Allinger, S.J. Angyal and G.A. Morrison, Interscience, New York, 1965, Chapter 4.

[17] "*Organic Chemistry*", J. McMurry, 3rd Ed., Brooks/Cole Publishing Company, California, USA, 1992, Chapter 25, pg. 961.

[18] R. K. Harris and R. A. Spragg, *J. Chem. Soc. (B)*, 1968, 684 – 691.

[19] A. Flores-Parra, G. Cadenas-Pliego, R. Contreras, N. Zuniga-Villarreal and M. de los Angeles Paz-Sandoval, *J. Chem. Ed.*, 1993, **70**, 556 – 559.

[20] E. W. Abel, M. Booth and K. G. Orrell, *J. Chem. Soc., Dalton Trans.*, 1979, 1994 – 2002.

[21] M. J. Fray, G. Bish, P. V. Fish, A. Stobie and F. Wakenhut, *Bioorg. Med. Chem. Lett.*, 2006, **16**, 4349 – 4353.

[22] B. Asproni, A. Pau, M. Bitti, M. Melosu, R. Cerri, L. Dazzi, E. Seu, E. Maciocco, E. Sanna, F. Busonero, G. Talani, L. Pusceddu, C. Altomare, G. Traponi and G. Biggio, *J. Med. Chem.*, 2002, **45**, 4655 – 4665.

[23] M. K. Piestrzeniewicz, D. Wilmanska, J. Szemraj and K. Studzian, *Zeit. für Natfor.*, 2004, **59**, 739 – 748.

[24] Y. Li, Y.-H. Lai, K. F. Mok and M. G. B. Drew, *Inorg. Chim. Acta*, 1999, **285**, 31 – 38.

[25] Y. Li, Y.-H. Lai, K. F. Mok and M. G. B. Drew, *Inorg. Chim. Acta*, 1998, **279**, 221 – 225.

[26] M. Rodriguez i Zubiri, A. M. Z. Slawin, M. Wainwright and D. J. Woollins, *Polyhedron*, 2002, **21**, 1929 – 1935.

[27] R. G. Kostyanovsky, V. N. Vonesensky, G. K. Kadorkina and Yu. I. El'natanov, *Org. Mag. Spectro.*, 1980, **15**, 412 – 418.

[28] R. G. Kostyanovski, Yu. I. El'natanov, Sh. M. Shikhaliev, S. M. Ignatov and I. I. Chevin, *Bull. Acad. USSR Div. Chem. Sci. (Engl. Trans.)*, 1982, **31**, 1433 – 1441.

[29] D. A. Binn, R. S. Button, V. Farazi, M. K. Neeb and C. L. Tapley, *J. Organomet. Chem.*, 1990, **393**, 143 – 152.

[30] B. A. Byron, A. Carroy, J.-M. Lehn and D. Parker, *J. Chem. Soc., Chem. Commun.*, 1984, 1546 – 1548.

[31] M. L. Clarke, A. M. Z. Slawin and J. D. Woollins, *Polyhedron*, 2003, **22**, 19 – 26.

[32] S. Mukhopadhyay, D. Mandal, D. Ghosh, I. Goldberg and M. Chadhuary, *Inorg. Chem.*, 2003, **42**, 8439 – 8445.

[33] D. G. Gilheany, *Chem. Rev.*, 1994, **94**, 1339 – 1374.

[34] "*Orbital Interactions in Chemistry*", T. A. Albright, J. K. Burdett and M.-H. Whangbo, Wiley, New York, 1985.

[35] D. G. Gilheany in, "*The Chemistry of Organophosphorus Compounds*", F.R. Hartley (Ed.); Wiley Interscience; Chichester, 1990; Vol. 1, Chapter 2, pgs. 9 – 49.

[36] D. S. Marynick, D. C. Rosen and J. Liebman, *J. Mol. Struct. Theochem.*, 1983, **94**, 47 – 50.

[37] C. A. Jolly, F. Chan and D. S. Marynick, *Chem. Phys. Lett.*, 1990, **174** (3–4), 320 – 324.

[38] R. F. W. Bader, J. R. Cheeseman, K. E. Laidig, K. B. Wiberg and C. Breneman, *J. Am. Chem. Soc.*, 1990, **112**, 6530 – 6536.

[39] A. M. Belostotskii, P. Aped and A. Hassner, *J. Mol. Struct. (Theochem.)*, 1997, **398 – 399**, 427 – 434.

[40] P. C. J. Kamer, A. van Rooy, G. C. Schoemaker and P. W. N. M. van Leeuwen, *Coord. Chem. Rev.*, 2004, **248**, 2409 – 2424.

[41] S. D. Ittel, L. K. Johnson and M. Brookhart, *Chem. Rev.*, 2000, **100**, 1169 – 1203.

[42] N. Miyaura and A. Suzuki, *Chem. Rev.*, 1995, **95**, 2457 – 2483.

[43] See L. Yin and J. Liebscher, *Chem. Rev.*, 2007, **107**, 133 – 173 and references therein.

[44] "*Palladium Reagents in Organic Synthesis*", R.F. Heck, 1985, Academic Press, Inc., Suffolk, UK.

[45] L. E. Overman and F. M. Knoll, *J. Am. Chem. Soc.*, 1980, **102**, 865 – 867.

[46] J. L. Baan and F. Bickelhaupt, *Tetrahedron Lett.*, 1986, **27**, 6267 – 6270.

[47] Most Pd-mediated hydrogenation reactions are heterogeneous (See "*Handbook of Organopalladium Chemistry for Organic Synthesis*" E. Neishi (Ed.), Wiley-Interscience, New York, 2002, Volume II, Chapter VII.2, pgs. 2719 – 2752 and references therein) although a few homogeneous processes have been reported (K. Tani, N. Ono, S. Okamoto and F. Sato, *J. Chem. Soc., Chem. Commun.*, 1993, 386 – 387)].

[48] J. Smidt, W. Hafner, R. Jira, R. Sieber, S. Sedlmeier and A. Sabel, *Angew. Chem. Int. Ed. Engl.*, 1962, **1**, 80 – 88.

[49] D. Forster, *Adv. Organometal. Chem.*, 1979, **17**, 255 – 267.

[50] See L. Negureanu, R. W. Hall, L. G. Butler and L. A. Simeral, *J. Am. Chem. Soc.*, 2006, **128**, 16816 – 16826 and references therein.

[51] A. L. McKnight and R. M. Waymouth, *Chem. Rev.*, 1998, **98**, 2587 – 2598.

[52] L. K. Johnson, C. M. Killian and M. Brookhart, *J. Am. Chem. Soc.*, 1995, **117**, 6414 – 6415.

[53] W. Keim, *Angew. Chem. Int. Ed. Engl.*, 1990, **29**, 235 – 244.

[54] J. Pietsch, P. Braunstein and Y. Chauvin, *New J. Chem.*, 1998, 467 – 472.

[55] P. Kuhn, D. Sémeril, D. Matt, M. J. Chetcuti and P. Lutz, *Dalton Trans.*, 2007, 515 – 528.

[56] L. Deng, T. K. Woo, L. Cavallo, P. M. Margl and T. Ziegler, *J. Am. Chem. Soc.*, 1997, **119**, 6177 – 6186.

[57] L. H. Schultz and M. Brookhart, *Organometallics*, 2001, **20**, 3975 – 3982.

[58] C. M. Killian, L. K. Johnson and M. Brookhart, *Organometallics*, 1997, **16**, 2005 – 2007.

[59] V. C. Gibson and S. K. Spitzmesser, *Chem. Rev.*, 2003, **103**, 283 – 316

[60] F. Speiser, P. Braunstein and L. Saussine, *Acc. Chem. Res.*, 2005, **38**, 784 – 793.

[61] Z. Guan and W.J. Marshall, *Organometallics*, 2002, **21**, 3580 – 3586.

[62] E. K. van der Beuken, W. J. J. Smeets, A. L. Spek and B. L. Feringa, *Chem. Commun.*, 1998, 223 – 224.

[63] O. Daugulis, M. Brookhart and P. S. White, *Organometallics*, 2002, **21**, 5935 – 5943.

[64] O. Daugulis and M. Brookhart, *Organometallics*, 2002, **21**, 5926 – 5934.

[65] E. Drent and P. H. M. Budzelaar, *Chem. Rev.*, 1996, **96**, 663 – 681.

[66] E. Drent, J. A. M. Broekhoven and M. J. Doyle, *J. Organomet. Chem.*, 1991, **417**, 235 – 251.

[67] M. Svensson, T. Matsubara and K. Morokuma, *Organometallics*, 1996, **15**, 5568 – 5576.

[68] A. Haras, A. Michalak, B. Rieger and T. Ziegler, *Organometallics*, 2006, **25**, 946 – 953.

[69] A. Haras, A. Michalak, B. Rieger and T. Ziegler, *J. Am. Chem. Soc.*, 2005, **127**, 8765 – 8774.

[70] P. W. N. M. van Leeuwen, C. F. Roobeek and H. van der Heijden, *J. Am. Chem. Soc.*, 1994, **116**, 12117 – 12118.

[71] T. C. Flood, J. E. Jenson and J. A. Statler, *J. Am. Chem. Soc.*, 1981, **103**, 4410 – 4414.

[72] C. Bianchini and A. Meli, *Coord. Chem. Rev.*, 2002, **225**, 35 – 66.

[73] J. Durand and B. Milani, *Coord. Chem. Rev.*, 2006, **250**, 542 – 560.

[74] D. Sirbu, G. Consiglio and S. Gischig, *J. Organomet. Chem.*, 2006, **691**, 1143 – 1150.

[75] A. D. Burrows, M. F. Mahon and M. Varrone, *Dalton Trans.*, 2003, 4718 – 4730.

[76] A. Aeby and G. Consiglio, *Inorg. Chim. Acta*, 1999, **296**, 45 – 51.

[77] A. Aeby, A. Gsponer and G. Consiglio, *J. Am. Chem. Soc.*, 1998, **120**, 11000 – 11001.

[78] I. P. Beletskaya and A. V. Cheprakov, *Chem. Rev.*, 2000, **100**, 3009 – 3066.

[79] J. K. Stille, *Angew. Chem. Int. Ed.*, 1986, **25**, 508 – 523.

[80] K. Sonogashira, *J. Organomet. Chem.*, 2002, **653**, 46 – 49.

[81] J. F. Hartwig, *Acc. Chem. Res.*, 1998, **31**, 852 – 860.

[82] A. Yamomoto, *J. Chem. Soc., Dalton Trans.*, 1999, 1027 – 1037.

[83] J. M. Brown and N. A. Cooley, *Chem Commun.*, 1988, **19**, 1345 – 1347.

[84] A. O. Aliprantis and J. W. Canary, *J. Am. Chem. Soc.*, 1994, **116**, 6985 – 6986.

[85] V. Farina and B. Krishnan, *J. Am. Chem. Soc.*, 1991, **113**, 9583 – 9595.

[86] W. de Graaf, S. Harder, J. Boersma, G. van Koten and J. A. Kanters, *J. Organomet. Chem.*, 1998, **358**, 545 – 562.

[87] C. A. Ghilardi, S. Midollini, S. Moneti and A. Orlandini, *Chem. Commun.*, 1986, 1771 – 1772.

[88] F.R. Hartley in "*Comprehensive Organometallic Chemistry; The Synthesis, Reactions and Structures of Organometallic Complexes*", G. Wilkinson, F.G.A. Stone and E.W. Abel (Eds.), Volume 6., 1982, Pergamon Press Inc., Elmsford, New York, USA. Pg. 473.

[89] M. L. Clarke, *Polyhedron*, 2001, **20**, 151 – 164.

[90] "*Inorganic Chemistry*", P. Atkins, T. Overton, J. Rourke, M. Weller and F. Armstrong, 4th Ed. OUP, Oxford, 2006, Chapter 18.

[91] L. M. Rendina and R. J. Puddephatt, *Chem. Rev.*, 1997, **97**, 1735 – 1754.

[92] P. Steffanut, J. A. Osborn, A. DeCian and J. Fisher, *Chem. A Eur. J.*, 1998, **4**, 2008 – 2017.

[93] C. U. Pittman Jr., Y. Kawabata and L. I. Flowers, *Chem. Commun.*, 1982, 473 – 474.

[94] F. Agbossou, J.-F. Carpentier and A. Mortreux, *Chem. Rev.*, 1995, **95**, 2485 – 2506.

[95] B. Soro, S. Stoccoro, G. Minghetti, A. Zucca, M. Agostina, M. Manassero and S. Gladiali, *Inorg. Chim. Acta*, 2006, **359**, 1879 – 1888.

[96] R. B. Bedford, S. L. Hazelwood and D. A. Albisson, *Organometallics*, 2002, **21**, 2599 – 2600.

[97] C. Mateo, C. Fernández-Rivas, D. J. Cárdenas and A. M. Echavarren, *Organometallics*, 1998, **17**, 3661 – 3669.

[98] "*Modern Rhodium-Catalysed Organic Reactions*", P.A. Evans (Ed.), Wiley-VCH, New York, 2005.

[99] R.P. Hughes in "*Comprehensive Organometallic Chemistry; The Synthesis, Reactions and Structures of Organometallic Compounds*", G. Wilkinson, F.G.A. Stone (Eds.), Volume 5, Pergamon Press Ltd., Oxford, 1982.

[100] See for examples: M.C. Simpson and D.J. Cole-Hamilton, *Coord. Chem. Rev.*, 1996, **155**, 163 – 207 and references therein

[101] D. Peña, A. J. Mimaard, A. H. M. de Vries, J. G. de Vries and B. L. Feringa, *Org. Lett.*, 2003, 475 – 478.

[102] X. Cui and K. Burgess, *Chem. Rev.*, 2005, **105**, 3272 – 3296.

[103] J. F. Young, J. A. Osborn, F. H. Jardine and G. Wilkinson, *Chem. Commun.*, 1965, 131 – 132.

[104] J. A. Osborn, F. H. Jardine, J. F. Young and G. Wilkinson, *J. Chem. Soc. (A)*, 1966, 1711 – 1732.

[105] "*Homogeneous Catalysis with Compounds of Rhodium and Iridium*", R.S. Dickson, D. Reidel Publishing Company, Dordrecht, Holland, 1985.

[106] R. G. Pearson, *Acc. Chem. Res.*, 1971, **4**, 152 – 160.

[107] J. Halpern, T. Okamoto and A. Zakhariev, *J. Mol. Cat.*, 1977, **2**, 65 – 68.

[108] H. Brunner in "*Applied Homogeneous Catalysis with Organometallic Compounds*", 2nd Edition, B. Cornlis, W.A. Herrmann (Eds.), Wiley-VCH, Weinheim, 2002, Chapter 2.2, pgs. 195 – 212.

[109] R. M. D. Hui, A. F. Peixoto, M. R. Axet, M. M. Pereira, M. J. Moreno, L. Kollár, C. Claver and S. Castillón, *J. Mol. Cat. (A)*, 2006, **247**(1–2), 275 – 282.

[110] J. Yu and J.B. Spencer, *J. Am Chem. Soc.*, 1997, **119**, 5257 – 5258.

[111] D. J. Law and R. G. Cavell, *J. Mol. Cat.*, 1994, **91**, 175 – 186.

[112] M. M. Taqui Khan, B. Taqui Khan, S. Begum and P. Jaypal Reddy, *J. Mol. Cat.*, 1988, **49**, 33 – 42.

[113] M. M. Taqui Khan, B. Taqui Khan and S. Begum, *J. Mol. Cat.*, 1986, **34**, 9 – 18.

[114] A. Jacobi, G. Gottfried and U. Winterhalter, *J. Organomet. Chem.*, 1998, **571**, 231 – 241.

[115] A. W. Gal and F. H. A. Bolder, *J. Organomet. Chem.*, 1977, **142**, 375 – 385.

[116] D. Cauzzi, M. Costa, N. Cucci, C. Graiff, F. Grandi, G. Predieri, A. Tiripicchio and R. Zanoni, *J. Organomet. Chem.*, 2000, **593–594**, 431 – 444.

[117] C. Claver, F. Gili, J. Viñas and A. Ruiz, *Polyhedron*, 1987, **6**, 1329 – 1335.

[118] J. P. Masson, A. A. Bahsoun, M. T. Youinou and J. A. Osborn, *Comptes Rendus Chimie*, 2002, **5**, 303 – 308.

[119] E. Cesarotti, A. Chiesa and G. D'Alfonso, *Tetrahedron Lett.*, 1982, **23**, 2995 – 2996.

[120] P. M. Maitlis, A. Haynes, G. J. Sunley and M. J. Howard, *J. Chem. Soc., Dalton Trans.*, 1996, 2187 – 2196.

[121] P. Torrence in "*Applied Homogeneous Catalysis with Organometallic Compounds*", 2nd Edition, B. Cornlis, W.A. Herrmann (Eds.), Wiley-VCH, Weinheim, 2002, Chapter 2.1, pgs. 104 – 136.

[122] C. M. Thomas and G. Süss-Fink, *Coord. Chem. Rev.*, 2003, **243**, 125 – 142.

[123] D. Forster, *J. Am. Chem. Soc.*, 1976, **98**, 846 – 848.

[124] A. Haynes, B. E. Mann, G. E. Morris and P. M. Maitlis, *J. Am. Chem. Soc.*, 1993, **115**, 4093 – 4100.

[125] G. W. Adamson, J. J. Daly and D. Forster, *J. Organomet. Chem.*, 1974, **71**, C17 – C19.

[126] H. Adams, N. A. Bailey, B. E. Mann, C. P. Manuel, C. M. Spencer and A. G. Kent, *J. Chem. Soc., Dalton Trans.*, 1988, 489 – 496.

[127] B. L. Smith, G. P. Torrence, M. A. Murphy and A. Aguiló, *J. Mol. Cat.*, 1987, **39**, 115 – 136.

[128] L. Gonsalvi, H. Adams, G. J. Sunley, E. Pitzel and A. Haynes, *J. Am. Chem. Soc.*, 2002, **124**, 13597 – 13612.

[129] Z. Freixa, P. C. J. Kamer, M. Lutz, A. L. Spek and P. W. N. M. van Leeuwen, *Angew. Chem. Int. Ed.*, 2005, **44**, 4385 – 4388.

[130] J. Rankin, A. D. Poole, A. C. Benyei and D. J. Cole-Hamilton, *Chem. Commun.*, 1997, 1835 – 1836.

[131] E. Daura-Oller, J. M. Poblet and C. Bo, *Dalton Trans.*, 2003, 92 – 98.

[132] C.-A. Carraz, E. J. Ditzel, A. G. Orpen, D. D. Ellis, P. G. Pringle and G. J. Sunley, *Chem. Commun.*, 2000, 1277 – 1278.

[133] P. Das, M. Boruah, N. Kumari, M. Sharma, D. Konwar and D. K. Dutta, *J. Mol. Cat. A*, 2002, **178**, 283 – 287.

[134] J. Dilworth, J. R. Miller, N. Wheatley, M. J. Baker and J. G. Sunley, *J. Chem. Soc., Chem. Commun.*, 1995, 1579 – 1581.

[135] M. J. Baker, M. F. Giles, A. G. Orpen, M. J. Taylor and R. J. Watt, *J. Chem. Soc., Chem. Commun.*, 1995, 197 – 198.

[136] R. W. Wegman, A. G. Abatjoglou and A. M. Harrison, *J. Chem. Soc., Chem. Commun.*, 1987, 1891 – 1892.

[137] D. K. Dutta, J. D. Woollins, A. M. Z. Slawin, D. Konwar, P. Das, M. Sharma, P. Bhattacharyya and S. M. Aucott, *Dalton Trans.*, 2003, 2674 – 2679.

[138] See: V. V. Grushin, *Chem. Rev.*, 2004, **104**, 1629 – 1662 and references therein.

[139] A. M. Z. Slawin, M. B. Smith and J. D. Woollins, *J. Chem. Soc., Dalton Trans.*, 1996, 4575 – 4581.

[140] C. D. Frohning, C. W. Kohlpaintner and H.-W. Bohnen in "*Applied Homogeneous Catalysis with Organometallic Compounds*", 2nd Edition, B. Cornlis, W.A. Herrmann (Eds.), Wiley-VCH, Weinheim, 2002, Chapter 2.1, pgs. 31 – 103.

[141] A. M. Trzeciak and J. J. Ziołkowski, *Coord. Chem. Rev.*, 1992, **190–192**, 883 – 900.

[142] D. Evans, J. A. Osborn and G. Wilkinson, *J. Chem. Soc. A*, 1968, 3133 – 3142.

[143] G. Yagupsky, C. K. Brown and G. Wilkinson, J. *Chem. Soc. A*, 1970, 1392 – 1401.

[144] C. K. Brown and G. Wilkinson, *J. Chem. Soc. A*, 1970, 2753 – 2764.

[145] B. Breit, *Acc. Chem. Res.*, 2003, **36**, 264 – 275.

[146] D. Gleich, R. Schmid and W. A. Herrmann, *Organometallics*, 1998, **17**, 4828 – 4834.

[147] C. A. Tolman, *Chem. Rev.*, 1977, **77**, 313 – 348.

[148] N. Sakai, S. Mano, K. Nozaki and H. Takaya, *J. Am. Chem. Soc.*, 1993, **115**, 7033 – 7034.

[149] T. Horiuchi, T. Ohta, E. Shirakawa, K. Nozaki and H. Takaya, J. *Org. Chem.*, 1997, **62**, 4285 – 4292.

[150] E. J. Zijp, J. I. van der Vlugt, D. M. Tooke, A. L. Spek and D. Vogt, *Dalton Trans.*, 2005, 512 – 517.

[151] J. J. Kim and H. Alper, *Chem. Commun.*, 2005, **24**, 3059 – 3061.

[152] A. D. Phillips, S. Bolaño, S. S. Bosquain, J.-C. Daran, R. Malacea, M. Peruzzini, R. Poli and L. Gonsalvi, *Organometallics*, 2006, **25**, 2189 – 2200.

[153] L.-L. Wang, R.-W. Guo, Y.-M. Li, A. S. C. Chan, *Tetrahedron: Asymm.*, 2005, 3198 – 3204.

[154] I. D. Kostas and C. G. Screttas, *J. Organomet. Chem.*, 1999, **585**, 1 – 6.

[155] I. D. Kostas, *Inorg. Chim. Acta*, 2003, **355**, 424 – 427.

[156] I. D. Kostas, B. R. Steele, F. J. Andreadaki and V. A. Potapov, *Inorg. Chim. Acta*, 2004, **357**, 2850 – 2854.

[157] O. Pàmies, M. Diéguez, G. Net, A. Ruiz and C. Claver, *Organometallics*, 2000, **19**, 1488 – 1496.

[158] G. Mora, S. van Zutphen, C. Thoumazet, X. F. Le Goff, L. Ricard, H. Grutzmacher and P. Le Flock, *Organometallics*, 2006, **25**, 5528 – 5532.

[159] I. D. Kostas, *J. Organomet. Chem.*, 2001, **634**, 90 – 98.

[160] I. D. Kostas, *J. Organomet. Chem.*, 2001, **626**, 221 – 226.

[161] See for example: C. E. Anderson, D. C. Apperley, A. S. Batsanov, P. W. Dyer and J. A. K. Howard, *Dalton Trans.*, 2006, 4134 – 4145 and references therein.

Chapter 2:

Synthesis and derivatisation of PNE ligands

2.1 Introduction

The development of new and innovative multidentate ligands is a constant area of development throughout the field of inorganic chemistry. Frequently, varieties of such ligands exhibit a range of advantages over their monodentate counterparts as polydentate ligands have a much greater potential to direct a metal's stoichiometry, stereochemistry and coordination number, factors that affect the reactivity of the complex as a whole.[1]

While an extensive variety of multidentate ligand types exist, it is especially desirable to combine a number of electronically differing donor fragments into a single ligand framework as this presents a given metal with a unique coordination environment and allows for facile electronic tuning of the metal centre in question. Specifically, the incorporation of a combination of hard (*e.g.* nitrogen and oxygen) and soft (*e.g.* phosphorus and sulphur) donors within the ligand scaffold may give rise to a number of attractive properties in its resulting metal complexes. By selecting a combination of donors that are quite different from one another, the differentiation between their resulting interactions with the metal centre will be increased, which, in turn, influences the bonding and reactivity of other ancillary ligands present at the metal centre.[2] Moreover, the ligand may behave in a 'hemilabile' manner: one donor fragment may reversibly dissociate from the metal centre, creating a vacant coordination site at the metal which is 'masked' in the ground state structure,[3] (Scheme 1.1, Chapter 1) a property that potentially has far-reaching applications in catalysis.

In the design of ligands for applications in both coordination chemistry and catalysis, it is desirable for a given ligand system to exert a high degree of control over the metal to which it is coordinated. The use of *bis*-chelating ring systems, such as piperazine, morpholine and thiomorpholine are ideal in this regard due to the rigid and pre-defined coordination that these ligands display. Furthermore, the ligation of these saturated rings has been shown to confer a number of added benefits to their resulting complexes such as an increased resistance to demetallation and metal aggregation processes.[4] An additional feature of these cyclic amines is the possibility for further functionalisation by the introduction of an additional donor, *e.g.* a pendant phosphine donor arm at nitrogen.[5]

This chapter details the synthesis of a range of PNE ligands, comprising an N^E saturated ring fragment (where N^E = piperazine, morpholine, thiomorpholine and piperidine) with a pendant phosphine donor present at the *N*-heterocyclic ring position. A ligand family of this nature permits in-depth coordination studies on these systems through the systematic variation of the E donor whilst incorporating a variety of electronically disparate donor fragments.

2.2 Synthetic methodology for ligand formation

As with the synthesis of many phosphine-containing compounds, the preparation of the target multidentate PNE ligand systems commenced from versatile phosphine chloride 'building-blocks'.[6] On reaction of an R_2PCl precursor with a vinyl Grignard reagent, the corresponding vinyl phosphine is afforded, which can subsequently be reacted with a cyclic secondary amine under basic conditions, to afford the desired PNE compounds, as shown in Scheme 2.1.

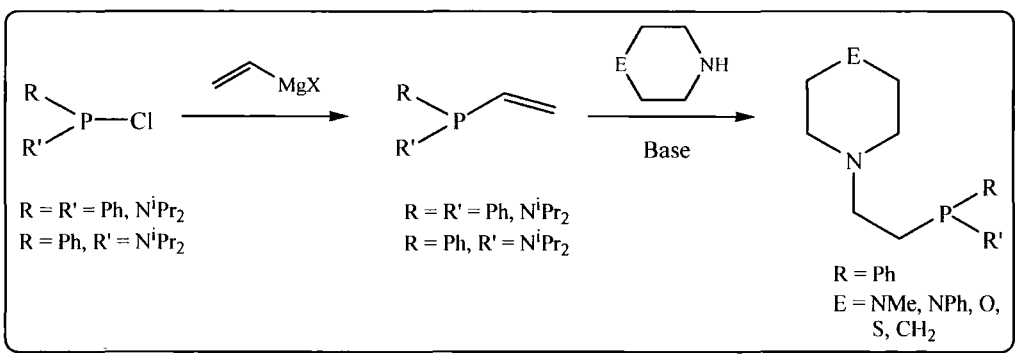

Scheme 2.1: General synthetic strategy for the preparation of the target PNE ligands

One significant advantage of employing the above methodology in the synthesis of the PNE systems is that both the pendent arm along with the phosphine donor are introduced in the same step, thus minimising the number of reactions required to generate the target species, potentially limiting the losses of yield that are often inherent in multi-step syntheses. A further attractive feature of this approach is that the cyclic secondary amines employed are all available from commercial sources, further facilitating ligand synthesis.

2.2.1 Synthesis of chlorophosphine precursors

The sterically demanding *bis*(diisopropylamino)chlorophosphine (**2.1-1**) was prepared according to a literature procedure as shown in Scheme 2.2.[7] The product was obtained in good yield (72 %) and displayed a characteristic singlet at δ_P = + 140.6 ($CDCl_3$) in its ^{31}P $\{^1H\}$ NMR spectrum.

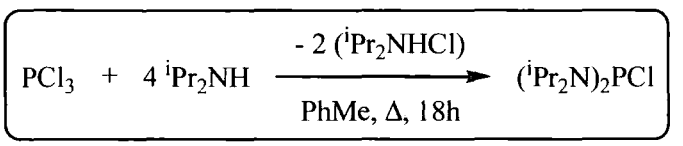

Scheme 2.2: Synthesis of $(^iPr_2N)_2PCl$ (**2.1-1**)

In addition to the synthesis of **2.1-1**, the synthesis of the related phenyl-(diisopropylamino)chlorophosphine (**2.1-2**) was undertaken in a two step procedure, as detailed in Scheme 2.3. The 'mixed' chlorophosphine **2.1-2** was a particularly attractive target due to the fact that it is notably less sterically encumbered than the *bis*(alkylamino)chlorophosphine **2.1-1**, but retains an electron-withdrawing alkyl amino fragment at the phosphorus centre. Additionally, this compound offers a convenient 'half-way house' in both electronic and steric terms between the *bis*(dialkylamino)- and diphenyl-substituted phosphines.

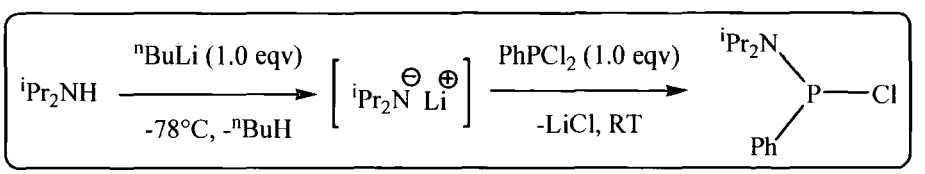

Scheme 2.3: Synthesis of phenyl(diisopropylamino)chlorophosphine (**2.1-2**)

The desired phenyl(diisopropylamino)chlorophosphine (**2.1-2**) was obtained in excellent yield (82 %) following purification by distillation under reduced pressure. The target compound gave a singlet resonance in its ^{31}P $\{^1H\}$ NMR spectrum (δ_P = + 134.0 ppm $\{CDCl_3\}$), consistent with the literature value for this compound.[8]

In both the ^{1}H and $^{13}C\{^{1}H\}$ NMR spectra of **2.1-2** at 30 °C, the resonances attributed to the phenyl substituent were observed to be sharp and well-defined, however the signals associated with the diisopropylamide substituent were noted to be severely broadened, indicating dynamic behaviour of this functionality. On lowering the temperature to – 20 °C, the broadened resonances were observed to sharpen, with four methyl signals being observed (in accordance with the chiral nature of the central phosphorus atom), in agreement with the observations made by Cowley and co-workers.[9] Figure 2.1.

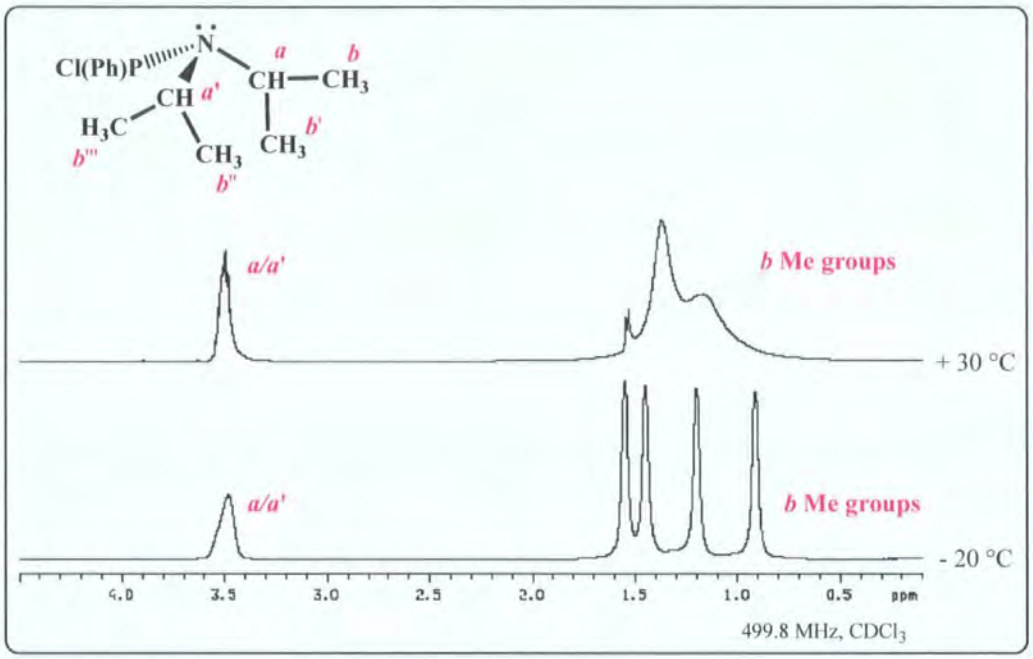

Figure 2.1: Representative ^{1}H NMR spectra of **2.1-2** at 30 °C and – 20 °C (aromatic region omitted for clarity)

The origin of the fluxional behaviour of **2.1-2** has been attributed to rotation about the P–N bond, with the energy barrier for this process having been determined to be 12.8 kcal mol^{-1} (CCl_3F).[9] This experimentally derived value is entirely in line with the observation that energy rotation barriers around P–N bonds bearing secondary alkyl groups tend to be of the order of 13.4 ± 0.2 kcal mol^{-1}.[10]

The dynamic behaviour in solution of **2.1-2** at room temperature is in direct contrast to the well-resolved spectra of the related *bis*(diisopropylamino)-chlorophosphine (**2.1-1**) at this temperature. It has been observed that the barrier of

rotation around P–N bonds is principally dependent on the steric congestion around the phosphorus centre[11] and it is presumed, therefore, that the significant steric demands offered by the presence of the two dialkylamino groups in **2.1-1** prevents rotation about its two P–N bonds. However, replacement of one of these groups by a less sterically demanding phenyl group appears to permit free rotation about this bond.

2.2.2 Synthesis of vinyl phosphines

The synthesis of the various vinyl phosphines all proceeded in accordance with Scheme 2.4, *i.e.* by reaction of the requisite chlorophosphine with an appropriate vinyl Grignard reagent, such as vinyl magnesium bromide (**2.2-1**). Following isolation and purification by distillation under reduced pressure, the vinyl phosphines **2.3-1** – **2.3-3** were all obtained as pale yellow or colourless oils in good to excellent yield. It is noteworthy that prolonged exposure of these compounds to light resulted in a distinct orange colouration, although this appears to have no noticeable effect on their chemical properties.

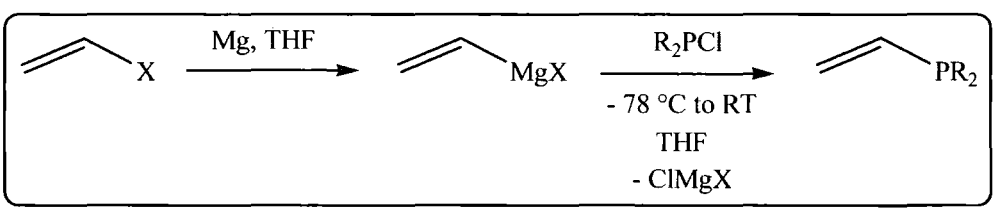

		Yield
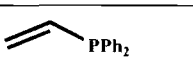	**2.3-1**	65%
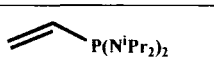	**2.3-2**	61%
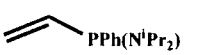	**2.3-3**	81%

Scheme 2.4: Synthesis of vinyl phosphines **2.3-1** – **2.3-3**

The use of vinyl magnesium bromide (**2.2-1**) proved successful for the preparation of the desired vinyl phosphines on a small scale (<2 g). However, upon scale-up to larger multigram quantities, the extraction of the target compounds with hexane proved to be a difficult and lengthy process, which consequently led to considerably reduced yields. In an effort to minimise this problem, the synthesis was attempted using the commercially available vinyl magnesium chloride, which proved more efficient as the extraction of the resulting magnesium chloride by-product proved to be more facile. Using this latter reagent, the yields of the multigram scale syntheses were comparable with the smaller scale reactions and even showed improvement on those performed using the vinyl bromide Grignard (**2.2-1**). It is unclear why the use of vinyl magnesium chloride improved the ease of the reaction work-up, however due to the enhanced yields obtained using this method, subsequent syntheses were performed using this reagent. Initially, the syntheses of the vinyl phosphines **2.3-1** – **2.3-3** (Scheme 2.4) were undertaken using equimolar quantities of the Grignard and chlorophosphine, however it was found that use of excess vinyl magnesium chloride (typically between 1.2 and 1.3 equivalents) afforded higher product yields in all cases, following isolation and purification.

Whilst few problems were experienced in the synthesis of **2.3-2** and **2.3-3**, it was noted during the synthesis of **2.3-1** that fast Grignard addition (> 3 – 4 cm^3 min^{-1}) or the presence of trace impurities in the commercial Grignard reagent afforded the formation of the reductively-coupled tetraphenyldiphosphine. The presence of this latter compound was readily detected in the reaction mixture by *in situ* ^{31}P NMR spectroscopy as this compound exhibits a characteristic singlet resonance at $\delta_P = -15.7$ (s).[12] Since tetraphenyldiphosphine is a solid, its removal proved to be facile as the required vinyl phosphine product **2.3-1** could be separated by vacuum distillation, although the formation of $Ph_2P–PPh_2$ served to reduce the overall yields of the reaction.

It is noteworthy that the yields obtained for compounds **2.3-2** and **2.3-3** were comparable or exceeded that of **2.3-1**. Given that it has been noted that Grignard reagents attack P–N bonds almost as easily as the P–Cl bond,[13] it might have been expected that this side-reaction would compromise the yields for these species, however it has been demonstrated that this is not the case in these systems.

2.2.3 Characterisation of 2.3-1 – 2.3-3

The use of ^{31}P $\{^{1}H\}$ NMR spectroscopy proved to be of great importance in confirming the formation of the vinyl phosphine products. Compounds **2.3-1** – **2.3-3** all demonstrated a characteristic shift to lower frequency relative to those of their parent chlorophosphines by ^{31}P $\{^{1}H\}$ NMR spectroscopy, Table 2.1. This is presumed to be a direct consequence of the replacement of the chloride substituent with a less electronegative vinyl functionality, which results in an increase in shielding of the phosphorus nucleus.[14]

		^{31}P $\{^{1}H\}$ NMR*	
		Vinyl phosphine δ_P	Parent chlorophosphine δ_P
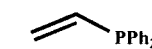	**2.3-1**	– 10.7 (s)	+ 81.5 (s)
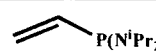	**2.3-2**	+ 54.2 (s)	+ 140.6 (s)
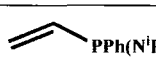	**2.3-3**	+ 34.7 (s)	+ 133.0 (s)

*202.3 MHz, $CDCl_3$

Table 2.1: ^{31}P $\{^{1}H\}$ NMR spectroscopic data for **2.3-1** – **2.3-3**

In the ^{1}H NMR spectra of the vinyl phosphines **2.3-1** – **2.3-3**, the vinylic protons were all observed as multiplets due to coupling across the vinyl functionality, and as a result of coupling to the phosphorus centre. Indeed, upon further analysis it was shown that these three vinylic protons gave rise to an ABMX spin system. Although extensive efforts were made to determine coupling constants with the use of ^{31}P $[^{1}H]$ NMR spectroscopy at high field, due to the second order nature of these systems, none of these values could be reliably assigned.[15]

In contrast to its parent chlorophosphine, **2.1-2**, which exhibited dynamic behaviour at 20 °C, **2.3-3** exhibited well-defined $^{1}H/^{13}C$ $\{^{1}H\}$ NMR spectra at this temperature. This difference has been attributed to the replacement of a chloro substituent by a more sterically demanding vinyl moiety, which inhibits rotation about the P–N bond.

The phenyl substituents in the vinyl phosphines **2.3-1** and **2.3-3** were all observed as multiplets, with overall integration of 10H and 5H, respectively, in the aromatic regions of their ^{1}H NMR spectra as expected. In both **2.3-2** and **2.3-3**, the resonances attributed to the isopropyl substituents all showed the expected characteristic doublet and septet signals associated with this functionality. In **2.3-2**, the resonances associated with the terminal isopropyl methyl protons were observed as two doublets, each integrating to 12H, with vicinal coupling to the methine proton being readily detected. The resonance assigned to the isopropyl methine proton was observed as a doublet of septets, showing coupling to both the terminal methyl protons and the phosphorus nucleus, as determined by ^{1}H $\{^{31}$P$\}$ NMR spectroscopy. The ^{13}C $\{^{1}$H$\}$ NMR spectra of the vinyl phosphines **2.3-1** – **2.3-3** proved less complicated than their respective ^{1}H NMR spectra with the required number of resonances being observed in each case.

Mass spectrometric analysis (ES^{+}) of **2.3-1** and **2.3-2** gave rise to molecular ions at m/z = 213.1 and m/z = 259.2, respectively. In contrast, despite repeated attempts, a molecular ion could not be observed for **2.3-3**, with only a number of unattributable fragmentation products being observed instead.

2.3 Synthesis of diphenylphosphine PNE compounds

Following the synthesis of the vinyl phosphine precursors, the synthesis of a family of variously-substituted, potentially tridentate PNE ligands was possible. The preparation of the required compounds all proceeded according to the same synthetic strategy, namely a base-promoted Michael addition of the vinyl phosphine to the requisite cyclic secondary amine, the mechanism for which is proposed in Scheme 2.5.

The correct choice of conditions for this addition reaction has proven to be of importance in determining the success of product formation, with the concentration of the catalyst in solution being the most important consideration of all. Previous work has indicated that this addition proceeds cleanly and in near-quantitative yield using catalytic quantities of sodamide ($NaNH_2$) in the aprotic solvent THF,[5] which is presumably a direct result of the low amide concentration in this solvent. Indeed, the use of more soluble bases such as methyl lithium is noticeably less successful as this

leads to only partial product formation,[16] while the use of butyl lithium and sodium acetate show no activity for this transformation.[17]

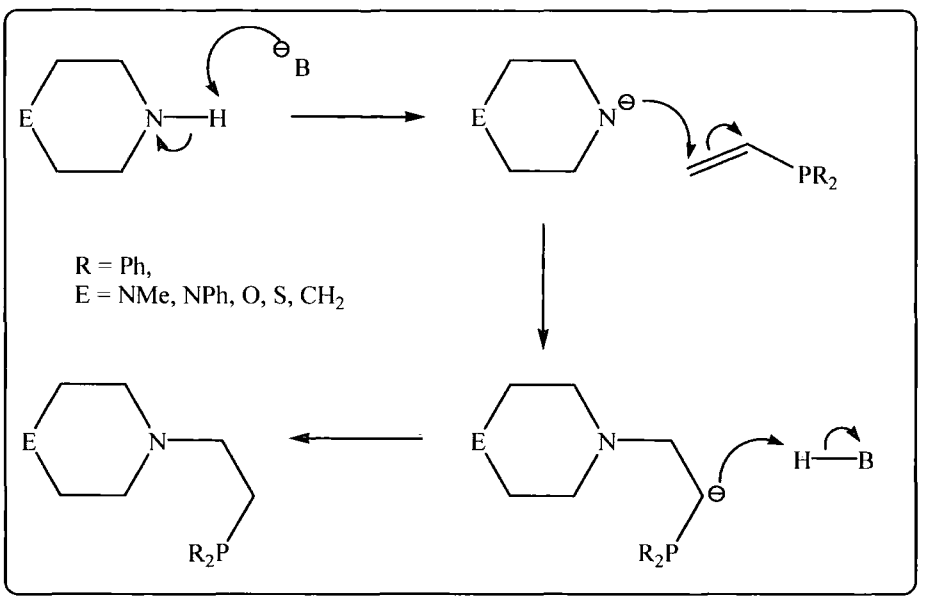

Scheme 2.5: Proposed mechanism of base-promoted Michael addition of diphenylvinyl-phosphine to cyclic secondary amines

The synthesis of the PNE compounds **2.4-1** – **2.4-5** was performed according to a slight variation of a reported procedure,[5] a THF solution containing stoichiometric quantities of the required vinyl phosphine and secondary amine were heated to reflux for around 12h with a catalytic quantity of sodamide. Following the work-up of the reaction mixture, the required products were isolated as highly viscous yellow-orange oils (**2.4-1** – **2.4-4**) or as a waxy orange solid (**2.4-5**) in good to near-quantitative yield Scheme 2.6.

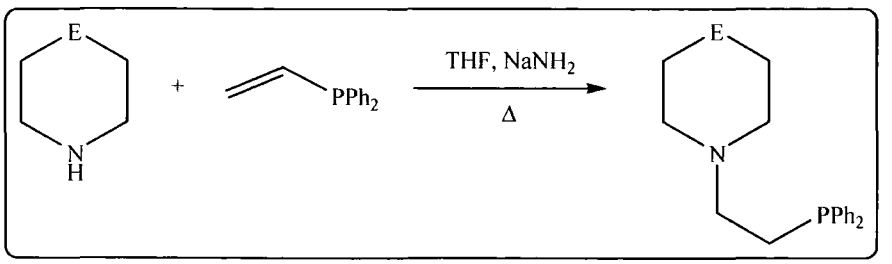

E =		Yield	$^{31}P\{^{1}H\}$ NMR*	MS§
			δ_P	*m/z*
NMe	**2.4-1**	94 %	– 19.1 (s)	313.2
O	**2.4-2**	95 %	– 18.2 (s)	300.1
S	**2.4-3**	96 %	– 18.3 (s)	316.1
CH_2	**2.4-4**	92 %	– 17.8 (s)	298.3
NPh	**2.4-5**	83 %	– 18.1 (s)	375.3

*202.3 MHz, $CDCl_3$; §ES^+, $[MH^+]$

Scheme 2.6: Synthesis, $^{31}P\{^{1}H\}$ NMR spectroscopic and mass spectrometric data for compounds **2.4-1 – 2.4-5**

2.3.1 Characterisation of 2.4-1 – 2.4-5

The formation of **2.4-1 – 2.4-5** was initially established with the aid of *in situ* ^{31}P NMR spectroscopy, with the compounds demonstrating resonances with a distinct shift to lower frequency relative to the parent vinyl phosphine {**2.3-1**; $\delta_P = -10.7$ (s)}, Scheme 2.6. All the phosphines **2.4-1 – 2.4-5** were isolated using an identical work-up procedure; the crude reaction mixtures were treated under nitrogen with an aqueous degassed solution of ammonium bromide to destroy the sodamide catalyst before extraction of the products into CH_2Cl_2. In all cases, satisfactory multinuclear NMR spectroscopic and mass spectrometric analyses were obtained.

It is interesting to note that, in all cases, regioselective anti-Markonikov addition of the vinyl functionality occurred; no trace of the Markonikov product was observed. It is presumed that the origin of this selectivity lies in the presence of a tertiary phosphorus centre adjacent to the vinyl functionality, which stabilises the secondary carbanion intermediate, Figure 2.2. The origin of this carbanion stabilisation by heteroatoms in the α-position [$RE–CR_2^-$] has several components. Classical overlap of the lone pair with the empty *d*-orbitals of P provides only a minor contribution, since

the *d*-orbitals are too diffuse and too high in energy. This in turn means that both the overlap integral and the energy separation are unfavourable. For ER (E = PR, S and SiR_2 and the higher analogous), there is a more significant contribution from σ-hyperconjugation (delocalisation of charge into E–R σ*-orbitals).[18]

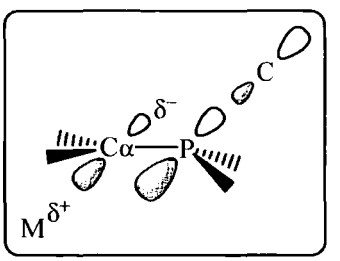

Figure 2.2: Stabilisation of negative charge at C_α by phosphorus

A factor comparable in importance to σ-hyperconjugation is the σ-bond strength. There is a size difference between the 3*p* orbitals in the C–H compounds. In the carbanion the C orbital increases in size, resulting in a stronger σ-bond. In an oxygen- or carbon-substituted system, the orbital mismatch is in the opposite direction: the *p* orbital at oxygen or carbon is smaller than that at carbon of the anion, and this size difference is exacerbated in the carbanion.

In order to avoid ambiguity in the following discussions of the structures of the PNE compounds, the labelling designation is shown in Figure 2.3. The P–N ethylene bridge positions are designated α and β in accordance with their position relative to phosphorus and the saturated ring positions are designated γ and δ. When a methylene substituent is present at the 3-position of the saturated ring, these protons are designated ε. If an *N*-methyl group is present in this 3-position of the heterocycle, the methyl protons are denoted as ζ.

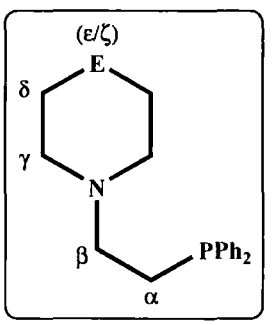

Figure 2.3: Labelling designation for PNE ligands (**2.4-1** – **2.4-5**)

In an effort to simplify discussions of the product structures, every effort has been made to perform NMR experiments in the same solvent ($CDCl_3$) to facilitate comparison between the individual species. In all cases, assignment of all resonances was assisted with the use of 2D NMR experiments (*i.e.* ^1H–^1H COSY, ^1H–^{13}C $\{^1H\}$ HETCOR and ^1H–^1H NOESY) at a range of temperatures.

2.3.2 Characterisation of *N*-methylpiperazine-*N'*-ethylene-diphenylphosphine (2.4-1)

The synthesis of *N*-methylpiperazine-*N'*-ethylene-diphenylphosphine **2.4-1** was initially performed using an excess of *N*-methylpiperazine relative to the vinyl phosphine (**2.3-1**) in accordance with literature precedent.[5] However it was subsequently found that reaction of stoichiometric quantities of the amine and phosphine afforded the required product with similar yields and hence this latter methodology was employed. The PNN(Me) product **2.4-1** was obtained in excellent near-quantitative yield (94%) following work-up and isolation.

The ^{1}H NMR spectrum of **2.4-1** obtained at 30 °C exhibited severe line broadening for all methylene resonances in accordance with rapid conformational exchange of the piperazine ring in solution.[19] On lowering the temperature, the initially broad resonance centred at δ_H = 2.42 reached coalescence at 0 – 10 °C with resonances corresponding to the individual sets of γ- and δ-rings protons evident at – 20 °C, Figure 2.4. The assignment of the saturated ring protons was made with the aid of low temperature 2D NMR spectroscopy experiments.

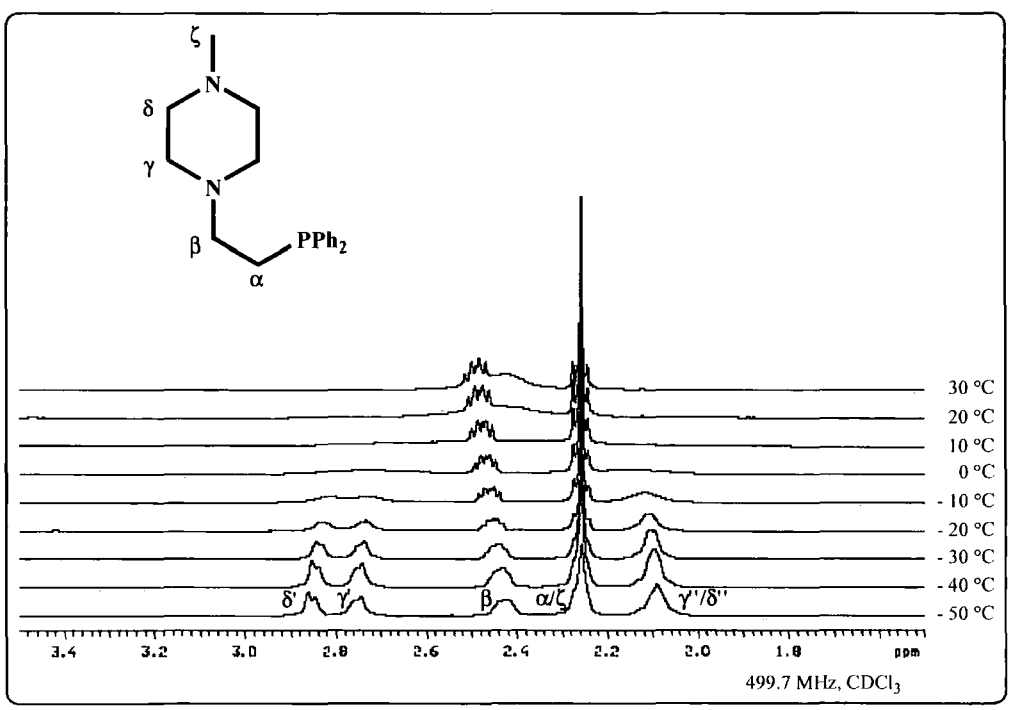

Figure 2.4: ^{1}H NMR spectroscopic data of **2.4-1** as a function of temperature (aromatic region omitted for clarity as no change observed)

Interestingly, the resonance attributed to the *N*-methyl group remained sharp on lowering the temperature of the sample. This is in agreement with previous low temperature NMR spectroscopic studies of *N*-methylpiperazine in which no broadening of this resonance was noted on lowering the temperature to – 90 °C in CD_2Cl_2.[19]

Unfortunately, reliable energy barriers for the inversion processes at the two nitrogen centres cannot be reported for **2.4-1** as there are a number of different dynamic processes occurring in solution. Moreover, due to the unsymmetrical substitution at the two nitrogens, the inversion barriers for these heteroatoms will differ. To unambiguously determine experimental values for these two processes is complex and would be misleading as it is difficult to differentiate these inversion processes from those associated with conformational changes of the ring.

In contrast to the ^1H NMR spectrum, the ^{13}C $\{^1H\}$ NMR spectrum of **2.4-1** was well-resolved at room temperature. The expected five aliphatic resonances were observed which correspond to the four methylene and the single methyl carbons. The α-bridge carbon was noted as a doublet resonance ($^1J_{CP}$ = 12.0 Hz) with this coupling constant being comparable to related species such as DPPE.[20] The aromatic region of the spectrum was as expected with coupling to phosphorus apparent in the phenyl ring carbons being consistent with expected values.[21]

Although **2.4-1** was isolated as a viscous oil, prolonged standing of a sample under a nitrogen atmosphere afforded crystals that were suitable for analysis by X-ray diffraction, the resulting molecular structure determination being shown in Figure 2.5.

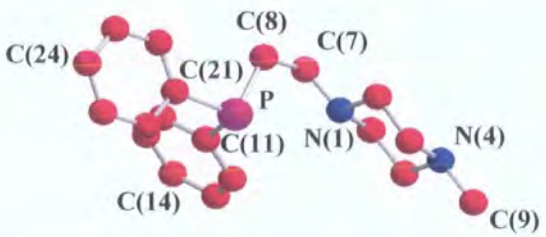

Figure 2.5: Ball and stick representation of the structure of **2.4-1***

	Bond Length/Å		**Bond Angle/°**
P–C(Ph)[a]	1.839(3)	C(2)–N(1)–C(6)	109.5(2)
P–C(8)	1.859(3)	C(3)–N(4)–C(5)	109.2(3)
N(1)–C(7)	1.469(4)	C(11)–P–C(21)	102.43(14)
N(1)–C(9)	1.465(4)	P–C(8)–C(7)–N(1)	42.5(3)
		$\Sigma_{\angle N(1)}$	334.6[a,b]
		$\Sigma_{\angle N(4)}$	330.7[a,b]
		$\Sigma_{\angle P}$	301.98[a,b]

[a]average; [b]angle summation, Individual e.s.d.'s in parentheses

Table 2.2: Selected bond distances (Å) and angles (°) for **2.4-1**

In the solid state, the piperazine ring adopts the least-energy chair conformation with both the substituents at nitrogen being equatorial. The internal ring angles are similar: C(2)–N(1)–C(6) = 109.5(2)° and C(3)–N(4)–C(5) = 109.2(3)° and consistent with related compounds.[22,23] A noticeable twist is evident in the P–C(8)–C(7)–N(1) bridge with the torsion angle for this fragment being 42.5°, giving rise to a *gauche* conformation with convergent P and N(1) lone pairs.

Both the N(1) and N(4) atoms show near-tetrahedral geometry as indicated by the summation of the angles of the substituents at these atoms ($\Sigma_{\angle N(1)}$ = 334.6° and $\Sigma_{\angle N(4)}$ = 330.7°) with only slight deviation from the ideal tetragonal angle (328.5°). The angles about P are noticeably narrowed ($\Sigma_{\angle P}$ = 302.0°). The two phenyl rings adopt a near-perpendicular arrangement with the intersection between the two phenyl planes being 98.0°.

* Molecular structure determination performed by Dr A. S. Batsanov

2.3.3 Characterisation of morpholine-*N*-ethylene-diphenylphosphine (2.4-2)

The synthesis of the PNO ligand **2.4-2** was performed using an identical methodology to that used for the synthesis of the PNN(Me) compound **2.4-1** as discussed previously, *i.e.* by reaction of equimolar quantities of vinyl phosphine (**2.3-1**) and morpholine.

The ^{1}H NMR spectrum of **2.4-2** obtained at 20 °C again demonstrated line broadening in the aliphatic region for the methylene ring protons (although this was not nearly as marked as that observed for the PNN(Me) variant **2.4-1**). Two broad resonances (each integrating to 4H) were observed at this temperature, which were observed to split into four 2H multiplets at lower temperatures and have been assigned to the individual sets of axial and equatorial γ- and δ-ring methylene protons (although definitive assignment of these proved impossible). Both sets of signals were noted to coalesce between – 10 and – 30 °C, Figure 2.6.

The resonances attributed to the α- and β-methylene protons in the ^{1}H NMR spectrum were well-resolved at 20 °C and changed little at lower temperatures. The aromatic region of the spectrum was as expected, with two multiplets (integrating to 4H and 6H) being observed which correspond to the *ortho*- and *meta*-/*para*-phenyl ring protons. No changes were noted in the aromatic region at lower temperatures.

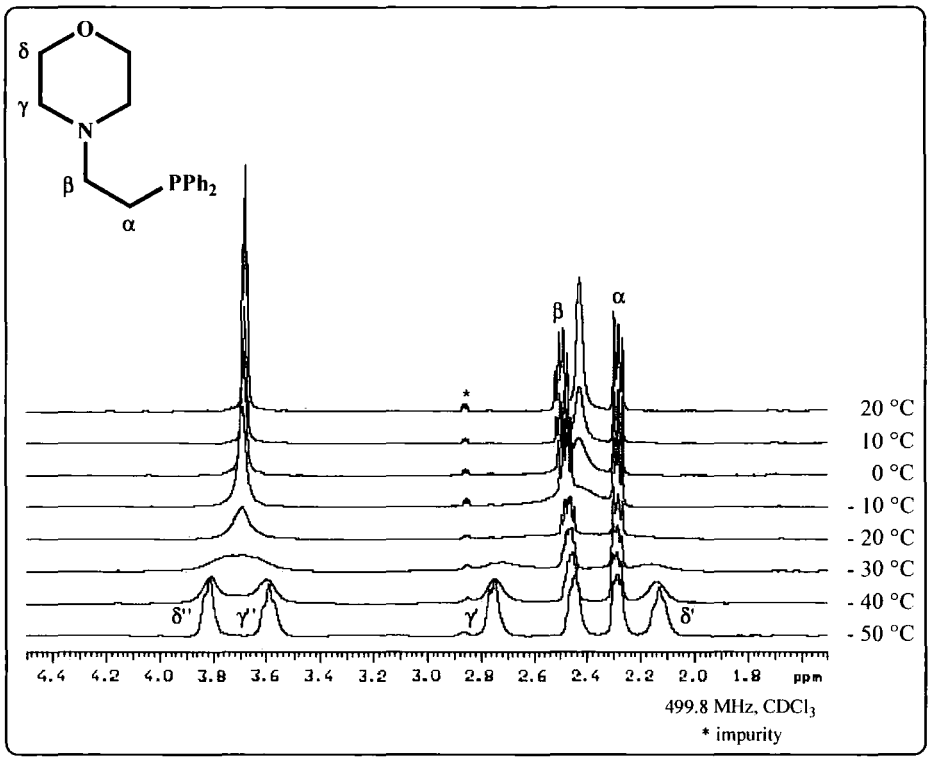

Figure 2.6: ^{1}H NMR spectroscopic data of **2.4-2** as a function of temperature (aromatic region omitted for clarity as no change observed)

It has been demonstrated that morpholine and substituted morpholines have a strong preference to exist in the chair conformation,[24,25] with hydrogen bonding between the oxygen and the adjacent methylene protons assisting the preference for this conformation.[26] However, it has been noted that this hydrogen bonding does not significantly affect the ring motion in morpholines as the free energy barriers for these inversion processes tend to be low, typically in the order of 6 kcal mol^{-1}.[27] Studies on tetrahydropyran have determined that the free energy barrier for inversion at oxygen ($\Delta G^{\ddagger}$ = 10.2 kcal mol^{-1}) is entirely consistent with the energy barriers noted for cyclohexane ($\Delta G^{\ddagger}$ = 10.1 kcal mol^{-1})[28] and piperidine ($\Delta G^{\ddagger}$ = 10.3 kcal mol^{-1})[19] with the incorporation of oxygen not significantly impacting upon the changes in conformation of the ring.[29] Indeed, these studies are consistent with the low temperature behaviour of **2.4-2** as the γ- and δ-ring methylene signals did not require low temperatures to bring the individual sets of peaks into resonance.

The ^{13}C {^{1}H} NMR spectrum of **2.4-2** was well-resolved at room temperature with the required four resonances being observed in the aliphatic region. Assignments of these signals were again made with the aid of low temperature ^{1}H–^{1}H COSY and ^{1}H–

^{13}C $\{^1H\}$ 2D NMR experiments. Coupling of both the α- and β-bridge carbons to phosphorus was observed with the coupling constants being of the expected magnitudes (C_α: $^1J_{CP}$ = 12.1 Hz; C_β: $^2J_{CP}$ = 23.0 Hz). The aromatic region was again as expected, with coupling to the ^{31}P nucleus being noted for all but the *para*-phenyl carbons.

2.3.4 Characterisation of thiomorpholine-*N*-ethylene-diphenylphosphine (2.4-3)

The synthesis of the PNS analogue mirrored that of the previously discussed PNN(Me) (**2.4-1**) and PNO (**2.4-2**) ligands, *i.e.* by reaction of thiomorpholine with 1.0 equivalents of diphenylvinylphosphine (**2.3-1**). In contrast to the syntheses of **2.4-1** and **2.4-2**, it proved essential to use a stoichiometric quantity of the amine relative to the phosphine as the removal of excess thiomorpholine was not a trivial procedure.

The ^1H NMR spectrum of **2.4-3** at 20 °C revealed the signals associated with the γ- and δ-ring protons to be two multiplets, with an overall integration of 8H. The resonances attributed to the α- and β-bridge protons were observed as two well-resolved multiplets, each integrating to 2H, at lower frequency relative to the ring protons. The assignment of these resonances was confirmed with the use of 2D ^1H–^1H COSY and ^1H–^{13}C $\{^1H\}$ HETCOR NMR experiments at room temperature.

It was surprising that the aliphatic region of the ^1H NMR spectrum of **2.4-3** was well-defined at room temperature as this was in direct contrast to the related PNN(Me) (**2.4-1**) and PNO (**2.4-2**) compounds discussed above. However, as the ring resonances in **2.4-3** were observed as two 4H multiplets, it is likely that rapid ring inversion is occurring, rendering these protons magnetically equivalent at room temperature. Consequently, the ^1H NMR spectrum of this compound was recorded at lower temperatures, Figure 2.7.

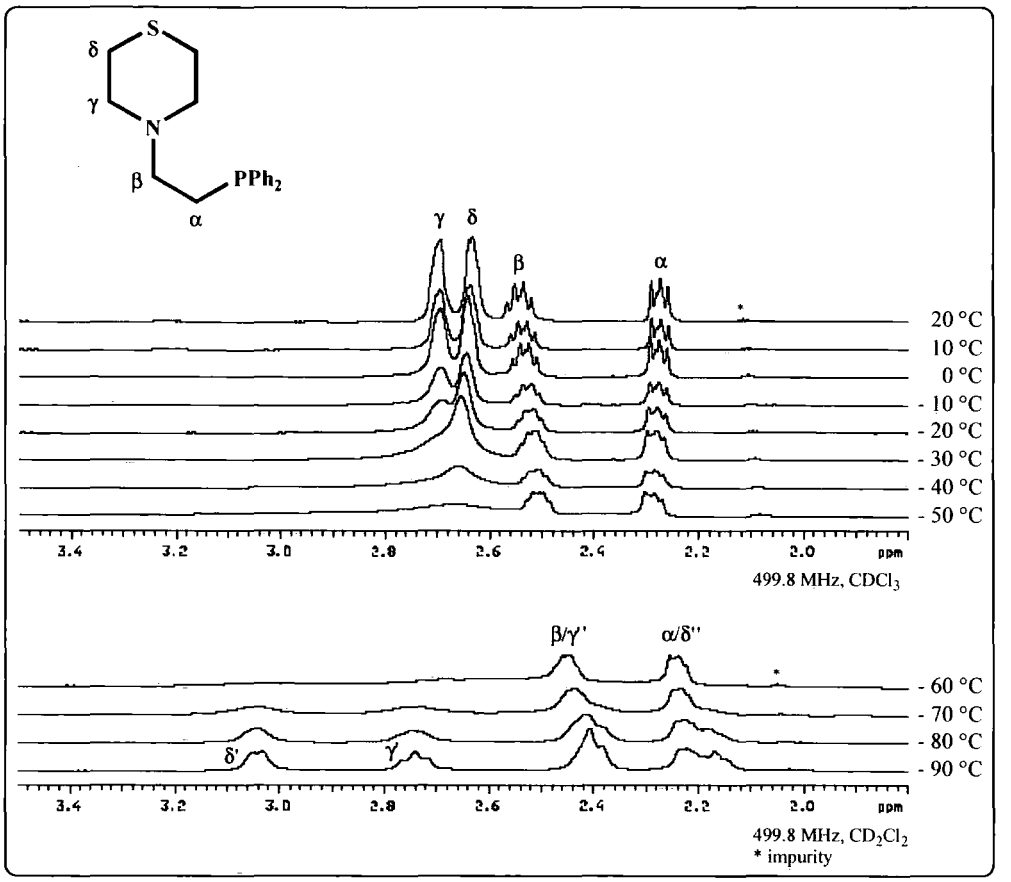

Figure 2.7: ^{1}H NMR spectra of **2.4-3** as a function of temperature (aromatic region omitted for clarity as no change observed)

On recording the ^{1}H NMR spectrum of **2.4-3** at low temperature, the resonances attributed to the sets of γ- and δ-ring protons started to broaden with the two resonances collapsing into a single broad signal at – 30 °C. Upon reaching the low temperature limit of $CDCl_3$ (– 50 °C), used initially in order to facilitate comparison with the spectra of **2.4-1** and **2.4-2**, the signals for the ring protons of **2.4-3** had yet to completely coalesce. Consequently, the solvent of this sample was changed to CD_2Cl_2, which allowed spectral acquisition to – 90 °C. At – 80 °C, the individual sets of ring protons started to come into resonance with their complete emergence being observed at – 90 °C. The resonances attributed to the α- and β-bridge carbons were coincident with those of the γ''- and δ''-ring protons. Definitive assignment of these signals was made by 2D ^{1}H–^{1}H COSY and ^{1}H–^{13}C {^{1}H} NMR experiments at – 90 °C. The aromatic regions of these spectra were as expected with multiplets integrating to 6H and 4H being observed

which corresponded to the phenyl protons in the *meta-/para-* and *ortho*-positions, respectively.

A coalescence temperature for the ring inversion processes cannot be determined for this system as, due to the similarity of the γ- and δ-ring protons in terms of chemical shift, these protons collapsed into a single broad resonance and therefore could not be differentiated.

The ^{13}C $\{^1H\}$ NMR spectrum of **2.4-3** at room temperature was as expected with four resonances evident in the aliphatic region. The α- and β-bridge carbon signals were observed as doublet resonances through coupling to the ^{31}P nucleus with their coupling constants being consistent with **2.4-1** and **2.4-3** (C_α: $^1J_{CP}$ = 12.4 Hz; C_β: $^2J_{CP}$ = 23.0 Hz). The γ- and δ-ring carbons were observed as singlet resonances although it is noteworthy that the signal associated with the δ-carbon was observed at significantly lower frequency than was observed in the related PNN(Me) (**2.4-1**) and PNO (**2.4-2**) compounds. At lower temperatures no appreciable change was noted in the ^{13}C $\{^1H\}$ NMR spectrum of **2.4-3**, although at – 90 °C the α-carbon was observed as a singlet. The aromatic region was again unremarkable with coupling to phosphorus being exhibited for all phenyl ring carbons except those in the *para-* position; no changes were noted at lower temperatures.

In contrast to the wealth of information in the literature regarding piperazines and morpholines (*vide supra*), there have been comparatively few studies on thiomorpholine and its derivatives. However, it has been shown that unsubstituted thiomorpholine adopts the least energy chair conformer with substituents at nitrogen tending to lie in the equatorial position.[30] It has been noted that the incorporation of a sulphur heteroatom into a saturated ring system has a profound effect on the ring geometry as a result of its larger nature (being a third-row element).[19] This 'splaying' of the ring angles appears to impact directly upon the dynamic motion of the ring in solution as the inversion barriers are clearly lower in thiomorpholino compounds than their related morpholine analogues, as demonstrated by the lower temperatures required to bring the individual ring protons into resonance for the former. It is somewhat surprising to note however that sulphur inversion barriers in thian *cyclo*-$\{S(CH_2CH_2)_2CH_2\}$ and dithian *cyclo*-$\{S(CH_2CH_2)_2S\}$ have been calculated as being 14.6 kcal mol^{-1},[31] and 10.3 kcal mol^{-1},[32] respectively, although it is indicated by these

values that the placement of a second heteroatom in a cyclic thioether appears to lower the energy barrier for ring inversion.

2.3.5 Characterisation of piperidine-*N*-ethylene-diphenylphosphine (2.4-4)

The synthesis of the piperidine-*N*-ethylene-diphenylphosphine (**2.4-4**) mirrored that of the previously synthesised diphenylphosphines with stoichiometric quantities of piperidine and diphenylvinylphosphine (**2.3-1**) again being employed. As was the case for compounds **2.4-1** – **2.4-3**, the piperidine-based derivative **2.4-4** was noted to exhibit dynamic behaviour in solution and thus NMR analyses were performed at low temperature, Figure 2.8.

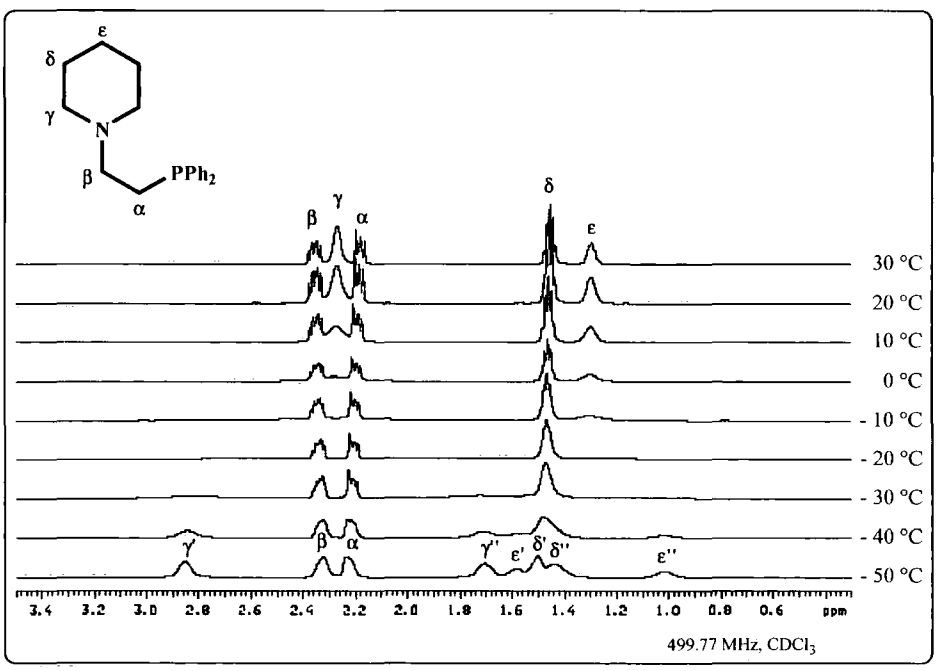

Figure 2.8: ^{1}H NMR spectra of compound **2.4-4** as a function of temperature (aromatic region omitted for clarity as no noticeable change)

Analysis of compound **2.4-4** by ^{1}H NMR spectroscopy at room temperature produced some interesting results; unlike the previously discussed compounds **2.4-1**, **2.4-2** and **2.4-3**, the resonance attributed to the δ-methylene protons in **2.4-4** was well-defined with only the signals associated with the γ- and ε-protons being broadened at

room temperature, Figure 2.8. On lowering the temperature, the resonance corresponding to the γ-ring protons was observed to coalesce at 0 °C. At – 50 °C, two resonances, each integrating to 2H, corresponding to the axial and equatorial γ-methylene ring protons were observed. The behaviour of the ε-CH_2 proton resonance was similar with the coalescence temperature for this resonance being noted to occur at – 20 °C, while at – 50 °C, two signals were observed, each with integration of 1H, again consistent with the diastereotopic nature of these protons. The resonance attributed to the δ-methylene ring protons was observed to split into two individual signals at – 50 °C, although this signal was not observed to coalesce. This is consistent with other previous observations made for piperidine itself, which is noted to adopt a frozen chair conformation at – 63 °C (CD_3OD) with an inversion barrier of 10.4 kcal mol^{-1}.[19] Little change was noted in the resonances attributed to the α- and β-protons or the aromatic region of the spectrum with decreasing temperature.

The ^{13}C {^1H} NMR spectrum of **2.4-4** displayed three singlet resonances in the aliphatic region corresponding to the piperidine ring carbons and the aromatic region as expected with coupling of the four phenyl resonances to the ^{31}P nucleus being noted in all but the *para*-ring carbons. The signals associated with the α- and β-bridge carbons were both observed as doublet resonances, again due to coupling to phosphorus (C_α: $^1J_{CP}$ = 11.9 Hz; C_β: $^2J_{CP}$ = 23.9 Hz).

2.3.6 Preparation of *N*-phenylpiperazine-*N'*-ethylene-diphenylphosphine (2.4-5)

The *N*-phenylpiperazine-*N'*-ethylene-diphenylphosphine compound (**2.4-5**) was synthesised using an identical methodology to that previously detailed, *i.e.* by reaction of equimolar quantities of *N*-phenylpiperazine and diphenylvinylphosphine (**2.3-1**) in accordance with Scheme 2.6. In contrast to compounds **2.4-1** – **2.4-4**, **2.4-5** was afforded as an orange waxy solid following repeated freeze-thaw drying cycles *in vacuo*.

The ^1H NMR spectrum of **2.4-5** was well-defined at room temperature with the resonances attributed to the piperazine γ- and δ-ring protons being observed as two 4H pseudo triplets with a vicinal coupling constant of 4.8 Hz. The two sets of α- and β-

methylene bridge protons were observed as multiplets, each integrating to 2H, Figure 2.9.

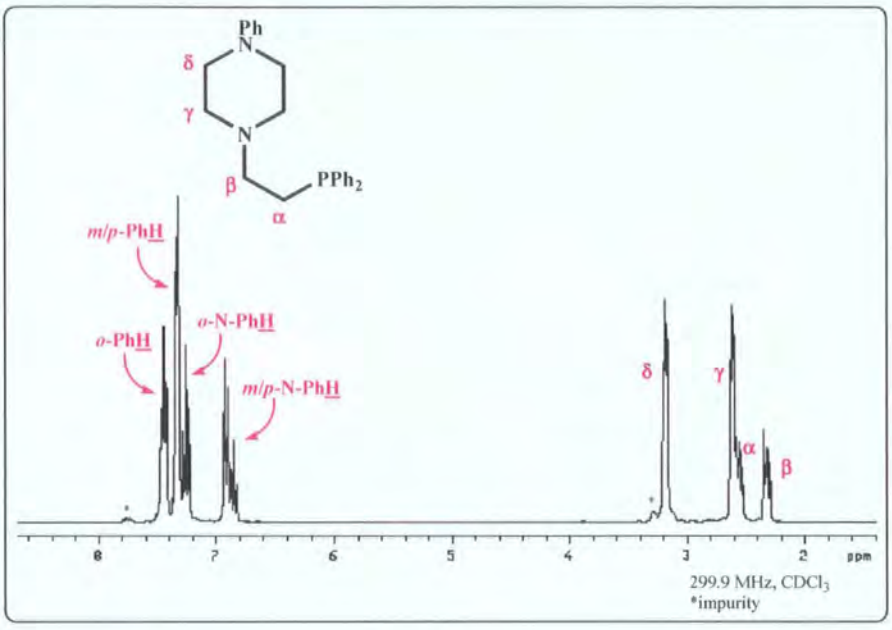

Figure 2.9: ^{1}H NMR spectrum of compound **2.4-5** at 20 °C

The introduction of a phenyl group at nitrogen is found to have a profound effect on the dynamic behaviour of the piperazine ring in solution, as no broad resonances were observed in the ^{1}H NMR spectrum of **2.4-5** at 20 °C. Indeed, aromatic rings located at the heterocyclic nitrogen of saturated *N*-containing heterocyclic rings are known to exhibit a strong preference to lie in the equatorial position,[33] inducing the ring to adopt the least-energy chair conformation.[34] The equatorial placement of the aromatic substituent is favoured purely on steric grounds as 1,3-steric interactions between the adjacent methylene protons of the piperazine ring and the *ortho*-phenyl protons strongly disfavour the alternative axial conformer as has been demonstrated in *N*-phenylpiperazine.[35] Moreover, as the aromatic substituent is adjacent to nitrogen, a heteroatom with a lone pair, there is the possibility of mesomeric delocalisation of this lone pair into the phenyl ring although this process is disfavoured as donation of the lone pair into the ring exacerbates this 'steric clash' as a result of planarisation of the heterocyclic nitrogen. Whilst the conformationally-flexible nature of piperazine allows for twisting of the saturated ring to minimise these 'steric clashes', deviation of the ring from the molecular plane reduces the effectiveness of the orbital overlap between the nitrogen lone pair and the π-electron framework of the aromatic ring.[36]

In contrast to **2.4-1** {PNN(Me)}, where inversion was presumed to occur at both nitrogens, the presence of a phenyl substituent at one heterocyclic amine in **2.4-5** {PNN(Ph)} exerts a 'locking effect', inhibiting inversion processes at this nitrogen. As the saturated ring resonances associated with the γ- and δ-ring protons were observed as two multiplets (rather than four individual signals which would signify a 'frozen' ring conformation), it is believed that inversion of the tertiary aliphatic nitrogen is still occurring in this compound at room temperature. While few studies have been performed on the nature of ring inversion in *N*-phenylpiperazine and its derivatives, high ring inversion barriers have been reported for *N*-phenylpiperidine (72 kcal mol^{-1}),[26] a value that is significantly larger than ring inversion barriers for piperazine (10.3 kcal mol^{-1})[19] and *N*-methylpiperazine (11.9 kcal mol^{-1}).[19]

The aromatic region of the ^{13}C {^{1}H} NMR spectrum of **2.4-5** was noticeably complicated by the presence of a third phenyl substituent, however unambiguous assignment of these resonances was made with the aid of ^{1}H–^{13}C {^{1}H} HETCOR and ^{1}H–^{13}C {^{1}H} HMBC 2D NMR experiments. While the *N*-phenyl resonances were observed as singlet resonances, the signals arising from the phosphorus-bound phenyl substituents all showed coupling to the ^{31}P nucleus. The resonances attributed to the γ- and δ-ring carbons were observed as two singlets, whereas the α- and β-bridge carbon signals both showed coupling to phosphorus with the one-bond coupling to C_α (23.1 Hz) being markedly larger than that to C_β (12.1 Hz).

2.3.7 Preparation of piperazine-*N*,*N'*-diethyltetraphenyldiphosphine (2.4-7)

Following the successful synthesis of the PNE compounds (**2.4-1** – **2.4-5**) with a variety of E donor atoms, it was desirable to extend this synthetic methodology to create a symmetrical, potentially tetradentate PNNP species comprising a piperazine core unit. The synthesis of the target PNNP species (**2.4-7**) again employed the base-promoted vinyl addition methodology described above, by reaction of two equivalents of diphenylvinylphosphine (**2.3-1**) to one equivalent of piperazine in accordance with Scheme 2.7.

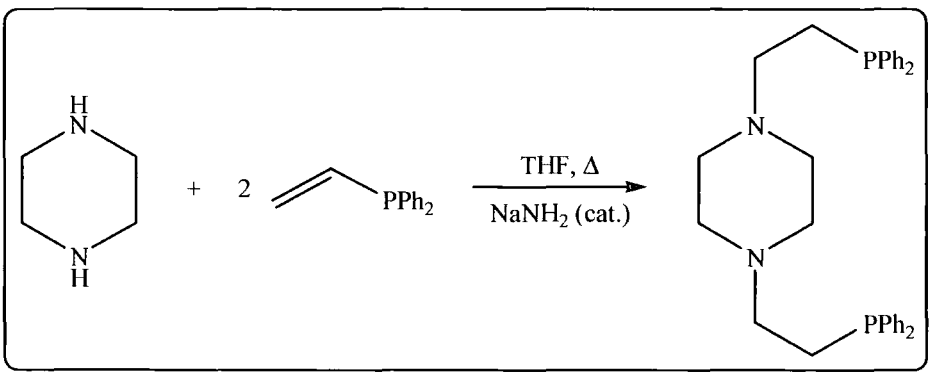

	$^{31}P\{^{1}H\}$ NMR* δ_P
2.4-7	– 19.1 (s)

*161.9 MHz, $CDCl_3$, – 50 °C

Scheme 2.7: Synthesis and $^{31}P\{^{1}H\}$ NMR spectroscopic data of PNNP (**2.4-7**)

Following an analogous work-up to that detailed in previous sections, **2.4-7** was obtained as a beige-coloured waxy solid in good yield (77 %). The product exhibited a sharp singlet by $^{31}P\{^{1}H\}$ NMR spectroscopy and satisfactory mass spectrometric data {*m/z* = 511.1 $[MH]^+$}. Due to the waxy nature of this species, purification was attempted by recrystallisation from a variety of solvents, but this was found not to be successful.

As with the compounds **2.4-1** – **2.4-4**, the ^{1}H NMR spectrum of **2.4-7** was severely broadened at room temperature and thus NMR spectra were recorded at low temperature, Figure 2.10. Due to its high degree of symmetry, the ^{1}H NMR spectrum of **2.4-7** was significantly simplified at – 50 °C with the signals attributed to the α/α′- and β/β′-methylene bridge protons being observed as multiplet resonances, each integrating to 4H. The axial and equatorial ring protons (γ/γ′) were observed as two 4H doublets with geminal coupling of 7.8 Hz, consistent with two-bond coupling in a heterocyclic ring.[37] The appearance of separate axial and equatorial resonances is indicative of 'freezing out' of the least energy chair conformation at low temperature.[38]

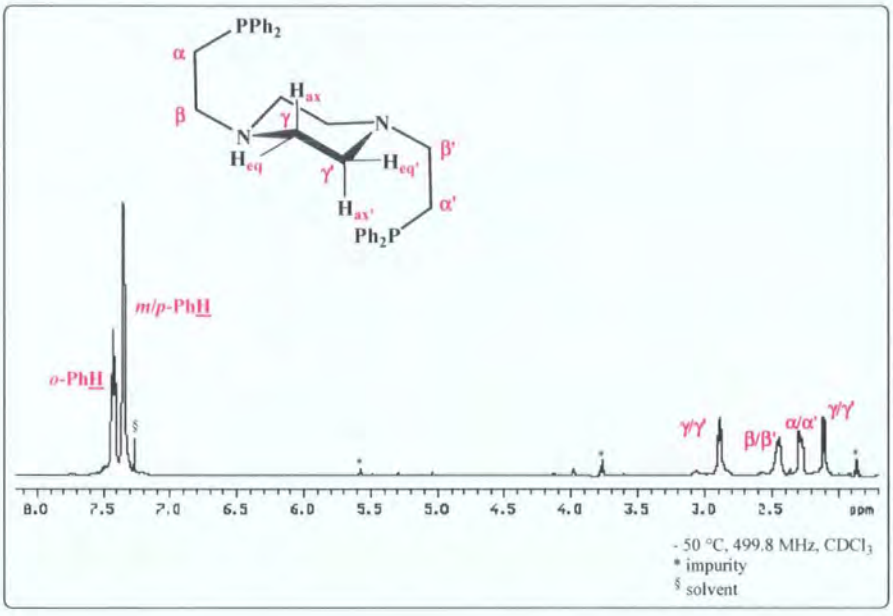

Figure 2.10: ^{1}H NMR spectrum of PNNP (**2.4-7**) at – 50 °C

The ^{13}C {^{1}H} NMR spectrum of **2.4-7** was also simplified by the symmetrically-substituted nature of this compound with three resonances being exhibited in the aliphatic region. The signal associated with the α/α′-carbons was observed as a doublet resonance as a result of one-bond coupling to the ^{31}P nucleus ($^{1}J_{CP}$ = 10.6 Hz), however the signal attributed to the β/β′-carbons showed a larger coupling to phosphorus ($^{2}J_{CP}$ = 24.4 Hz). The expected singlet resonance was observed for each of the γ/γ′-carbons. The aromatic region of the spectrum was reminiscent of the mono-substituted compounds **2.4-1** – **2.4-5** with coupling to phosphorus being noted for all but the *para*-phenyl carbon atoms.

2.4 Synthesis of HCl derivatives of PNE systems

Due to the fluxional nature of some of the PNE species in solution (**2.4-1** – **2.4-4** and **2.4-7**), the characterisation of the species by multinuclear NMR spectroscopy proved challenging and low temperature studies were invoked in order to definitively confirm their proposed structures. Consequently an alternative, complementary method of characterisation was sought that would circumvent the need for these low temperature studies.

As previously discussed, the inversion processes at heteroatoms in saturated heterocyclic ring systems, combined with associated ring inversion, results in the magnetic equivalence of the ring methylene groups, which, depending on the rate of inversion relative to the NMR time-scale, can lead to broadening of the observed resonances. It has been noted that the coordination of the nitrogen lone pair with a Lewis acid (such as borane)[38] or by protonation[39] hinders these inversion processes and favours the adoption of a static structure with the least favoured conformer being assumed.[38] Thus inhibition of the ring inversion has the effect of differentiating the faces of the heterocycle hence breaking one of the planes of symmetry through this ring. This therefore allows the individual ring resonances to be observed at room temperature in both the ^{1}H and ^{13}C $\{^{1}H\}$ NMR spectra of the compound in question.[40] Thus the synthesis of the hydrochloride salts of the PNE ligands **2.4-1** – **2.4-4** and **2.4-7** were undertaken.

The synthesis of the HCl derivatives all proceeded according to an identical methodology; anhydrous HCl gas was bubbled through an ethereal solution of the required compound under a nitrogen atmosphere. This reaction resulted in the immediate precipitation of pale yellow-white solids, which were collected by filtration and dried under vacuum. The salts obtained were all purified by recrystallisation from chloroform/diethyl ether.

2.4.1 Preparation of *N*-methylpiperazine-*N'*-ethylene-diphenylphosphine dihydrochloride (2.5-1)

Using the procedure detailed above, the diamine hydrogen chloride salt **2.5-1** was prepared and isolated as a white crystalline solid after recrystallisation in excellent yield (95 %). Elemental analyses confirmed the formation of the doubly protonated species. Two broad signals corresponding to these ammonium protons were observed in the ^{1}H NMR spectrum of **2.5-1**, the assignment of which was confirmed with the use of 2D NMR experiments. Interestingly, these two resonances were noticeably broadened to different extents $\{\nu_{½} = N(H^{+})NP = 34.4$ Hz; $NN(H^{+})P = 46.9$ Hz$\}$, something that is presumed to reflect their location in different environments. The ^{31}P $[^{1}H]$ NMR

spectrum of **2.5-1**, in which a singlet resonance was observed {$\delta_{P\{1H\}} = -20.0$ (s)}, is consistent with the fact that protonation of the phosphine fragment had not occurred.

It has been noted that useful comparisons may be made between the $^{1}H/^{13}C$ $\{^{1}H\}$ NMR spectra of saturated heterocyclic rings at low temperature and their corresponding hydrochloride salts.[41] This comparison has the potential to assist the characterisation of the parent compound through contrasting the low temperature spectrum of the parent amine and the room temperature spectrum of the corresponding ammonium salt. Comparisons of the NMR spectroscopic data for compounds **2.4-1** (PNN) and **2.5-1** (PNN.2HCl) is shown below in Table 2.3.

	^{1}H NMR* δ_H		^{13}C $\{^{1}H\}$ NMR§ δ_C	
	2.4-1 (– 50 °C)	**2.5-1** (20 °C)	**2.4-1** (– 50 °C)	**2.5-1** (20 °C)
α	2.82[b]	2.63[b]	24.9 (d) (12.1 Hz)	27.7 (d) (17.7 Hz)
β	2.72[b]	3.12[b]	54.3 (s)	55.1 (s)
γ	2.07/2.41[b]	3.54/4.04[b]	54.1 (s)	48.3 (s)
δ	2.23[a,b]	3.85/3.62[b]	52.0 (s)	50.0 (s)
ζ	2.23[a] (s)	2.89 (s)	45.1 (s)	43.2 (s)

*499.8 MHz, $CDCl_3$; §125.7 MHz, $CDCl_3$; [a]overlap of signals; [b]multiplet resonances

Table 2.3: Selected ^{1}H and ^{13}C $\{^{1}H\}$ NMR spectroscopic data for **2.4-1** and **2.5-1**

The ^{1}H NMR spectrum of **2.5-1** compared favourably with the low temperature spectra of **2.4-1** thus confirming the assignment of the resonances for the γ- and δ-ring protons (by comparison of the relevant 2D NMR spectra). The aliphatic ring resonances of **2.5-1** were well-resolved at room temperature, which facilitated their assignment although a marked shift to higher frequency was noted for all of these resonances in comparison to those of the parent compound **2.4-1**. Moreover, a shift to higher frequency was noted for the β-methylene bridge protons, which is in contrast to that observed for the protons attributed to those in the α-position, as these were noted to exhibit a slight shift to lower frequency. The aromatic region of the spectra remained unchanged by protonation and resembled that of the diamine **2.4-1**.

The ^{13}C $\{^{1}H\}$ NMR spectrum of **2.5-1** strongly resembled that of the parent diamine **2.4-1**. In accordance with previous observations on related systems, all

aliphatic resonances, except the α-bridge carbon, displayed shifts to lower frequency with the resonance demonstrating the largest shift being that of the γ-carbon.[40] It is noteworthy that a significant increase in the $^{1}J_{CP}$ coupling constant for the α-carbon of **2.5-1** was observed relative to the diamine **2.4-1**, which is presumably due to more favourable orbital overlap in the static conformer. The aromatic region of this spectrum was again unremarkable and resembled that of **2.4-1**.

2.4.2 Preparation of morpholine-*N*-ethylene-diphenylphosphine hydrochloride (2.5-2)

The morpholine-*N*-ethylene-diphenylphosphine hydrochloride salt **2.5-2** was again synthesised by reaction of the parent phosphine **2.4-2** with excess gaseous HCl in diethyl ether. Following recrystallisation, the product was obtained in excellent yield (91 %) as a white crystalline solid. The ^{1}H NMR spectrum of the product exhibited a broad singlet resonance ($\nu_{½}$ = 25.2 Hz), integrating to 1H, which was shown by a combination of ^{31}P [^{1}H] {δ_P = – 19.6 (s)} and 2D nOesy NMR experiments to correspond to protonation at nitrogen. The NMR spectra of the PNO.HCl salt **2.5-2** was again compared with that of the parent amine **2.4-2**, Table 2.4.

	^{1}H NMR* δ_H		^{13}C {^{1}H} NMR§ δ_C	
	2.4-2 (– 50 °C)	**2.5-2** (20 °C)	**2.4-2** (– 50 °C)	**2.5-2** (20 °C)
α	2.30	2.67	24.5 (d) (12.0 Hz)	22.1 (d) (16.5 Hz)
β	2.44	2.99	54.4 (d) (23.0 Hz)	55.7 (d) (28.7 Hz)
γ	2.77/3.59	2.78/3.41	52.3	51.9
δ	2.13/3.83	3.90/4.23	65.8	63.7

*499.8 MHz, $CDCl_3$; §125.7 MHz, $CDCl_3$

Table 2.4: Selected ^{1}H and ^{13}C{^{1}H} NMR spectroscopic data for **2.4-2** and **2.5-2**

The ^{1}H NMR spectrum of **2.5-2** closely resembled the low temperature spectrum of **2.4-2** as the expected six aliphatic resonances were observed. Further comparisons between the data for **2.4-2** and **2.5-2** revealed a shift to higher frequency for the α- and

β-methylene bridge protons along with similar shifts being observed for the H_δ ring protons in **2.5-2**. Comparatively little shift was observed in the resonances associated with the H_γ ring protons, which appeared at approximately the same shifts as in the parent compound **2.4-2**. No appreciable differences were observed between the two spectra in the aromatic regions.

In the $^{13}C\{^1H\}$ NMR spectrum, the resonances attributed to the C_α-bridge carbon and the γ- and δ-ring carbons of **2.5-2** were observed to come into resonance at lower frequency than the signals observed for the parent compound **2.4-2**. The only exception to this is the β-ring carbon, which exhibits a higher frequency shift relative to the corresponding resonance in **2.4-2**. As was noted previously for compound **2.5-1**, the α- and β-bridge carbons exhibit greater couplings to the ^{31}P nucleus in **2.5-2** than were observed in the parent amine (**2.4-2**). The aromatic region of the spectrum for **2.5-2** showed no notable differences to that of **2.4-2**.

Slow diffusion of diethyl ether into a chloroform solution of **2.5-2** afforded colourless, block-shaped crystals that were suitable for analysis by single crystal X-ray diffraction, Figure 2.11.

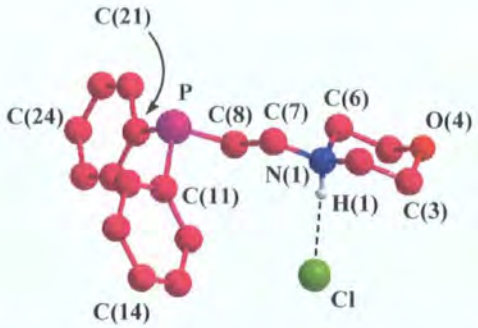

Figure 2.11: Ball and stick representation of PNO.HCl (**2.5-2**)[†]

	Bond Length/Å		**Bond Angle/°**
P–C(8)	1.8540(11)	C(11)–P–C(21)	102.64(5)
N(1)–C(7)	1.5006(13)	C(2)–N(1)–C(6)	109.27(8)
N(1)–H(1)	0.869(15)	C(3)–O(4)–C(5)	109.37(12)
C(Ph)–P	1.8325[a]	N(1)–H(1)–Cl	176.4(13)
Cl–H(1)	3.0294(10)	P–C(8)–C(7)–N(1)	173.4[a]
		$\Sigma_{\angle N(1)}$	333.29[a,b]
		$\Sigma_{\angle P}$	304.19[a,b]

[a]average; [b]angle summation

[†] Molecular structure determination performed by Dr A. S. Batsanov

Table 2.5: Selected bond lengths (Å) and angles (°) for **2.5-2**

The molecular structure of **2.5-2** demonstrates that the morpholine fragment adopts the expected chair conformation in the solid state with internal ring angles {C(2)–N(1)–C(6): 109.27(8)° and C(3)–O(4)–C(5): 109.37(12)°} consistent with literature values.[42,43] The sum of the angles about N(1) ($\Sigma_{\angle N(1)} = 333.29°$) are indicative of a near-tetrahedral geometry about this atom with a slight broadening from the ideal value of 327.9° evident, which is a direct result of the presence of the proton at the nitrogen as a bonding pair of electrons occupies less geometrical space than a lone pair. A short N(1)–H(1) bond {0.869(15) Å} was observed with the interaction between H(1) and Cl atoms being {3.0294(10) Å}. The coordinated electron pair of N(1) and the phosphorus lone pair adopt a pseudo-*anti* conformation with the P–C(8)–C(7)–N(1) torsion angle being 173.4°. The phenyl groups at phosphorus show a near-perpendicular arrangement, with a value of 84.75° between the mean planes.

2.4.3 Attempted preparation of thiomorpholine-*N*-ethylene-diphenylphosphine hydrochloride (2.5-3)

The preparation of the thiomorpholine-*N*-ethylene-diphenyl-phosphine hydrochloride derivative **2.5-3** was attempted according to the previously discussed methodology, *i.e.* by reaction of the parent amine (**2.4-3**) with excess anhydrous HCl. Although the formation of a light-coloured precipitate was observed, this solid was subsequently shown by NMR spectroscopy and mass spectrometry not to be the target product as only a number of unassignable resonances were obtained. It is interesting to note, however, that no trace of the parent amine was observed in this mixture.

It is surprising that the synthesis of **2.5-3** was unsuccessful given the facile near-quantitative formation of the HCl derivatives of the related compounds **2.5-1** and **2.5-2**. Indeed, successful, high yielding preparations for the synthesis of related substituted thiomorpholine.HCl salts are detailed in the literature using the exact same synthetic methodology as that detailed here.[44] The reasons for the failure of the reaction remain unclear.

2.4.4 Preparation of piperidine-*N*-ethylene-diphenylphosphine hydrochloride (2.5-4)

The piperidine-*N*-ethylene-diphenyl-phosphine hydrochloride derivative **2.5-4** was synthesised according to the previously detailed methodology, *i.e.* by reaction of the parent amine **2.4-4** with excess anhydrous HCl. Following recrystallisation, the target product was obtained in excellent yield (93 %) as a white crystalline solid, with analyses by mass spectrometry and CHN confirming the proposed formulation. The ^{1}H NMR spectrum of **2.5-4** demonstrated the presence of a broad singlet ($\nu_{½}$ = 23.0 Hz), integrating to 1H which was shown, by the use of 2D NMR experiments, to correspond to the ammonium proton. Furthermore, the ^{31}P [^{1}H] NMR spectrum of the product demonstrated that protonation at phosphorus had not occurred {$\delta_{P[1H]}$ = – 19.4 (s)}. The aliphatic regions of the ^{1}H and ^{13}C {^{1}H} NMR spectra of **2.5-5** were compared with the low temperature spectra of the parent amine **2.4-4**, Table 2.6.

	^{1}H NMR* δ_H		^{13}C {^{1}H} NMR§ δ_C	
	2.4-4 (– 50 °C)	**2.5-4** (20 °C)	**2.4-4** (– 50 °C)	**2.5-4** (20 °C)
α	2.33	2.64	25.9 (d) (11.9 Hz)	22.4 (d) (12.1 Hz)
β	2.42	2.89	56.1 (d) (23.9 Hz)	55.0 (d) (27.3 Hz)
γ	1.80/2.95	2.54/3.38	54.5 (s)	53.1
δ	1.53/1.60	1.72/2.11[a]	26.1 (s)	22.8
ε	1.12/1.67	1.29/1.67[a]	24.6 (s)	22.2

*499.7 MHz, $CDCl_3$; §125.7 MHz, $CDCl_3$; [a]overlapping resonances

Table 2.6: Selected ^{1}H and ^{13}C {^{1}H} NMR spectroscopic data for **2.4-4** and **2.5-4**

Comparison of the low temperature ^{1}H NMR spectrum of **2.4-4** with that at room temperature of **2.5-4** revealed the two to be very similar. The α-bridge protons of **2.5-4** were observed to shift to higher frequency relative to those observed in **2.4-4**, whereas a shift to lower frequency was observed for the protons in the β-position of **2.5-4** in comparison to those of the parent amine. Surprisingly, the resonances attributed to the γ- and δ-ring protons of **2.5-4** were observed at higher frequency than those of **2.4-4**, with significant differences in chemical shift being noted for all four signals. By

comparison, the resonances associated with the ε-protons of **2.5-4** were shown to be similar in terms of chemical shift to those of **2.4-4**.

The ^{13}C {^{1}H} NMR spectrum of **2.5-4** was shown to be largely comparable with that of **2.4-4**. As expected, the α- and β-bridge carbons of **2.5-4** were both observed as doublet resonances, with the coupling constant exhibited by C_β ($^{2}J_{CP}$ = 27.3 Hz) being the larger of the two. Few differences were noted in the remaining aliphatic resonances and the aromatic regions of the two spectra were near-identical and unremarkable.

2.4.5 Preparation of piperazine-*N*,*N*′-diethylene-tetraphenyldiphosphine dihydrochloride (2.5-6)

The PNNP dihydrochloride salt (**2.5-6**) was obtained as an off-white coloured crystalline powder in good yield (88 %). Purification of **2.5-6** by recrystallisation using a number of solvent combinations was attempted with little success, with this compound (in contrast to **2.5-1**, **2.5-2** and **2.4-4**) showing very limited solubility in polar and/or chlorinated solvents. Unfortunately the poor solubility of **2.5-6** limited extensive analysis of the product by NMR spectroscopy as the dilute $CDCl_3/CD_2Cl_2$ solutions of **2.5-6** did not give reliable 2D NMR spectra. Attempts were made to grow single crystals for X-ray crystallographic studies, but despite repeated attempts, suitable crystals could not be obtained.

	^{1}H NMR δ_H		^{13}C {^{1}H} NMR[§] δ_C	
	2.4-7* (– 50 °C)	**2.5-6**✧ (20 °C)	**2.4-7** (– 50 °C)	**2.5-6** (20 °C)
α	2.29	3.09	25.8 (10.6 Hz)	23.0 (17.3 Hz)
β	2.46	3.55	55.3 (24.4 Hz)	55.0 (28.4 Hz)
γ′	2.11	2.63	53.1	48.7
γ″	2.90	3.83	-	-

*499.8 MHz, $CDCl_3$; ✧299.9 MHz, $CDCl_3$; §125.7 MHz, $CDCl_3$

Table 2.7: Selected ^{1}H and ^{13}C {^{1}H} NMR spectroscopic data for **2.4-7** and **2.5-6**

The ^{31}P [^{1}H] NMR spectrum of **2.5-6** was noticeably broadened (δ_P = – 19.9,

br s, $\nu_{½}$ = 20.9 Hz), in contrast to the parent diphosphine **2.4-7** which afforded a sharp singlet resonance. No change in the appearance of the signal for **2.5-6** was observed on lowering the temperature to – 20 °C. Unfortunately, the poor solubility of **2.5-6** precluded studies at lower temperatures as the compound precipitated from solution. Satisfactory analysis of **2.5-6** by mass spectrometry was obtained {*m/z* = 511.3 $[MH–2HCl]^+$}.

The ^1H NMR spectrum of **2.5-6** revealed a shift to higher frequency of all aliphatic proton resonances relative to the free diamine **2.4-7**. In accordance with the symmetrical nature of the piperazine ring, four resonances were noted, which correspond to the α- and β-methylene bridge and the γ'- and γ''-methylene ring protons. A broad singlet resonance corresponding to the ammonium protons was observed for **2.5-6**, but at a noticeably lower frequency {δ_H = 7.77 (br s, $\nu_{½}$ = 29.4 Hz)} than recorded for the previously synthesised hydrochloride salts. It is interesting to note that the resonances attributed to the phenyl substituents of **2.5-6** were not observed as individual multiplets corresponding to protons at the *meta-/para-* and *ortho*-ring positions, but appeared as overlapping resonances with an overall integration of 20H.

The ^{13}C {^1H} NMR spectrum of **2.5-6** strongly resembled that of the parent compound **2.4-7** as only three aliphatic resonances were observed. A slight shift to lower frequency of the γ-carbon for **2.5-6** relative to **2.4-7** was noted, along with a slight increase in the magnitude of the coupling to phosphorus of the α- and β-carbon resonances. The aromatic region of the spectrum was comparable to that observed for **2.4-7**.

2.5 Preparation and characterisation of PNE sulphide derivatives

Whilst the successful synthesis of a selection of PNE ligands has been demonstrated in the above sections, the oily nature of the majority of these phosphines (**2.4-1** – **2.4-4**) precluded the acquisition of satisfactory CHN analysis and hence an assessment of their purity. Whilst PNN(Me) (**2.4-1**) was found to crystallise over an extended period of time, disappointingly the morpholine (**2.4-2**), thiomorpholine (**2.4-3**) and piperidine (**2.4-4**) derivatives remained as viscous liquids. In order to obtain more easily purified, air stable, solid products, the corresponding phosphine sulphides were prepared.

The synthesis of the phosphine sulphides **2.6-1** – **2.6-4** was identical in each case; a solution of the required PNE compound in CH_2Cl_2 was stirred at room temperature with *ca.* one equivalent of elemental sulphur until *in situ* analysis by ^{31}P NMR spectroscopy indicated complete conversion to the desired product, Scheme 2.8. Following removal of the solvent under vacuum, the resulting products were purified by recrystallisation from CH_2Cl_2/hexane.

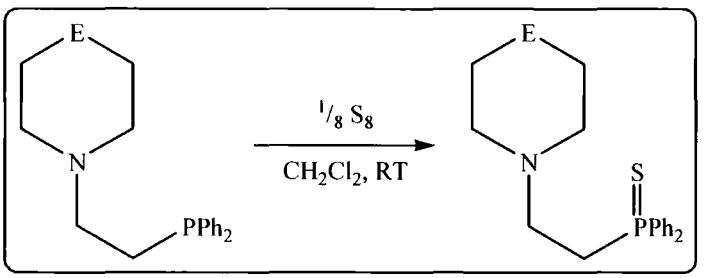

Scheme 2.8: Synthesis of phosphine sulphide derivative of PNE ligands

E =		Yield	MS $(ES^+)^{\diamond}$ *m/z*	$^{31}P\{^1H\}$ NMR δ_P	
				Phosphine sulphide*	Parent ligand§
NMe	**2.6-1**	84 %	345.2	+ 41.4 (s)	– 19.1 (s)
O	**2.6-2**	81 %	332.2	+ 41.5 (s)	– 18.2 (s)
S	**2.6-3**	82 %	348.1	+ 41.6 (s)	– 18.3 (s)
CH_2	**2.6-4**	79 %	330.1	+ 41.5 (s)	– 17.8 (s)

*202.3 MHz, $CDCl_3$; § 161.9 MHz, $CDCl_3$; $^{\diamond}[MH]^+$

Table 2.8: Synthesis, mass spectrometric and $^{31}P\{^1H\}$ NMR spectroscopic data for **2.6-1** – **2.6-4**

All of the resulting sulphides **2.6-1** – **2.6-4** gave a single resonance by $^{31}P\{^1H\}$ NMR spectroscopy, which was shifted to higher frequency relative to that of the parent phosphines, in accordance with the change in oxidation state of phosphorus {from P(III) to P(V)}. In each case, satisfactory mass spectrometric and CHN analyses were obtained. Severely broadened ^1H NMR spectra were obtained for the compounds **2.6-1**, **2.6-2** and **2.6-4**, with the obtained spectra closely resembling those of their parent phosphines. A representative spectrum for **2.6-1** is shown in Figure 2.12.

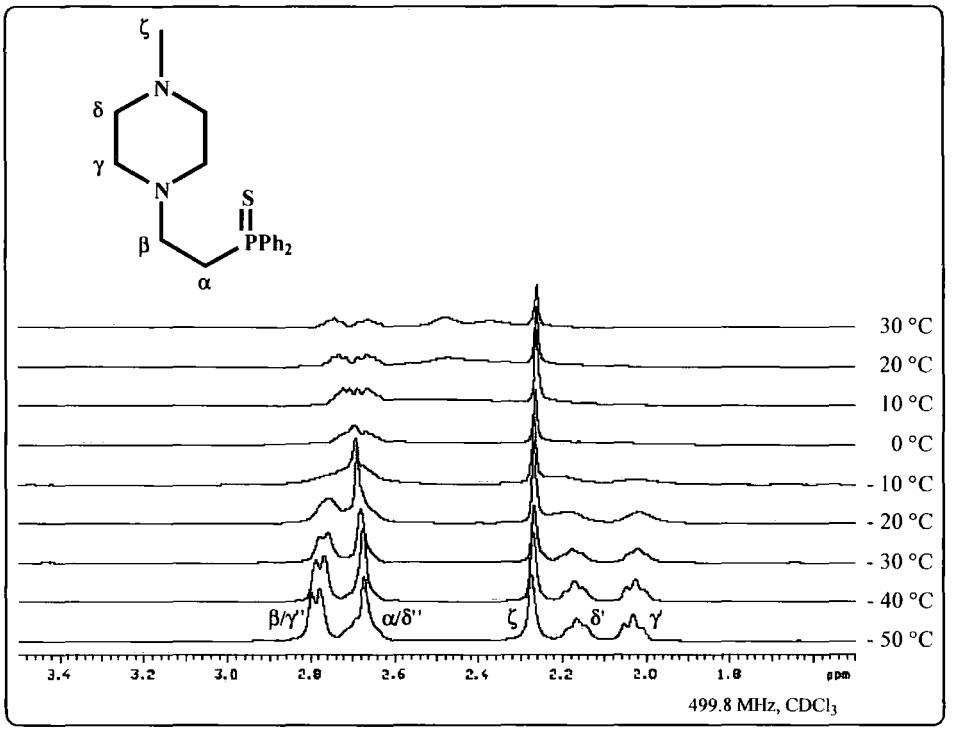

Figure 2.12: ^{1}H NMR spectra for compound **2.6-1** as a function of temperature (aromatic region omitted for clarity)

The ^{13}C {^{1}H} NMR spectra of **2.6-1** – **2.6-4** again strongly resembled those of the parent tertiary phosphines. The only significant differences noted were in the magnitudes of the $^{1}J_{CP}$ coupling constants for the carbons adjacent to phosphorus, *i.e.* the α-bridge and *ipso*-phenyl carbons, in accordance with the oxidation of the phosphorus centre, Table 2.9.[45] Other features of these spectra were unexceptional.

E =	$^{13}C\{^{1}H\}$ NMR*			
	α-bridge carbon		*ipso*-phenyl carbon	
	Parent phosphine	Phosphine sulphide	Parent phosphine	Phosphine sulphide
NMe	24.9 (d) (12.1 Hz)	29.0 (d) (57.0 Hz)	137.6 (d) (12.9 Hz)	132.0 (d) (81.2 Hz)
O	24.5 (d) (12.1 Hz)	30.0 (d) (56.6 Hz)	137.3 (d) (12.6 Hz)	133.1 (d) (81.1 Hz)
S	25.7 (d) (12.4 Hz)	29.7 (d) (56.0 Hz)	138.7 (d) (12.9 Hz)	133.2 (d) (80.9 Hz)
CH_2	25.9 (d) (11.9 Hz)	30.1 (d) (56.2 Hz)	138.8 (d) (12.4 Hz)	133.1 (d) (80.6 Hz)

*125.7 MHz, $CDCl_3$

Table 2.9: Selected $^{13}C\{^{1}H\}$ NMR spectroscopic data for phosphines **2.4-1** – **2.4-4** and phosphine sulphides **2.6-1** – **2.6-4**

2.6 Attempted preparation of aminophosphine-containing *N*-methylpiperazine-*N'*-ethylene-phosphines

2.6.1 Attempted preparation of *N*-methylpiperazine-*N'*-ethylene-*bis*(diisopropyl-amino)phosphine (2.7-1)

Following the successful synthesis of the diphenylphosphine-containing species (**2.4-1** – **2.4-5**) detailed in Section 2.3, the syntheses of the analogous *bis*(diisopropylamino)-phosphine-substituted species were attempted (Scheme 2.9) with a view to creating a further family of ligands with an electron-rich phosphine centre by the placement of two amino substituents at phosphorus.[46]

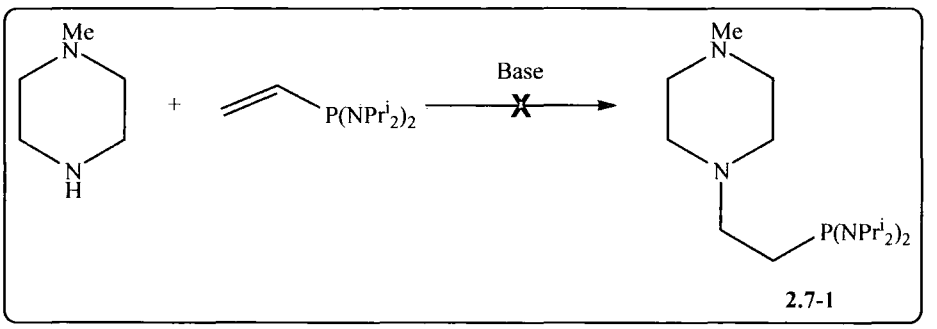

2.7-1

Scheme 2.9: Attempted synthesis of *N*-methylpiperazine-*N'*-ethylene *bis*(diisopropylamino)phosphine

The synthesis of the *bis*(diisopropylamino)phosphine ligand was initially attempted as detailed by Davies and co-workers;[5] four equivalents of *N*-methylpiperazine with one equivalent of *bis*(diisopropylamine)vinylphosphine (**2.3-2**) were heated in THF with a catalytic quantity of sodamide. *In situ* analysis of the product mixture by ^{31}P $\{^1H\}$ NMR spectroscopy demonstrated the appearance of a singlet resonance at δ_P = + 69.8 ppm, at higher frequency relative to the parent vinyl phosphine $\{\delta_P$ = + 53.3 ppm (s)$\}$. The reaction mixture was subjected to an identical work-up as detailed previously, *i.e.* by quenching of the $NaNH_2$ catalyst with aqueous ammonium bromide before extraction into CH_2Cl_2. Following isolation, analysis of the product by ^{31}P NMR spectroscopy revealed that the resonance attributed to the product was no longer present and only a number of presumed decomposition products were instead observed, Table 2.10, Entry 1.

The failure of the procedure was surprising given the success of this methodology using diphenylvinylphosphine (**2.3-1**). Although amino-substituted phosphines are noted to be significantly more sensitive to decomposition than their alkyl and aryl counterparts through cleavage of the P–N bond,[47] aminophosphines are sensitive to oxygen alone.[6] Moreover the parent vinylphosphine ($^iPr_2N)_2PCH{=}CH_2$ (**2.3-2**) is known to be tolerant to deoxygenated water[48] so it was assumed that employing an aqueous work-up would not have been an issue in the preparation of this compound.

Entry	Me(ppz) (eqv.)*	**2.3-2**	Base	Solvent	$^{31}P\{^{1}H\}$ NMR δ_P = + 69.8/69.9	
					Observed *In situ*	Observed after work-up
1	4	1	$NaNH_2$	THF	➳	×
2	1	1.5	$NaNH_2$	THF	➳	×
3	1	1	$NaNH_2$	THF	➳	×
4	1	1	-	THF	×	×
5	1	1	NEt_3	CH_2Cl_2	(➳)	×
6	1	1.5	NEt_3	CH_2Cl_2	(➳)	×
7	1	1	K_2CO_3	THF	(➳)	×
8	1	1	K_2CO_3	MeCN	×	×
9	1	1	K_2CO_3	CH_2Cl_2	×	×
10	1	1	DBU	THF	×	×
11	1	1	DBU	CH_2Cl_2	×	×

➳ = product observed; (➳) = product observed but 100% completion not achieved;

× = product not obtained

NB. Me(ppz) = *N*-methylpiperazine

Table 2.10: Reaction conditions employed for the attempted synthesis of **2.7-1**

The addition reaction outlined in Scheme 2.9 (*vide supra*) was reattempted using analogous conditions (*i.e.* heating to reflux in THF with $NaNH_2$ catalyst), but with a differing stoichiometry; here a slight excess of the phosphine (**2.3-2**, 1.5 equivalents) was reacted with one equivalent of *N*-methylpiperazine. As was observed in the initial synthesis, a singlet resonance was noted in the *in situ* $^{31}P\{^{1}H\}$ NMR spectrum of the reaction mixture {δ_P = 69.9 ppm (s)}. Again, following an aqueous work-up of the product, it was found that this resonance was no longer present with only a number of presumed decomposition products being observed, Table 2.10, Entry 2. A further attempt to synthesise the target product using this methodology was made, employing stoichiometric quantities of the phosphine (**2.3-2**) and the amine, however, an identical outcome was encountered, with a singlet resonance at δ_P = 69.8 ppm being observed *in situ*, which was lost following work-up, Table 2.10, Entry 3.

In an attempt to simplify the synthesis of the target product and minimise the work-up required, stoichiometric quantities of the reagents were heated in THF with the absence of base, however no reaction was noted and only unreacted starting materials were detected in the resulting ^{31}P NMR spectrum of the reaction mixture, Table 2.10,

Entry 4. This is in agreement with a previous observation which noted that a base is required to promote this addition reaction.[17]

Due to the disappointing outcome of the above syntheses, an alternative synthetic methodology was sought for the formation of **2.7-1**. It has been shown that the addition of vinyl phosphites to substituted piperazines proceeds cleanly and rapidly with the use of a soluble base such as triethylamine in CH_2Cl_2 solvent.[49] This approach was especially attractive for the synthesis of this P–N bond-containing phosphine as the work-up for this transformation merely involves the removal of the volatile triethylamine and CH_2Cl_2 solvent *in vacuo*, thereby eliminating the need for an aqueous work-up. The reaction was attempted using equimolar quantities of the phosphine (**2.3-2**) and *N*-methylpiperazine with an excess of the base and the resulting mixture was allowed initially to react at room temperature for 3h. *In situ* ^{31}P NMR analysis again afforded a singlet resonance at δ_P = + 68.9 ppm, but only in 64 % yield relative to the parent phosphine (by integration). Despite heating the mixture to reflux for a further 12h in an attempt to push the reaction to completion, no further reaction was observed and the percentage composition of the presumed product unchanged.

In an effort to find a set of reaction conditions that permitted the clean synthesis and subsequent isolation of the desired product, a number of different solvent and catalyst combinations were screened, with emphasis on soluble hindered bases, *i.e.* DBU, and bases that show limited solubility in organic solvents, *i.e.* K_2CO_3 (5 mol %), in order to simplify the reaction work-up, Table 2.10, Entries 7 – 11. Disappointingly, however, the only conditions that showed even traces of reaction were reaction with K_2CO_3 in THF, Table 2.10, Entry 7, yet following removal of the base by filtration and removal of the solvent, the desired resonance were not observed by ^{31}P NMR spectroscopy or by mass spectrometric analysis of the obtained products.

2.6.2 Attempted synthesis of *N*-methylpiperazine-*N'*-ethylene *bis*(diisopropylamino)phosphine sulphide (2.7-2)

In an effort to synthesise an aminophosphine-containing PNE compound, an alternative methodology for this transformation was sought. It has been reported that vinylphosphine sulphides undergo an identical addition to secondary amines under base-catalysed additions with anti-Markonikov regiochemistry.[50] Consequently, the corresponding *bis*(diisopropylamino)vinyl phosphine sulphide (**2.3-5**) was synthesised and the addition of this protected phosphine sulphide to *N*-methylpiperazine attempted, Scheme 2.10.

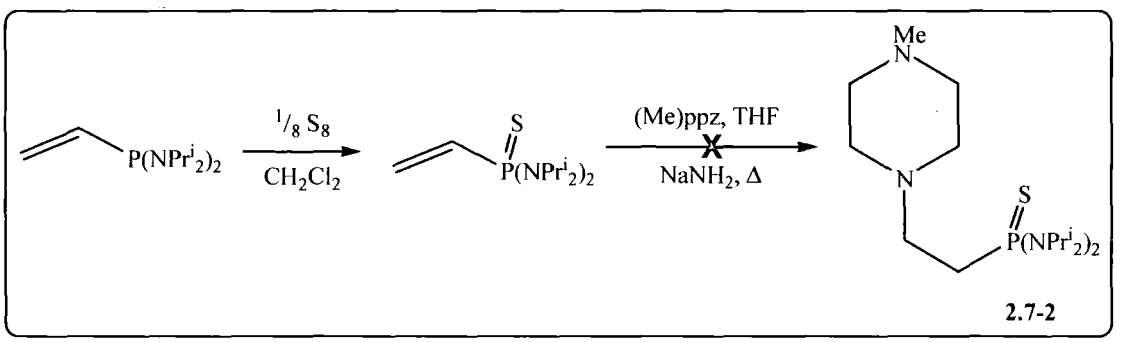

Scheme 2.10: Attempted synthesis of **2.7-3** using (^{i}Pr$_2$N)$_2$P(S)CH=CH$_2$ (**2.3-5**)

The necessary *bis*(diisopropylamino)vinylphosphine sulphide (**2.3-5**) was prepared from its parent tertiary phosphine **2.3-2** by reaction with *ca.* one equivalent of elemental sulphur in CH_2Cl_2 at room temperature. Following isolation and recrystallisation, **2.3-5** was isolated as a solid in excellent yield (75 %). The solid nature of this P(V) compound significantly facilitated further reaction, due to both its ease of handling and its tolerance to atmospheric conditions. The attempted synthesis of **2.7-2** was, however, performed under anhydrous conditions in order to minimise possible complications that may arise from the presence of air and moisture in the reaction mixture. Consequently, equimolar quantities of *N*-methylpiperazine and the phosphine sulphide **2.3-5** were heated in THF with a catalytic quantity of sodamide, Scheme 2.10, however analysis of the product mixture by ^{31}P NMR spectroscopy showed that no trace of reaction had occurred and only numerous peaks attributed to decomposition products

were observed. Analysis of the resulting mixture by mass spectrometry also failed to provide any evidence of the required product.

2.6.3 Attempted Synthesis of *N*-methylpiperazine-*N'*-ethylene-diisopropylamino-phenylphosphine (2.7-3)

In a final attempt to synthesise an analogue of compounds (**2.4-1** – **2.4-5**) with an amino group present at the phosphorus atom, the addition reaction between the 'mixed' (diisopropylamino)phenylphosphine (**2.3-3**) with *N*-methylpiperazine was attempted in accordance with Scheme 2.11.

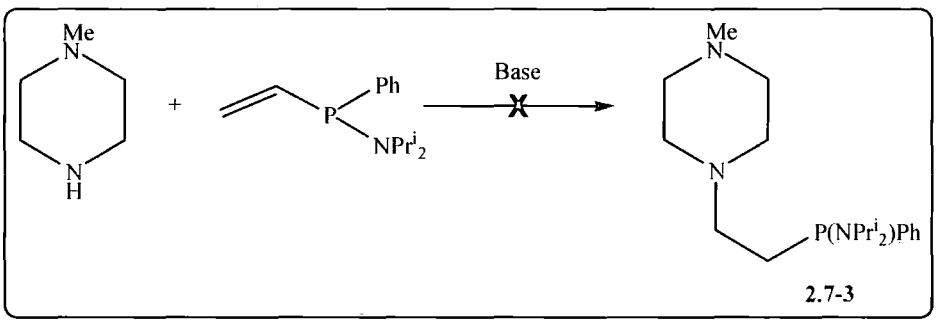

Scheme 2.11: Attempted synthesis of *N*-methylpiperazine-*N'*-ethylene-diisopropyl-amino(phenyl)phosphine (**2.7-3**)

Initially the synthesis of **2.7-3** was attempted by heating a slight excess of the amine (1.5 eqv. relative to the phosphine) in THF with a catalytic quantity of sodamide, but again as found with the attempted synthesis of **2.7-1** (*vide supra*), the desired product **2.7-2** was not obtained. Indeed, *in situ* analysis by ^{31}P NMR spectroscopy demonstrated the formation of many unidentifiable phosphorus-containing products for this transformation. An alternative synthetic methodology was attempted as detailed in Table 2.10, Entry 7 (*vide supra*), employing a catalytic quantity of K_2CO_3 (5 mol %) in THF, but again no reaction was observed to take place and only a mixture of products containing traces of the starting materials were observed for this reaction.

It is presumed that the origin of the failure of the synthesis of **2.7-1** – **2.7-3** lies in the mechanism of the Michael addition. It has already been established that the anti-Markonikov nature of this addition results from the stabilisation of the intermediate

carbanion by orbital overlap with the α-P–R σ*-orbital, Figure 2.2 (*vide supra*).[18] It is believed that the presence of electronegative amino-substituents at phosphorus raises the energy of the P–R σ*-orbitals, thereby disfavouring interaction of these with the adjacent carbanion orbital. This poor orbital overlap results in the amino-phosphines being poor substrates for these conjugate addition reactions as the intermediate carbanion is destabilised, thus inhibiting product formation.

2.7 Attempts to lengthen the PNE P–N bridge: Attempted synthesis of *N*-methylpiperazine-*N'*-propylene-diphenylphosphine

Given the success of the synthesis of the diphenylphosphino-containing PNE systems from diphenylvinylphosphine, an attempt was made to synthesise a PNE species with a three-carbon P–N bridge using a similar methodology. In these attempted transformations, allyldiphenylphosphine was employed in place of the vinyl-functionalised phosphine with the aim of generating the desired extended three carbon linker.

The allyldiphenylphosphine (**2.3-4**) was synthesised according to Scheme 2.12, *i.e.* by reaction of Ph_2PCl with allyl Grignard (**2.2-2**) at low temperature. Following isolation and purification by distillation under reduced pressure, this product was afforded as a colourless oil in good yield (64 %).

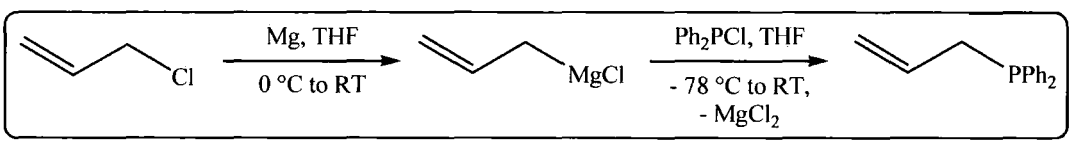

		$^{31}P\{^1H\}$ NMR* δ_P
PPh2	**2.3-4**	– 14.6 (s)

*161.9 MHz, $CDCl_3$

Scheme 2.12: Synthesis and $^{31}P\{^1H\}$ NMR spectroscopic data of **2.3-4**

The addition of the allyldiphenylphosphine (**2.3-4**) to *N*-methylpiperazine was undertaken according to the previously detailed methodology, *i.e.* stoichiometric

quantities of **2.3-4** and diamine were heated to reflux in THF with a catalytic quantity of sodamide. The reaction mixture was subject to an aqueous work-up and the product extracted into CH_2Cl_2. The product from this reaction, **2.4-6**, was isolated as a viscous orange oil in excellent yield (90 %).

Initial analysis of **2.4-6** by ^{31}P $\{^1H\}$ NMR spectroscopy indicated the formation of a diphenylalkylphosphine from the observed chemical shift $\{\delta_P = -18.6$ (s)$\}$ and satisfactory mass spectrometric analysis consistent with the addition of the allyl phosphine to the piperazine was obtained $\{m/z = 327.2\ [MH]^+\}$. However, further spectroscopic analysis revealed that **2.4-6** was in fact the 1,2-disubstituted compound with a methyl group present at the β-bridge carbon instead of the desired 1,3-disubstituted product, Scheme 2.13. The presence of the methyl group was unambiguously confirmed by the use of DEPT 135/DEPT 90 NMR techniques and the regiochemistry of the product confirmed with the use of 2D ^1H–^1H nOesy, ^1H–^1H COSY and ^1H–$^{13}C\{^1H\}$ HETCOR NMR experiments.

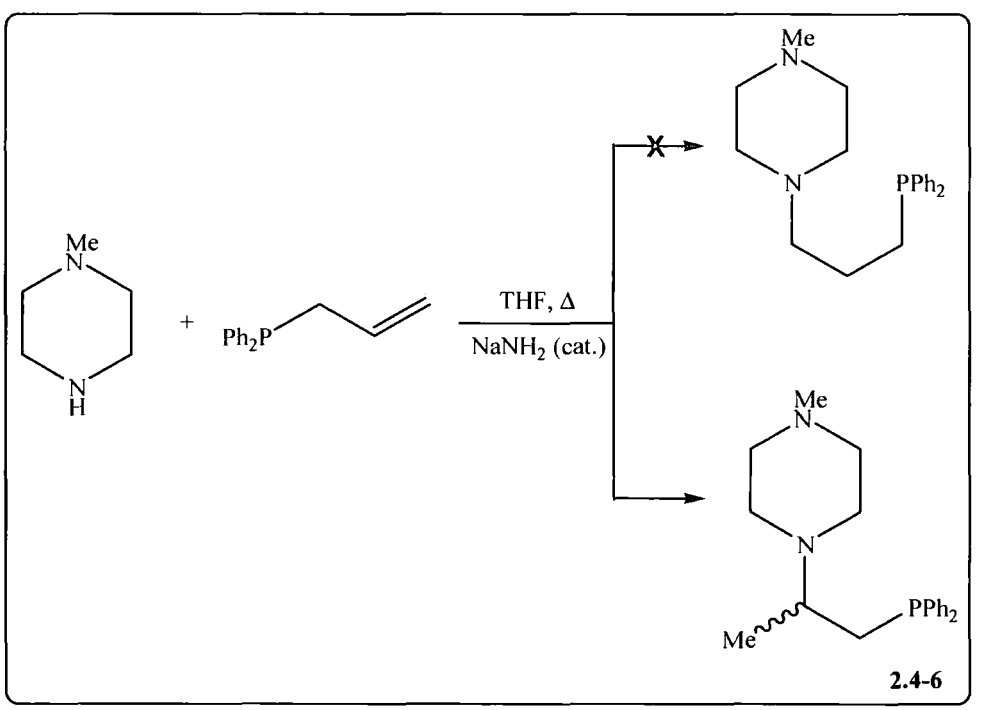

Scheme 2.13: Synthesis of *N*-methylpiperazine-*N'*-1-methyl-ethyl-diphenylphosphine (**2.4-6**)

The formation of the methylated 1,2-substituted product is believed to arise from base-catalysed isomerisation of the allyldiphenylphosphine to diphenyl-prop-2-ene-phosphine **2.3-4(a)**, in accordance with comparable observations in the literature.[51,52] A proposed mechanism for this process is shown in Scheme 2.14. The isomeric unsaturated compound **2.3-4(a)** undergoes base-catalysed Michael addition to the piperazine moiety, leading to the observed product, with the mechanism for the vinyl addition being entirely analogous to that detailed in Scheme 2.5 (*vide supra*).

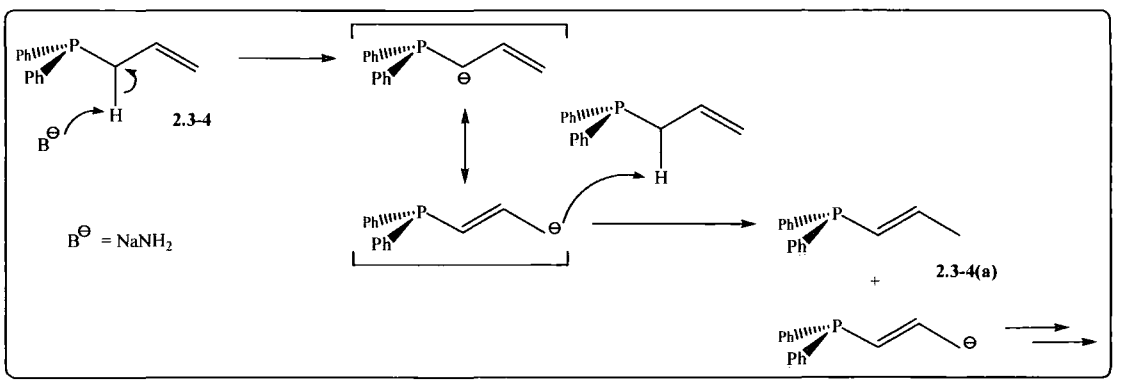

Scheme 2.14: Proposed rearrangement of allyldiphenylphosphine {**2.3-4**} to diphenyl-prop-2-ene-phosphine {**2.3-4(a)**}

The ^{1}H NMR spectrum of **2.4-6** at room temperature was reminiscent of that of the related PNN(Me) compound **2.4-1**, as at 20 °C, the spectrum of **2.4-6** exhibited severely broadened methylene and methine resonances, with only the signals for the *N*-bridge methyl and *N*-methyl substituents being well-resolved. The ι-bridge methyl was observed as a doublet resonance with a $^{4}J_{PH}$ coupling of 6.0 Hz, which was confirmed with the aid of ^{1}H $\{^{31}P\}$ NMR experiments.

Upon lowering the temperature to – 50 °C, the ^{1}H NMR signals attributed to the methylene and methine protons were observed to sharpen. The assignment of these resonances was again aided by the use of low temperature 2D NMR experiments, Figure 2.13. Notably, the presence of the methyl group on the P–N bridge renders the α-methylene protons magnetically inequivalent and consequently these diastereotopic protons are observed as two multiplets, each integrating to 1H. Other features of the aliphatic spectral region were reminiscent of the related PNN moiety **2.4-1**, Section 2.3.2 (*vide supra*).

The aromatic region of **2.4-6** at – 50 °C resembled that of the room temperature spectrum, although at the lower temperature, the signal associated with the *ortho*-phenyl protons was noted to split from a 4H multiplet into two 2H resonances. Independent of the sample temperature, the *meta*- and *para*-phenyl ring protons were observed as overlapping multiplets integrating to 6H.

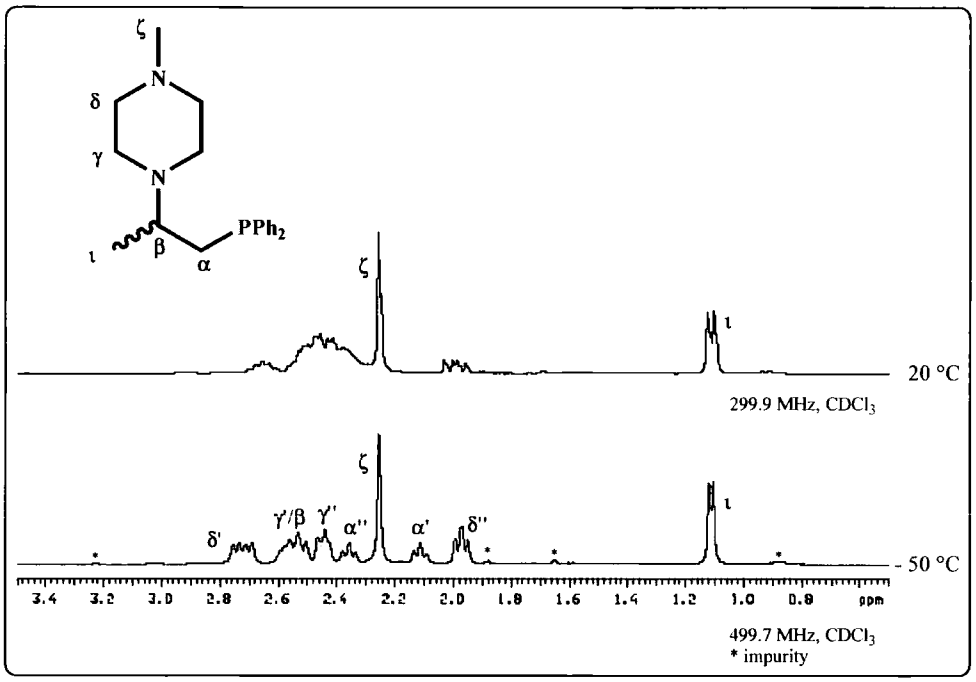

Figure 2.13: Representative ^{1}H NMR spectra of **2.4-6** at + 20 °C and – 50 °C

In the aliphatic region of the ^{13}C {^{1}H} NMR spectrum of **2.4-6**, the methine and methyl carbons were easily distinguishable from the methylene carbon resonances with the use of DEPT 135/DEPT 90 NMR experiments. The α-methylene and β-methine bridge carbons both demonstrate coupling to ^{31}P with the β-carbon displaying the larger value ($^{1}J_{CP}$ = 13.2 Hz, $^{2}J_{CP}$ = 16.1 Hz). Coupling to phosphorus was also noted for the ι-carbon ($^{3}J_{CP}$ = 7.3 Hz). Interestingly, the resonance associated with the δ-ring carbon was notably broadened at room temperature ($\nu_{1/2}$ = 49.2 Hz), although sharpening of this resonance occurred at lower temperatures. The aromatic region of this spectrum was unremarkable and as expected with coupling to phosphorus being observed for all but the *para*-phenyl carbons at room temperature.

2.7.1 Synthesis and characterisation of *N*-methylpiperazine-*N'*-ethylene(1-methyl)-diphenylphosphine.HCl (2.5-5)

In an effort to assist the characterisation of **2.4-6**, the synthesis of the corresponding hydrochloride salt **2.5-5** was undertaken, which was prepared in an entirely analogous manner to that detailed previously for the generation of **2.5-1**, **2.5-2**, **2.5-4** and **2.5-6** (Section 2.4). Dry gaseous HCl (excess) was bubbled through an ethereal solution of **2.4-6** resulting in the immediate precipitation of a white solid. Following recrystallisation from chloroform/diethyl ether, **2.5-5** was obtained as a white crystalline solid in almost quantitative yield (98 %).

In line with the other HCl salts prepared previously (Section 2.4), analysis of **2.5-5** by ^{31}P [^{1}H] NMR spectroscopy indicated that protonation of the phosphine moiety had not occurred {$\delta_{P[1H]} = -17.3$ (s)}. The most striking feature of the ^{1}H NMR spectrum of **2.5-5** is that only one resonance, integrating to 1H, corresponding to a single ammonium proton was observed. This is in contrast to the related PNN species **2.5-1**, in which two broad resonances corresponding to protonation at both nitrogens were clearly observed under identical reaction conditions. Further analysis by ^{1}H–^{1}H COSY and nOesy NMR experiments also indicated that **2.4-6** had reacted with only one equivalent of HCl (despite a large excess in the reaction) with mono-protonation occurring exclusively at the terminal NMe fragment. Additionally **2.5-5** afforded CHN and mass spectrometric analyses consistent with the formation of a mono-protonated species.

In contrast to the related MeNNP.2HCl salt **2.5-1**, which exhibited a well-defined ^{1}H NMR spectrum at 20 °C, the ^{1}H NMR spectrum of **2.5-5** {MeNN(Me)P.HCl} at room temperature demonstrated broadening of all methylene and methine resonances. On lowering the temperature of the sample of **2.5-5**, these CH_2 and CH signals were noted to sharpen with a well-defined spectrum being observed at – 50 °C, a situation indicative of mono-protonation.

Whilst the signal associated with the methyl protons in the ζ-position was noted as a singlet resonance, coupling to phosphorus was again noted for the ι-bridge methyl protons of **2.5-5** with the magnitude of the $^{4}J_{PH}$ coupling (6.4 Hz) being of a similar value to that observed for the parent diamine **2.4-6** ($^{4}J_{PH}$ = 6.0 Hz). The aromatic region of the spectrum of **2.5-5** was as expected and unremarkable. The ^{13}C {^{1}H} NMR

spectrum of **2.5-5** was as expected, with the resonance attributed to the ι-methyl carbon being observed as a doublet resonance ($^3J_{CP}$ = 8.0 Hz) as a result of coupling to phosphorus.

In an effort to definitively confirm the regiochemistry of the methyl-substituted P–N bridge, crystallisation of a sample of **2.5-5** was undertaken. It was found that slow diffusion of diethyl ether into a concentrated chloroform solution produced single crystals of **2.5-5** suitable for study by X-ray diffraction, Figure 2.14.

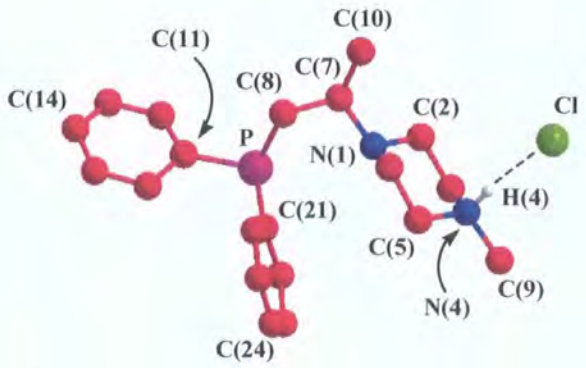

Figure 2.14: Ball and Stick representation of **2.5-5**‡

	Bond Length/Å		Bond Angle/°
P–C(8)	1.851(6)	C(11)–P–C(21)	101.4(2)
N(1)–C(7)	1.473(6)	C(2)–N(1)–C(6)	109.6(4)
N(4)–C(9)	1.473(6)	C(3)–N(4)–C(5)	110.4(3)
N(1)–H(1)	0.83(4)	N(4)–H(4)–Cl	168(4)
C(Ph)–P	1.854[a]	N(1)–C(7)–C(8)–P	54.4
Cl–H(1)	3.002(2)	$\Sigma_{\angle N(1)}$	335.6[a,b]
		$\Sigma_{\angle N(4)}$	337.1[a,b]
		$\Sigma_{\angle P}$	305.1[a,b]

[a]average value, [b]angle summation, Individual e.s.d.'s in parentheses

Table 2.11: Selected bond distances (Å) and angles (°) for **2.5-5**

The molecular structure of **2.5-5** confirmed both the regiochemistry of the methyl-substituted bridge and that protonation had occurred solely at the N(4) position, observations consistent with the structure proposed by NMR spectroscopy. A sample of crystals of **2.5-5** were harvested and their units cells checked against the parameters

‡ Molecular structure determination performed by Dr A. S. Batsanov

obtained for the original crystal and identical values were obtained for each suggesting that the obtained structure is representative of the bulk sample of **2.5-5**.

Summation of the bond angles about the heteroatoms reveal tetrahedral geometry about both the amine $\{\Sigma_{\angle N(1)} = 335.6°\}$ and ammonium $\{\Sigma_{\angle N(4)} = 337.1°\}$ functionalities with the angle summation about phosphorus being slightly smaller as expected $\{\Sigma_{\angle P} = 305.1°\}$. The P and N(1) lone pairs adopt a pseudo *gauche* arrangement with a pronounced twist through the N(1)–C(7)–C(8)–P bridge of 54.4°. The phenyl substituents at P are not found in a perpendicular arrangement as the mean ring planes intersect at 63.2°. Whilst minimal distortion from planarity was noted in the C(21)–C(24) ring, significant distortion from planarity was noted in the C(11)–C(14) ring, which is indicative of ring-motion in the solid state and is representative of the mean statistical position of this ring in space.

2.8 Evaluation of the electronic character of the phosphine component of the PNE systems – synthesis and analysis of the Se=PNE derivatives

Phosphines are known to coordinate well to chalcogens to give the corresponding P(V) species as previously demonstrated (Section 2.5). Whilst these reactions may be of use synthetically, the corresponding phosphine selenides have an additional beneficial property, namely that the magnitude of the inherent $^{1}J_{SeP}$ coupling constant (^{77}Se = 7.58 %, I = ½) may be used as a convenient probe of the donor properties of the parent phosphine (and hence their potential as ligands).[53]

The donor characteristics (or basicity) of a phosphine ligand is principally dependent on the proportion of *s*-character of the phosphorus–metal bond.[53] As coupling between two spin-active nuclei in NMR spectroscopy is principally exhibited between their *s*-orbitals (due to their proximity to the nuclei in question),[54] it follows that an examination of the magnitudes of the resulting coupling constants can provide an indication of the extent of the *s*-character of this bond and therefore the donor ability of the parent phosphine. It has been demonstrated that the greater the *s*-character of the phosphorus-selenium bond, the larger the magnitude of $^{1}J_{SeP}$ and hence the less Lewis basic the parent phosphine.[53]

Several factors have been noted to impact on the magnitude of this $^{1}J_{SeP}$ coupling constant, which include the formal hybridisation of phosphorus and the

electronic nature of its substituents. Moreover, the placement of bulky substituents at phosphorus has the effect of widening the angle about the phosphorus centre, something that results in lower magnitudes of $^{1}J_{SeP}$.[53] Additionally, the introduction of electron-withdrawing substituents presents higher values of $^{1}J_{SeP}$ as a result of the electron poor nature of the Lewis acidic phosphine.[55]

With this in mind, the syntheses of the selenide derivatives of the various PNE compounds (**2.8-1** – **2.8-7**) were undertaken with a view to evaluating the donor characteristics of the phosphine centre in order to assess their potential as ligands. The synthetic methodology for this transformation is shown in Scheme 2.15.

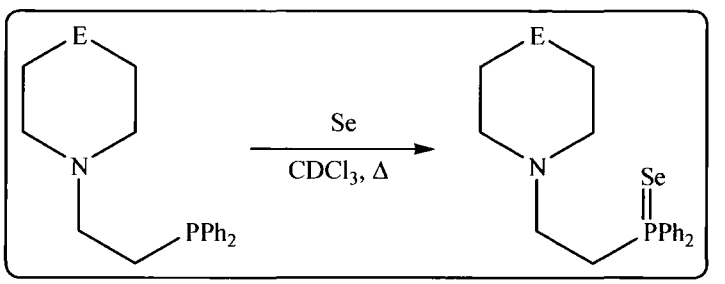

Compound	$^{31}P\{^{1}H\}$ NMR* δ_P	$^{1}J_{SeP}$ /Hz	Yield /%
(Me)NNP=Se (**2.8-1**)	+ 32.3	726	93
ONP=Se (**2.8-2**)	+ 32.4	727	95
SNP=Se (**2.8-3**)	+ 32.8	726	92
CNP=Se (**2.8-4**)	+ 32.2	725	93
(Ph)NNP=Se (**2.8-5**)	+ 32.6	725	90
(Me)NN(Me)P=Se (**2.8-6**)	+ 34.3	727	91
Se=PNNP=Se (**2.8-7**)	+ 32.3	726	89

*121.4 MHz, $CDCl_3$

Scheme 2.15: Synthesis and $^{31}P\{^{1}H\}$ NMR spectroscopic data of phosphine selenides **2.8-1** – **2.8-7**

All the selenide derivatives **2.8-1** – **2.8-7** were synthesised in an identical manner; under nitrogen, a Young's tap NMR tube was charged with a $CDCl_3$ solution of the required phosphine and an excess (5 equivalents) of elemental 'grey' selenium. The tube was placed in an oil bath and warmed gently until analysis by ^{31}P NMR spectroscopy showed complete conversion to the required product (typically 2–3 h). All selenide compounds were synthesised and characterised by NMR spectroscopy in

$CDCl_3$ for comparative purposes, as alteration of the solvent can, unexpectedly, have profound effects on not only the shift, but also the magnitude of $^1J_{SeP}$.[56]

The phosphine selenides **2.8-1** – **2.8-7** were all obtained in near-quantitative yields following isolation by filtration to remove excess, unreacted selenium and removal of the solvent *in vacuo*. Satisfactory mass spectrometric data were obtained for compounds **2.8-1** – **2.8-7** with molecular ion peaks being observed in all cases. The ^1H and ^{13}C $\{^1H\}$ NMR spectra of **2.8-1** – **2.8-7** are entirely unremarkable as they closely resemble their parent PNE species and the related phosphine sulphide derivatives.

All of the selenides **2.8-1** – **2.8-7** exhibited a sharp singlet in their ^{31}P $\{^1H\}$ NMR spectra at higher frequency than was observed for the parent species $\{\delta_P \approx -19.0$ (s)$\}$ with satellites resulting from coupling between ^{31}P and ^{77}Se being observed. From a comparison of these $^1J_{SeP}$ values with a range of other selenides, Table 2.12, it is evident that the phosphine donor component in the PNE systems is a relatively good Lewis base and is comparable to other similarly-substituted phosphines and is, as may be expected, similar to $Ph_2P(R)P{=}Se$ (R = ^{n}Bu, Me).[57] Furthermore, the magnitudes of $^1J_{SeP}$ for each of the compounds is essentially independent of the nature of the E donor, as would be expected.

Compound	$^1J_{SeP}$ /Hz	Compound	$^1J_{SeP}$ /Hz
$Me_3P{=}Se$	684[a] [56]	^{n}Bu$(Ph)_2P{=}Se$	730[b] [57]
$^n Bu_3P{=}Se$	693[b] [57]	$Ph_2(Me)P{=}Se$	731[a] [58]
$^n Bu_2(Ph)P{=}Se$	715[b] [57]	$Ph_3P{=}Se$	738[a] [59]
2.8-4	725[a]	$(Et_2N)_2PhP{=}Se$	761[a] [60]
2.8-5	725[a]	$(Me_2N)_3P{=}Se$	790[a] [61]
2.8-6	726[a]	$(pyrr)Ph_2P{=}Se$	812[a] [21]
2.8-3	726[a]	$(pyrr)(^iPr_2N)_2P{=}Se$	842[a] [21]
2.8-2	727[a]	$(EtO)_3P{=}Se$	935[a] [59]
2.8-7	726[a]	$(MeO)_3P{=}Se$	940[a] [61]
2.8-1	726[a]	$(^iPrO)_3MeP{=}Se$	1023[a] [59]

[a] $CHCl_3/CDCl_3$; [b] CH_2Cl_2/CD_2Cl_2

Table 2.12: Representative $^1J_{PSe}$ values for a range of phosphine/phosphite selenides

2.9 Conclusions/Summary

This chapter has detailed synthetic methodologies for the preparation of a family of potentially polydentate PNE ligands by a concise synthetic pathway. The synthesis of the known chlorophosphine precursors, namely ($^{i}Pr_2N)_2PCl$ (**2.1-1**) and ($^{i}Pr_2N$)PhPCl (**2.1-2**) was performed along with an examination of the spectroscopic behaviour of **2.1-2** at low temperature. These chlorophosphines, along with Ph_2PCl, were successfully converted into their corresponding vinyl compounds by reaction with a vinyl Grignard.

Reaction of the diphenylvinylphosphine (**2.3-1**) with a doubly-bridged HN^E ring compound (where E = NMe, NPh, O, S, CH_2) affords, in near-quantitative yields, the corresponding $Ph_2PCH_2CH_2N(CH_2CH_2)_2E$ derivatives with regioselective addition of the vinyl functionality. When E = NMe, O, S, and CH_2 (**2.4-1** – **2.4-4**), dynamic ring inversion processes are observed in the ^{1}H NMR spectra of these products and extensive low temperature multinuclear NMR spectroscopic studies were undertaken to fully characterise these species in solution. The PNN(Me) compound (**2.4-6**) was found to crystallise over long periods of time; X-ray diffraction studies revealed the expected chair conformation of the saturated six-membered ring in the solid state. The addition of diphenylvinylphosphine (**2.3-1**) to heterocyclic secondary amines was extended to generate a PNNP (**2.4-7**) system by reaction of the diphenylvinylphosphine (**2.3-1**) with piperazine.

A range of PNE and PNNP derivatives were synthesised for a variety of reasons: the phosphine sulphides of E = NMe (**2.6-1**), O (**2.6-2**), S (**2.6-3**) and CH_2 (**2.6-4**) were synthesised as the parent PNE species were oily in nature which precluded the assessment of their purity. Satisfactory CHN analytical data were obtained on their phosphine sulphide derivatives. As dynamic behaviour in solution was observed for the parent PNE compounds in solution when E = NMe (**2.4-1**), O (**2.4-2**), S (**2.4-3**), CH_2 (**2.4-4**) and also for the PNNP counterpart (**2.4-7**), the hydrochloride salts were synthesised with the aim of limiting the ring inversion processes. Surprisingly the synthesis of PNS.HCl was unsuccessful. The resulting cations (**2.5-1**, **2.5-2**, **2.5-4**, and **2.5-6**) all displayed well resolved NMR spectra at room temperature. X-ray diffraction studies performed on the ONP.HCl salt (**2.5-2**) confirmed the expected chair conformation of the six-membered ring in the solid-state.

Despite repeated attempts, a set of conditions under which the Michael addition of the P-amino-substituted vinylphosphines **2.3-2** and **2.3-3** to *N*-methylpiperazine

could not be found. The failure of these syntheses are attributed to the aminovinylphosphines being poor substrates for the Michael addition reaction.

Attempts to prepare analogues of the PNN compounds that possess a C_3-rather than a C_2-P-N bridge by reaction of allyldiphenylphosphine (**2.3-4**) with *N*-methylpiperazine did not produce the desired compound, since the allylphosphine underwent a base-catalysed rearrangement to form an internal double bond {**2.3-4(a)**}, which subsequently reacted with the piperazine moiety to afford a two-carbon P^N bridge with a methyl group located at the *beta* position relative to the phosphine (**2.4-6**). The corresponding hydrochloride salt **2.5-5** of this species was synthesised and crystals suitable for X-ray diffraction studies were analysed, which confirmed the regiochemistry of this product.

The selenides of all the phosphine-containing PNE and PNNP (**2.8-1** – **2.8-7**) species were synthesised in order to probe the electronic donor characteristics of the phosphine fragments by NMR spectroscopic methods. These studies indicated that the phosphine components have Lewis basicities that are comparable with related phosphines such as $Ph_2(R)P{=}Se$ (R = Me, ^{n}Bu) and thus are expected to coordinate readily to metal centres.

2.10 References

[1] G. Helmchen and A. Pfaltz, *Acc. Chem. Res.*, 2000, **33**, 336 – 345.

[2] T. G. Appleton, H. C. Clark and L. E. Manzer, *Coord. Chem. Rev.*, 1973, **10**, 335 – 422.

[3] P. Braunstein and F. Naud, *Angew. Chem. Int. Ed.*, 2001, **40**, 680 – 699.

[4] M. Boiocchi, M. Bonizzoni, L. Fabbrizzi, F. Foti, M. Licchelli, A. Taglietti and M. Zema, *Dalton Trans.*, 2004, 653 – 658.

[5] M. Bassett, D. L. Davies, J. Neild, L. J. S. Prouse and D. R. Russell, *Polyhedron*, 1991, **10**, 501 – 507.

[6] "*A Guide to Organophosphorous Chemistry*", L. D. Quin, A. John Wiley & Sons 2000, pg 45.

[7] J. R. Doyle and D. Drew, *Inorg. Synth.*, 1990, **28**, 346 – 349.

[8] M. Mag, J. Muth, K. Jahn, A. Peyman, G. Kretzschmar, J. W. Engles and E. Uhlmann, *Bioorg. & Med. Chem.*, 1997, **12**, 2213 – 2220.

[9] A. H. Cowley, M. J. S. Dewar, W. R. Jackson and W. B. Jennings, *J. Am. Chem. Soc.*, 1970, **92**, 5206 – 5213.

[10] J. Anagnosis and M. M. Turnbull, *Polyhedron*, 2004, **23**, 125 – 133.

[11] B. Wrackmeyer, C. Kohler, W. Milius, J. M. Grevy, Z. Garcia-Hernandez and R. Contreras, *Heteroatom Chem.*, 2002, **13**, 667 – 676.

[12] K. M. Abraham and J. R. van Wazer, *Inorg. Chem.*, 1975, **14**, 1099 – 1103.

[13] A. B. Burg and P. J. Slota, *J. Am. Chem. Soc.*, 1958, **80**, 1107 – 1109.

[14] "*Spectroscopic Methods in Organic Chemistry*", D. H Williams and I. Flemming, 5th Ed., McGraw-Hill, Maidenhead, 1995, pg. 71.

[15] "*NMR Spectroscopy: Basic Principles, Concepts and Applications in Chemistry*", H. Günther, 2nd Ed. J. Wiley and Sons, Chichester, 1995, pgs. 181 – 194.

[16] Von. G. Markl and B. Merkl, *Tetrahedron Lett.*, 1981, **22**, 4459 – 4462.

[17] M. S. Rahman, J. W. Steed and K.-K. Hii, *Synthesis*, 2000, **9**, 1320 – 1326.

[18] "*Organic Synthesis: The Roles of Boron and Silicon*", S. E. Thomas, OUP, Oxford, 1994, pg. 49 and 78.

[19] R. K. Harris and R. A. Spragg, *J. Chem. Soc. (B)*, 1968, 684 – 691.

[20] R. Castro, M. L. Durán, J. A. García-Vázquez, J. Romero, A. Sousa, E. E. Castellano and J. Zukerman-Schpector, *J. Chem. Soc., Dalton Trans.*, 1992, 2559 – 2564.

[21] See for example: C. E. Anderson, A. S. Batsanov, P. W. Dyer, J. Fawcett and J. A. K. Howard, *Dalton Trans.*, 2006, 5362 – 5378.

[22] J. Guillon, P. Grellier, M. Labaird, J.-M. Leger, R. Deprez-Poulain, I. Forfar, P. Dallemagne, N. Lemaitre, F. Pehourcq, J. Rochette, C. Sergheraert and C. Jarry, *J. Med. Chem.*, 2004, **47**, 1997 – 2009.

[23] M. Yoyavel, S. Selvanayagam, D. Velmurugan, S. S. S. Raj, H. K. Fun, M. Marappan and M. Kandaswamy, *Acta Cryst. E.*, 2003, **59**, o83.

[24] M. Aroney and R. J. W. Le Fèvre, *J. Chem. Soc.*, 1958, 3002 – 3008.

[25] C. E. Anderson, P. W. Dyer, K. Miqueu and J.-M. Sotiropolous, unpublished results.

[26] L. Fielding, N. Hamilton, R. McGuire and A. C. Campbell, *Magn. Res. Chem.*, 1996, **34**, 59 – 62.

[27] L. Lunazzi, D. Casarini, M. A. Cremonini and J. E. Anderson, *Tetrahedron*, 1991, **47**, 7465 – 7470.

[28] "*Conformational Analysis*", E. L. Eliel, N. L. Allinger, S. J. Angyal and G. A. Morrison, Interscience, New York, 1965, Chapter 4.

[29] G. Gatti, A. L. Segre and C. Morandi, *J. Chem. Soc. (B)*, 1967, 1203 – 1204.

[30] A. C. Fantoni, R. R. Filgueira, L. M. Boggia and W. Caminati, *J. Mol. Spec.*, 1980, **84**, 493 – 502.

[31] E. W. Abel, M. Booth, K. G. Orrell and G. M. Pring, *J. Chem. Soc., Dalton Trans.*, 1981, 1944 – 1950.

[32] W. Faistt, H. Friebolin, S. Kabuss and H. G. Schmid, *Org. Magn. Reson.*, 1969, 67 – 86.

[33] N. L. Allinger, J. G. D. Carpenter and F. M. Karkowski, *J. Am. Chem. Soc.*, 1965, **87**, 1232 – 1236.

[34] M. Aroney and R. J. W. Le Fèvre, *J. Chem. Soc.*, 1960, 2162 – 2168.

[35] S. A. Gorman, J. D. Hepworth and D. Mason, *J. Chem. Soc., Perkin Trans. 2*, 2000, 1889 – 1895.

[36] G. Hallas, R. Marsden, J. D. Hepworth and D. Mason, *J. Chem. Soc., Perkin Trans. 2*, 1984, 149 – 153.

[37] "*Spectroscopic Methods in Organic Chemistry*", D. H. Williams and I. Fleming, 5th Edition, 1995, Cambridge, pg. 98.

[38] A. Flores-Parra, G. Cadenas-Pliego, R. Contreras, N. Zuniga-Villarreal and M. de los Angeles Paz-Sandoval, *J. Chem. Ed.*, 1993, **70**, 556 – 559.

[39] A. R. Katritzky, N. G. Akhmedov, H. Yang, C. D. Hall, *Magn. Reson. Chem.*, 2005, **43**, 673 – 675.

[40] Z. Dega-Szafran, M. Szafran and A. Katrusiak, *J. Mol. Struct.*, 2004, **704**, 129 – 137.

[41] A. J. Jones, C. P. Beeman, M. U. Hasan, A. F. Casy and M. M. A. Hassan, *Can. J. Chem.*, 1976, **54**, 126 – 135.

[42] R. A. Coxall, L. F. Lindoy, H. A. Miller, A. Parkin, S. Parsons, P. A. Tasker and D. J. White, *Dalton Trans.*, 2003, 55 – 64.

[43] G. L. Olson, H.-C. Cheung, K. D. Morgan, J. F. Blount, L. Todaro, L. Berger, A. B. Davidson and E. Boff, *J. Med. Chem.*, 1981, **24**, 1026 – 1034.

[44] L. A. Burrows and E. E. Reid, *J. Am. Chem. Soc.*, 1934, **56**, 1720 – 1724.

[45] K. Bieger, J. Tejeda, R. Réau, F. Dahan and G. Bertrand, *J. Am. Chem. Soc.*, 1994, **116**, 8087 – 8094.

[46] M. L. Clarke, D. J. Cole-Hamilton, A. M. Z. Slawin and J. D. Woollins, *Chem. Commun.*, 2000, 2065 – 2066.

[47] S. Priya, M. S. Balakrishna, J. T. Mague and S. M. Mobin, *Inorg. Chem.*, 2003, **42**, 1272 – 1281.

[48] R. B. King and P. M. Sundaram, *J. Org. Chem.*, 1984, **49**, 1784 – 1789.

[49] P. Herczegh, T. B. Buxton, J. C. McPherson (III), Á. Kovács-Kulyassa, P. D. Brewer, F. Sztaricskai, G. G. Stroebel, K. M. Plowman, D. Farasiu and J. F. Hartmann, *J. Med. Chem.*, 2002, **45**, 2338 – 2341.

[50] D. V. Griffiths, H. J. Groombridge, P. M. Mahoney, S. P. Swetnam, G. Walton and D. C. York, *Tetrahedron*, 2005, **61**, 4595 – 4600.

[51] D. Cavalla, W. B. Cruse and S. Warren, *J. Chem. Soc., Perkin Trans. 1*, 1987, 1883 – 1898.

[52] D. J. Collins, S.-A. Mollard, N. Rose and J. M. Swan, *Austr. J. Chem.*, 1974, **27**, 2365 – 2372.

[53] D. W. Allan and B. F. Taylor, *J. Chem. Res. (S)*, 1981, 220 – 221.

[54] "*NMR Spectroscopy in Inorganic Chemistry*", J. A. Iggo, OUP, Oxford, 1999, pgs. 42 – 43.

[55] N. G. Anderson and B. A. Kaey, *Chem. Rev.*, 2001, **101**, 997 – 1030.

[56] A. Cogne, A. Grand, J. Laugier, J. B. Robert and L. Wiesenfeld, *J. Am. Chem. Soc.*, 1980, **107**, 2238 – 2242.

[57] S. O. Grim, E. D. Walton and L. C. Satak, *Can. J. Chem.*, 1980, **58**, 1476 – 1479

[58] D. Cauzzi, C. Graiff, R. Pattacini, G. Prrdieri, A. Tiripicchio, S. Kahlal and J.-Y. Saillard, *Eur. J. Inorg. Chem.*, 2004, 1063 – 1072.

[59] L. A. Woźniak and M. J. Stec, *Tetrahedron Lett.*, 1999, **40**, 2637 – 2640.

[60] P. W. Dyer, J. Fawcett, M. J. Hanton, R. D. W. Kemmitt, R. Padda and N. Singh, *Dalton Trans*, 2003, 104 – 113.

[61] E. Krawczyk, A. Skowrońska and J. Michalski, *J. Chem. Soc., Perkin Trans. 2*, 2000, 1135 – 1140.

Chapter 3:

Complexation of PNE ligands with Pd

3.1 Introduction

Palladium complexes find extensive application in the areas of coordination chemistry and catalysis. From a synthetic point of view, palladium is an ideal metal for use in such areas since it exists in a number of stable oxidation states. Pd(II) is the most commonly employed, something that can be ascribed to the diamagnetic nature of these square planar d^8 complexes, which facilitates their study by NMR spectroscopy.[1] As a soft late transition metal, Pd binds especially well to softer donor fragments, such as phosphines and thiols, although harder donors (*e.g.* amines and nitriles) also coordinate well to this metal,[2] thus permitting the synthesis of an extensive variety of palladium complexes.

Organometallic palladium derivatives find numerous applications in the area of homogeneous catalysis, as, in many respects, Pd compounds are highly reactive and yet are stable enough to be used as recyclable reagents.[3] The widespread occurrence of palladium in catalysis can be attributed to many factors, not least that these complexes display wide-ranging activity, frequently with high stereo-, regio- and chemo-selectivies in the resulting products.[4] Indeed, it is widely acknowledged that the type of coordinated ligand(s) has a significant effect on both the catalytic activity of the palladium initiator in question and the nature of the resultant products.[5] It is for this reason that the development of new and innovative ligands for palladium remains a constant area of activity.

The following studies will focus on an exploration of the coordination chemistry of the previously discussed PNE ligands with a variety of palladium complexes in order to gain an understanding of the fundamental behaviour of the resulting complexes in both the solution and solid state.

3.2 Coordination of PNE ligands with '$PdCl_2$' fragments

As a starting point to explore the coordination chemistry of the PNE compounds with Pd(II) centres, the reaction of the PNE ligands (**2.4-1** – **2.4-5**) with $PdCl_2(MeCN)_2$ was undertaken. These complexations were performed by reaction of equimolar quantities of the requisite PNE ligands with $[PdCl_2(MeCN)_2]$ in CH_2Cl_2 solution, Scheme 3.1. In the case of **3.1-1** – **3.1-3** (E = NMe, O and S, respectively), the reaction proceeded with the rapid formation of a yellow precipitate.

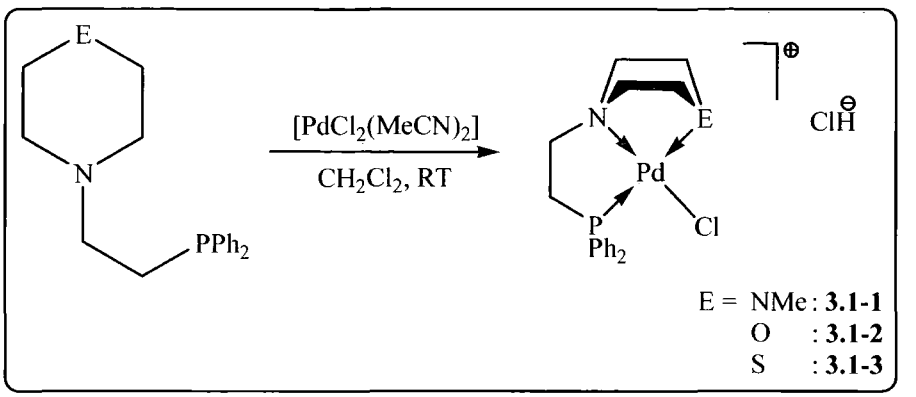

		Yield	$^{31}P\{^1H\}$ NMR* (complex)		$^{31}P\{^1H\}$ NMR§ (parent ligand)
			δ_P	$\nu_{1/2}$ /Hz	δ_P
$[PdCl\{\kappa^3\text{-PNNMe}\}]^+ Cl^-$	**3.1-1**	68 %	+ 46.5[a] (+ 45.7[b])	- -	– 19.1[d]
$[PdCl\{\kappa^3\text{-PNO}\}]^+ Cl^-$	**3.1-2**	67 %	+ 50.4[c]	24	– 18.2[d]
$[PdCl\{\kappa^3\text{-PNS}\}]^+ Cl^-$	**3.1-3**	80 %	+ 49.8[c]	27	– 18.3[d]

*121.4 MHz; §202.3 MHz; [a]CD_3OD; [b]D_2O; [c]d_6-DMSO; [d]$CDCl_3$

Scheme 3.1: Synthesis and $^{31}P\{^1H\}$ NMR spectroscopic data of **3.1-1** – **3.1-3**

All products **3.1-1** – **3.1-3** were obtained as yellow powders in good yield following isolation. Owing to the poor solubility of these complexes in common solvents, such as $CHCl_3$ and CH_2Cl_2, preliminary NMR spectroscopic analysis was performed in polar solvents such as CD_3OD, D_2O and d_6-DMSO. It is noteworthy that the $[PdCl\{\kappa^3\text{-PNNMe}\}]^+ Cl^-$ complex **3.1-1** proved to be slightly more soluble in water

and methanol, whereas $[PdCl\{\kappa^3\text{-PNO}\}]^+ Cl^-$ (**3.1-2**) and $[PdCl\{\kappa^3\text{-PNS}\}]^+ Cl^-$ (**3.1-3**) showed only very limited solubility in DMSO.

In the $^{31}P\{^1H\}$ NMR spectra of all complexes **3.1-1** – **3.1-3**, coordination shifts ($\Delta\delta_P = \delta_{coordinated} - \delta_{free}$) of + 65.6, + 68.6 and + 68.1 ppm were noted for products **3.1-1**, **3.1-2** and **3.1-3**, respectively, signifying complexation of the phosphorus donor to the Pd centre.[6] In all cases, satisfactory mass spectrometric analyses were obtained with peaks corresponding to $[M–Cl]^+$ being observed. In addition, CHN analyses consistent with an empirical formula of '$[PdCl_2(PNE)]$' were obtained.

In an effort to confirm the tridentate binding of the PNE ligands to the '$PdCl_2$' fragment, conductimetry experiments were attempted on the resulting complexes. For complex **3.1-1**, a molar conductance consistent with the formation of a 1:1 electrolyte was obtained (Λ_M (MeOH) = 68 Ω cm^2 mol^{-1}),[7,8] thus confirming the ionic nature of **3.1-1**. Regrettably the limited solubility of both **3.1-2** and **3.1-3** precluded conductimetry experiments being performed on these complexes.

3.2.1 Characterisation of 3.1-1

The $[PdCl\{\kappa^3\text{-PNNMe}\}]^+ Cl^-$ complex **3.1-1** behaved in a noticeably different way from the other members of this family of complexes as it showed sparing solubility in solvents such as D_2O and CD_3OD, which facilitated its characterisation in the solution state. The ^1H NMR spectrum of **3.1-1** clearly indicated a tridentate binding of **2.4-1** to Pd with well-defined resonances attributed to the γ- and δ-ring protons being observed in addition to the signals corresponding to the α- and β-bridge protons. Significantly, the signal attributed to the ζ-*N*-methyl protons was clearly observed as a doublet resonance due to coupling to phosphorus, a situation only achieved upon coordination of the terminal amine donor to the Pd centre (*NB.* the *N*-$C\underline{H}_3$ signal is observed as a singlet in the free ligand **2.4-1**). The origin of this coupling was confirmed using $^1H\{^{31}P\}$ NMR experiments, as shown in Figure 3.1; the doublet signal observed in the $^1H[^{31}P]$ spectrum (Figure 3.1, A) collapses to a singlet resonance with the use of ^{31}P decoupling (Figure 3.1, B). The aromatic region of the spectra were as expected with three multiplet resonances being attributed to protons at the *ortho*-, *meta*- and *para*-positions of the phosphine phenyl substituents.

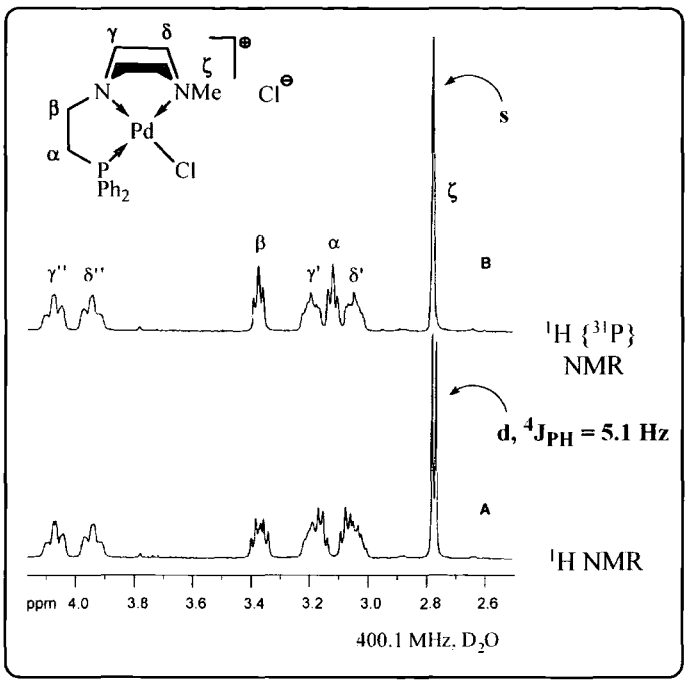

Figure 3.1: Comparative ^{1}H [^{31}P]/^{1}H {^{31}P} NMR spectra of **3.1-1** (aromatic region omitted for clarity)

The ^{13}C {^{1}H} NMR spectrum of **3.1-1** was entirely as expected with the required number of resonances being observed. The signal attributed to the α-bridge carbon was observed as a doublet resonance, resulting from coupling to phosphorus, although it is noteworthy that, in contrast to the ^{1}H NMR spectrum, the signal associated with the ζ-carbon was observed as a singlet resonance. All other aliphatic resonances were observed as the expected singlets, while the resonances in the aromatic region of the spectrum were observed as doublet signals, again as a result of coupling to the ^{31}P nucleus.

3.2.2 Crystallographic analysis of 3.1-1

3.2.2.1 Molecular structure of 3.1-1(a)

The $[PdCl\{\kappa^3\text{-PNNMe}\}]^+ Cl^-$ complex **3.1-1** was found to be very sparingly soluble in chlorinated solvents upon moderate heating. Slow evaporation of a highly dilute solution of **3.1-1** in CH_2Cl_2 gave rise to small crystals that were suitable for study by X-ray diffraction.

The resulting molecular structure obtained from these crystals proved surprising as, instead of the predicted $[PdCl\{\kappa^3\text{-PNNMe}\}]^+ Cl^-$ salt, the molecular structure of these crystals was shown to be that of the neutral P–N-chelated $[PdCl_2\{\kappa^2\text{-PN(NMe)}\}]$ **3.1-1(a)** complex as shown in Figure 3.2.

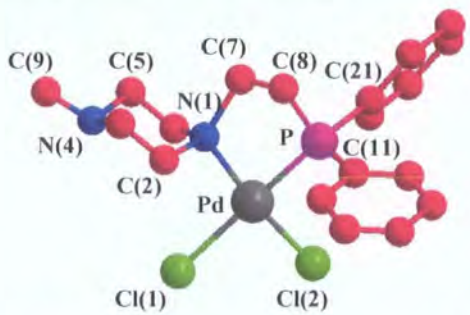

Figure 3.2: Ball and stick representation of **3.1-1(a)***

	Bond Length /Å			Bond Angle /°	
	3.1-1(a)	**2.4-1**		**3.1-1(a)**	**2.4-1**
Pd–P	2.2024(6)	-	N(1)–Pd–P	86.27(4)	-
Pd–N(1)	2.1181(16)	-	Cl(1)–Pd–Cl(2)	91.97(2)	-
Pd–Cl(1)	2.3903(6)	-	P–Pd–Cl(2)	87.98(2)	-
Pd–Cl(2)	2.3056(5)	-	N(1)–Pd–Cl(1)	94.02(4)	-
P–C(8)	1.8226(19)	1.859(3)	P–Pd–Cl(1)	174.94(2)	-
N(1)–C(7)	1.507(2)	1.469(4)	N(1)–Pd–Cl(2)	173.55(5)	-
P–C(Ph)	1.807[a]	1.839[a]	C(11)–P–C(21)	109.08(9)	102.43(14)
			C(2)–N(1)–C(6)	108.48(14)	109.5(2)
			C(3)–N(4)–C(5)	109.58(16)	109.2(3)
			$\Sigma_{\angle N(1)}$	328.86[b]	334.6[b]
			$\Sigma_{\angle N(4)}$	333.33[b]	330.7[b]
			$\Sigma_{\angle P}$	323.77[b]	301.98[b]
			N(1)–C(7)–C(8)–P	54.1(18)	– 42.5(3)

[a]average; [b]angle summation; e.s.d.'s in parentheses

Table 3.1: Selected bond distances (Å) and bond angles (°) for **3.1-1(a)** (Comparative values for free ligand **2.4-1** included)

* Molecular structure determination performed by Dr. A. S. Batsanov

The molecular structure of [$PdCl_2$\{κ^2-PN(NMe)\}] {**3.1-1(a)**} demonstrated the expected square planar geometry about the Pd centre, with the PNN(Me) ligand (**2.4-1**) coordinating the metal in a bidentate P–N fashion. A slight tetragonal distortion about the Pd centre was noted with the Cl(1) atom being located 5.07° above the N(1)–Pd–P plane whereas the Cl(2) atom was found to lie 2.92° below this plane. The ligand bite angle in **3.1-1(a)**, 86.27(4)°, is slightly less than the expected value of 90° and consequently, a pronounced twist in the N(1)–C(7)–C(8)–P ligand backbone {54.16(18)°} is observed to compensate for this smaller angle. As a result of the small bite angle of **3.1-1(a)**, slight distortions in the remaining angles about the Pd centre were noted, with the greatest of these being that for N(1)–Pd–Cl(1) {94.02(4)°}. Interestingly, comparison of the torsion angles of the complex **3.1-1(a)** and the free ligand **2.4-1** reveal opposite twists in the N(1)–C(7)–C(8)–P backbone between these two species. As expected, the phenyl rings at phosphorus adopt a staggered configuration with the intersection of their mean ring planes being 66.2°.

The P–Pd distance in **3.1-1(a)** is observed to be slightly longer than that of the N(1)–Pd bond with values within the range noted for similar $PdCl_2$ centres coordinated with five-membered P–N chelates.[9,10] Comparison of the palladium-chloride bond lengths reflects the greater *trans* influence of the phosphorus donor moiety compared with that of nitrogen, as the Pd–Cl(1) bond (located *trans* to P), is noticeably longer than Pd–Cl(2), again, in line with similar P–N-chelated complexes.[11]

The mono-coordinated piperazine ring of **3.1-1(a)** retains a chair conformation with little distortion noted upon coordination of the N(1) atom {by comparison with the free ligand structure (**2.4-1**)}. Indeed, comparison of the C(2)–N(1)–C(6) and C(3)–N(4)–C(5) angles between the structures of compounds **3.1-1(a)** and **2.4-1** reveals only a slight reduction in angle about N(1) upon complexation. Moreover, both the internal ring angles in complex **3.1-1(a)** are comparable to those of the free ligand **2.4-1**. As expected, the piperazino methyl substituent C(9) is found to lie in an equatorial position with the lone pair at N(4) occupying the axial position.

Comparison of the angle summations about the phosphine donors in **3.1-1(a)** and **2.4-1** reveals an opening of the angles upon coordination, presumably in order to relieve steric strain. In contrast, the angle at the N(1) donor narrows upon complexation, the angle in the complex **3.1-1(a)** {$\Sigma_{\angle N(1)} = 328.86°$} being noticeably smaller than that

of the free ligand **2.4-1** {$\Sigma_{\angle N(1)} = 334.6°$}. As expected, little change was noted in the angles about the pendant N(4) donor atom in **3.1-1**.

3.2.2.2 Synthesis and molecular structure of 3.1-1(c)

Following the unexpected isolation of a neutral bidentate form of **3.1-1** (which contrasts with the conductimetry data obtained), additional experiments were undertaken in order to unambiguously determine the molecular structure of **3.1-1** for the bulk sample of this compound in both the solution and the solid state. As **3.1-1** showed sparing solubility in alcoholic solvents, full multinuclear NMR spectroscopic analysis of this complex was obtained in CD_3OD, although the resulting $^1H/^{13}C$ {^1H} NMR spectra obtained closely resembled those in D_2O solution, again with a doublet resonance observed for the signal attributed to the ζ-*N*-methyl protons (indicating coordination of the terminal nitrogen donor to Pd). Due to the hygroscopic nature of methanol, the ^1H NMR spectra of **3.1-1** (CD_3OD) were dominated by the presence of adventitious water and thus attempts to chemically dry the NMR sample with $MgSO_4$ were undertaken.

The water-containing CD_3OD sample of **3.1-1** was treated with an excess of $MgSO_4$ and the resulting suspension allowed to stir at room temperature for several hours. Upon removal of the drying agent by filtration and subsequent analysis by NMR spectroscopy, slow evaporation of the sample afforded crystals which were suitable for analysis by X-ray diffraction. In contrast to the previously observed molecular structure of **3.1-1(a)** in which the MeNNP ligand was coordinated to Pd in a κ^2-P–N fashion, the crystals grown from the $MgSO_4$-dried methanol solution demonstrated tridentate ligation of the MeNNP ligand (**2.4-1**) to Pd. The surprising feature of this molecular structure, **3.1-1(c)**, was the nature of the anion as, instead of the expected chloride counterion, the anion was shown to be half an equivalent of the unusual $[Mg(SO_4)_2(H_2O)_4]^{2-}$ species along with three waters of crystallisation, as shown in Figure 3.3.

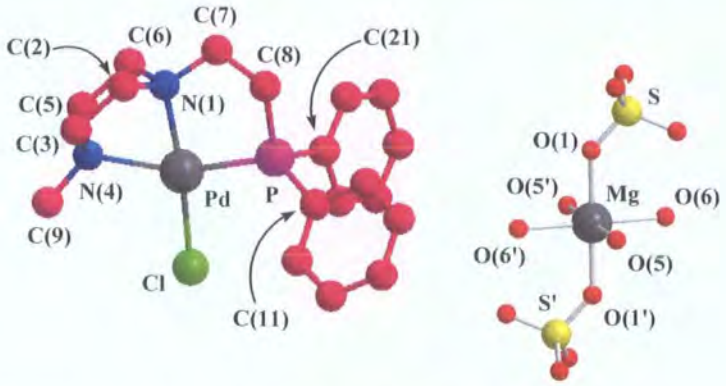

Figure 3.3: Ball and stick representation of **3.1-1(c)**[†]

	Bond Length /Å			Bond Angle /°	
	3.1-1(c)	**3.1-1(a)**		**3.1-1(c)**	**3.1-1(a)**
Pd–P	2.2243(5)	2.2024(6)	N(1)–Pd–P	87.35(4)	86.27(4)
Pd–N(1)	2.0325(14)	2.1181(16)	N(1)–Pd–N(4)	72.29(6)	-
Pd–N(4)	2.1426(14)	-	P–Pd–Cl(2)	99.520(18)	87.98(2)
Pd–Cl(1)	-	2.3903(6)	Cl(1)–Pd–Cl(2)	-	91.97(2)
Pd–Cl(2)	2.2897(5)	2.3056(5)	N(4)–Pd–Cl(2)	101.33(4)	-
P–C(8)	1.8322(17)	1.8226(19)	N(1)–Pd–Cl(1)	-	94.02(4)
N(1)–C(7)	1.496(2)	1.507(2)	N(4)–Pd–P	158.57(4)	-
P–C(Ph)	1.8096[a]	1.807[a]	P–Pd–Cl(1)	-	174.94(2)
O(1)–S	1.4733[a]	-	N(1)–Pd–Cl(2)	171.85(4)	173.55(5)
Mg–O(1)	2.0478[a]	-	C(11)–P–C(21)	104.75(8)	109.08(9)
Mg–O(5/5')	2.1005[a]	-	C(2)–N(1)–C(6)	107.60(13)	108.48(14)
			C(3)–N(4)–C(5)	107.27(14)	109.58(16)
Mg–O(6/6')	2.0520[a]	-	$\Sigma_{\angle N(1)}$	332.42[b]	328.86[b]
			$\Sigma_{\angle N(4)}$	329.86[b]	333.33[b]
			$\Sigma_{\angle P}$	319.84[b]	323.77[b]
			N(1)–C(7)–C(8)–P	47.41(17)	54.16(18)
			Mg–O(1)–S	137.64(8)	-

[a]average; [b]angle summation; e.s.d.'s in parentheses

Table 3.2: Selected bond lengths (Å) and bond angles (°) for **3.1-1(c)**
(Comparative parameters for complex **3.1-1(a)** included)

The $[PdCl(\kappa^3\text{-PNNMe})]^+$ cation **3.1-1(c)** adopts a distorted square planar geometry about the Pd centre. The N(1)–Pd–P bite angle in **3.1-1(c)** {87.35(4)°} is largely comparable to that observed in the related neutral bidentate complex **3.1-1(a)** {86.27(4)°} although a significantly less pronounced twist in the N(1)–C(7)–C(8)–P

[†] Molecular structure determination performed by Dr A. S. Batsanov

bridge was noted in **3.1-1(c)** {47.41(17)°} relative to that displayed in **3.1-1(a)** {54.16(18)°}. Binding of the terminal N(4) donor in **3.1-1(c)**, is shown to severely distort the coordination geometry about the Pd centre. The second N(1)–Pd–N(4) bite angle in **3.1-1(c)** {72.29(6)°} was notably smaller in comparison to that of the P–N chelate {87.35(4)°} as a result of the constrained nature of the piperazine ring, although this value is entirely consistent with the related compounds [$PdCl_2\{\kappa^2$-$MeN(CH_2CH_2)_2NMe)\}$] and [$PdCl_2\{\kappa^2$-$MeN(CH_2CH_2)_2NH\}$] (**3.4**, *vide infra*), which exhibit N–Pd–N bite angles of 71.8° [12] and 72.16(8)°, respectively.

The small N(1)–Pd–N(4) and N(1)–Pd–P bite angles in **3.1-1(c)** results in a small N(4)–Pd–P angle {158.57(4)°}. As a consequence of these steric constraints, opening of the N(4)–Pd–Cl(2) {101.33(4)°} and P–Pd–Cl(2) {99.520(18)°} angles are observed, placing the bound chloride in an approximate equidistant position between the P and N(4) donor atoms. Indeed, the N(1)–Pd–Cl(2) angle, 171.85(4)°, confirms this situation, with only a moderate deviation from linearity being noted. Furthermore, a slight tetrahedral distortion about Pd is noted in **3.1-1(c)**, with the phosphorus donor being projected 6.79° above the N(1)–Pd–N(4) plane, whilst the Cl(2) atom is found 5.25° below this plane.

Comparison of the Pd–P bond lengths between the bidentate κ^2-PN complex **3.1-1(a)** and the tridentate κ^3-PNN compound **3.1-1(c)** reveal this metric parameter to be slightly longer in **3.1-1(c)** with its distance of 2.2243(5) Å being entirely consistent with other systems containing *trans*-coordinating nitrogen and phosphorus donors arranged in a constrained ligand framework.[13] Conversely, the Pd–N(1) bond distance in **3.1-1(c)** {2.0325(14) Å} is noted to be slightly shorter than observed in **3.1-1(a)** {2.1181(16) Å}, although a longer Pd–N(4) bond length is evident in **3.1-1(c)** {2.1426(14) Å}. The coordination of the terminal N(4) donor to Pd induces a shortening of the Pd–Cl(2) bond in **3.1-1(c)** in comparison to the distance determined for **3.1-1(a)**.

Binding of the N(4) donor to the Pd centre in **3.1-1(c)** results in near-equivalence of the C(2)–N(1)–C(6) and C(3)–N(4)–C(5) internal piperazine ring angles, which is reflected in the rigidly symmetrical nature of this chelated ring. Summation of the angles about the nitrogen atoms reveal broadly comparable values for **3.1-1(c)** {$\Sigma_{\angle N(1)} = 332.42°$; $\Sigma_{\angle N(4)} = 329.86°$}, which are shown to be similar in magnitude to the bound N(1) atom in **3.1-1(a)** {$\Sigma_{\angle N(1)} = 328.86°$} as expected. Furthermore, the sum of angles about the phosphorus donor is shown to be largely comparable in both

complexes **3.1-1(a)** and **3.1-1(c),** with a near-perpendicular intersection of the phenyl ring mean planes in **3.1-1(c)** (91.7°).

Along with the $[PdCl\{\kappa^3\text{-PNNMe}\}]^+$ cation, the asymmetric unit of **3.1-1(c)** comprised half an equivalent of the $[Mg(SO_4)_2(H_2O)_4]^{2-}$ anion. The central magnesium atom binds two monodentate sulphato ligands in a *trans* arrangement, with four coordinated water molecules completing its octahedral coordination sphere. An extensive hydrogen bonding network is observed between the bound water molecules, the sulphato oxygen atoms and the uncoordinated waters present in the crystal lattice, Figure 3.4. While *bis* sulphato anions, such as those in the minerals leonite[14,15] $\{K_2Mg(SO_4)_2.4H_2O\}$ and bloedite[16,17] (astrakhanite[18]) $\{Na_2Mg(SO_4)_2.4H_2O\}$ are known, to date only one other example of this type of anion exists in a synthetic solid, namely that of *cis*-$Mg(SO)_4(H_2O)\{OC(NH_2)_2\}_4$.[19]

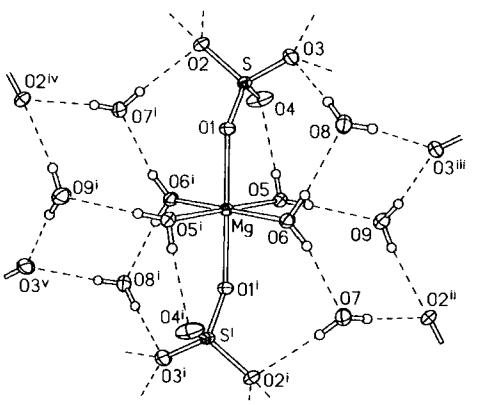

Figure 3.4: An anion and water molecules of crystallisation in structure **3.1-1(c)**.

Symmetry operations: (i) 1-x, 1-y, 1-z; (ii) x, ½ -y, ½ +z; (iii) 1-x, -y, 1-z; (iv) 1-x, ½ +y, ½ - z; (v) x, y+1, z.

Selected bond distances (Å) and angles (°): Mg–O(1) 2.048(1), Mg–O(5) 2.100(1), Mg–O(6) 2.052(1), S–O(1) 1.473(1), other S–O (av.) 1.473(4), O(1)–Mg–O(5) 90.17(5), O(1)–Mg–O(6) 90.16(5), O(5)–Mg–O(6) 92.02(5), Mg–O(1)–S 137.64(8).

It was subsequently found that this unusual $[PdCl\{\kappa^3\text{-PNNMe}\}]^+ Cl^-$ $.½[Mg(SO_4)_2(H_2O)_4]$ species **{3.1-1(c)}** could be prepared on a preparative scale by treating a suspension of $[PdCl\{\kappa^3\text{-PNNMe}\}]^+ Cl^-$ in methanol with an excess of $MgSO_4$ (*ca.* 5 eqv.). Whilst the $^1H/^{13}C\{^1H\}$ NMR spectra of **3.1-1(c)** were identical to that of

3.1-1(a) in CD_3OD, only a peak corresponding to $[PdCl\{\kappa^3\text{-PNNMe}\}]^+$ was observed by mass spectrometry for both complexes **3.1-1(a)** and **3.1-1(c)**. Although every effort was made to identify the aqua ligands of complex **3.1-1(c)**, due to rapid exchange on the NMR time-scale, these could not be observed by ^1H NMR spectroscopy and attempts to identify the $[Mg(SO_4)_2(H_2O)_4]^{2-}$ counterion by IR/Raman spectroscopy and mass spectrometry also proved unsuccessful although conductimetry experiments confirmed the presence of a 2:1 electrolyte (Λ_M (MeOH) = 360 Ω cm^2 mol^{-1}).[7,8] The crystals of **3.1-1(c)** were found to desolvate rapidly when isolated from methanolic solution and thus satisfactory CHN analyses could not be obtained. However, crystallisation of the preparative sample of **3.1-1(b)** afforded crystals with unit cells identical to those originally characterised therefore indicating that the obtained molecular structure of **3.1-1(c)** is likely to be representative of the bulk sample structure.

3.2.3 Verification of the solution behaviour of 3.1-1

3.2.3.1 Addition of Cl^- to 3.1-1

As two forms of the complex **3.1-1** were isolated and characterised crystallographically, it was questioned whether these isomers were interconverting in solution with the terminal amine displaying reversible coordination to the Pd centre, as shown in Scheme 3.2. Specifically, it was important to establish whether an equilibrium between the κ^2-PN and κ^3-PNN forms of **3.1-1** was operational with both forms being present in solution.

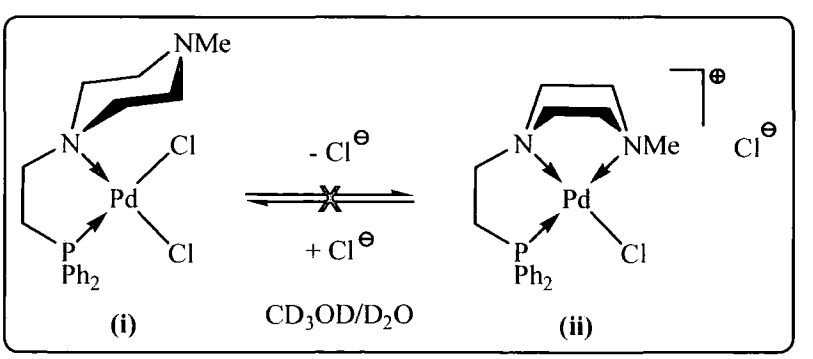

Scheme 3.2: Proposed interconversion of $[PdCl_2\{\kappa^2\text{-PN(NMe)}\}]$ and $[PdCl\{\kappa^3\text{-PNNMe}\}]^+ Cl^-$ forms of **3.1-1** in solution

In order to establish the possibility of interconversion of the bidentate $[PdCl_2\{\kappa^2\text{-PN(NMe)}\}]$ {Scheme 3.2, (**i**)} and tridentate $[PdCl\{\kappa^3\text{-PNNMe}\}]^+ Cl^-$ {Scheme 3.2, (**ii**)} forms of **3.1-1** in solution, a series of experiments were undertaken in which sources of Cl^- were added to D_2O and CD_3OD solutions of **3.1-1** and subsequently studied by ^1H and ^{31}P NMR spectroscopies. Initially D_2O and CD_3OD solutions of **3.1-1** were treated with NaCl, but it was found that no noticeable changes were observed spectroscopically in either sample upon the addition of up to 40 equivalents of NaCl. Addition of further amounts of NaCl resulted in the formation of yellow powders from both the D_2O and CD_3OD solutions of **3.1-1** with precipitation of this solid being complete, in both cases, upon the addition of *ca.* 100 equivalents of NaCl. It is believed that the precipitation of the complex from solution merely indicates the preferential solubility of NaCl in both D_2O and CD_3OD compared to that of compound **3.1-1**.

In order to circumvent the problem of precipitation, a biphasic experiment was attempted in which a solution of **3.1-1** in D_2O was suspended above an initially colourless solution of $CDCl_3$. Addition of increasing numbers of equivalents of NaCl (1 – 100 eqv.) resulted in the decolouration of the upper aqueous phase with concomitant colouration of the lower organic fraction, with no precipitation of the complex being noted under these conditions. Unfortunately, analysis of the samples by both ^1H and $^{31}P\{^1H\}$ NMR spectroscopies gave rise to spectra consistent with those of the parent complex with the signal attributed to the ζ-NMe protons being consistently observed as a doublet resonance by ^1H NMR spectroscopy. It is therefore concluded that an equilibrium of the type illustrated in Scheme 3.2 is not in operation under the conditions explored, however it is noteworthy that removal of the upper aqueous phase resulted in the immediate precipitation of **3.1-1** from the organic fraction.

3.2.3.2 Addition of phosphine to 3.1-1

Following the failure of the above experiments to establish the presence of interconversion of the neutral and cationic isomers of **3.1-1** in solution, an attempt to "trap out" the bidentate $[PdCl_2\{\kappa^2\text{-PN(NMe)}\}]$ complex **3.1-1(a)** by reaction with an ancillary phosphine ligand was made. Thus, a solution of **3.1-1** in D_2O was treated with

an equimolar quantity of the water-soluble phosphine $Cy_2PCH_2CH_2NMe_3Cl$ and the resulting solution again studied by ^1H and ^{31}P $\{^1H\}$ NMR spectroscopies, Scheme 3.3.

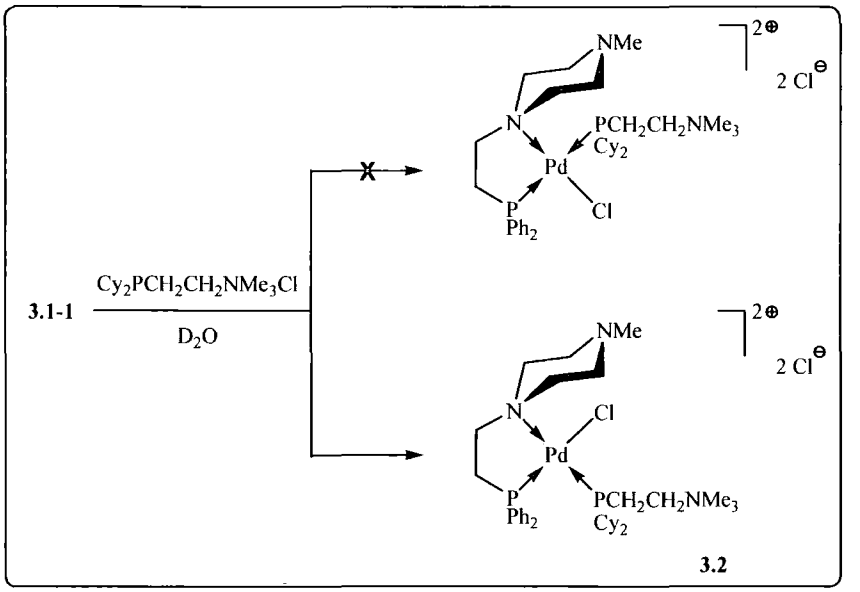

		^{31}P $\{^1H\}$ NMR*	
		δ_P	$^2J_{PP}$ /Hz
$[PdCl\{\kappa^3\text{-PNNMe}\}]^+ Cl^-$	**3.1-1**	+ 45.7	-
$[PdCl\{\kappa^2\text{-PN(NMe)}\}$ $\{\kappa^1\text{-P(Cy}_2)CH_2CH_2NMe_3\}]^{2+}$ $2Cl^-$	**3.2**	+ 54.8 + 44.1	12.0 12.0

*121.4 MHz, D_2O

Scheme 3.3: Synthesis of *cis*-$[PdCl\{\kappa^2\text{-PN(N)}\}\{\kappa^1\text{-P(Cy}_2)CH_2CH_2NMe_3\}]^{2+}$ $2Cl^-$ (**3.2**)

The ^{31}P $\{^1H\}$ NMR spectrum of **3.2** clearly demonstrates the presence of a second phosphine donor at the Pd centre with both signals being observed as doublet resonances. The small magnitude of the $^2J_{PP}$ coupling of these peaks (12.0 Hz) is indicative of the mutual *cis* coordination of these two donors about the metal site.[20,21] Regrettably, the ^1H and ^{13}C $\{^1H\}$ NMR spectra of the *bis*(phosphine) complex **3.2** were severely broadened and thus precluded full characterisation of this complex.

The observation of a *cis*-PP coordinated isomer of **3.2**, along with the lack of structural isomerisation exhibited by **3.1-1** in solution in the presence of excess chloride, indicate that **3.1-1** exists primarily in the tridentate $[PdCl\{\kappa^3\text{-PNNMe}\}]^+ Cl^-$ {**3.1-1(b)**} form. The bidentate $[PdCl\{\kappa^2\text{-PN(NMe)}\}]$ {**3.1-1(a)**} isomer (characterised only by crystallographic methods) is believed to comprise only a small percentage of the bulk sample as this isomer could not be identified by any other spectroscopic method. Moreover, conductimetry experiments on the bulk sample of **3.1-1** (*vide supra*)

were consistent with a 1:1 electrolyte, providing a further indication that this compound mainly adopts the ionic $[PdCl\{\kappa^3\text{-PNNMe}\}]^+ Cl^-$ {**3.1-1(b)**} formulation.

3.2.4 Characterisation of 3.1-2 and 3.1-3

The characterisation of complexes **3.1-2** and **3.1-3** proved substantially more challenging than that of **3.1-1** as both **3.1-2** and **3.1-3** exhibited only extremely limited solubility in all organic solvents. Whereas **3.1-3** was shown to be sparingly soluble in d_6-DMSO, by contrast, **3.1-2** was almost completely insoluble in this solvent and hence only ^1H NMR spectroscopic data could be reported for **3.1-3** (with the obtained spectrum being consistent with the proposed structure). In both cases, the poor solubility of both **3.1-2** and **3.1-3** precluded the acquisition of satisfactory ^{13}C $\{^1H\}$ NMR spectra. Both complexes however afforded satisfactory mass spectrometric analysis (ES^+) with molecular ion peaks corresponding to $[PdCl\{\kappa^3\text{-PNE}\}]^+$ being observed (**3.1-2**: *m/z* = 441.9; **3.1-3**: *m/z* = 457.9). Satisfactory CHN analyses were also obtained corresponding to an empirical formula of $[PdCl_2\{PNE\}]$ for both **3.1-2** (E = O) and **3.1-3** (E = S).

3.2.5 Solid-state NMR spectroscopy of 3.1-1 – 3.1-3 and 3.4

In order to confirm the nature of ligand coordination in all complexes **3.1-1** – **3.1-3** and to verify their composition in the bulk sample, a series of ^{31}P and natural abundance ^{15}N solid state NMR experiments were undertaken. To date, few ^{15}N solid-state NMR studies of metal-coordinated amines exist and therefore the $[PdCl_2\{\kappa^2\text{-}MeN(CH_2CH_2)_2NH\}]$ complex **3.4** was prepared in order to provide a reference for the ^{15}N NMR spectroscopic data obtained for complexes **3.1-1** – **3.1-3**.

The synthesis of $[PdCl_2\{\kappa^2\text{-}MeN(CH_2CH_2)_2NH\}]$ (**3.4**) was performed according to a variation of a literature procedure,[22] namely by reaction of neat *N*-methylpiperazine with K_2PdCl_4. The desired product was afforded in excellent yield (94 %). Analysis of **3.4** by NMR spectroscopy and mass spectrometry gave data consistent with the proposed structure. Complex **3.4** proved an ideal choice for a ^{15}N NMR

spectroscopic reference due to facile differentiation of the two observed resonances (*via* depolar dephasing experiments) therefore permitting a direct comparison between the NMe donor components in compounds **3.4** and **3.1-1**.

		Nucleus	NMR Spectroscopy		Assignment
			δ	$\nu_{1/2}$ /Hz	
$[PdCl\{\kappa^3\text{-}PNNMe\}]^+ Cl^-$	**3.1-1**	$^{31}P^a$	+ 55.1	1.5	$Ph_2\underline{P}$
		$^{15}N^b$	– 331.2	25	$\underline{N}(CH_2CH_2)_2NMe$
			– 342.7	20	$N(CH_2CH_2)_2\underline{N}Me$
$[PdCl\{\kappa^3\text{-}PNO\}]^+ Cl^-$	**3.1-2**	$^{31}P^a$	+ 48.6, + 51.9, + 53.5, + 55.8[c]	-	$Ph_2\underline{P}$
		$^{15}N^b$	– 290.4, – 312.8, – 332.3, – 338.9	-	$\underline{N}(CH_2CH_2)_2O$
$[PdCl\{\kappa^3\text{-}PNS\}]^+ Cl^-$	**3.1-3**	$^{31}P^a$	+ 51.1	2.0	$Ph_2\underline{P}$
		$^{15}N^b$	– 329.9	20	$\underline{N}(CH_2CH_2)_2S$
$[PdCl_2\{\kappa^2\text{-}MeN(CH_2CH_2)_2NH\}]$	**3.4**	$^{15}N^b$	– 350.2	33	$HN(CH_2CH_2)_2\underline{N}Me$[d]
			– 362.5	51	$H\underline{N}(CH_2CH_2)_2NMe$[d]

[a]121.4 MHz, [b]30.4 MHz, [c]overlapping resonances; [d]assignment confirmed by dipolar dephasing experiments

Table 3.3: Selected solid-state NMR spectroscopic data for **3.1-1** – **3.1-3** and **3.4**

From the natural abundance ^{15}N NMR spectroscopic data, Table 3.3, it is clear that complexes **3.1-1** and **3.1-3** exist in the tridentate $[PdCl\{\kappa^3\text{-}PNE\}]^+ Cl^-$ form in the solid state from comparison of their respective chemical shifts with the $[PdCl_2\{\kappa^2\text{-}NN\text{-}(Me)ppzH\}]$ reference species **3.4**. In **3.1-1**, two environments are clearly observed in ^{15}N NMR spectra with the $N(CH_2CH_2)_2\underline{N}Me$ donor ($\delta_N = -342.7$) coming into resonance in the same region as the $HN(CH_2CH_2)_2\underline{N}Me$ donor in the $[PdCl_2\{\kappa^2\text{-}NN\text{-}(Me)ppzH\}]$ reference compound **3.4** ($\delta_N = -350.2$). Additionally, the chemical shift of the $\underline{N}(CH_2CH_2)_2NMe$ donor in **3.1-1** is shown to be broadly similar to that for the $\underline{N}(CH_2CH_2)_2S$ donor in complex **3.1-2** with $\delta_N = -331.2$ and -329.9 for compounds **3.1-1** and **3.1-3**, respectively. In both complexes **3.1-1** and **3.1-3**, only one environment is observed in their ^{31}P NMR spectra as expected, with the observed chemical shifts comparing favourably with the solution-state data (Scheme 3.1).

The ^{31}P and ^{15}N NMR spectral data for the $[PdCl\{\kappa^3\text{-}PNO\}]^+ Cl^-$ complex **3.1-2** are somewhat more complicated as, in each spectrum, four separate environments are observed. As previous analyses of this compound by CHN and mass spectrometry

indicated an empirical formula of [$PdCl_2${PNO}], it is presumed that the PNO ligand **2.4-2** binds to the Pd centre in a number of different ways. This difference in coordination behaviour in **3.1-2** can tentatively be ascribed to the presence of the harder oxygen donor in the parent ligand, which has a lower affinity for the soft palladium metal, thus presumably favouring bidentate κ^2-PN chelation of the Pd centre over the alternative tridentate ligation.

3.2.6 Molecular structure of 3.4

The reference compound [$PdCl_2\{\kappa^2$-*NN*-(Me)ppzH}] **3.4** was found to produce crystals suitable for study by X-ray diffraction upon slow cooling to 5 °C of a hot aqueous solution of this complex. The molecular structure of **3.4** confirmed the bidentate ligation of the Pd centre by the piperazine ring as shown in Figure 3.4.

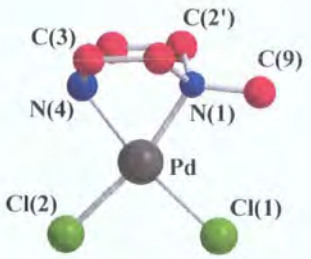

Figure 3.4: Ball and stick representation of **3.4**‡

	Bond Length /Å		**Bond Angle /°**
Pd–N(1)	2.041(2)	N(1)–Pd–N(4)	72.16(8)
Pd–N(4)	2.066(2)	Cl(1)–Pd–Cl(2)	93.37(2)
Pd–Cl(1)	2.3107(7)	N(1)–Pd–Cl(1)	96.36(6)
Pd–Cl(2)	2.3055(6)	N(4)–Pd–Cl(2)	98.12(5)
N(1)–C(9)	1.478(3)	N(1)–Pd–Cl(2)	170.28(6)
N(4)–H(1)	0.83(4)	N(4)–Pd–Cl(1)	168.52(6)
		C(2)–N(1)–C(2')	109.12(18)
		C(3)–N(1)–C(3')	107.92(17)
		$\Sigma_{\angle N(1)}$	331.26[a]
		$\Sigma_{\angle N(4)}$	329.52[a]

[a]angle summation, e.s.d.'s in parentheses

Table 3.4: Selected bond lengths (Å) and bond angles (°) for **3.4**

‡ Molecular structure determination performed by Dr A. S. Batsanov

The neutral [$PdCl_2\{\kappa^2$-$MeN(CH_2CH_2)_2NH\}$] complex **3.4** displayed a symmetrical, but distorted, square planar geometry about the Pd centre as a result of the constraining nature of the chelating piperazine unit. The small N(1)–Pd–N(4) bite angle {72.16(8)°} was shown to be consistent with that observed in the chelating diamine in complex **3.3-1(b)** {72.29(6)°} (*vide supra*) and the related [$PdCl_2\{\kappa^2$-*NN*-$MeN(CH_2CH_2)_2NMe)\}$] species {71.8°}.[12] This small bite angle in **3.4** is reflected in the larger N(1)–Pd–Cl(1) {96.36(6)°} and N(4)–Pd–Cl(2) {98.12(5)°} angles. As expected, only slight differences were noted in the Pd–N(1) {2.041(2) Å} and Pd–N(4) {2.066(2) Å} bond distances although the Pd–Cl(1) bond length {2.3107(7) Å} was observed to be slightly longer than the corresponding Pd–Cl(2) distance {2.3055(6) Å}. Summation of the angles about the nitrogen donors reveal a larger angle about the tertiary amine N(1) {$\Sigma_{\angle N(1)} = 331.26°$}, than the secondary amine N(4) {$\Sigma_{\angle N(4)} = 329.52°$} although the C(2)–N(1)–C(2′) {109.12(18)°} and C(3)–N(1)–C(3′) {107.92(17) °} angles are broadly comparable.

3.2.7 Synthesis and molecular structure of 3.1-4

In a further attempt to clarify the nature of the coordination of the PNE ligands to the '$PdCl_2$' fragments, the corresponding [$PdCl_2\{\kappa^2$-$PN(CH_2)\}$] complex **3.1-4** was synthesised. As the PNC ligand **2.4-4** comprises a piperidine ring, it lacks a heteroatom in the 4-position of the saturated ring thus allowing only P–N coordination of this ligand to a '$PdCl_2$' moiety. The bidentate complex **3.1-4** was synthesised using an analogous methodology to that used to prepare complexes **3.1-1** – **3.1-3**, *i.e.* by reaction of equimolar quantities of the PNC ligand with [$PdCl_2(MeCN)_2$] as detailed in Scheme 3.4. In an identical manner to the synthesis of **3.1-1** – **3.1-3**, addition of the ligand **2.4-4** to a CH_2Cl_2 solution of the palladium precursor resulted in the immediate formation of a yellow precipitate.

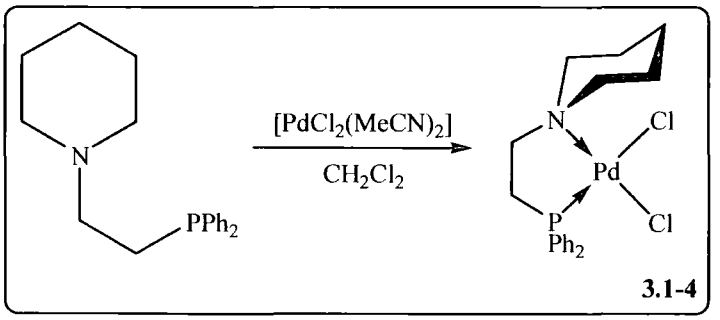

3.1-4

		Yield	^{31}P {^{1}H} NMR	
			δ_P (complex)[a]	δ_P (parent ligand)[b]
[$PdCl_2$\{κ^2-PN(CH_2)\}]	**3.1-4**	57 %	+ 49.9 (s)	– 17.8 (s)

[a]161.9 MHz, d_6-DMSO; [b]202.3 MHz, $CDCl_3$

Scheme 3.4: Synthesis and ^{31}P {^{1}H} NMR spectroscopic data of [$PdCl_2$\{κ^2-PN(CH_2)\}] (**3.1-4**)

The [$PdCl_2$\{κ^2-PN(CH_2)\}] complex **3.1-4** was isolated in good yield following isolation and purification. In contrast to the complexes **3.1-1** – **3.1-3**, **3.1-4** was found to have sparing solubility in common organic solvents such as $CHCl_3$ (presumably as a result of its neutral character) and showed appreciable solubility in polar solvents such as MeOH and DMSO. The ^{31}P {^{1}H} NMR spectrum of **3.1-4** exhibited a sharp singlet resonance (δ_P = 49.9 ppm) with a large coordination chemical shift ($\Delta\delta_P$ ($\delta_{coordinated}$ – δ_{free}) = + 67.7 ppm) consistent with binding of the phosphorus to the palladium centre.[6] Additionally, a molecular ion corresponding to $[M–Cl]^+$ (*m/z* = 438.1) was observed by mass spectrometry ($MALDI^+$), while satisfactory CHN analyses consistent with the proposed formulation were obtained.

The higher solubility of **3.1-4** in DMSO permitted the full characterisation of this complex by multinuclear NMR spectroscopy. The ^{1}H NMR spectrum of **3.1-4** was consistent with the proposed bidentate structure with the expected number of aliphatic resonances being observed. Interestingly, the protons at the ε-position of the ring were not observed as a 2H multiplet, but appeared as two individual resonances (each integrating to 1H) with the signal at highest frequency being attributed to that in the *endo*-position of the saturated ring due the closer proximity of this substituent to the Pd centre, as shown in Figure 3.5. Conversely, the resonance at lower frequency is associated with the proton in the *exo*-position in accordance with similar observations

made previously.[23] The aromatic region of this spectrum was as expected, with an overall integration of 10H corresponding to the two phenyl substituents at phosphorus.

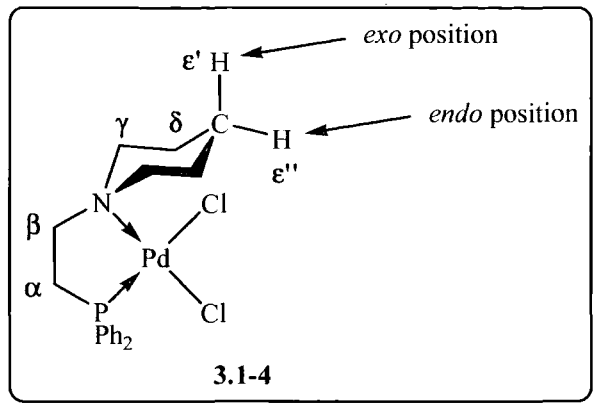

3.1-4

Figure 3.5: Designation of *endo* and *exo* ε-protons in **3.1-4**

The ^{13}C $\{^1H\}$ NMR spectrum of **3.1-4** was also consistent with bidentate κ^2-P–N ligation to Pd, with the expected number of signals being observed. The α-bridge carbon is observed as a doublet whilst all other aliphatic signals appear as singlet resonances. The signals attributed to the phenyl substituents are all observed as doublets resulting from coupling to the ^{31}P nucleus.

It is noteworthy that, in contrast to the parent ligand **2.4-4**, fluxionality of the uncoordinated ring fragment in **3.1-4** was not observed in solution, something that is attributed to binding of the heterocyclic nitrogen to palladium. Indeed, the well-resolved ^1H and ^{13}C $\{^1H\}$ NMR spectra of **3.1-4** at 20 °C are reminiscent of those observed for the hydrochloride ligand derivative **2.5-4** in which protonation at the tertiary nitrogen eliminates the saturated ring inversion processes.

Upon slow evaporation of a dilute solution of **3.1-4** in $CHCl_3$ under air, crystals suitable for analysis by X-ray diffraction were obtained, the molecular structure being shown in Figure 3.6. The gross molecular structure of **3.1-4** is consistent with the structure predicted by NMR spectroscopy/mass spectrometry, with the ligand binding to Pd in a κ^2-P–N bidentate manner.

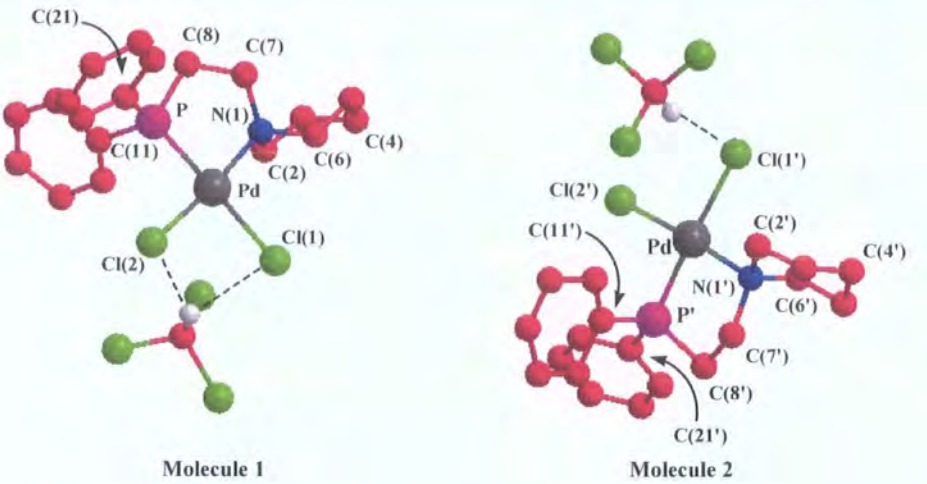

Figure 3.6: Ball and stick representation of **3.1-4**[§]

	Bond Length /Å			Bond Angle /°	
	Molecule 1	Molecule 2		Molecule 1	Molecule 2
Pd–P	2.199(6)	2.197(7)	N(1)–Pd–P	85.7(5)	86.3(5)
Pd–N(1)	2.100(17)	2.098(17)	Cl(1)–Pd–Cl(2)	90.7(2)	91.5(2)
Pd–Cl(1)	2.395(6)	2.380(6)	P–Pd–Cl(2)	88.7(2)	89.4(2)
Pd–Cl(2)	2.313(6)	2.315(6)	N(1)–Pd–Cl(1)	94.9(5)	93.0(5)
P–C(8)	1.86(2)	1.83(2)	P–Pd–Cl(1)	178.4(2)	176.6(2)
N(1)–C(7)	1.49(3)	1.50(3)	N(1)–Pd–Cl(2)	174.3(5)	173.8(5)
P–C(Ph)	1.83(2)[a]	1.82(2)[a]	C(11)–P–C(21)	105.8(9)	107.5(11)
H(1)–Cl(1)	3.62(2)	3.59(2)	C(2)–N(1)–C(6)	104.8(16)	108.8(17)
H(1)–Cl(2)	3.38(2)	-	C(3)–C(4)–C(5)	109(2)	110(2)
			$\Sigma_{\angle N(1)}$	322.5[b]	329.0[b]
			$\Sigma_{\angle P}$	323.2[b]	322.0[b]
			N(1)–C(7)–C(8)–P	43(2)	51(3)

[a]average; [b]angle summation; e.s.d.'s in parentheses

Table 3.5: Selected bond distances (Å) and bond angles (°) for **3.1-4**

The molecular structure determination revealed eight molecules of **3.1-4** in the unit cell, as shown in Figure 3.6. The asymmetric unit was found to comprise two molecules of chloroform linked to the palladium chloride substituents by hydrogen bonds. Interestingly, the chloroform hydrogen atom associated with Molecule 1 is found to hydrogen-bond to both metal-bound chlorides, whilst the solvent unit associated with

[§] Molecular structure determination performed by Dr A. S. Batsanov

Molecule 2 exhibits only one hydrogen bond to the C(1′) atom with no second hydrogen bond being observed.

The geometry about Molecule 1 is rigidly square planar with no appreciable distortion being noted, however Molecule 2 experiences a slight tetragonal distortion with the Cl(1′) atom being located 3.35° above the P–Pd–N(1) plane, whilst the Cl(2′) atom is found to lie 4.41° below this plane. The P–N bite angles of the two molecules are broadly comparable {Molecule 1: 85.7(5)°; Molecule 2: 86.3(5)°} with both being slightly smaller than the ideal value of 90°. As was found in the related structures of **3.1-1(a)** and **3.1-1(b)**, the N(1)–C(7)–C(8)–P backbone was found to adopt a staggered conformation in both molecules of **3.1-4**, although it is noteworthy that the twist of this N(1)–C(7)–C(8)–P bridge experienced in Molecule 1 {43(2)°} is significantly less that that observed in Molecule 2 {51(3)°}; however this appears to have little impact on the gross molecular geometry.

Comparison of the Pd–P bond lengths in the two molecules of **3.1-4** reveal these to be near-identical {Molecule 1: 2.199(6) Å; Molecule 2: 2.197(7) Å } and significantly longer than observed for the Pd–N bond lengths {Molecule 1: 2.100(17) Å; Molecule 2: 2.098(17) Å}, however both sets of bond distances are entirely in line with typical values observed in complexes of this nature {Pd–P: 2.3 – 2.35 Å; Pd–N: 2.0 – 2.2 Å}.[2] In both Molecules 1 and 2, the greater *trans*-influence of phosphorus relative to that of nitrogen is evident in the differing Pd–Cl bond distances as the Pd–Cl(1/1′) (lying *trans* to P) has an average bond length of 2.388 Å whereas the average Pd–Cl(2/2′) (situated *trans* to N) bond distance is considerably shorter as expected, being 2.314 Å.[24]

The piperidine ring in both molecules of **3.1-4** is found to adopt the expected chair conformation with the C(2)–N(1)–C(6) bond angle {Molecule 1: 104.8(16)°; Molecule 2: 108.8(17)°} and is found to be comparable to that observed for the bidentate complex **3.1-1(a)** ([$PdCl_2\{\kappa^2$-PN(NMe)}]; C(2)–N(1)–C(6): 108.48(14)°) and consistent with other Pd-bound piperidine ligands.[25] The C(3)–C(4)–C(5) angle of **3.1-4** {Molecule 1: 109(2)°; Molecule 2: 110(2)°} is found to be near-tetrahedral as expected. Summation of the bond angles about the nitrogen and phosphorus donor atoms in **3.1-4** reveal these angles to be broadly similar {$\Sigma_{\angle N(1)} = 325.8°$; $\Sigma_{\angle P} = 322.6°$}, with the angle summation being entirely consistent with those previously observed in the molecular structure of [$PdCl_2\{\kappa^2$-PN(NMe)] {**3.1-1(a)**} {$\Sigma_{\angle N(1)} = 328.86°$; $\Sigma_{\angle P} = 323.77°$}.

3.2.8 Attempted synthesis of 3.1-5

The attempted synthesis of **3.1-5** was performed in an analogous manner to that of **3.1-1 – 3.1-4**, *i.e.* by reaction of stoichiometric quantities of *N*-phenyl-*N'*-ethylene-diphenylphosphine (**2.4-5**) with $[PdCl_2(MeCN)_2]$ in CH_2Cl_2, as shown in Scheme 3.5. In contrast to the syntheses of the related complexes **3.1-1 – 3.1-4**, rapid precipitation of solid was not noted in this reaction, although upon allowing the reaction mixture to stir at room temperature for 12h, the formation of a dark brown solid and a light orange solution was observed to occur.

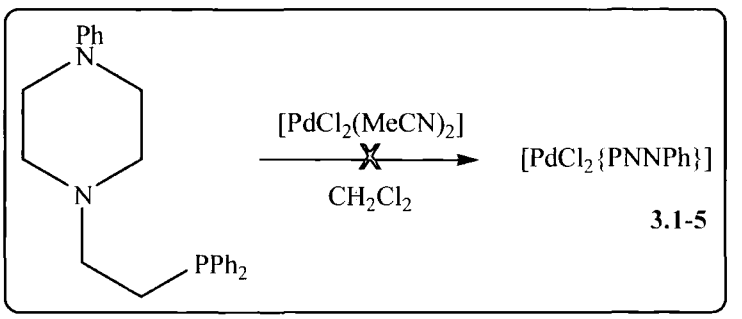

Scheme 3.5: Attempted synthesis of $[PdCl_2\{PNNPh\}]$ (**3.1-5**)

Upon separation of the brown precipitate from the supernatant solution by filtration, this solid again was shown to be almost completely insoluble in common organic solvents (*e.g.* $CDCl_3$, d_6-DMSO) which precluded its analysis by NMR spectroscopy. Analysis of the precipitated solid by mass spectrometry disappointingly did not indicate the presence of the target product, as only a number of presumed degradation products were observed. Subsequent analysis of the soluble orange material by $^{31}P\{^1H\}$ NMR spectroscopy/mass spectrometry also revealed the presence of presumed decomposition products with no trace of the target product being observed in this fraction.

There remain few examples of *N*-phenylpiperazine-containing ligand systems in which the aliphatic tertiary amine has been demonstrated to coordinate to metal centres,[26,27] although to date, no examples of κ^2-*NN*-chelating *N*-phenylpiperazine complexes exist. It has been demonstrated that *N*-phenylpiperazine exhibits a strong preference to exist solely in the chair conformation in solution,[28,29] something which is presumed to disfavour the chelation of the saturated ring to metal sites. It is surprising

however that the alternative neutral [$PdCl_2\{\kappa^2$-PN(NPh)}] complex was not observed in place of the target cationic species **3.1-5**, although the reasons for the observed ligand degradation remain unclear.

3.2.9 Complexation of 2.4-7 with '$PdCl_2$' fragments

Following the successful synthesis of the $[PdCl\{\kappa^3$-PNE}$]^+$ Cl^- complexes **3.1-1** – **3.1-3** and the [$PdCl_2\{\kappa^2$-PN(CH_2)}] compound **3.1-4**, the complexation of the related PNNP ligand **2.4-7** with '$PdCl_2$' fragments was undertaken. Given the potentially four-coordinate nature of **2.4-7**, two principal coordination modes were envisaged for the complexation of this ligand to a single '$PdCl_2$' fragment; **2.4-7** could bind to Pd in an analogous manner to that shown for complexes **3.1-1** and **3.1-3**, *i.e.* in a three coordinate [κ^3-PNN(P)] manner {**3.1-6(a)**} (maintaining a pendent phosphine donor component). Alternatively, coordination of all four ligand donor fragments of **2.4-7** could occur with the resulting complex being that of the doubly-charged species **3.1-6(b)**.

The synthesis of the monometallic complex **3.1-6** was attempted as shown in Scheme 3.6 (A). In an analogous manner to the preparation of complexes **3.1-1** – **3.1-4**, equimolar quantities of **2.4-7** and [$PdCl_2(MeCN)_2$] were allowed to react at room temperature in CH_2Cl_2, although in contrast to **3.1-1** – **3.1-4**, the formation of a precipitate was not observed even with prolonged reaction times. Although the soluble nature of this product facilitated its analysis in the solution state, the target product was not observed by either ^1H or ^{31}P $\{^1H\}$ NMR spectroscopies as only severely broadened resonances were observed in both spectra. In an effort to establish whether any dynamic processes associated with coordination were operative upon binding of **2.4-7** to the single Pd site, low temperature NMR spectroscopic studies of **3.1-6** were undertaken. However, these spectra recorded at – 50 °C merely demonstrated the presence of numerous unassignable resonances with the target species not being identified. It is noteworthy that a resonance corresponding to a free phosphine donor {δ_P = – 19.1 (s)} was not observed in the low temperature ^{31}P $\{^1H\}$ NMR spectrum of **3.1-6**.

Additionally, analysis of the product by mass spectrometry ($MALDI^+$) also failed to confirm the presence of the desired complex as only the presence of numerous Pd-containing high molecular weight products was observed (by comparison with

theoretical isotope patterns). Despite extensive efforts, structural assignments of these products could not be made.

From the results of this complexation, it is concluded that simple ligation of the PNNP ligand (**2.4-7**) to Pd does not take place. Specifically, the formation of a mono-metallic 'PNNP-$PdCl_2$' complex does not occur. It is believed that the tetradentate ligand **2.4-7** participates in a number of intermolecular ligations between different Pd sites, resulting in the formation of polymetallic arrays, which proved impossible to characterise.

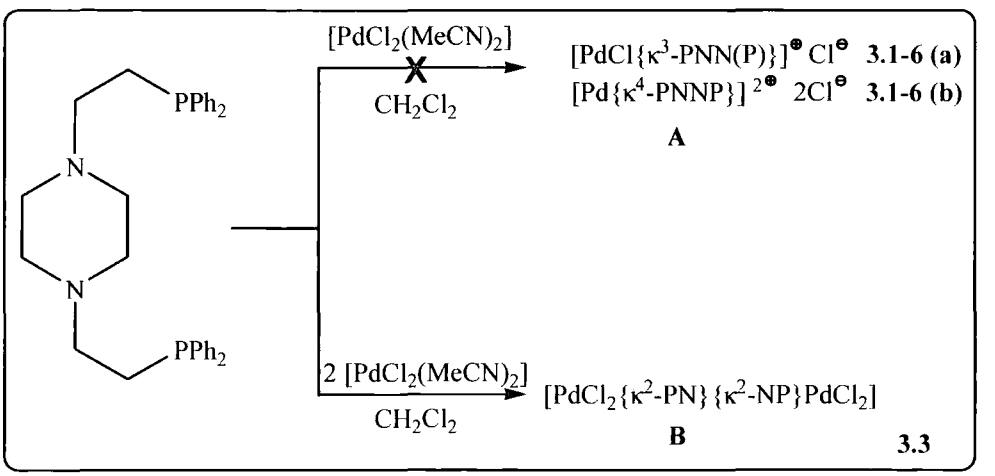

Scheme 3.6: Complexation of **2.4-7** with '$PdCl_2$' fragments

As the simple coordination of the PNNP ligand to a '$PdCl_2$' fragment is clearly a disfavoured process, the complexation of **2.4-7** to '$PdCl_2$' was repeated with a modification of the reaction stoichiometry, Scheme 3.6 (B). By reaction of this tetradentate species with two equivalents of $[PdCl_2(MeCN)_2]$, it was hoped that coordination of the two metal centres to the ligand framework would occur with both metal centres being ligated in a P^N fashion in the resulting bimetallic species **3.3**.

Upon reaction of the **2.4-7** with two equivalents of $[PdCl_2(MeCN)_2]$, the formation of an orange precipitate was noted although this product (**3.3**) demonstrated extremely limited solubility in organic solvents, which precluded its analysis by NMR spectroscopy. However the presence of the target product was not observed by mass spectrometry (ES/MALDI) as again only a number of high molecular weight Pd-containing species were noted.

Again, it is believed that the simple complexation of **2.4-7** to Pd centre is not a favoured process. The potentially tetradentate nature of **2.4-7** presents the metal with a number of potential coordination modes, which results in the formation of more than one product. From the mass spectra of both products **3.1-6** and **3.3**, it is presumed that the favoured outcome of these complexations (regardless of reaction stoichiometry) is the formation of extended polymetallic arrays rather than the target monometallic products although it is regrettable that the products from these reactions could not be isolated and characterised.

3.3 Complexation of PNE ligands with 'PdCl(Me)' fragments (3.5-1 – 3.5-4)

In an effort to further explore the coordination of the PNE ligands with Pd(II) centres, the complexation of the PNE ligands **2.4-1** – **2.4-4** was undertaken with [PdCl(Me)(cod)]. Specifically, given the sparing solubility of the previously discussed palladium dichloride complexes **3.1-1** – **3.1-4** in organic solvents, it was thought that the replacement of one chloride substituent at Pd with a methyl group would result in a greater degree of solubility in the resulting complexes, thus facilitating study of the resulting [PdCl(Me){PNE}] compounds in the solution state.

The complexation of **2.4-1** – **2.4-4** with 'PdCl(Me)' was undertaken as detailed in Scheme 3.7, *i.e.* by reaction of equimolar quantities of the required PNE ligand with [PdCl(Me)(cod)] in CH_2Cl_2. In contrast to the related [$PdCl_2${PNE}] complexes **3.1-1** – **3.1-4**, no solid precipitation was noted in the formation of **3.5-1** – **3.5-4** with the obtained products demonstrating considerable solubility in chlorinated solvents.

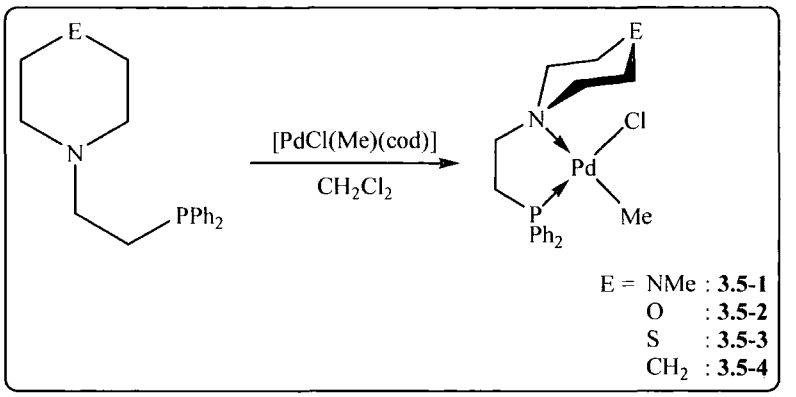

		MS		Yield	$^{31}P\{^1H\}$ NMR	
		m/z $[M-Cl]^+$	*m/z* $[M-Me]^+$		δ_P* (Complex)	δ_P§ (Parent phosphine)
[PdCl(Me){κ^2-PN(NMe)}]	**3.5-1**	433.0[a]	454.3[a]	76 %	+ 45.7 (s)	– 19.1 (s)
[PdCl(Me){κ^2-PN(O)}]	**3.5-2**	440.1[b]	420.1[b]	69 %	+ 43.1 (s)	– 18.1 (s)
[PdCl(Me){κ^2-PN(S)}]	**3.5-3**	436.0[b]	458.0[b]	66 %	+ 43.5 (s)	– 19.2 (s)
[PdCl(Me){κ^2-PN(CH_2)}]	**3.5-4**	418.1[b]	438.0[b]	68 %	+ 44.6 (s)	– 17.8 (s)

*161.9 MHz, $CDCl_3$; §202.3 MHz, $CDCl_3$; [a]EI^+; [b]$MALDI^+$ (dithranol matrix)

Scheme 3.7: Synthesis, mass spectrometric and $^{31}P\{^1H\}$ NMR spectroscopic data of **3.5-1** – **3.5-4**

All products **3.5-1** – **3.5-4** were isolated as yellow-orange powders in good yield following isolation and purification, with satisfactory mass spectrometric and CHN analyses being obtained in all cases. These complexes exhibited a single resonance in their $^{31}P\{^1H\}$ NMR spectra at higher frequency than the signal observed for their parent phosphines, indicating the formation of one structural isomer in all cases. Complexes **3.5-1** – **3.5-4** demonstrated an average complexation shift {$\Delta\delta_P$ ($\delta_{coordinated} - \delta_{free}$) = + 62.8 ppm (average)} indicating phosphine coordination to the metal fragment.[6] Furthermore, the $^{31}P\{^1H\}$ chemical shifts of complexes **3.5-1** – **3.5-4** were shown to be comparable with other [PdCl(Me){κ^2-PN}] complexes in the literature.[30,31]

The ^1H NMR spectra of **3.5-1** – **3.5-4** all clearly demonstrated the presence of the metal-bound methyl group by the presence of a signal at low frequency (*ca.* δ_H =

0.60 ppm). In compounds **3.5-2** – **3.5-4**, this resonance was clearly observed as a doublet, with the magnitude of the $^{3}J_{PH}$ coupling being consistent with similar compounds in the literature,[32] however, the palladium methyl protons were observed as a singlet resonance in **3.5-1** with no coupling to phosphorus observed.

Whilst the α- and β-bridge protons were observed as well-defined multiplets in all complexes **3.5-1** – **3.5-4**, the resonances attributed to the γ- and δ-ring protons in complexes **3.5-1** – **3.5-3** were observed to exhibit moderate broadening at 20 °C. Upon lowering the temperature of the samples, the aliphatic regions of these spectra were observed to sharpen, a situation consistent with the bidentate κ^2-PN ligand coordination to the 'PdCl(Me)' centre. Additionally, the signal associated with the ζ-*N*-C$\underline{H}_3$ protons in the [PdCl(Me){κ^2-PN(NMe)}] compound **3.5-1** was observed as a singlet resonance (in contrast to the [PdCl{κ^3-PNNMe}]$^+$ Cl$^-$ complex **3.1-1** in which this signal was observed as a doublet), providing an indication that this terminal donor fragment is not bound to the metal centre in this complex. Interestingly, in contrast to the [PdCl$_2${κ^2-PN(CH$_2$)}] compound **3.1-4**, in which the ε-ring protons were observed as two resonances, the ε-protons of the related complex [PdCl(Me){κ^2-PN(CH$_2$)}] (**3.5-4**) were noted to appear as a single 2H multiplet. In all complexes **3.5-1** – **3.5-4**, the aromatic regions of these spectra were as expected and unremarkable.

On the basis of electronic grounds, the phosphine donor in **3.5-1** – **3.5-4** was presumed to lie *trans* to the chloride donor with the amine and methyl functionality adopting a mutual *trans* arrangement.[33,34,35] In an effort to confirm this proposed regiochemistry, a series of 1D nOe difference NMR experiments were undertaken, with a representative example being shown in Figure 3.7. In all cases, selective irradiation of the metal-bound methyl gave rise to only one response corresponding to the *ortho*-phenyl protons, thus indicating the mutual *cis* arrangement of the methyl and phosphine ligands about the palladium centre.

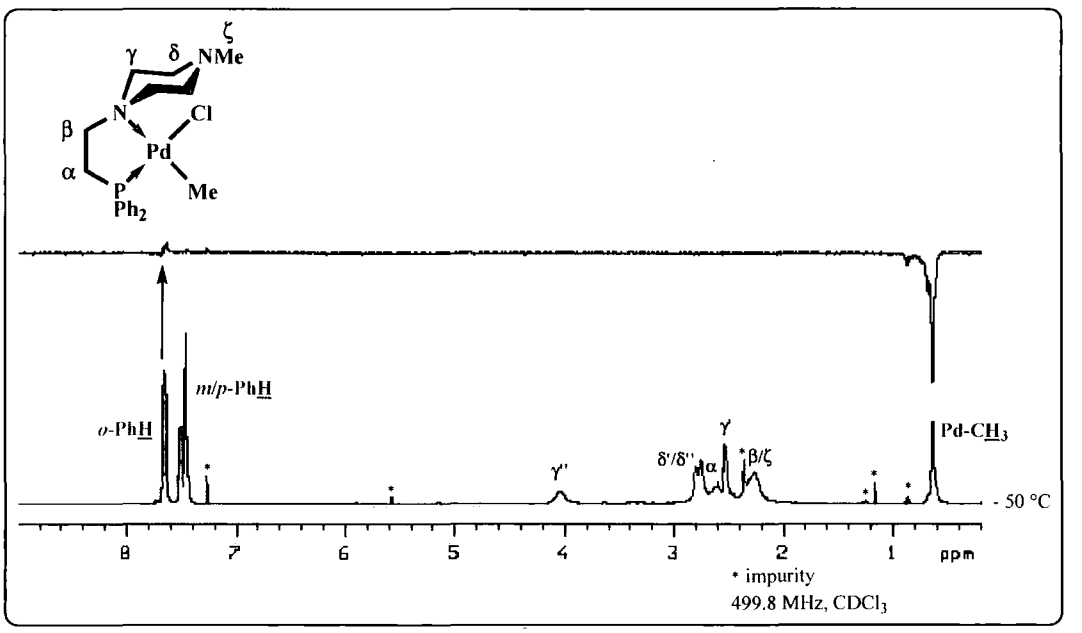

Figure 3.7: Representative ^{1}H and 1D nOe difference NMR spectra for **3.5-1**

The ^{13}C $\{^{1}H\}$ NMR spectra of compounds **3.5-1** – **3.5-4** were as expected and consistent with the proposed structures. In all complexes, the palladium-bound methyl carbon was observed to come into resonance at extremely low frequency (*ca.* – 5.2 ppm), with this resonance being observed as a doublet signal in **3.5-4** with the associated coupling constant being of the expected value ($^{2}J_{CP}$ = 3.4 Hz).[30] In all complexes **3.5-1** – **3.5-4**, the signals attributed to the α-bridge carbons were observed as doublet resonances as a result of coupling to phosphorus while the remaining aliphatic resonances were observed as singlets. The aromatic regions of these spectra were as expected with the required number of signals being observed.

3.4 Complexation of PNE ligands with '$PdMe_2$' fragments (3.6-1 – 3.6-4)

In an effort to extend the range of palladium complexes synthesised and also to explore access to their corresponding Pd(0) compounds, the complexation of the PNE ligands **2.4-1** – **2.4-4** with $PdMe_2$(tmeda) was undertaken. The synthesis of these [$PdMe_2${PNE}] complexes was of particular interest as the Pd centre comprises two 'non-dissociable' alkyl substituents, thus favouring bidentate ligand coordination to the metal centre. Additionally, given the strong *trans* influence of these metal-bound alkyl

groups, it was questioned whether coordination of the harder amine and ether donors to the '$PdMe_2$' site would be favoured over the softer thiol and phosphine donor fragments, thus resulting in a variation in ligand coordination in the ensuing complexes.

The syntheses of the [$PdMe_2${PNE}] complexes were all performed using stoichiometric quantities of the required PNE ligand (**2.4-1** – **2.4-4**) with $PdMe_2$(tmeda), Scheme 3.8. All reactions were performed at low temperature in toluene solution as, in the presence of chlorinated solvents such as CH_2Cl_2 or $CHCl_3$, substitution of the methyl group situated *trans* to phosphorus can be a facile process.[36]

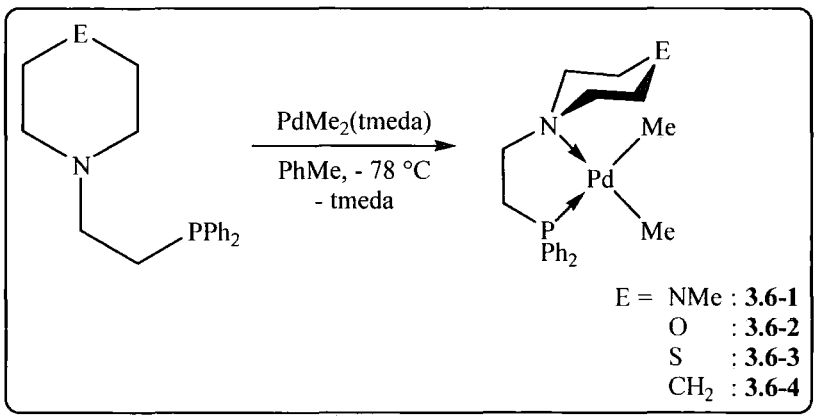

		$^{31}P\{^1H\}$ NMR	
		Complex* δ_P	Parent ligand§ δ_P
[$PdMe_2\{\kappa^2$-PN(NMe)}]	**3.6-1**	+ 16.8 (s)[a]	– 19.1 (s)[a]
[$PdMe_2\{\kappa^2$-PN(O)}]	**3.6-2**	+ 16.0 (s)[b]	– 18.1 (s)[a]
[$PdMe_2\{\kappa^2$-PN(S)}]	**3.6-3**	+ 16.2 (s)[c]	– 19.2 (s)[a]
[$PdMe_2\{\kappa^2$-PN(CH_2)}]	**3.6-4**	+ 16.5 (s)[c]	– 17.8 (s)[a]

*202.3 MHz, d_8-PhMe; [a] – 50 °C; [b] – 60 °C; [c] – 30 °C; §202.3 MHz, $CDCl_3$,

Scheme 3.8: Synthesis and $^{31}P\{^1H\}$ NMR spectroscopic data for complexes **3.6-1** – **3.6-4**

While rapid coordination of the ligand to Pd was observed in all cases, the resulting complexes were noted to be extremely thermally sensitive with rapid onset of decomposition (signified by a darkening of the reaction solution and precipitation of a black solid), even at low temperatures. In an effort to limit product decomposition, the minimum reaction times were employed in all cases with the product being rapidly removed from solution and stored at – 20 °C under a nitrogen atmosphere to preserve the samples. It is interesting to note that the only complex that demonstrated sufficient

stability to permit isolation and purification was that of the [$PdMe_2\{\kappa^2$-PN(O)}] compound (**3.6-2**), with this complex being afforded in moderate yield (44 %). Although satisfactory mass spectrometric analysis was obtained for **3.6-2** (*m/z* = 420.1, $[M–CH_3]^+$), the thermal instability of the remaining complexes **3.6-1**, **3.6-3** and **3.6-4**, even in the solid state, precluded analysis by this technique.

The ^{31}P {^1H} NMR spectra of compounds **3.6-1** – **3.6-4** all exhibited a sharp singlet resonance at low temperature with the chemical shift of these signals being consistent throughout this family of complexes. The [$PdMe_2\{\kappa^2$-$PN(CH_2)$}] compound **3.6-4** proved useful in the structural assignment of the related compounds **3.6-1** – **3.6-3** as the similarity in chemical shift between **3.6-1** – **3.6-4** provided an indication that the mode of coordination remains constant throughout this series with κ^2-PN ligation to Pd occurring in all cases. Comparison of δ_P of compounds **3.6-1** – **3.6-4** with the related crystallographically characterised compound [$PdMe_2\{\kappa^2$-PN-$Ph_2NCH_2CHN(Me_2$-$C_6H_3)$}] reported by Green and co-workers[36] further confirmed the proposed structures of these products, Table 3.6.

	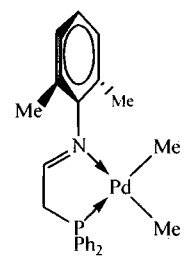	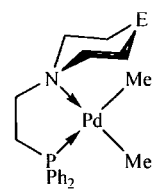
^{31}P {^1H} NMR δ_P	+ 21.3 (s)[a] [36]	+ 16.4 (s)[a,b]

[a] d_8-PhMe; [b] average δ_P shift quoted for comparative purposes

Table 3.6: Comparative ^{31}P {^1H} NMR spectroscopic data of **3.6-1** – **3.6-4** with the literature compound [$PdMe_2\{\kappa^2$-PN-$Ph_2NCH_2CHN(Me_2$-$C_6H_3)$}][36]

While it was expected on electronic grounds that the ligation of the harder donors to the '$PdMe_2$' fragment would be favoured over the softer donor fragments, from the ^{31}P {^1H} NMR spectroscopic data of **3.6-1** – **3.6-4**, this was shown not to be the case as phosphine coordination was noted in all complexes. Indeed, it has been reported previously that amine ligands do not coordinate well to '$PdMe_2$' fragments,[34]

although the presence of an nitrogen donor in a P–N ligand system does not appear to inhibit chelation of this ligand to the metal.[37]

The thermally sensitive nature of **3.6-1** – **3.6-4** limited the characterisation of these compounds due to rapid decomposition of these species, typically above – 20 °C both in the solution- and solid-state. Compounds **3.6-1** and **3.6-2** exhibited sufficient stability to allow their characterisation by multinuclear spectroscopy, however rapid degradation was noted for the remaining complexes **3.6-3** and **3.6-4** (even at low temperatures), thus preventing the acquisition of reliable ^{1}H and ^{13}C $\{^{1}H\}$ NMR spectroscopic data.

The ^{1}H NMR spectra of **3.6-1** and **3.6-2** were consistent with the proposed structures. Whilst two resonances corresponding to the metal-bound methyl groups were observed in the ^{1}H NMR spectrum of **3.6-1**, only one methyl resonance was noted in the ^{1}H NMR spectrum of **3.6-2** (an observation consistent with the spectroscopic analysis of the [$PdMe_2$(tmeda)] starting material[34]). The remaining features of these spectra resembled those of the related [PdCl(Me){κ^2-PN(E)}] complexes **3.5-1** and **3.5-2** with the required number of both aliphatic and aromatic resonances being observed.

The ^{13}C $\{^{1}H\}$ NMR spectra of **3.6-1** and **3.6-2** both exhibited two resonances at low frequency, which were attributed to the metal-bound methyl carbons. In **3.6-1**, these signals were both noted as singlet resonances however, in **3.6-2**, a singlet and a doublet of doublet resonances were observed (with the multiplicity of the latter resulting from coupling to phosphorus through different pathways around the chelate ring[38]). The aliphatic regions of these spectra were both as expected, although it is noteworthy that the signals attributed to the α-bridge carbons were observed as singlet resonances for both compounds. The aromatic regions of these spectra of **3.6-1** and **3.6-2** both displayed the required number of resonances although the aryl carbon-phosphorus coupling constants were obscured in both cases by toluene solvent resonances.

The instability of the [$PdMe_2${κ^2-PN(E)}] complexes **3.6-1** – **3.6-4** is surprising given the relative stability of the [$PdMe_2$(tmeda)] precursor, which is stable to temperatures as high as 60 °C,[39] however few reports of crystallographically characterised P–N-chelated dimethylpalladium complexes have been reported.[36] Whilst similar [$PdMe_2$(κ^2-PN)] compounds such as [$PdMe_2${κ^2-*PN*-Ph_2P-(1,2-C_6H_4)-CH_2NMe_2}][34] and [$PdMe_2${κ^2-*PN*-Ph_2P-(1,2-C_6H_4)-CH(Me)NMe_2}][39] have been found to be stable in the solid-state at low temperatures, these complexes display extremely

limited lifetimes in the solution-state with the rapid onset of decomposition at room temperature.

The decomposition of dimethylpalladium compounds coordinated with neutral two-electron donors in the absence of competing ligands has been studied previously, with the two principal pathways for this process being shown in Scheme 3.9.[40] These studies have suggested that the initial step of the decomposition process is loss of a ligand from the metal's coordination sphere and subsequent elimination of a methyl proton into this vacant coordination site. If the two methyl groups remain situated in a *cis*-arrangement, pathway (a) is the dominant process with ethane being the chief decomposition product formed in a concerted mechanism. If isomerisation of the bound methyl substituents about Pd occurs, pathway (b) dominates with the decomposition products being largely composed of methane along with the concomitant formation of PdC.

Deuterium labelling studies have confirmed that proton abstraction from the coordinated ligands does not take place, even when the ligand comprises protons in the α-position, although it is appreciated that the auxiliary ligand appears to influence the rate of alkane elimination.[40]

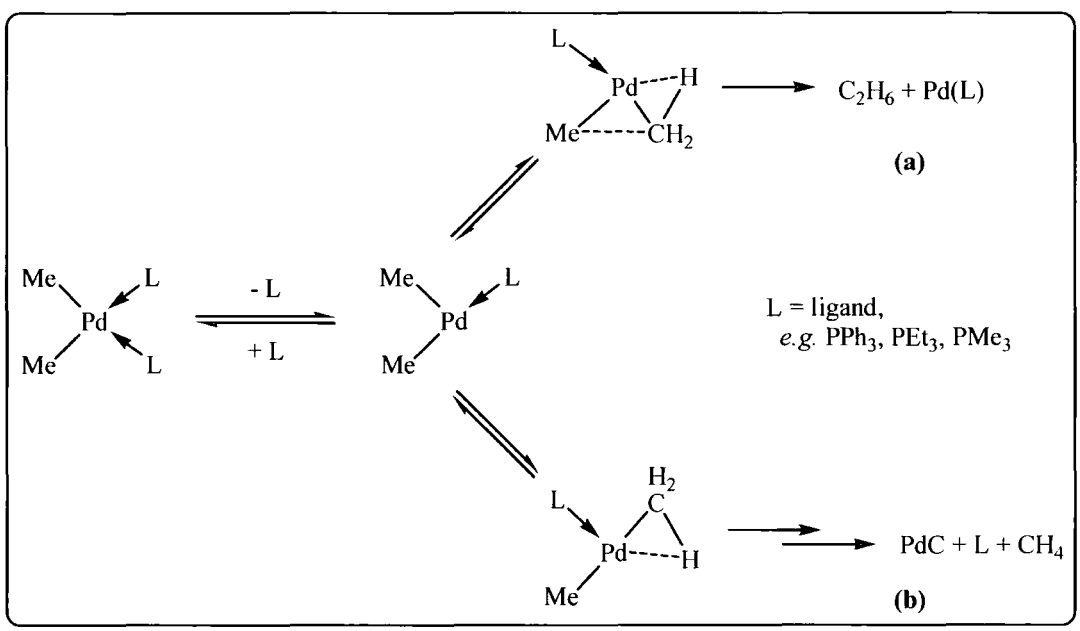

Scheme 3.9: Principal decomposition pathways for $[PdMe_2(L)_2]$ complexes[40]

Harder donors, such as nitrogen, coordinate less well to the soft Pd centre than phosphorus-based ligands,[24] and therefore dissociation of the N-donor from Pd is a more facile process than observed for phosphine donor fragments. Moreover, upon reductive elimination of the alkane degradation products, the coordination of nitrogen donors to the zerovalent Pd^0 centre is unfavourable, a situation reflected in the structure of $[PdN(CH_2CH_2PPh_2)_3]$ in which only coordination of the three phosphine donors is noted to the Pd^0 centre with the tertiary amine remaining uncoordinated.[41] It is therefore believed that the rapid decomposition of complexes **3.6-1** – **3.6-4** is a result of the poorly coordinating nature of the ligand to the '$PdMe_2$' fragment. As a result of the weak nitrogen-palladium bond, it is presumed that dissociation of the amine donor is a facile process, which generates a vacant coordination site at the metal and, in turn, promotes decomposition of the $[PdMe_2\{\kappa^2\text{-PN(E)}\}]$ complexes.

3.5 Conclusions/Summary

This chapter has detailed the coordination of the PNE ligands to '$PdCl_2$', '$PdCl(Me)$' and '$PdMe_2$' fragments and the characterisation of the resulting complexes.

Reaction of ligands **2.4-1** – **2.4-3** with $[PdCl_2(MeCN)_2]$ demonstrated a surprising difference in coordination behaviour of the ligands with the '$PdCl_2$' fragment although the low solubilities of the resulting complexes (**3.1-1** – **3.1-3**) in common organic solvents restricted their analysis in the solution state. The neutral $[PdCl_2\{\kappa^2\text{-PN(NMe)}\}]$ compound **3.1-1(a)** was characterised crystallographically, through a combination of NMR spectroscopy, mass spectrometry and CHN analyses. All complexes **3.1-1** – **3.1-3** were shown to principally adopt an ionic formulation, *i.e.* $[PdCl\{PNE\}]^+ Cl^-$, in the bulk sample. Experiments to determine the presence of an equilibrium between the $[PdCl_2\{\kappa^2\text{-PN(NMe)}\}]$ and $[PdCl\{\kappa^3\text{-PNNMe}\}]^+ Cl^-$ forms of **3.1-1** failed to establish the interconversion of these isomers in solution, however **3.1-1** was shown to react with $MgSO_4$ in CD_3OD to generate the unusual $[PdCl\{\kappa^3\text{-PNNMe}\}].½[Mg(SO_4)_2.4H_2O]$ compound **3.1-1(c)**.

Further analysis of **3.1-1** – **3.1-3** by solid-state NMR spectroscopy definitively showed **3.1-1** and **3.1-3** to exist as the tridentate $[PdCl\{\kappa^3\text{-PNE}\}]^+ Cl^-$ isomers, however a number of different coordination environments were observed in the ^{15}N and ^{31}P NMR

spectra of **3.1-2**, thus indicating that simple ligation of the PNO ligand to the '$PdCl_2$' fragment does not occur.

The [$PdCl_2\{\kappa^2$-PN(CH_2)}] compound **3.1-4**, as expected, demonstrated κ^2-PN ligand coordination to the metal site and was characterised by X-ray diffraction. Reaction of **2.4-5** and **2.4-7** to '$PdCl_2$' moieties failed to generate the target product in either case.

Reaction of ligands **2.4-1** – **2.4-4** with [PdCl(Me)(cod)] successfully afforded the [PdCl(Me)$\{\kappa^2$-PN(E)}] complexes **3.5-1** – **3.5-4**. Analysis of **3.5-1** – **3.5-4** by nOe difference NMR experiments confirmed the mutual *cis*-arrangment of the phosphine and methyl groups about the metal centre.

The [$PdMe_2\{\kappa^2$-PN(E)}] complexes **2.6-1** – **2.6-4**, synthesised by reaction with [$PdMe_2$(tmeda)], demonstrated extremely limited thermal stability with rapid decomposition noted both in the solution and solid states at ambient temperature which precluded full characterisation of these complexes. In all complexes, κ^2-PN coordination of the ligand to the '$PdMe_2$' fragment was noted although the facile decomposition of compounds **2.6-1** – **2.6-4** is tentatively attributed to the poorly coordinating nature of the amine donor.

3.6 References

[1] P. S. Pregosin and R. W. Kunz, "*^{31}P and ^{13}C NMR of Transition Metal Complexes*", Springer-Verlag, Berlin, 1979.

[2] P. M. Maitlis and M. J. H. Russell in "Comprehensive Organometallic Chemistry; The Synthesis, Reactions and Structures of Organometallic Compounds", G. Wilkinson, F. G. A. Stone and E.W. Abel (Eds.), Pergamon Press, New York, 1983, Volume 6, Chapter 38.1.

[3] R.F. Heck, "*Palladium Reagents in Organic Synthesis*", 1985, Academic Press, Inc., Suffolk, UK.

[4] "*Handbook of Organopalladium Chemistry for Organic Synthesis*" E. Neishi (Ed.), Wiley-Interscience, New York, 2002, Volumes I and II.

[5] G. Helmchen and A. Pfaltz, *Acc. Chem. Res.*, 2000, **33**, 336 – 345.

[6] P. E. Garrou, *Chem. Rev.*, 1981, **81**, 229 – 266.

[7] T. D. DuBois and D. W. Meek, *Inorg. Chem.*, 1969, **8**, 146 – 150.

[8] R. L. Dutta, D. W. Meek and D. H. Busch, *Inorg. Chem.*, 1970, **9**, 1215 – 1226.

[9] G. Cross, B. K. Vriesema, G. Boven, R. M. Kellogg and F. van Bolhuis, *J.Organomet. Chem.*, 1989, **370**, 357 – 381.

[10] J. M. Camus, P. R. García, J. Andrieu, P. Richard and R. Poli, *J. Organomet. Chem.*, 2005, **690**, 1659 – 1668.

[11] N. D. Jones, S. Jo Ling Foo, B. O. Patrick and B. R. James, *Inorg. Chem.*, 2004, **43**, 4056 – 4063.

[12] O. Hassel and B. F. Pedersen, *Proc. Chem. Soc. London*, 1959, 394.

[13] A. Bacchi, M. Carcelli, M. Costa, A. Fochi, C. Monici, P. Pelagetti, C. Pelizzi, G. Pelizzi and L. M. S. Rosa, *J. Organomet. Chem.*, 2000, **593**, 180 – 191.

[14] D. Jarosch, *Z. Kristallogr.*, 1985, **173**, 75 – 79.

[15] B. Hertweck, G. Giester and E. Libowitsky, *Am. Mineral.*, 2001, **86**, 1282 – 1292.

[16] F. C. Hawthorne, *Can. Mineral.*, 1985, **23**, 669 – 674.

[17] C. Vizcayno and M. T. Garia-Gonzalez, *Acta Cryst., Sect. C*, 1999, **55**, 8 – 11.

[18] I. M. Rumanova and G. I. Malitskaya, *Kristallografica*, 1959, **4**, 510 – 525.

[19] T. Todorov, R. Petrova, K. Kossev, J. Macicek and O. Angelova, *Acta Cryst., Sect. C*, 1998, **54**, 456 – 458.

[20] S. M. Aucott, A. M. Z. Slawin and J. D. Woollins, *J. Chem. Soc., Dalton Trans.*, 2000, 2559 – 2575.

[21] T. Chivers, K. McGregor and M. Parvez, *Inorg. Chem.*, 1993, **32**, 5119 – 5125.

[22] R. R. Fenton, F. Huq and T. W. Hambley, *Polyhedron*, 1999, **18**, 2149 – 2156.

[23] M. V. Baker, B. W. Skelton, A. H. White and C. C. Williams, *J. Chem. Soc., Dalton Trans.*, 2001, 111 – 120.

[24] T. G. Appleton, H. C. Clark and L. E. Manzer, *Coord. Chem. Rev.*, 1973, **10**, 335 – 422.

[25] D. Schildbach, M. Arroyo, S. Martin-Barrios, L. Sierra, F. Villafane and C. Strohman, *Organometallics*, 2004, **23**, 3228 – 3238.

[26] C.-Q. Quitmann and K. Müller-Buschbaum, *Zeit. für Anorg. Allgem. Chemie*, 2005, **631(2–3)**, 350 – 354.

[27] L.Wei, S. Ray Banerjee, M. K. Levadala, J. Babich and J. Zubieta, *Inorg. Chim. Acta*, 2004, **357**, 1499 – 1516.

[28] N. L. Allinger, J. G. D. Carpenter and F. M. Karkowski, *J. Am. Chem. Soc.*, **87**, 1232 – 1236.

[29] M. Aroney and R. J. W. Le Fèvre, *J. Chem. Soc.*, 1960, 2162 – 2168.

[30] K. R. Reddy, W.-W. Tsai, K. Surekha, G.-H. Lee, S.-M. Peng, J.-T. Chen and S.-T. Liu, *J. Chem. Soc., Dalton Trans.*, 2002, 1776 – 1782.

[31] H. A. Ankersmit, B. H. Løken, H. Koojiman, A. L. Spek, K. Vrieze and G. van Koten, *Inorg. Chim. Acta*, 1996, **252**, 141 – 155.

[32] O. Daugulis and M. Brookhart, *Organometallics*, 2002, **21**, 5926 – 5934.

[33] G. Müller, M. Klinga, P. Oswald, M. Leskelä, *Zeit. Für Naturforsch. B*, 2002, **57**, 803 – 809.

[34] W. De Graaf, S. Harder, J. Boersma, G. van Koten and J. A. Kanters, *J. Organomet. Chem.*, 1998, **358**, 545 – 562.

[35] E. K. van den Beuken, W. J. J. Smeets, A. L. Spek and B. L. Feringa, *Chem Commun.*, 1998, 223 – 224.

[36] K. S. Coleman, M. L. H. Green, S. I. Pascu, N. H. Rees, A. R. Cowley and L. H. Rees, *J. Chem. Soc., Dalton Trans.*, 2001, 3384 – 3395

[37] F. Dahan, P. W. Dyer, M. J. Hanton, M. Jones, D. P. Mingos, A. J. P. White and A.-M. Williamson, *Eur. J. Inorg. Chem.*, 2002, 732 – 742.

[38] M.J. Hanton, Ph.D. Thesis, University of Leicester 2003.

[39] W. Graaf, J. Boersma, W. J. J. Smeets, A. L. Spek and G. van Koten, *Organometallics*, 1989, **8**, 2907 – 2917.

[40] Z. Yuan, D. Jiang, S. J. Naftel, T.-K. Sham and R. J. Puddephatt, *Chem. Mater.*, 1994, **6**, 2151 – 2158.

[41] C. A. Ghilardi, S. Midollini, S. Moneti and A. Orlandini, *Chem. Commun.*, 1986, 1771 – 1772.

Chapter 4:

Complexation of PNE ligands with Pt

4.1 Introduction

The use of platinum complexes in organometallic and coordination chemistry is widespread with a large range of complexes of varying types being found throughout the literature. Platinum is a particularly attractive metal for use in coordination chemistry due to its propensity to form stable diamagnetic complexes which facilitates their isolation and subsequent characterisation.[1] A further attractive feature of platinum is that the ^{195}Pt nucleus (I = ½, 33.7 %), is readily detected by NMR spectroscopy. The presence, or absence, of coupling by other NMR spin active nuclei to Pt has the potential to greatly assist structural characterisation of platinum-containing complexes.[2]

Although the typically slow rates of reductive elimination and ligand substitution from Pt complexes generally restrict the application of these compounds in homogeneous catalysis,[3] the greater thermodynamic and kinetic stability shown by platinum complexes relative to their palladium and nickel counterparts can potentially be used to great advantage. Indeed, transient intermediates in Ni and Pd catalytic cycles are often isolable compounds in their analogous Pt compounds which may facilitate characterisation and hence, in turn, providing mechanistic insights into catalytic processes.[4]

Following the successful complexation studies of the PNE ligands (**2.4-1** – **2.4-4**) with Pd(II) centres, as detailed in the previous chapter, it was desirable to synthesise a variety of platinum complexes in order to further probe the coordination behaviour of the PNE ligands.

4.2 Complexation of PNE ligands with [$PtCl_2$(cod)]

The synthesis of a range of PNE-coordinated platinum complexes was initially attempted using '$PtCl_2$' fragments in an effort to generate a family of Pt-containing $[PtCl\{\kappa^3\text{-PNE}\}]^+ Cl^-$ species. These complexations were performed by reaction of stoichiometric quantities of [$PtCl_2$(cod)] and the required PNE ligand (**2.4-1** – **2.4-3**), Scheme 4.1.

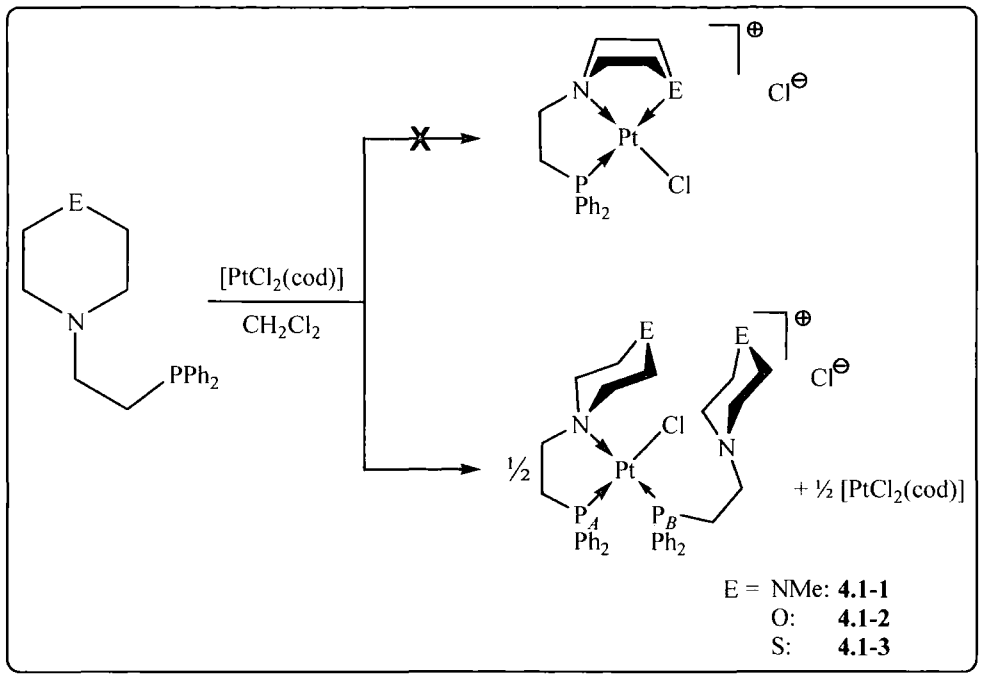

Scheme 4.1: Reaction of $[PtCl_2(cod)]$ with ligands **2.4-1 – 2.4-3**

From the reaction with each PNE ligand with $[PtCl_2(cod)]$, a fine white-pale yellow powder was isolated. The ^{31}P $\{^1H\}$ NMR spectra of all compounds **4.1-1 – 4.1-3** proved surprising as, in each spectrum, two distinct phosphorus environments were noted, with coupling to the ^{195}Pt nucleus being observed in all cases. Integration of the two environments showed a 1:1 ratio in all cases, Table 4.1.

		^{31}P $\{^1H\}$ NMR*					
		P_A			P_B		
		δ_P	$^1J_{PtP}$ /Hz	$\nu_{½}$ /Hz	δ_P	$^1J_{PtP}$ /Hz	$\nu_{½}$ /Hz
$[PtCl\{\kappa^2\text{-PN(NMe)}\}\{\kappa^1\text{-P(NNMe)}\}]^+ Cl^-$	**4.1-1**	+ 35.7	3748	78	+ 1.6	3186	66
$[PtCl\{\kappa^2\text{-PN(O)}\}\{\kappa^1\text{-P(NO)}\}]^+ Cl^-$	**4.1-2**	+ 35.9	3767	80	+ 0.8	3241	77
$[PtCl\{\kappa^2\text{-PN(S)}\}\{\kappa^1\text{-P(NS)}\}]^+ Cl^-$	**4.1-3**	+ 35.8	3771	72	+ 0.9	3208	55

*121.4 MHz, $CDCl_3$

Table 4.1: ^{31}P $\{^1H\}$ NMR spectroscopic data for complexes **4.1-1 – 4.1-3**

Although initial assignment of the $^{31}P\{^{1}H\}$ NMR spectra of **4.1-1 – 4.1-3** proved difficult, comparison with previous reports in the literature indicated that the data obtained was consistent with double ligation of the Pt centre by the PNE ligands. The resonance at *ca.* δ_P = + 35.8 ppm in all spectra can be attributed to the P_A donor (Scheme 4.1), which is bound to the Pt centre as part of a bidentate P–N chelate. The large coordination chemical shifts experienced by these donor atoms upon coordination ($\Delta\delta_P$ ($\delta_{P\ coordinated} - \delta_{P\ free}$) = *ca.* + 54.3 ppm) are consistent with the formation of a five-membered ring at the Pt centre.[5] The larger value of $^{1}J_{PtP}$ is indicative of the P_A donor fragment being located *trans* to the more electronegative chloride ligand.[6] The second resonance at *ca.* δ_P = + 1.1 ppm is associated with a second PNE ligand bound to the Pt centre, in each case, coordinated in a monodentate fashion *via* the phosphine donor only. The smaller coordination chemical shift of the P_B donor ($\Delta\delta_P$ ($\delta_{P\ coordinated} - \delta_{P\ free}$) = *ca.* + 19.7 ppm) is consistent with the idea that the second PNE ligands are ligated in a monodentate fashion.[5]

Unfortunately, due to the broadened nature of the resonances in the $^{31}P\{^{1}H\}$ NMR spectra of **4.1-1 – 4.1-3**, the secondary $^{2}J_{PP}$ coupling between the two phosphine donors could not be resolved. Given the small magnitude of *cis*-$^{2}J_{PP}$ coupling (typically being ~ 20 Hz[7]), it is unsurprising that these couplings were obscured as the broadening in all resonances **4.1-1 – 4.1-3** was typically greater than 60 Hz. It is evident, however, that the phosphine donors do not adopt a *trans* arrangement about the Pt centre as the magnitude of *trans*-$^{2}J_{PP}$ coupling constants are generally large (~ 500 Hz[8]) and hence would have been evident even with the moderate broadening observed in these spectra.

The structural assignments of complexes **4.1-1 – 4.1-3** are consistent with those found by Sadler and co-workers for a comparable bidentate P–N chelated Pt-system, $[PtCl(Me_2NCH_2CH_2PPh_2)_2]Cl.H_2O$, a comparison of relevant spectroscopic data[9] (and associated numbering scheme) being shown in Table 4.2. Studies on the behaviour of this complex in solution have revealed two distinct forms, namely $[PtCl\{\kappa^2\text{-}(N\text{–}P_A)\}\{\kappa\text{-}(P_B)\}]Cl$ and $[Pt\{\kappa^2\text{-}(N\text{–}P_C)_2\}]Cl_2$, depending on solution pH. In the $[PtCl\{\kappa^2\text{-}(N\text{–}P_A)\}\{\kappa\text{-}(P_B)\}]Cl$ complex, the chelated P_A moiety exhibits a single singlet resonance (δ_P = + 36.5 ppm), at higher frequency than that of the monodentate P_B donor (δ_P = – 0.5 ppm). In the doubly chelated $[Pt\{\kappa^2\text{-}(N\text{–}P_C)_2\}]Cl_2$ complex, only one singlet resonance, P_C, is observed (δ_P = + 33.7 ppm) as a result of the symmetrical environment about Pt.

	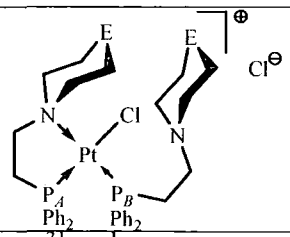		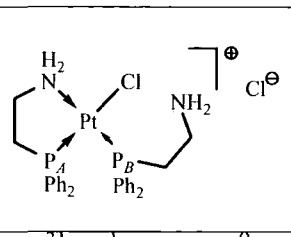		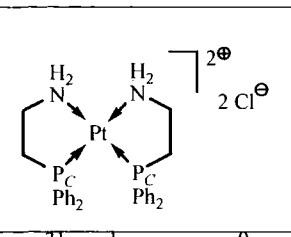	
	$^{31}P\{^{1}H\}$ NMR[a] **4.1-1 – 4.1-3**		$^{31}P\{^{1}H\}$ NMR[9]		$^{31}P\{^{1}H\}$ NMR[9]	
	δ_P[§]	$^{1}J_{PtP}$ /Hz[§]	δ_P	$^{1}J_{PtP}$ /Hz	δ_P	$^{1}J_{PtP}$ /Hz
P_A	+ 35.8	3762	+ 36.5	3691	–	–
P_B	+ 1.1	3211	– 0.5	3187	–	–
P_C	–	–	–	–	+ 33.7	3300

[§]average for **4.1-1 – 4.1-3** quoted for comparative purposes; [a]202.3 MHz, $CDCl_3$; [b]109.3 MHz, $CDCl_3$.

Table 4.2: Comparative $^{31}P\{^{1}H\}$ NMR spectroscopic data for complexes **4.1-1 – 4.1-3** and $[PtCl\text{-}\{\kappa^2\text{-}(N\text{–}P_A)\}\{\kappa^1\text{-}(P_B)\}]Cl$ and $[Pt\{\kappa^2\text{-}(N\text{–}P_C)_2\}]Cl_2$[9]

It is noteworthy that no trace of the doubly-chelated $[Pt\{\kappa^2\text{-}PN(E)\}_2]Cl_2$ complexes were observed in the reactions outlined above. The absence of these homoleptic complexes is presumed to be due to the steric demands of the PNE ligands, as chelation of the second P^N(E) ligand would result in a steric clash of the two E donor moieties given the *cis*-arrangement of the phosphine donor fragments.

Unfortunately, completely satisfactory ^{1}H and $^{13}C\{^{1}H\}$ NMR data could not be obtained for any of the complexes **4.1-1 – 4.1-3** as the spectra were all subject to considerable broadening, something suggestive of fluxionality of the pendent donor arms in solution. Despite lowering the temperature of the NMR samples, both the ^{1}H and $^{13}C\{^{1}H\}$ NMR spectra remained severely broadened. In all the ^{1}H NMR spectra of the crude reaction products **4.1-1 – 4.1-3**, the presence of olefinic resonances (flanked by Pt satellites) was observed. Comparison of the chemical shifts of these resonances with an authentic sample of $[PtCl_2(cod)]$ indicated that the samples of **4.1-1 – 4.1-3** contained the unreacted metal complex. The overall integration of these signals corresponded to the samples containing 0.5 equivalents of this $[PtCl_2(cod)]$ starting material thereby providing further evidence of the double ligation of one Pt site by two PNE ligands.

Analysis of the product mixtures **4.1-1 – 4.1-3** by mass spectrometry afforded spectra consistent with previous structural assignments, Table 4.3 (see Scheme 4.2 for assignments). In all compounds, two distinct sets of peaks were observed with the first

corresponding to the expected $[PtCl\{\kappa^2\text{-}PN(E)\}\{\kappa^1\text{-}P(NE)\}]^+$ ion while a second minor fragment resulting from loss of the monodentate ligand from this latter complex was noted.

		MALDI$^+$ Mass Spectrometry			
		m/z	Assignment	*m/z*	Assignment
$[PtCl\{\kappa^2\text{-}PN(NMe)\}\{\kappa^1\text{-}P(NNMe)\}]^+ Cl^-$	**4.1-1**	855	$[ii]^+$	543	$[ii - (MeNNP)]^+$
$[PtCl\{\kappa^2\text{-}PN(O)\}\{\kappa^1\text{-}P(NO)\}]^+ Cl^-$	**4.1-2**	829	$[ii]^+$	529	$[ii - (ONP)]^+$
$[PtCl\{\kappa^2\text{-}PN(S)\}\{\kappa^1\text{-}P(NS)\}]^+ Cl^-$	**4.1-3**	861	$[ii]^+$	546	$[ii - (SNP)]^+$

Table 4.3: Mass spectrometric data for **4.1-1 – 4.1-3**

{See Scheme 4.2 for structural assignments (*vide infra*)}

From the observed spectroscopic analyses, it is believed that coordination of the PNE ligands **2.4-1 – 2.4-3** to the '$PtCl_2$' fragment occurs as shown in Scheme 4.2. Upon initial P–N bidentate coordination of the PNE ligand (*i*), the strongly *trans*-influencing phosphine donor (P_A) labilises the chloride co-ligand lying *trans* to itself, creating a vacant coordination site. The second phosphine donor (P_B) coordinates *trans* to P_A, and following isomerisation within the Pt coordination sphere, the *cis*-P,P complex (*ii*) is afforded. Due to the sterically demanding nature of the N^E ring fragment, the doubly chelated product (*iii*) is not observed and the presumed equilibrium in this step lies towards that of species (*ii*).

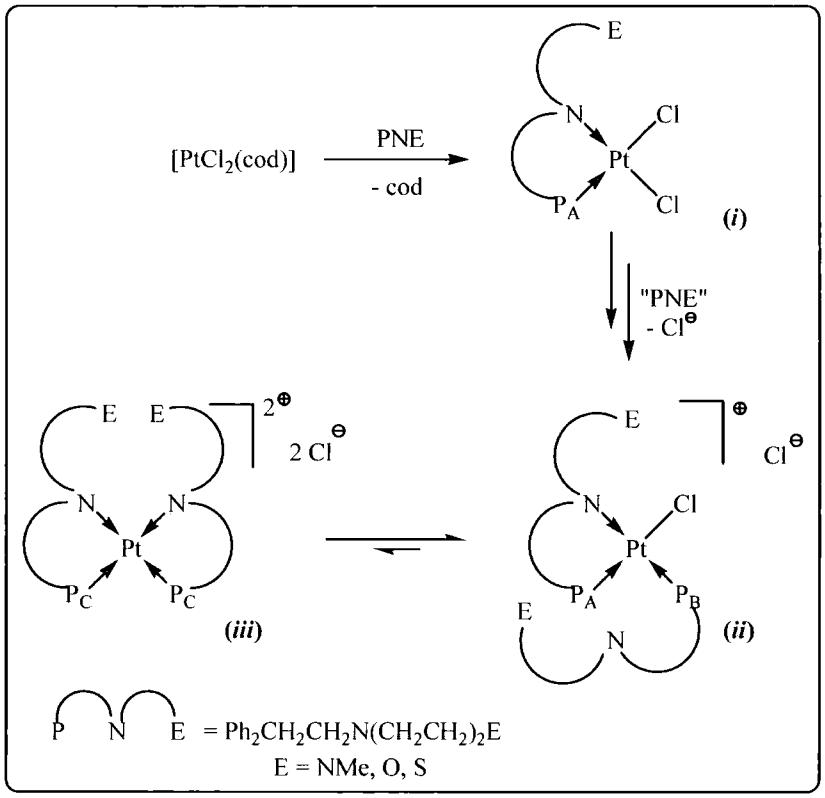

Scheme 4.2: Proposed mechanism of PNE ligand additions to $[PtCl_2(cod)]$

4.2.1 Molecular structure of 4.1-2.HCl

In an effort to definitively confirm the structures of the various platinum complexes obtained through reaction of equimolar quantities of $[PtCl_2(cod)]$ and the PNE ligands **2.4-1** – **2.4-3**, the solid materials isolated were recrystallised by slow diffusion of hexane into CH_2Cl_2 solutions of the crude complexes under air. Colourless needles suitable for analysis by X-ray diffraction were obtained from the crude sample containing **4.1-2**. The resulting molecular structure (Figure 4.1) revealed the crystalline material to be that of the hydrochloride salt of **4.1-2** with the tertiary nitrogen of the pendent morpholine ring having been protonated. Since no trace of this doubly-charged cation was observed by mass spectrometric or NMR spectroscopic analysis of the bulk sample containing **4.1-2**, it is believed that since recrystallisation was undertaken using non-dried solvents, the HCl resulted from hydrolysis of the product mixture of **4.1-2**. However, the gross molecular structure obtained is entirely consistent with the structures proposed for **4.1-1** – **4.1-3** on the basis of their spectroscopic analyses.

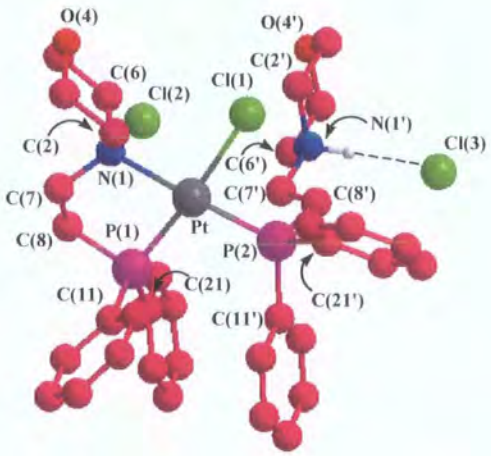

Figure 4.1: Ball and stick representation of **4.1-2.HCl***

	Bond Length /Å		**Bond Angle /°**
Pt–P(1)	2.231(2)	P(1)–Pt–N(1)	84.1(2)
Pt–N(1)	2.197(8)	P(1)–Pt–P(2)	98.84(9)
Pt–P(2)	2.245(2)	N(1)–Pt–Cl(1)	91.4(2)
Pt–Cl(1)	2.363(2)	P(2)–Pt–Cl(1)	85.76(9)
N(1)–C(7)	1.481(13)	P(1)–Pt–Cl(1)	173.02(11)
P(1)–C(8)	1.820(11)	P(2)–Pt–N(1)	176.9(3)
P(1)–C(11)	1.795(11)	C(11)–P(1)–C(21)	108.8(5)
P(1)–C(21)	1.817(9)	C(2)–N(1)–C(6)	105.3(8)
P(2)–C(8′)	1.808(10)	C(3)–O(4)–C(5)	109.3(10)
N(1′)–C(7′)	1.501(12)	C(11′)–P(2)–C(21′)	99.6(4)
P(2)–C(11′)	1.826(10)	C(2′)–N(1′)–C(6′)	110.4(8)
P(2)–C(21′)	1.835(10)	C(3′)–O(4′)–C(5′)	110.4(9)
H(1)–Cl(3)	2.118	$\Sigma_{\angle P(1)}$	319.4[a]
		$\Sigma_{\angle N(1)}$	327.5[a]
		$\Sigma_{\angle P(2)}$	309.7[a]
		$\Sigma_{\angle N(1')}$	334.2[a]
		P(1)–C(8)–C(7)–N(1)	59.25
		P(2)–C(8′)–C(7′)–N(1′)	165.11

[a]angle summation; [c]e.s.d.'s in parentheses

Table 4.4: Selected bond lengths (Å) and bond angles (°) for **4.1-2.HCl**

The square planar platinum centre in **4.1-2.HCl** is ligated with two equivalents of the PNO ligand **2.4-2** with one ligand moiety chelating the metal in a bidentate P–N fashion (retaining a pendant ether donor fragment) and the second PNE system acting as a monodentate phosphine ligand. The phosphine components of the two ligands were

* Molecular structure determination performed by Dr A. S. Batsanov

observed to bind to Pt in a mutually *cis* arrangement with a chloride being found *trans* to the chelated phosphine donor, thus completing the square planar coordination environment. A slight distortion from planarity about the metal centre was observed with the bound chloride {Cl(1)} being located 5.27° below the P(1)–Pt–P(2) plane, however no distortion was noted about the bound N(1) atom.

The N(1′)–H(1) bond was found to adopt a pseudo *anti* configuration with respect to the coordinated P(2) electron pair, which is reflected in the P(2)–C(8′)–C(7′)–N(1′) torsion angle of 165.11°. As a result of the chelation of the P(1) and N(1) donor atoms to Pt, the P(1)–C(8)–C(7)–N(1) bridge exhibits a staggered configuration {59.25°}.

The sum of angles about the N(1′) atom {$\Sigma_{\angle N(1')} = 334.2°$} is entirely consistent with that observed for the previously synthesised protonated ligand $Ph_2PCH_2CH_2NH^+(CH_2CH_2)_2O$ **(2.5-2)** {333.29°} (Chapter 2, Section 2.4.2). As expected, the sum of angles about the phosphine donor atoms P(1) {$\Sigma_{\angle P(1)} = 319.4°$} and P(2) {$\Sigma_{\angle P(2)} = 309.7°$} were smaller than the angle noted about the coordinated N(1) {$\Sigma_{\angle N(1)} = 327.5°$} atom.

The bond angles about the Pt centre reveal a slight deviation from ideal square planar geometry, with the P(1)–Pt–P(2) angle exhibiting the largest distortion {98.84(9)°}. Comparison of the C(11)–P(1)–C(21) versus the C(11′)–P(2)–C(21′) bond angles reveal a large difference between the chelated and monodentate phosphorus donors. The C(11′)–P(2)–C(21′) angle in the monodentate phosphine moiety was noted to be significantly narrower {99.6(4)°} than that observed for the C(11)–P(1)–C(21) angle in the chelated ligand {108.8(5)°}, presumably as a result of constraints imposed on the latter by it being part of a five-membered ring.

The Pt–P(1), Pt–P(2) and Pt–N(1) bond lengths lie within the expected range,[3] with the Pt–P(1) and Pt–P(2) bonds being the longer as expected. Comparison of the Pt–P(1) and Pt–P(2) bond lengths reveal the latter of the two to be slightly longer, in line with previous observations,[10] reflecting the weaker *trans* influence of the chloride ligand relative to that of the N(1) donor.[11] The remaining bond lengths associated with the κ^1-P and the κ^2-P–N bound ligands are largely comparable, thus indicating that the differing coordinating modes have little impact on the gross molecular structure of the PNE scaffolds.

4.3 Direct synthesis of 4.1-1 – 4.2-3

Following the formation of the doubly ligated platinum complexes **4.1-1** – **4.1-3** as mixtures in solution with unreacted $[PtCl_2(cod)]$, the direct stoichiometric synthesis of these complexes was undertaken. This was achieved using a variation of the reaction stoichiometry, *i.e.* by reaction of two equivalents of the requisite PNE ligand with one equivalent of the $[PtCl_2(cod)]$ precursor, Scheme 4.3.

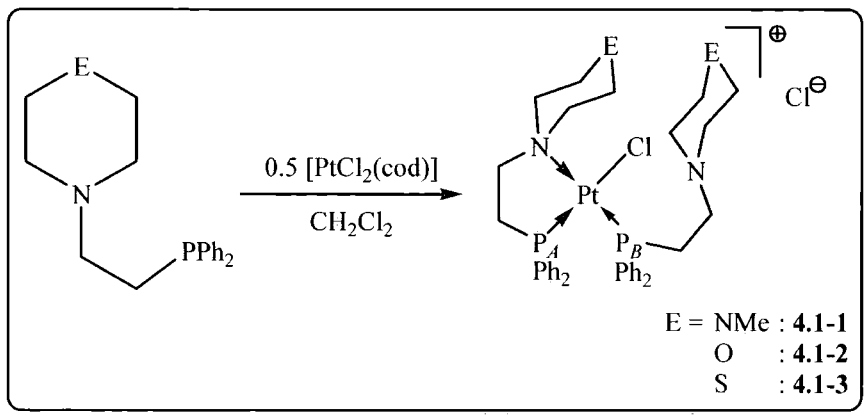

		Yield
$[PtCl\{\kappa^2\text{-PN(NMe)}\}\{\kappa^1\text{-P(NNMe)}\}]^+ Cl^-$	**4.1-1**	52 %
$[PtCl\{\kappa^2\text{-PN(O)}\}\{\kappa^1\text{-P(NO)}\}]^+ Cl^-$	**4.1-2**	56 %
$[PtCl\{\kappa^2\text{-PN(S)}\}\{\kappa^1\text{-P(NS)}\}]^+ Cl^-$	**4.1-3**	64 %

Scheme 4.3: Stoichiometric synthesis of $[PtCl\{\kappa^2\text{-PN(E)}\}\{\kappa^1\text{-P(NE)}\}]^+ Cl^-$ (**4.1-1** – **4.1-3**)

The $^{31}P\{^1H\}$ NMR spectroscopic data obtained for the complexes prepared in this manner were identical to those obtained previously for complexes **4.1-1** – **4.1-3** using the synthesis described earlier in Scheme 4.1 and thus is consistent with the generation of Pt complexes ligated with two equivalents of the PNE ligands, Table 4.5. Analysis of each reaction mixture obtained using this revised stoichiometry by ^1H NMR spectroscopy clearly confirmed the absence of unreacted $[PtCl_2(cod)]$.

Notably, even in the absence of unreacted $[PtCl_2(cod)]$, substantial broadening of all NMR spectra of complexes **4.1-1** – **4.1-3** was observed. Although the molecular structure of **4.1-2** (*vide supra*) demonstrated the protonation of the pendent amine fragment, this resonance could not be identified in the ^1H NMR spectra of **4.1-1** – **4.1-3**.

		$^{31}P\{^{1}H\}$ NMR*					
		P_A			P_B		
		δ_P	$^{1}J_{PtP}$ /Hz	$\nu_{½}$ /Hz	δ_P	$^{1}J_{PtP}$ /Hz	$\nu_{½}$ /Hz
$[PtCl\{\kappa^2\text{-}PN(NMe)\}\{\kappa^1\text{-}P(NNMe)\}]^+ Cl^-$	**4.1-1**	+ 35.6	3760	78	+ 1.6	3168	83
$[PtCl\{\kappa^2\text{-}PN(O)\}\{\kappa^1\text{-}P(NO)\}]^+ Cl^-$	**4.1-2**	+ 36.1	3716	71	+ 1.3	3151	56
$[PtCl\{\kappa^2\text{-}PN(S)\}\{\kappa^1\text{-}P(NS)\}]^+ Cl^-$	**4.1-3**	+ 35.9	3771	72	+ 1.4	3146	60

*121.4 MHz, $CDCl_3$

Table 4.5: $^{31}P\{^{1}H\}$ NMR spectroscopic data for complexes **4.1-1** – **4.1-3** prepared according to Scheme 4.3

Similarly, the mass spectrometric analyses of complexes **4.1-1** – **4.1-3** formed according to Scheme 4.3 proved to be identical to those attained for complexes **4.1-1** – **4.1-3**, demonstrating the presence of the required species, along with a minor fragmentation peak corresponding to loss of one PNE ligand moiety. No evidence was found for protonation in any of the samples.

It is surprising that the PNE ligands display a strong preference for double ligation of the '$PtCl_2$' fragment. It was initially presumed that reaction of stoichiometric quantities of the PNE ligand and the $[PtCl_2(cod)]$ precursor would lead to the formation of the neutral $[PtCl_2\{\kappa^2\text{-}PN(E)\}]$ complex. Alternatively, it was speculated that coordination of the terminal E donor to the Pt(II) centre could occur, resulting in the formation of the charged $[PtCl\{\kappa^3\text{-}PNE\}]^+ Cl^-$ complexes, a situation reminiscent of that previously observed in the analogous Pd complexes (Chapter 3, Section 3.2). It is clear, however, that simple chelation of the PNE moieties to the '$PtCl_2$' fragment is not the favoured reaction in these systems.

Whilst cyclooctadiene is generally viewed as a labile ancillary ligand in complexes such as $[PtCl_2(cod)]$, complete displacement of this co-ligand can prove problematic unless comparatively harsh reaction conditions or strongly coordinating ligands, such as chelating *bis*-phosphine donors, are employed.[12] Indeed, complete displacement of this olefin is facilitated by the incorporation of strongly *trans*-influencing ligands at Pt, which reduce the availability of Pt $d\pi$-electrons for back-

bonding to the π^*-orbitals of the olefin. This increases the lability of the cyclooctadiene ligand as a whole, enabling facile displacement from Pt under mild conditions.[13] It is believed that the combination of the poor lability of the ancillary cyclooctadiene ligand from $[PtCl_2(cod)]$ combined with the facile substitution of chloride ligands from square planar Pt(II) centres[1] serve to favour double coordination of the PNE ligands to the metal centre over selective formation of mono-ligated species.

4.4 Attempted derivatisation of 4.1-1 – 4.1-3

Following the selective synthesis and isolation of the doubly-ligated $[PtCl\{\kappa^2\text{-}PN(E)\}\{\kappa^1\text{-}P(NE)\}]^+ Cl^-$ complexes **4.1-1** – **4.1-3**, experiments were undertaken to probe the behaviour of these complexes in both the solution- and solid-state. Initially, the abstraction of the bound chloride ligand from **4.1-1** – **4.1-3** was undertaken *via* reaction with sodium hexafluorophosphate in an attempt to form the dihexafluoro-phosphate salts **4.2-1** – **4.2-3**, as detailed in Scheme 4.4(a). Two equivalents of the sodium salt were employed in this transformation to enable both exchange of the halide counterion and abstraction of the bound chloride. Since $NaPF_6$ has only sparing solubility in CH_2Cl_2, no noticeable reaction was detected after two days at room temperature (*via* $^{31}P\{^1H\}$ NMR spectroscopy). A small quantity of MeOH was therefore added to the reaction mixtures in order to solubilise the $NaPF_6$ and promote the required reactions. However, *in situ* analysis of the reaction mixtures by $^{31}P\{^1H\}$ NMR spectroscopy afforded only a resonance attributed to the free PF_6^- anion. Following isolation of the products, analysis by multinuclear NMR spectroscopy again afforded unassignable, severely broadened spectra with the required singlet resonances for the *bis*-chelated Pt complexes not being observed in their $^{31}P\{^1H\}$ NMR spectra. Mass spectrometric analysis of the obtained products also failed to demonstrate the presence of the required complexes, with only the parent complexes being observed and thus these syntheses were abandoned.

The failure of these reactions is believed to give an indication that the complexation of the second pendent amine is unfavourable on steric grounds as the coordination of this donor results in an disfavoured steric clash between the two ring fragments. Although the conformationally flexible six-membered rings are capable of

twisting to relieve this steric interaction, the lack of formation of the doubly-chelated complexes **4.2-1** – **4.2-3** indicates that these configurations are too high in energy to result in stable *bis*-chelated Pt complexes.[14]

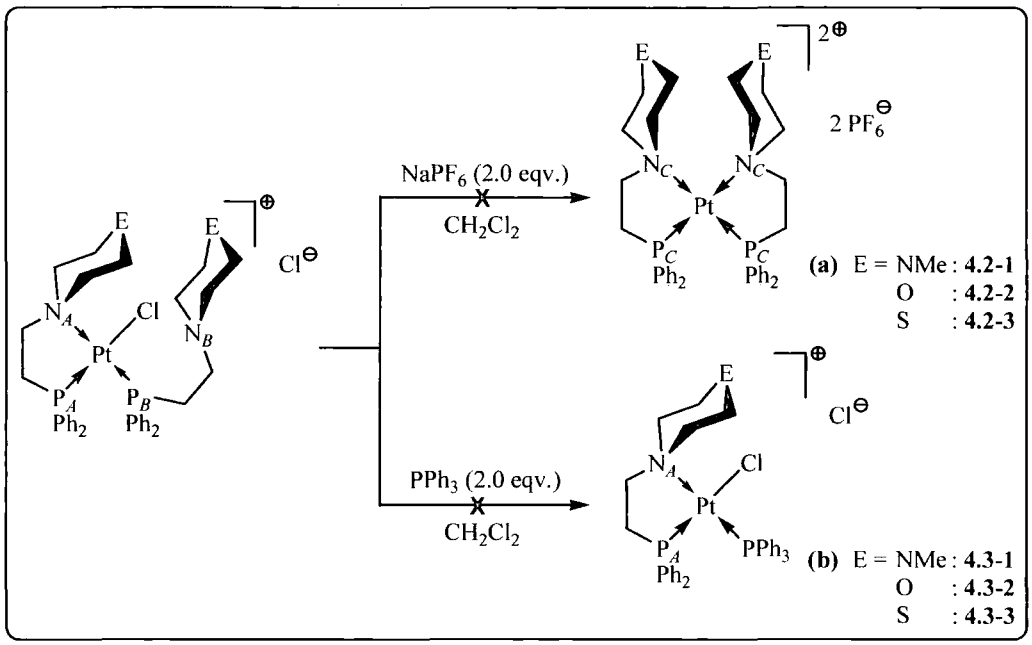

Scheme 4.4: Attempted derivatisation of complexes **4.1-1** – **4.1-3**

In an attempt to generate the $[PtCl(PPh_3)\{\kappa^2\text{-}PN(E)\}]^+ Cl^-$ derivatives **4.3-1** – **4.3-3** by selective substitution of the monodentate PNE phosphine donor, the complexes **4.1-1** – **4.1-3** were allowed to react with equimolar quantities of triphenylphosphine, according to Scheme 4.4(b). Upon the addition of one equivalent of PPh_3 to complexes **4.1-1** – **4.1-3**, *in situ* analysis of the reaction mixtures by $^{31}P\ \{^1H\}$ NMR spectroscopy afforded extremely broadened spectra with the required product resonances not being observed. Following removal of the solvent and washing of the resulting white powders with hexane, analysis by multinuclear NMR spectroscopy again afforded severely broadened spectra in all cases with the requisite complexes **4.3-1** – **4.3-3** not being observed. In an effort to ensure these reactions had reached completion and to generate the required triphenylphosphine complexes, the product mixtures were redissolved in CH_2Cl_2 and a further equivalent of PPh_3 added. Again, only the unreacted parent complexes and free PPh_3 were observed in the $^{31}P\ \{^1H\}$ NMR spectra of the resulting reaction mixtures and thus the syntheses were abandoned.

4.5 Reaction of PNE ligands with $[PtCl\{\mu\text{-}Cl\}(PEt_3)]_2$ (4.4-1 – 4.4-4)

In an effort to generate another family of Pt complexes that demonstrated well-defined coordination of the PNE ligand to the metal centre, an alternative platinum precursor complex was sought. Dimeric platinum complexes with bridging chlorides, especially those comprising phosphine co-ligands, are excellent precursor species due to their reactive nature as they are susceptible to cleavage of the chloro bridge by a range of nucleophiles.[15] Moreover, complexation reactions employing these dimeric precursors do not depend on the displacement of a chelating co-ligand, such as cyclooctadiene, which can complicate the nature of metal ligation.[16] Thus, the complexation of the PNE ligands **2.4-1** – **2.4-4** was attempted employing half an equivalent of $[PtCl\{\mu\text{-}Cl\}(PEt_3)]_2$ as detailed in Scheme 4.5.

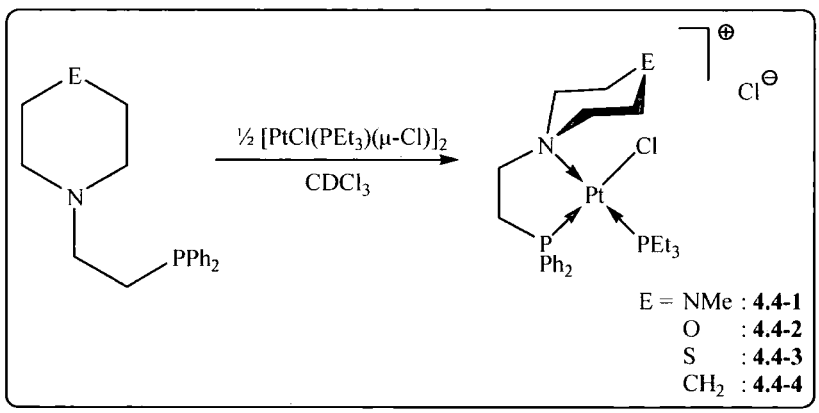

		Yield
$[PtCl(PEt_3)\{\kappa^2\text{-}PN(NMe)\}]^+ Cl^-$	**4.4-1**	81 %
$[PtCl(PEt_3)\{\kappa^2\text{-}PN(O)\}]^+ Cl^-$	**4.4-2**	83 %
$[PtCl(PEt_3)\{\kappa^2\text{-}PN(S)\}]^+ Cl^-$	**4.4-3**	78 %
$[PtCl(PEt_3)\{\kappa^2\text{-}PN(CH_2)\}]^+ Cl^-$	**4.4-4**	77 %

Scheme 4.5: Synthesis of $[PtCl(PEt_3)\{\kappa^2\text{-}PN(E)\}]^+ Cl^-$ complexes **4.4-1** – **4.4-4**

The synthesis of all complexes **4.4-1** – **4.4-4** was performed on an NMR scale (*ca.* 70 mg of Pt dimer) in order to facilitate characterisation of the products. Isolation of the resulting cationic platinum species proved facile and, following purification by recrystallisation, the $[PtCl(PEt_3)\{\kappa^2\text{-}PN(E)\}]^+ Cl^-$ species **4.4-1** – **4.4-4** were obtained in excellent isolated yields as white crystalline solids. In all cases, satisfactory CHN and mass spectrometric analyses corresponding to the proposed structures were obtained.

The ^{31}P $\{^{1}H\}$ NMR spectra of complexes **4.4-1** – **4.4-4** all displayed the expected two phosphorus environments, each exhibiting mutual ^{31}P coupling as well as coupling to the ^{195}Pt nucleus, Table 4.6. The resonance attributed to the triethylphosphine co-ligand was observed at lowest frequency (*ca.* δ_P = + 6.5 ppm), with a similar chemical shift to that of the dimeric precursor (δ_P = + 10.2 ppm). The PNE phosphine moiety was observed to come into resonance at higher frequency (*ca.* δ_P = + 32.4 ppm) as a result of greater deshielding of this phosphorus donor by its two aromatic substituents.[17] The small magnitude of the $^{2}J_{PP}$ coupling constants observed in all complexes provides an indication of *cis* coordination of the two phosphino donor moieties.[8,18]

		^{31}P $\{^{1}H\}$ NMR (Pt–{PNE})*			^{31}P $\{^{1}H\}$ NMR (Pt–PEt_3)*		
E =		δ_P	$^{1}J_{PtP}$/Hz	$^{2}J_{PP}$ /Hz	δ_P	$^{1}J_{PtP}$/Hz	$^{2}J_{PP}$ /Hz
NMe	**4.4-1**	+ 34.4	3822	17.2	+ 6.4	3020	17.2
O	**4.4-2**	+ 34.2	3803	17.6	+ 6.6	3027	17.6
S	**4.4-3**	+ 34.1	3792	17.4	+ 6.5	3037	17.2
CH_2	**4.4-4**	+ 34.2	3834	17.5	+ 5.9	2971	17.2

*161.9 MHz, $CDCl_3$

Table 4.6: ^{31}P $\{^{1}H\}$ NMR spectroscopic data for complexes **4.4-1** – **4.4-4**

The ^{1}H NMR spectra of **4.4-1** – **4.4-4** exhibited the required number of resonances for the coordinated ligands. In all complexes, the signals attributed to the ethyl substituents of the PEt_3 co-ligand were observed as a doublet of triplet and a doublet of quartet resonances for the methyl and methylene protons, respectively, as a result of mutual coupling between these protons and phosphorus. Confirmation of this multiplicity was obtained with the use of ^{1}H $\{^{31}P\}$ NMR spectroscopy.

The resonances associated with the saturated N^E ring protons were noted to be slightly broadened at room temperature in complexes **4.4-1**, **4.4-2** and **4.4-3**, presumably as a result of pyramidal inversion of the pendent heteroatom donor (as observed previously, Chapter 2). On lowering the temperature of the samples to 10 °C, the resonances attributed to the saturated ring protons of **4.4-1** – **4.4-3** were observed to sharpen. It is interesting to note however, that further reduction of the temperature to – 50 °C in **4.4-3** led to severe broadening of these signals, an observation

that is consistent with the faster rate of inversion of sulphur in saturated thioether rings compared with their N- and O-containing analogues (See Chapter 2, Section 2.3).

Surprisingly, in the ^{1}H NMR spectrum of **4.4-4**, the ε-ring protons were not observed as a single resonance, but appeared as two distinct signals, each integrating to 1H. The diastereotopic nature of these protons can be attributed to the presence of the platinum centre,[19] as the ε-*endo* proton (δ_H = 1.63 ppm) was observed at noticeably higher frequency to the proton in the ε-*exo* position (δ_H = 1.46 ppm) {*c.f.* **3.1-4**, Chapter 3}. Additionally, in the ^{1}H NMR spectra of **4.4-1**, the resonance attributed to the δ-ring protons was observed as a single resonance integrating to 4H. This was in direct contrast to the protons at the γ-ring position, which were observed as two distinct 2H resonances as expected. In all complexes **4.4-1** – **4.4-4**, the aromatic region was as expected, with an overall integration of 10H, corresponding to the two phenyl substituents at the PNE phosphine fragment.

Although the small magnitude of the $^{2}J_{PP}$ coupling constants in the ^{31}P {^{1}H} NMR spectra of complexes **4.4-1** – **4.4-4** indicated a *cis* arrangement of the phosphine donors about the platinum centre, a series of 2D nOe NMR experiments were undertaken in an effort to unequivocally confirm this proposed regiochemistry. A representative example of **4.4-3** is shown in Figure 4.2.

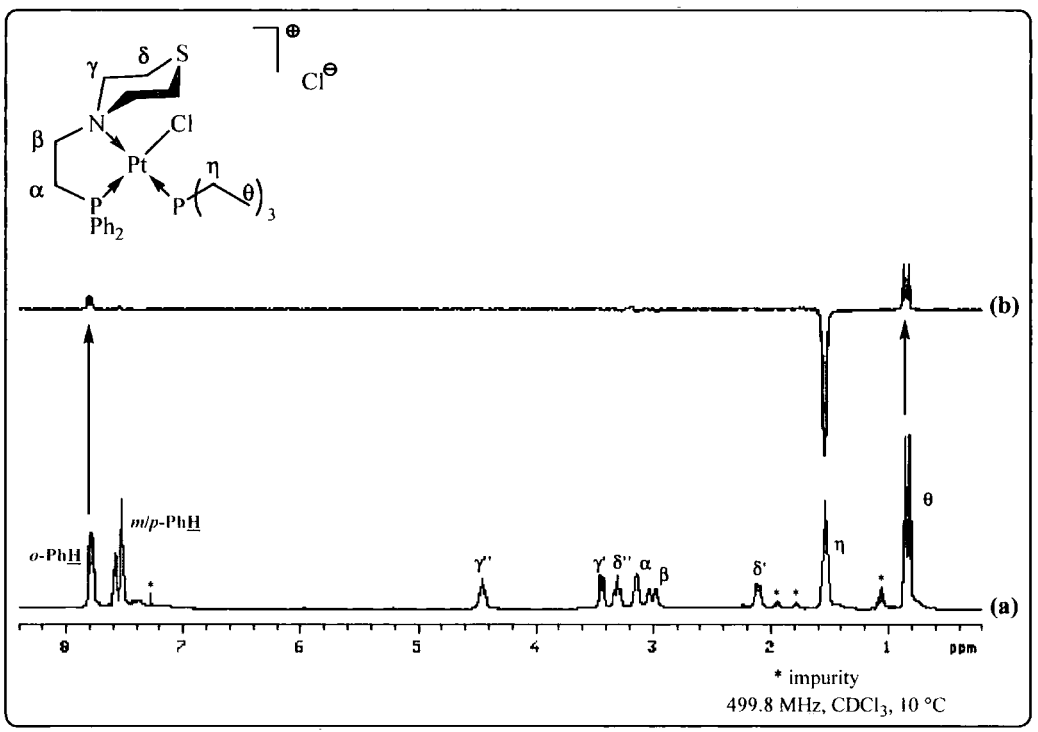

Figure 4.2: ^{1}H NMR (a) and 1D nOe (b) spectra of **4.4-3**

In the 1D nOe NMR spectra of all complexes **4.4-1** – **4.4-4**, selective irradiation of the PEt_3 methylene signal gave rise to two principal responses, corresponding to the PEt_3 methyl and *ortho*-phenyl protons. The absence of a response corresponding to the γ-/δ-ring protons further indicated that the phosphine donors were located *cis* to each other and thus confirmed the original structural assignment.

The ^{13}C $\{^1H\}$ NMR spectra of complexes **4.4-1** – **4.4-4** were as expected with each exhibiting the required number of resonances corresponding to the proposed structures. In all cases, the signals associated for the ethyl substituents of the PEt_3 co-ligand were observed as doublet resonances, resulting from coupling to the ^{31}P nucleus. Whilst the resonance attributed to the α-bridge carbon was observed as a doublet resonance, the other remaining signals were typically noted as singlet resonances. The aromatic region of all spectra were as expected with extensive coupling to phosphorus being noted for all the phenyl ring carbon resonances.

4.5.1 Molecular structure of 4.4-4

The complexes **4.4-1** – **4.4-4** were found to be stable under atmospheric conditions and slow evaporation of a CH_2Cl_2 solution of **4.4-4** afforded crystals suitable for study by X-ray diffraction. The gross molecular structure of **4.4-4** was as expected and confirmed the *cis* arrangement of the phosphine donors about the Pt centre as predicted by NMR spectroscopic studies. The PNC ligand **2.4-4** was shown to ligate the metal in a P–N fashion with the piperidine ring adopting the expected chair conformation, Figure 4.3.

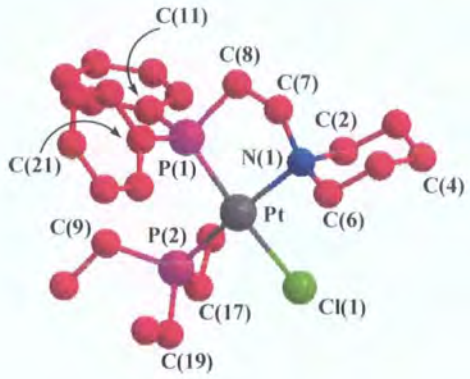

Figure 4.3: Ball and stick representation of **4.4-4**[†]

	Bond Length /Å		**Bond Angle /°**
Pt–P(1)	2.2259(5)	P(1)–Pt–N(1)	84.14(5)
Pt–N(1)	2.1873(16)	P(1)–Pt–P(2)	99.15(2)
Pt–P(2)	2.2607(6)	N(1)–Pt–Cl(1)	91.31(4)
Pt–Cl(1)	2.3697(5)	P(2)–Pt–Cl(1)	85.39(2)
P(1)–C(8)	1.821(2)	P(1)–Pt–Cl(1)	175.057(19)
N(1)–C(7)	1.504(3)	N(1)–Pt–P(2)	176.70(4)
P(1)–C(Ph)	1.810[a]	C(11)–P–C(21)	108.51(10)
P(2)–C(Et)	1.823[a]	C(2)–N(1)–C(6)	109.18(15)
		$\Sigma_{\angle P(1)}$	317.98[a,b]
		$\Sigma_{\angle P(2)}$	313.82[a,b]
		$\Sigma_{\angle N(1)}$	328.73[a,b]
		P(1)–C(8)–C(7)–N(1)	53.14

[a]average; [b]angle summation; e.s.d.'s in parentheses

Table 4.7: Selected bond lengths (Å) and bond angles (°) for **4.4-4**

The molecular structure of **4.4-4** demonstrated the expected square planar geometry about the Pt centre with little distortion as indicated by only slight deviation from linearity of the values of the P(1)–Pt–Cl(1) {175.057(19)°} and N(1)–Pt–P(2) {176.70(4)°} bond angles. Although the N(1) atom was observed to lie in the P(1)–Pt–P(2) plane, the Cl(1) atom was noted to lie 1.96° below this plane. The P(1)–Pt–N(1) bite angle {84.14(5)°} was found to be comparable to that for the previously discussed complex **4.1-2** (*vide supra*), with an associated twist noted in the P(1)–C(8)–C(7)–N(1) backbone {53.14°}. The P(1)–Pt–P(2) bond angle {99.15(2)°} is slightly larger than the ideal, with an associated opening of the N(1)–Pt–Cl(1) angle being noted.

[†] Molecular structure determination performed by Dr A. S. Batsanov

The metal-donor bond lengths in **4.4-4** are consistent with the related structure **4.1-2** shown above. The average P(2)–C(Et) bond distance {1.823 Å} is slightly longer than that observed for the P(1)–C(Ph) bond {1.810 Å}. Comparison of the angle summation about the P(1) and P(2) centres reveals the angle about the P(1) atom to be larger as a result of the increased steric demands about this donor atom. As expected, the sum of angles about the N(1) atom {$\Sigma_{\angle N(1)} = 328.73°$} is significantly larger than observed for the phosphorus donors {$\Sigma_{\angle P(1)} = 317.98°$; $\Sigma_{\angle P(2)} = 313.82$}.

The ethyl substituents about the P(2) centre were observed to adopt a 'splayed' arrangement in order to relieve the steric demands on the phosphorus donor. At the P(1) atom, the phenyl substituents were again noted to be found in a staggered orientation, in order to reduce steric constraints, with the intersection of the mean aromatic ring planes being 49.8°.

4.6 Conclusions/Summary

The stoichiometric reaction of the PNE ligands **2.4-1** – **2.4-3** with $[PtCl_2(cod)]$ did not afford the expected monometallic $[PtCl_2\{PNE\}]$ complexes, but instead double ligation of the Pt centre was shown to be the preferred product of these reactions. In all cases, complexes of formulation $[PtCl\{\kappa^2\text{-PN(E)}\}\{\kappa^1\text{-P(NE)}\}]^+ Cl^-$ (**4.1-1** – **4.1-3**) were obtained from reaction of equimolar quantities of the PNE ligand with $[PtCl_2(cod)]$ {along with 0.5 equivalents of unreacted $[PtCl_2(cod)]$}, presumably as a result of the poor lability of the ancillary cyclooctadiene ligand.

An HCl derivative of complex **4.1-2** {**4.1-2.HCl**} was found to crystallise by slow diffusion of hexane into a saturated CH_2Cl_2 solution of the complex mixture. The resulting molecular structure confirmed the nature of the complexation. Variation of the reaction stoichiometry, *i.e.* by treatment of two equivalents of ligand with one equivalent of $[PtCl_2(cod)]$, afforded the complexes **4.1-1** – **4.1-3** directly, thus providing confirmation of the nature of ligand coordination. In all cases, double chelation of the PNE ligands **2.4-1** – **2.4-3** to the Pt centre was not noted.

Attempts to form the doubly-chelated $[Pt\{\kappa^2\text{-PN(E)}\}_2\}]^{2+}$ $2PF_6^-$ complexes **4.2-1** – **4.2-3** by abstraction of the bound chloride from complexes **4.1-1** – **4.1-3** with $NaPF_6$ proved unsuccessful in all cases. The failure of these syntheses is attributed to the

sterically demanding nature of the pendent ring as it is presumed that coordination of the second amine donor would give rise to an unfavourable steric clash between this ring fragments. Attempts to selectively substitute the $\{\kappa^1$-P(NE)$\}$ donor from the $[PtCl\{\kappa^2$-PN(E)$\}\{\kappa^1$-P(NE)$\}]^+$ Cl^- complexes **4.1-1(a)** – **4.1-3(a)** with PPh_3 also proved unsuccessful as the required $[PtCl\{\kappa^2$-PN(E)$\}(PPh_3)]^+$ Cl^- complexes **4.3-1** – **4.3-3** were not obtained.

Reaction of the PNE ligands (**2.4-1** – **2.4-4**) with the more reactive $[PtCl(PEt_3)(\mu$-Cl$)]_2$ dimer rapidly and cleanly generated the required $[PtCl(PEt_3)\{\kappa^2$-PN(E)$\}]^+$ Cl^- complexes **4.4-1** – **4.4-4**. Complex **4.4-4** was found to crystallise from CH_2Cl_2/hexane with the molecular structure supporting the structure proposed by NMR spectroscopic studies and confirming the *cis* arrangement of the phosphines about the Pt centre.

4.7 References

[1] U. Belluco, "*Organometallic and Coordination Chemistry of Platinum*", 1974, Academic Press, New York, USA.

[2] P. S. Pregosin and R. W. Kunz, "*^{31}P and ^{13}C NMR of Transition Metal Complexes*", Springer-Verlag, Berlin, 1979.

[3] F. R. Hartley in "*Comprehensive Organometallic Chemistry; The Synthesis, Reactions and Structures of Organometallic Compounds*", G. Wilkinson, F. G. A. Stone and E. W. Abel (Eds.), Pergamon Press, New York, 1983, Volume 6, Chapter 39.

[4] M. L. Clarke, *Polyhedron*, 2001, **20**, 151 – 164.

[5] P. E. Garrou, *Chem. Rev.*, 1981, **81**, 229 – 266.

[6] Q. Folashade Mokuolu, P. A. Duckmanton, P. B. Hitchcock, C. Wilson, A. J. Blake, L. Shukla and J. B. Love, *Dalton Trans.*, 2004, 1960 – 1970.

[7] C. W. G. Ansell, M. K. Cooper, K. P. Dancey, P. A. Duckworth, K. Henrick, M. McPartin, G. Organ and P. A. Tasker, *J. Chem. Soc., Chem. Commun.*, 1985, 437 – 439.

[8] T. Chivers, K. McGregor and M. Parvez, *Inorg. Chem.*, 1993, **32**, 5119 – 5125.

[9] A. Habtemariam, B. Watchman, B. S. Potter, R. Palmer, S. Parsons, A. Parkin and P. J. Sadler, *J. Chem. Soc., Dalton Trans.*, 2001, 1306 – 1318.

[10] M. Bassett, D. L. Davies, J. Neild, L .J. S. Prouse and D. R. Russell, *Polyhedron*, 1991, **10**, 501 – 507.

[11] T. G. Appleton, H. C. Clark and L. E. Manzer, *Coord. Chem. Rev.*, 1973, **10**, 335 – 422.

[12] T. G. Appleton, R. D. Berry, J. R. Hall and D. W. Neale, *J. Organomet. Chem.*, 1989, **364**, 249 – 273.

[13] H. C. Clark and L. E. Manzer, *J. Organomet. Chem.*, 1973, **59**, 411 – 428.

[14] E. L. Eliel, N. L. Allinger, S. J. Angyal and G. A. Morrison, "*Conformational Analysis*", 1965, Interscience Publishers, New York, USA.

[15] N. M. Boag and M. S. Ravetz, *J. Chem. Soc., Dalton Trans.*, 1995, 3473 – 3474.

[16] F. R. Hartley, *Organomet. Chem. Rev. A*, 1970, **6**, 119 – 137.

[17] "*Handbook of Phosphorus-31 Nuclear Magnetic Resonance*", J. C. Tebby (Ed.), CRC Press, Boca Raton, Florida, USA, 1991.

[18] S. M. Aucott, A. M. Z. Slawin and J. D. Woollins, *J. Chem. Soc., Dalton Trans.*, 2000, 2559 – 2575.

[19] M. V. Baker, B. W. Skelton, A. H. White and C. C. Williams, *J. Chem. Soc., Dalton Trans.*, 2001, 111 – 120.

Chapter 5:

Complexation of PNE ligands with Rh

5.1 Introduction

Rhodium complexes find almost ubiquitous application in both coordination chemistry and homogeneous catalysis due to the wide ranging catalytic properties that these complexes exhibit.[1] Rh-mediated processes are particularly attractive as they are often extremely chemically selective and are capable of exhibiting high rates of stereoselectivity.[2] It is unsurprising, therefore, that there is a continuing drive towards the development of ligands that exhibit ever-increasing levels of control over their resulting complexes.

In terms of coordination chemistry, Rh is a particularly attractive metal due to the presence of the ^{103}Rh nucleus (I = ½, 100% abundant) as couplings to other NMR spin-active nuclei (such as the ^{31}P nucleus) are readily detected, which potentially aids the characterisation of the resulting complexes.[3] Moreover, the overwhelming majority of rhodium complexes are found in the Rh(I) and Rh(III) oxidation states, the diamagnetic nature of these further facilitates their study by NMR spectroscopic methods.[4]

The following studies will focus on examination of the coordination chemistry of the PNE ligands with Rh(I) centres and exploration of the behaviour of the resulting complexes in both the solid- and solution-states.

5.2 Coordination of 2.4-1 with [RhCl(PPh$_3$)$_3$]

As a starting point in the exploration of the coordination behaviour of the ligands **2.4-1** – **2.4-5** with Rh(I) centres, the reaction of the PNN(Me) ligand **2.4-1** with [RhCl(PPh$_3$)$_3$] was undertaken. Given the potentially tridentate nature of **2.4-1**, two likely coordination modes of the ligand to the 'RhCl' fragment were envisaged, with the ligand adopting either bidentate or tridentate coordination to the Rh centre, as shown in Scheme 5.1. Upon reaction of equimolar quantities of **2.4-1** with [RhCl(PPh$_3$)$_3$], *in situ* analysis of the reaction mixture by ^{31}P {^{1}H} NMR spectroscopy clearly indicated the formation of the bidentate [RhCl(PPh$_3$){κ^2-PN(NMe)}] complex (Scheme 5.1, **ii**).

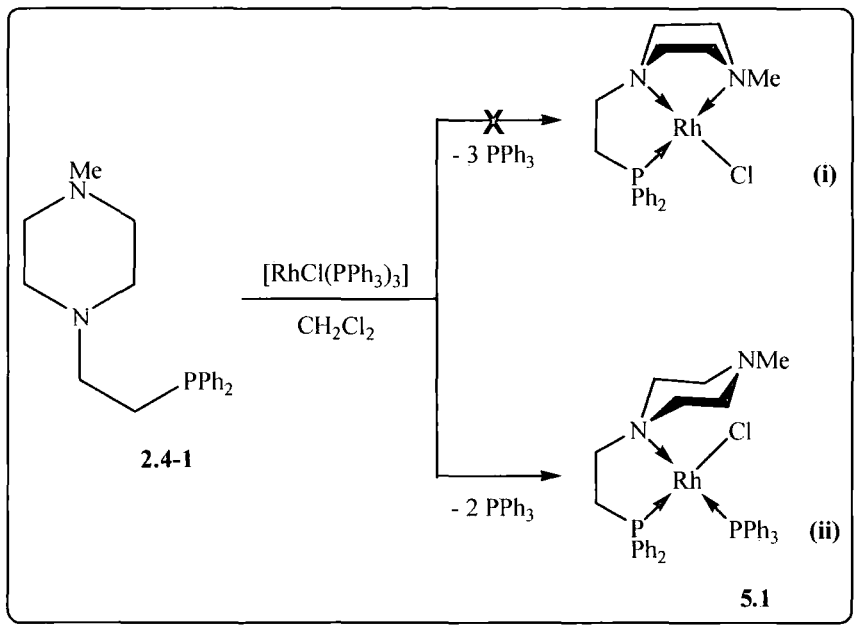

		$^{31}P\{^{1}H\}$ NMR*		
		δ_P	$^{1}J_{RhP}$/Hz	$^{2}J_{PP}$/Hz
5.1	$NCH_2CH_2\underline{P}Ph_2$ (dd)	+ 62.6	173.6	32.2
	$\underline{P}Ph_3$ (dd)	+ 36.8	125.9	32.2

*121.4 MHz, C_6D_6

Scheme 5.1: Synthesis and $^{31}P\{^{1}H\}$ NMR spectroscopic data for **5.1**

Both signals in the $^{31}P\{^{1}H\}$ NMR spectrum of **5.1** were observed as doublet of doublet resonances. The signal at lower frequency (δ_P = + 36.8 ppm) was attributed to that of the metal-bound triphenylphosphine ligand on the basis of its chemical shift (by comparison with similar compounds in the literature[5]). Furthermore, the magnitude of the $^{1}J_{RhP}$ coupling (125.9 Hz) was consistent with that exhibited by the $[RhCl(PPh_3)_3]$ precursor compound.[6] The resonance at higher frequency (δ_P = 62.6 ppm) was attributed to that of the bound PNE phosphine donor with the magnitude of the $^{1}J_{RhP}$ coupling being consistent with the $[RhCl(CO)\{\kappa^2\text{-PN-}Ph_2PCH_2CH_2NMe_2\}]$ complexes reported by des Abbayes and co-workers.[7] Additionally, the small magnitude of the $^{2}J_{PP}$ coupling constant (32.2 Hz) indicated the mutual *cis* arrangement of the phosphine donors about the rhodium centre,[8] thus supporting the proposed geometry of complex **5.1**.

The bidentate P–N coordination in **5.1** of the PNE ligand was further indicated by the observation of severely broadened resonances in both the ^{1}H and $^{13}C\{^{1}H\}$ NMR spectra of this compound. This spectral line broadening was reminiscent of the NMR

spectra obtained from the related bidentate P–N ligated complexes [PdCl(Me){κ^2-PN(NMe)}] (**3.5.1**) and [PtCl(PEt_3){κ^2-PN(NMe)}] (**4.4-1**) in which fluxionality of the uncoordinated amine donor was observed at room temperature. However, acquisition of ^1H and ^{13}C {^1H} NMR spectra of **5.1** at lower temperatures (– 50 °C) did not result in a significant sharpening of the resonances.

Regrettably, the purification of the *bis*-phosphine complex **5.1** did not prove a facile process as, despite repeated attempts by extraction and fractional crystallisation, free triphenylphosphine could not be completely removed from the sample. Over the course of these repeated recrystallisation attempts, the decomposition of the complex was gradually observed (signified by signals in its ^{31}P {^1H} NMR spectrum attributed to ligand degradation products) and thus this purification was abandoned.

Due to the purification difficulties of this complex, this synthetic methodology was not extended to the remaining ligands in this family (**2.4-2** – **2.4-4**) and an alternative source of Rh(I) was sought which would facilitate the synthesis of a series of PNE-containing Rh complexes.

5.3 Reaction of PNE ligands with $[Rh_2\{\mu\text{-}Cl\}_2(CO)_4]$

Following the failure to isolate the [RhCl(PPh_3){κ^2-PN(NMe)}] complex **5.1**, the complexation of the PNE ligands **2.4-1** – **2.4-4** was reattempted using the dimeric $[Rh_2\{\mu\text{-}Cl\}_2(CO)_4]$ precursor. The use of this dimeric complex was particularly attractive since it comprises labile CO ligands along with weakly bound bridging chlorides. On cleavage of this dimeric precursor, facile dissociation of the CO ligands from the metal's coordination sphere occurs, thereby facilitating both complex formation and its subsequent purification. Moreover, the presence of a carbonyl functionality at the rhodium centre provides an additional means of characterising the resulting complexes by infrared spectroscopy.

The reactions of **2.4-1** – **2.4-4** all proceeded according to the methodology detailed in Scheme 5.2, *i.e.* by reaction of the requisite ligand with half a molar equivalent of $[Rh_2\{\mu\text{-}Cl\}_2(CO)_4]$. Upon addition of **2.4-1** – **2.4-4** to the Rh precursor, the immediate evolution of the displaced CO gas from solution was noted, indicating rapid formation of the product.

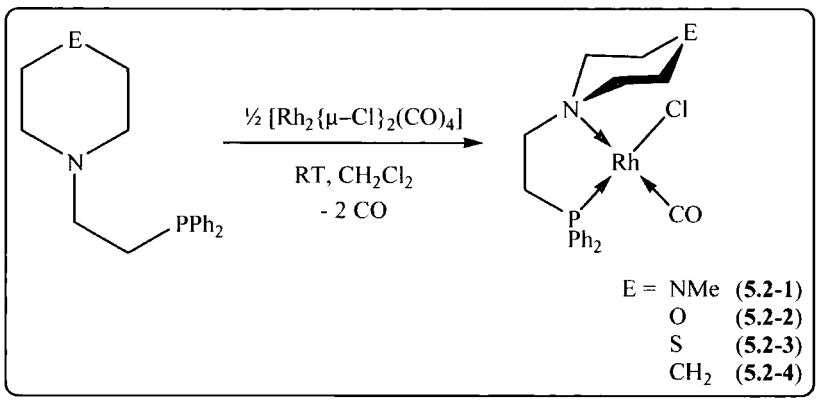

E =		Yield	MS (MALDI$^+$)^a *m/z*	IR^b /cm^{-1}
NMe	**5.2-1**	71 %	443.0	1998
O	**5.2-2**	75 %	430.0	2001
S	**5.2-3**	86 %	446.1	2000
CH_2	**5.2-4**	79 %	428.1	1998

^{a}[M–Cl]$^+$ observed in all complexes **5.2-1** – **5.2-4**; ^{b}$CHCl_3$ solution

Scheme 5.2: Synthesis, mass spectrometric and IR spectroscopic data of **5.2-1** – **5.2-4**

Following isolation and purification by recrystallisation, the [RhCl(CO){κ^2-PN(E)}] complexes **5.2-1** – **5.2-4** were all obtained in good yield (71 – 86 %) as yellow-brown solids with satisfactory CHN analyses. In all cases, mass spectrometric analyses (MALDI$^+$) were obtained with molecular ion peaks corresponding to [Rh(CO){PNE}]$^+$ fragments being noted. In complexes **5.2-1** – **5.2-4**, carbonyl absorption bands at *ca.* 2000 cm^{-1} were obtained by IR spectroscopy, thus indicating a *cis* arrangement of the carbonyl and phosphine donor fragments by comparison with similar compounds in the literature.[9,10]

5.3.1 NMR spectroscopic characterisation of [RhCl(CO){κ^2-PN(E)}]

5.3.2 Characterisation of 5.2-1 – 5.2-4 by ^{31}P {^{1}H} NMR spectroscopy

As expected, the [RhCl(CO){κ^2-PN(E)}] complexes **5.2-1** – **5.2-4** all exhibited the expected doublet resonances in their ^{31}P {^{1}H} NMR spectra (as a result of mutual coupling between the ^{31}P and ^{103}Rh nuclei) with the magnitudes of these couplings

being consistent with those for similar bidentate κ^2-P–N-ligated 'RhCl(CO)' centres in the literature.[7,10] However, it was notable that the resonances for complexes **5.2-1** and **5.2-3** were significantly broadened at 20 °C. This was in direct contrast to the sharp doublet resonances that were observed for the related derivatives **5.2-2** and **5.2-4**, Table 5.1.

E =		$^{31}P\{^1H\}$ NMR*			
		[RhCl(CO){κ^2-PN(E)}]			Parent ligand
		δ_P	$^1J_{RhP}$ /Hz	$\nu_{½}$ /Hz[a]	δ_P
NMe	**5.2-1**	+ 59.6 (br d)	160.2	51	– 19.1 (s)
O	**5.2-2**	+ 60.8 (d)	172.6	-	– 18.2 (s)
S	**5.2-3**	+ 54.7 (br d)	164.1	497	– 18.3 (s)
CH_2	**5.2-4**	+ 60.8 (d)	175.5	-	– 17.8 (s)

*202.3 MHz, $CDCl_3$; [a]defined as half average signal width at half height

Table 5.1: $^{31}P\{^1H\}$ NMR spectroscopic data for **5.2-1** – **5.3-4**
(Data for parent ligands **2.4-1** – **2.4-4** included for comparative purposes)

The unexpectedly broadened nature of the $^{31}P\{^1H\}$ NMR spectra of complexes **5.2-1** and **5.2-3** was suggestive of a dynamic process occurring in $CDCl_3$ solution in both these compounds which was absent in compounds **5.2-2** and **5.2-4**. In an effort to establish the origin of the fluxionality demonstrated by **5.2-1** and **5.2-3**, low temperature NMR studies of these complexes were undertaken.

5.3.2.1 $^{31}P\{^1H\}$ NMR spectroscopic analysis of 5.2-1

On lowering the temperature of a sample of **5.2-1** ($CDCl_3$), the appearance of the $^{31}P\{^1H\}$ NMR spectrum of this compound was observed to undergo significant change. The broad doublet resonance (attributed to the bound phosphine moiety) was observed to sharpen as the temperature was decreased, with the concomitant appearance of a second doublet resonance in this spectrum at 0 °C at slightly lower frequency than the major signal. Upon reaching – 50 °C, the presence of two distinct species was evident in the NMR spectrum in an approximate ratio of *ca.* 4:1, Figure 5.1. Both signals remain

as doublet resonances despite the change in temperature, consistent with the phosphine fragment being bound to the Rh centre in both species. On warming the sample to 20 °C, an identical broad resonance to that observed prior to cooling was noted, thereby indicating that this process is reversible.

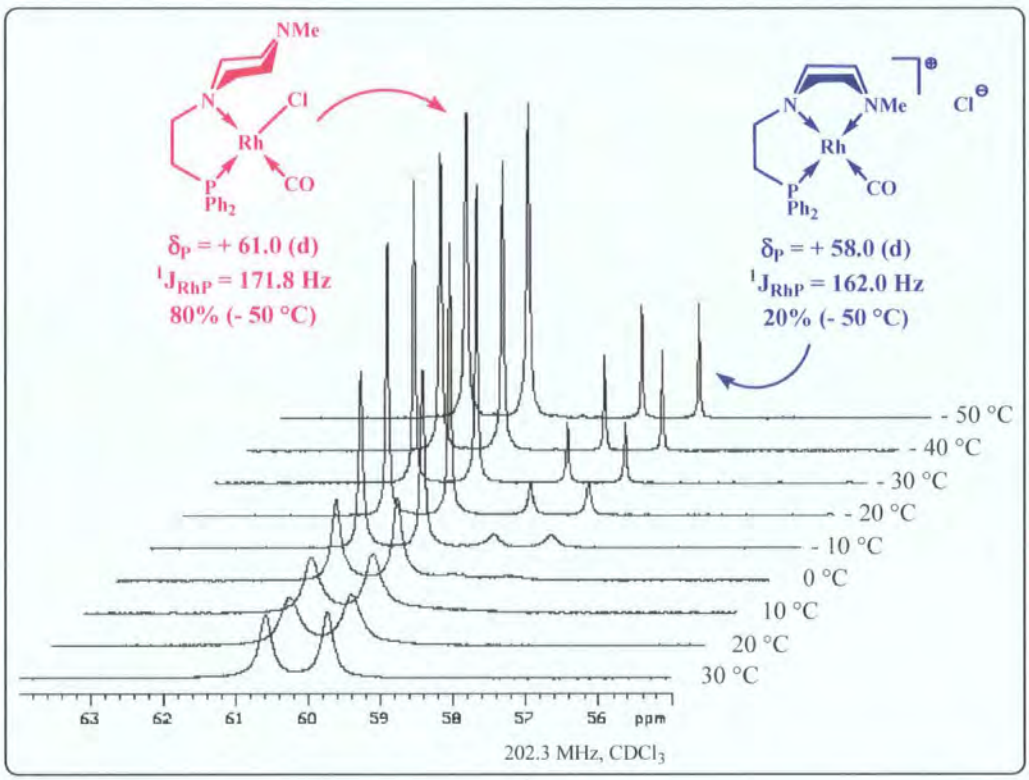

Figure 5.1: ^{31}P $\{^{1}H\}$ NMR spectra of **5.2-1** ($CDCl_3$) as a function of temperature

The two species observed in the low temperature ^{31}P $\{^{1}H\}$ NMR spectrum of **5.2-1** exhibited markedly different $^{1}J_{RhP}$ coupling constants, although the magnitude of these couplings remain within the expected limits for Rh(I) complexes.[3] The $^{1}J_{RhP}$ coupling observed for the major doublet species (δ_P = + 61.0 ppm; 171.8 Hz) is suggestive of the expected neutral [RhCl(CO){κ^2-PN(NMe)}] complex {**5.2-1(a)**} by comparison with the related complexes **5.2-2** and **5.2-4** as well as with similar literature compounds.[7,10,11] By contrast, the minor species exhibits a notably smaller $^{1}J_{RhP}$ value (δ_P = + 58.0 ppm; 162.0 Hz), which is consistent with a charged [Rh(CO){κ^3-PNNMe}]$^+$ Cl^- complex {**5.2-1(b)**}.[12]

5.3.2.2 ^{31}P {^{1}H} NMR spectroscopic analysis of 5.2-3

Following the surprising appearance of two environments in the low temperature ^{31}P {^{1}H} NMR spectrum of **5.2-1**, a series of low temperature NMR spectroscopic studies were undertaken on the related [RhCl(CO){PNS}] complex **5.2-3**. Specifically, it was of interest to establish whether reversible coordination of the thioether donor to the rhodium centre in **5.2-3** was occurring in an analogous manner to that observed for **5.2-1**.

As observed for **5.2-1**, lowering the temperature of a sample of **5.2-3** in $CDCl_3$ afforded two resonances at – 50 °C in its ^{31}P {^{1}H} NMR spectrum. Again, both signals were observed as doublet resonances, indicating that no dissociation of the phosphine fragment from the rhodium centre occurs on decreasing temperature.

Comparison of the chemical shifts and their $^{1}J_{RhP}$ coupling constants again were suggestive of a dynamic isomerisation process between [RhCl(CO){κ^2-PN(S)}] {**5.2-3(a)**} and [Rh(CO){κ^3-PNS}]$^{+}$ Cl^{-} {**5.2-3(b)**} forms of the complex. The major species (δ_P = + 60.6 ppm) was attributed to the neutral structure **5.2-3(a)** as the magnitude of the $^{1}J_{RhP}$ coupling (173.6 Hz) is consistent with that of **5.2-1(a)** and the related complexes **5.2-2** and **5.2-4**, as well as with similar compounds in the literature.[7,10,11] The minor species (δ_P = + 53.6 ppm) was noted to display a smaller magnitude of $^{1}J_{RhP}$ which, from comparison with data in the literature, is consistent with the formation of a [Rh(CO){κ^3-PNS}]$^{+}$ Cl^{-} compound {**5.2-3(b)**},[13] Figure 5.2. Interestingly, at – 50 °C, the integration of the resonances attributed to complexes **5.2-3(a)** and **5.2-3(b)** was approximately 4:1, an identical ratio to that observed for the related complex **5.2-1**.

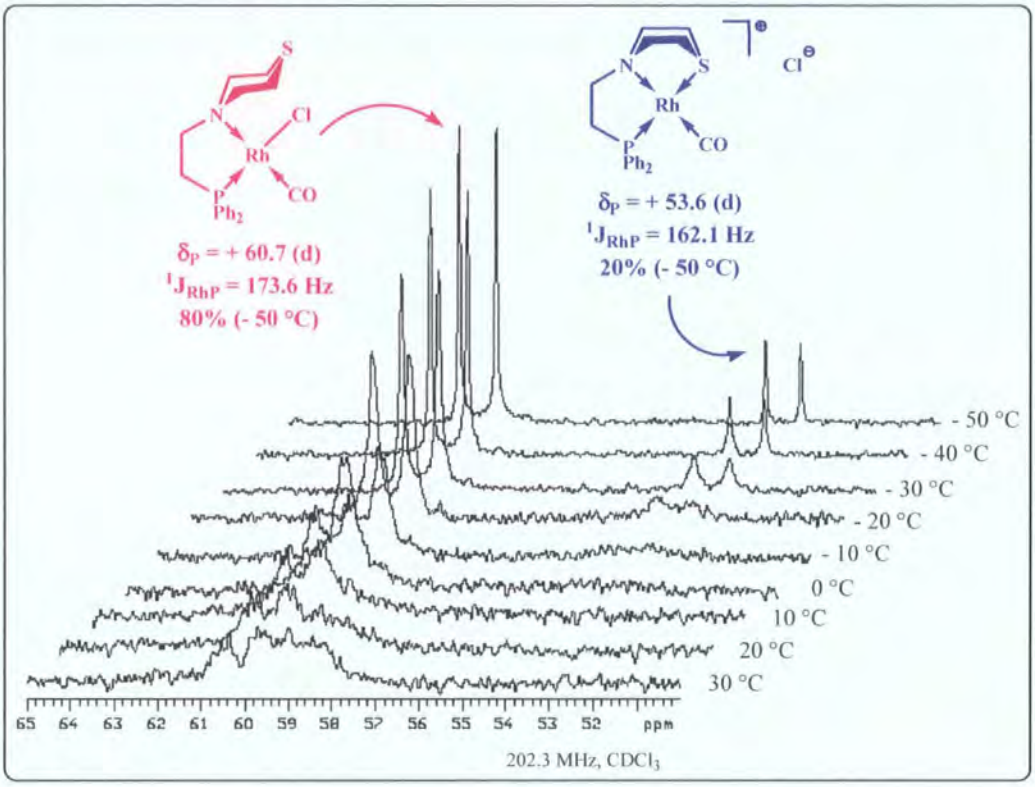

Figure 5.2: ^{31}P $\{^{1}H\}$ NMR spectra of **5.2-3** ($CDCl_3$) as a function of temperature

In contrast to the ^{31}P $\{^{1}H\}$ NMR spectra of **5.2-1** and **5.2-3**, the ^{31}P $\{^{1}H\}$ NMR spectra of the related compounds **5.2-2** and **5.2-4** were observed to be sharp well-defined doublet resonances at 20 °C, with the magnitudes of their $^{1}J_{RhP}$ couplings being consistent with κ^2-P–N ligation to the rhodium centre.[7,10] Indeed upon lowering the temperature of the ^{31}P $\{^{1}H\}$ NMR spectra of **5.2-2** and **5.2-4**, no changes were noted and thus confirmed the rigid bidentate coordination of these ligands to rhodium.

Whilst the static P–N ligand coordination of **5.2-4** was unsurprising (due to the absence of a third heteroatom donor fragment in the ligand framework), it was surprising that dynamic interconversion between the neutral [RhCl(CO){κ^2-PN(O)}] and charged [Rh(CO){κ^3-PNO}]$^+$ Cl^- forms of complex **5.2-2** was not observed in solution. Indeed, no change in the ^{31}P $\{^{1}H\}$ NMR spectrum of **5.2-2** was noted at lower temperatures. Although complex **5.2-2** comprises an additional, pendent ether donor fragment, the rigid κ^2-P–N ligation to the rhodium centre indicates that coordination of the hard ether donor to the soft Rh(I) centre is a disfavoured process. Indeed, this situation is supported by the observation that in comparable tridentate PNO ligands

systems, P–N chelation is the preferred coordination mode to Rh(I) centres with the oxygen remaining uncoordinated to the metal centre.[14,15,16]

In conclusion, the broad nature of the ^{31}P $\{^1H\}$ NMR spectra of complexes **5.2-1** and **5.2-3** is believed to result from a dynamic process that interconverts [RhCl(CO){κ^2-PN(E)}] {**5.2-1(a)/5.2-3(a)**} and [Rh(CO){κ^2-PN(E)}]$^+$ Cl^- {**5.2-1(b)/5.2-3(b)**} in $CDCl_3$ solution. Low temperature ^{31}P $\{^1H\}$ NMR spectroscopic studies on these two complexes clearly demonstrate the appearance of a second metal-bound phosphine environment at low temperature with magnitudes of the $^1J_{RhP}$ coupling constants comparing favourably with the proposed structural assignments. By contrast, the ^{31}P $\{^1H\}$ NMR spectra of complexes **5.2-2** and **5.2-4** indicated rigid bidentate P–N ligation of the rhodium centre. For ease of comparison, the chemical shifts and ^{31}P–^{103}Rh coupling constants are shown in Table 5.2.

		^{31}P $\{^1H\}$ NMR*			
		[RhCl(CO){κ^2-PN(E)}]		[Rh(CO){κ^2-PN(E)}]$^+$ Cl^-	
		δ_P	$^1J_{RhP}$ /Hz	δ_P	$^1J_{RhP}$ /Hz
NMe	**5.2-1(a)**[a]	+ 61.0	171.8	-	-
	5.2-1(b)[a]	-	-	+ 58.0	162.0
O	**5.2-2**	+ 60.8	172.6	-	-
S	**5.2-3(a)**[a]	+ 60.7	173.6	-	-
	5.2-3(b)[a]	-	-	+ 53.6	162.1
CH_2	**5.2-4**	+ 60.8	175.5	-	-

*202.3 MHz, $CDCl_3$; [a] – 50 °C

Table 5.2: ^{31}P $\{^1H\}$ NMR spectroscopic data for complexes **5.2-1 – 5.2-4**

5.3.3 NMR spectroscopic characterisation of 5.2-1 – 5.2-4

5.3.3.1 $^1H/^{13}C$ $\{^1H\}$ NMR spectroscopic analysis of 5.2-1

The ^1H NMR spectrum of **5.2-1** at 30 °C demonstrated severe broadening of most aliphatic resonances as a result of the presumed dynamic isomerisation process at the Rh centre. However, upon lowering the temperature of the sample to – 50 °C, the signals in the aliphatic region of the spectrum were observed to sharpen considerably, with the appearance of a number of new resonances, Figure 5.3. Interestingly, the

methyl and methylene signals observed corresponded to the presence of two forms of **5.2-1** in solution, namely the bidentate complex [RhCl(CO){κ^2-PN(NMe)}] {**5.2-1(a)**} and its tridentate counterpart [Rh(CO){κ^3-PNNMe}]$^+$ Cl^- {**5.2-1(b)**}.

The aromatic region of the ^{1}H NMR spectrum of **5.2-1** at 30 °C was observed to be moderately broadened, although upon lowering the temperature to – 50 °C, two distinct environments became apparent as was the case for the aliphatic region of this spectrum.

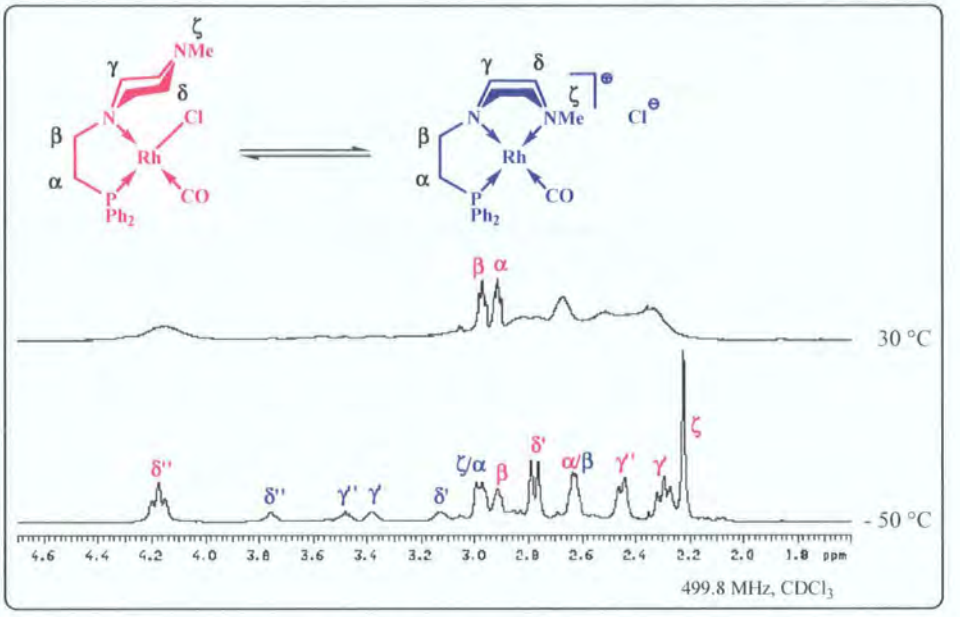

Structural assignment with the aid of low temperature 2D NMR experiments (*vide infra*)

Figure 5.3: Representative ^{1}H NMR spectra of **5.2-1** at 30 °C and – 50 °C ($CDCl_3$) (aromatic region omitted for clarity)

It is interesting to note that the resonance corresponding to the *N*-methyl group (ζ) in **5.2-1** was not observed as the expected sharp singlet resonance at 30 °C. This is in direct contrast to the situation for both the parent ligand (**2.4-1**) (Chapter 2, Section 2.3.2) and previous studies on the solution behaviour of uncoordinated heterocyclic amines such as *N*-methylpiperidine. Indeed, the latter low temperature NMR spectroscopic studies have shown that rapid ring inversion processes result in the magnetic equivalence of the axial and equatorial conformers of the ring (even at temperatures as low as – 90 °C) and consequently the signal attributed to these protons is observed as a sharp singlet resonance.[17] It is presumed that the interconversion processes between the bidentate [RhCl(CO){κ^2-PN(NMe)}] {**5.2-1(a)**} and tridentate

$[Rh(CO)\{\kappa^3\text{-PNNMe}\}]^+ Cl^-$ {**5.2-1(b)**} forms of this complex hinder the rate of ring inversion processes in structure **5.2-1(a)**, resulting in broadening of the resonance attributed to the ζ-protons in **5.2-1(a)**.

The 2D ^1H–^1H COSY NMR spectrum of **5.2-1** at – 50 °C was consistent with the ^{31}P $\{^1H\}$ NMR spectrum at this temperature and clearly indicated the presence of two environments. Indeed, the two sets of resonances were shown to correspond to two discrete structures through the lack of correlation cross peaks between these environments, Figure 5.4.

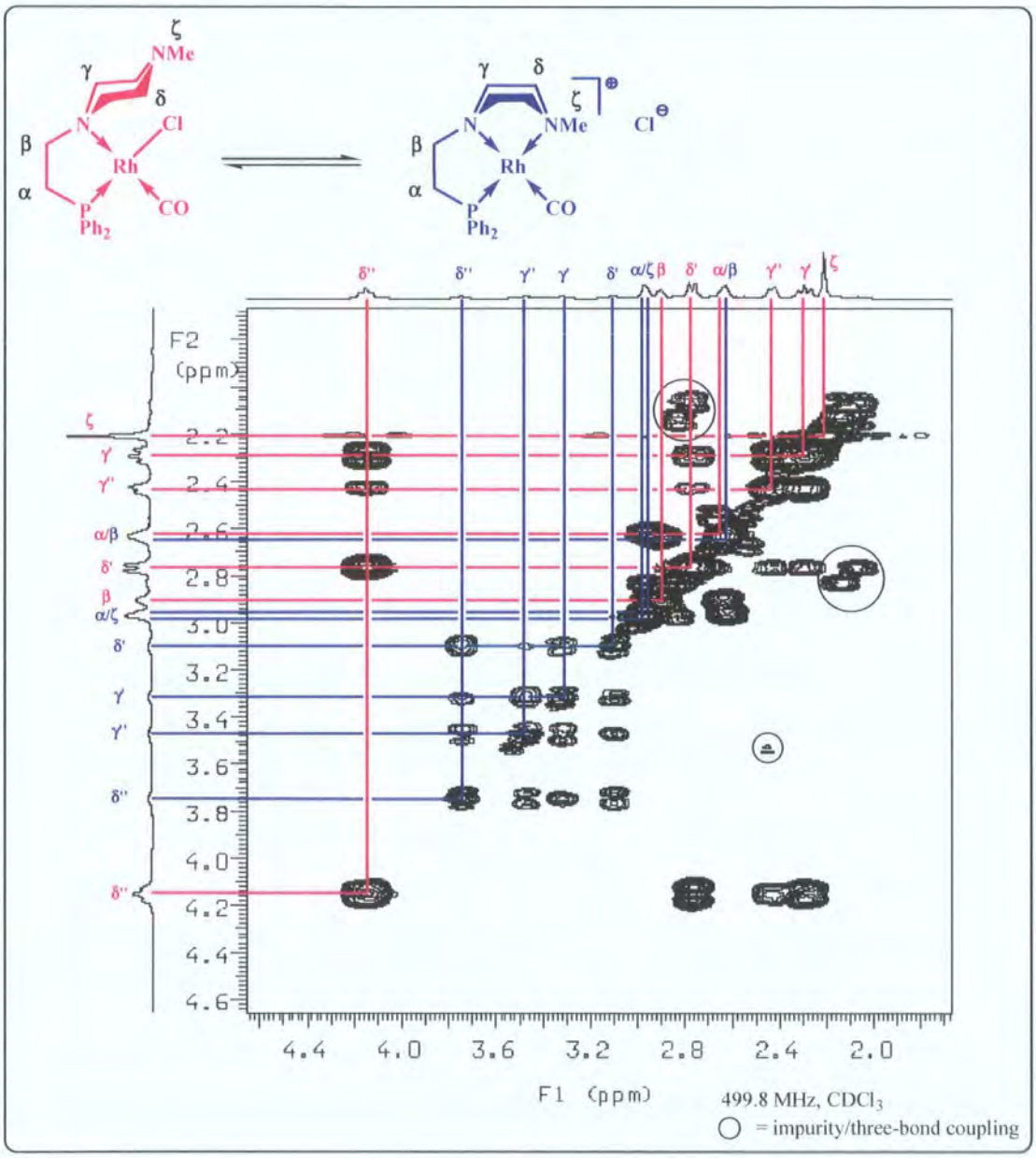

Figure 5.4: ^1H–^1H COSY NMR spectrum of **5.2-1** at – 50 °C ($CDCl_3$)
(aromatic region omitted for clarity)

The ^{1}H NMR spectrum of **5.2-1** at – 50 °C ($CDCl_3$) was consistent with the existence of the neutral [RhCl(CO){κ^2-PN(NMe)}] {**5.2-1(a)**} and charged [Rh(CO){κ^3-PNNMe}]$^+$ Cl^- {**5.2-1(b)**} structures proposed on the basis of the low temperature ^{31}P {^{1}H} NMR spectroscopic studies on this compound. In both structural isomers, distinct splitting patterns of the resonances associated with the γ- and δ-ring protons were observed, although it is interesting to note that the γ- and δ-positions in **5.2-1(b)** were notably closer in chemical shift than were observed for the bidentate isomer **5.2-1(a)**. The ζ-methyl signal for the cationic complex **5.2-1(b)** was expected to appear as a doublet resonance {as observed for the analogous [PdCl{κ^3-PN(NMe)}]$^+$ Cl^- complex (**3.1-1**)} although due to this resonance being coincident with the signal attributed to the δ-protons of **5.2-1(b)**, the expected multiplicity was not observed. Although not shown in Figure 5.4, the aromatic region of the spectrum for **5.2-1** at low temperature clearly demonstrated the presence of two distinct aromatic environments.

The ^{13}C {^{1}H} NMR spectrum of **5.2-1** recorded at 30 °C again demonstrated broadening of all aliphatic resonances, however, upon acquisition of the spectrum at low temperature (– 50 °C), the presence of the two structural isomers {**5.2-1(a)/5.2-1(b)**} was again apparent. The structural assignments of these resonances was made with the assistance of low temperature 2D ^{1}H–^{13}C HETCOR experiments, Figure 5.5.

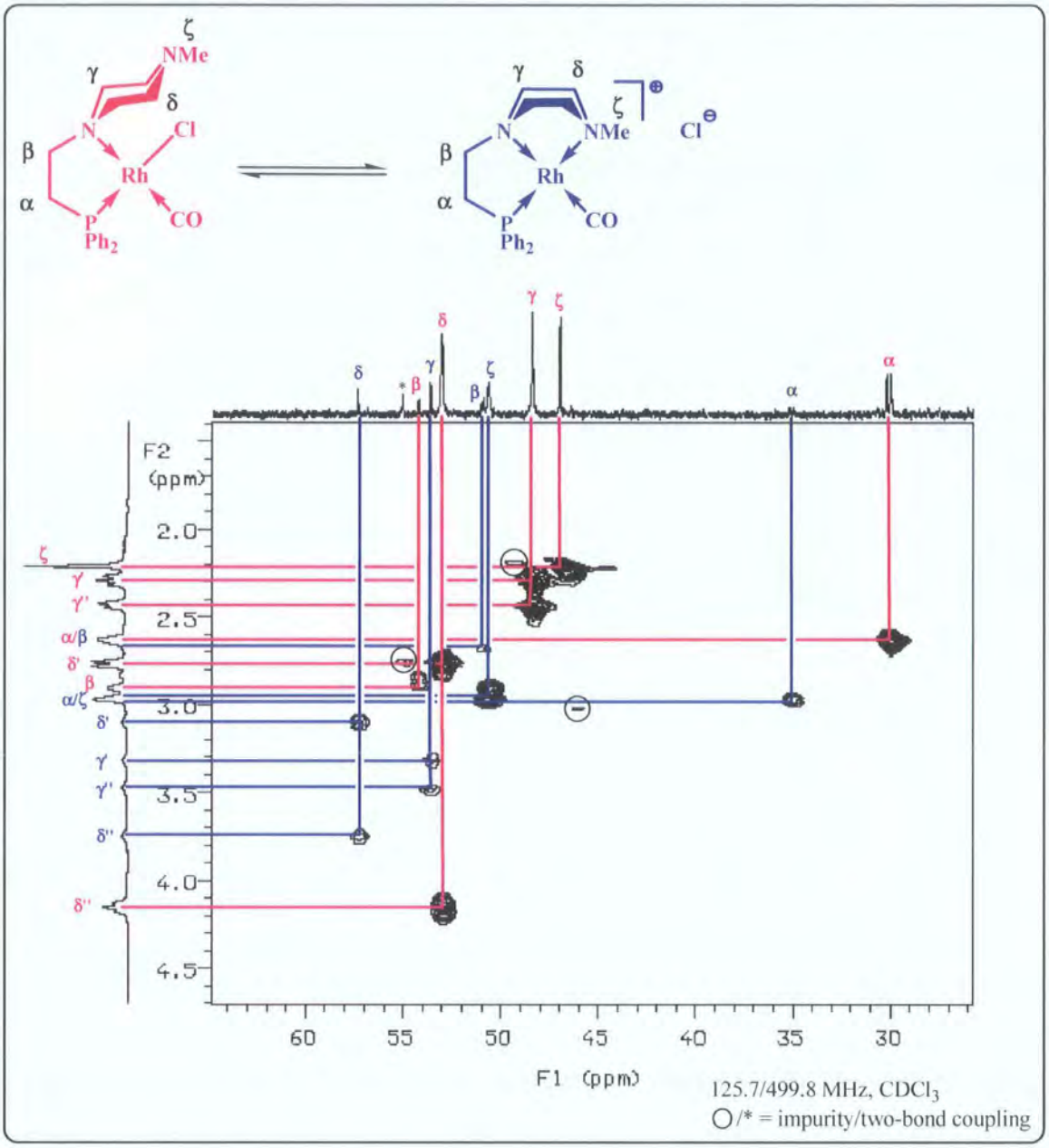

Figure 5.5: ^{1}H–^{13}C $\{^{1}H\}$ HETCOR NMR spectrum of **5.2-1** at – 50 °C ($CDCl_3$) (aromatic region omitted for clarity)

The ^{1}H–^{13}C $\{^{1}H\}$ HETCOR spectrum of **5.2-1** at – 50 °C clearly exhibited the expected correlations between the resonances attributed to the two isomeric forms of this complex. Indeed, this low temperature HETCOR NMR spectrum proved to be consistent with both the low temperature ^{31}P $\{^{1}H\}$ and ^{1}H–^{1}H COSY NMR spectra (*vide supra*) and thus supporting the existence of κ^2-P–N {**5.2-1(a)**}and κ^3-P–N {**5.2-1(b)**} structures in chloroform solution.

5.3.3.2 ^{1}H NMR spectroscopic analysis of 5.2-2 – 5.2-4

The ^{1}H NMR spectrum of **5.2-2** was observed to exhibit moderate broadening of the resonances attributed to the saturated morpholine ring protons at 30 °C, although the resonances associated with the α- and β-bridge protons were observed as well-defined multiplet signals at this temperature. Given that the previous study of the behaviour of **5.2-2** by ^{31}P {^{1}H} NMR spectroscopy had confirmed that this complex exists solely in the bidentate [RhCl(CO){κ^2-PN(O)}] form (by the use of low temperature studies), this fluxionality was thought to arise from ring inversion processes in the monodentate coordinated morpholine ring. Indeed, upon lowering the temperature of the sample, the resonances were observed to sharpen with a well-resolved spectrum being observed at 10 °C, Figure 5.6.

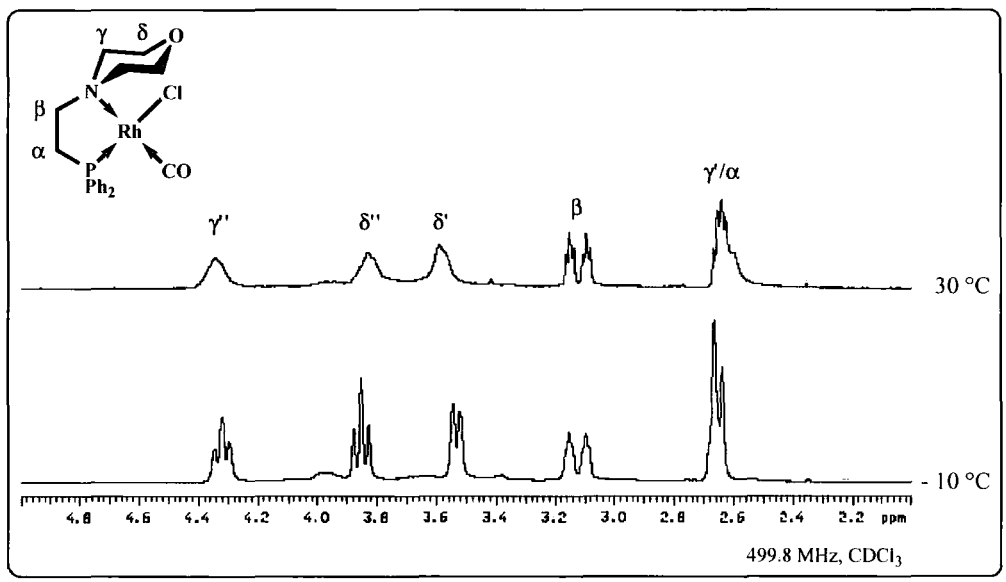

Figure 5.6: Comparison of ^{1}H NMR spectra of **5.2-2** at 30 °C and – 10 °C (aromatic region omitted for clarity)

It is noteworthy that only a small reduction in temperature was required to bring the morpholine ring signals into resonance. As expected, no change was noted in the aromatic region of the spectrum at low temperature, as two multiplet resonances with an overall integration of 10H were observed.

The ^{1}H NMR spectrum of **5.2-3** was noted to be severely broadened at room temperature, as a result of the proposed dynamic interconversion process between the

[RhCl(CO){κ^2-PN(S)}] {**5.2-3(a)**} and [Rh(CO){κ^3-PNS}]$^+$ Cl$^-$ {**5.2-3(b)**} isomers of this complex. In contrast to the low temperature ^{31}P {^{1}H} NMR spectroscopic studies, the ^{1}H NMR spectrum of **5.2-3** at – 50 °C ($CDCl_3$) still exhibited extreme line broadening, although it is notable that a further reduction in temperature to – 90 °C (CD_2Cl_2) failed to bring any of the expected signals into resonance.

It is surprising that well-resolved ^{1}H NMR spectroscopic data for **5.2-3** in chlorinated solutions could not be attained. It was thought that the low temperature ^{1}H NMR spectrum of this compound would be analogous to that of the related [RhCl(CO){PNNMe}] complex **5.2-1**, with resonances corresponding to the proposed [RhCl(CO){κ^2-PN(S)}] {**5.2-3(a)**} and [Rh(CO){κ^3-PNS}]$^+$ Cl$^-$ {**5.2-3(b)**} structures being observed. As demonstrated by low temperature multinuclear NMR spectroscopic studies on the parent PNS ligand **2.4-3**, very low temperatures were required to bring the saturated ring protons into resonance (*ca.* – 90 °C) as a result of the rapid conformational changes within the thiomorpholine ring fragment. The low energy barrier for inversion appears to be reflected in the behaviour of complex **5.2-3** as, despite repeated attempts in a variety of solvents (*i.e.* CCl_4, $(CD_3)_2CO$), sufficient spectral resolution for the full NMR characterisation of this complex could not be obtained.

The room temperature ^{1}H NMR spectrum of **5.2-4** at room temperature was as expected and was the only member of this complex family to exhibit a well-resolved spectrum at this temperature. The aliphatic region of this spectrum demonstrated the required number of resonances with correct integrations. Interestingly, the ε-methylene protons of the piperidine ring were observed as a single 2H multiplet, as opposed to the two resonances observed for the piperdine ε-protons for the related complexes [$PdCl_2${κ^2-PN(CH_2)}] (**3.1-4**) and [PtCl(PEt_3){κ^2-PN(CH_2)}] (**4.4-4**). The aromatic region of this spectrum was as expected, with two multiplet resonances being observed corresponding to the *ortho-* and *meta-/para-* phenyl protons.

5.3.3.3 ^{13}C {^{1}H} NMR spectroscopic analysis of 5.2-1 – 5.2-4

The ^{13}C {^{1}H} NMR spectra of complexes **5.2-1(a)** (observed at – 50 °C), **5.2-2** and **5.2-4** were consistent with bidentate P–N coordination of the rhodium centre. The ^{13}C {^{1}H} NMR spectrum of **5.2-2** was observed to exhibit moderate broadening of the aliphatic methylene resonances at 30 °C, as a result of dynamic ring inversion processes, although **5.2-4** exhibited a well-resolved spectrum at this temperature as expected.

In all complexes **5.2-1(a)**, **5.2-2** and **5.2-4**, the α-carbon was observed as a doublet resonance resulting from coupling to phosphorus with the remaining aliphatic resonances being observed as singlets. The aromatic regions of these spectra were as expected, with coupling to phosphorus being observed in the resonances attributed to the phenyl carbons.

The presence of the carbonyl group at the rhodium centre proved an additional means of characterising the regiochemistry of complexes **5.2-1(a)**, **5.2-2** and **5.2-4** as the resonance associated with the carbonyl carbon in the ^{13}C {^{1}H} NMR spectra was observed to couple to other spin-active nuclei in these complexes. As well as displaying the expected $^{1}J_{RhC}$ coupling, these resonances also displayed a secondary $^{2}J_{CP}$ coupling resulting from mutual coupling of phosphorus to the carbonyl carbon. Indeed, the small magnitude of these couplings provided an indication of the *cis* arrangement of the carbonyl and phosphine functionalities, as *trans* couplings tend to be larger in nature as a result of more favourable orbital overlap,[18] Table 5.3.

Unfortunately, the broadened nature of the ^{13}C {^{1}H} NMR spectrum of **5.2-3** (even at temperatures as low as – 90 °C) precluded the observation of the carbonyl carbon in this spectrum.

		^{13}C {^{1}H} NMR (Rh–CO)*		
		δ_C	$^{1}J_{RhC}$ /Hz	$^{2}J_{CP}$ /Hz
NMe	**5.2-1(a)**	188.0[a]	72.6[a]	17.9[a]
O	**5.2-2**	187.8	73.1	18.9
S	**5.2-3(a)**[b]	-	-	-
CH_2	**5.2-4**	188.1	72.0	18.2

*125.7 MHz, $CDCl_3$; [a] – 50 °C; [b]sufficient spectral resolution not achieved

Table 5.3: Selected ^{13}C {^{1}H} NMR spectroscopic data of complexes **5.2-1** – **5.2-4**

On the basis of the solution studies of the complex **5.2-1** – **5.2-4** it is concluded that a fluxional interconversion process between the bidentate [RhCl(CO){κ^2-PN(E)}] and tridentate [Rh(CO){κ^3-PNE}]$^+$ Cl$^-$ isomers of **5.2-1** and **5.2-3** is operative in $CDCl_3$ solution, in accordance with Scheme 5.3. By contrast, complexes **5.2-2** and **5.2-4** were shown to bind to Rh in a rigidly bidentate P–N manner.

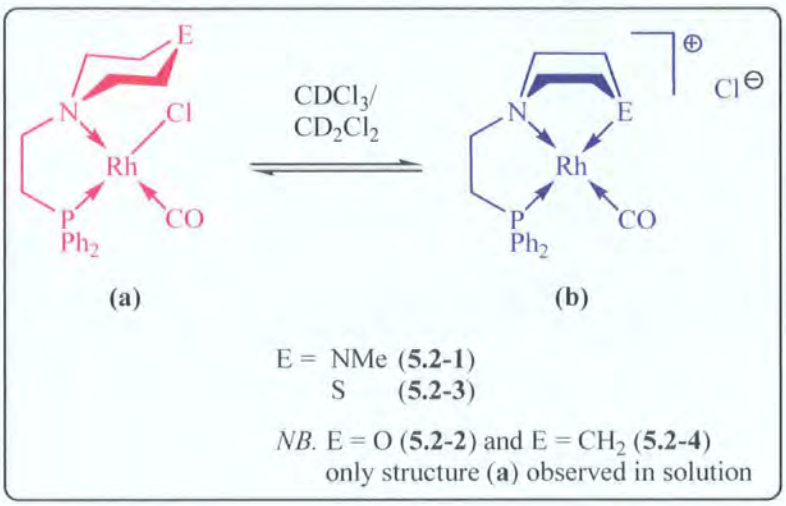

Scheme 5.3: Proposed isomerisation of [RhCl(CO){κ^2-PN(E)}] and [Rh(CO){κ^3-PNE}]$^+$ Cl$^-$ isomeric forms of **5.2-1** and **5.2-3**

The origin for this proposed dynamic exchange process is thought to lie in the regiochemistry of the rhodium carbonyl complexes **5.2-1** – **5.2-4**. On the basis of *trans* influence grounds, the phosphine donor lies *trans* to the chloride substituent,[19] a situation that is confirmed by the small magnitude of the *cis*-$^2J_{CP}$ couplings observed in the ^{13}C {^1H} NMR spectra of complexes **5.2-1** – **5.2-4**. The strongly *trans* influencing phosphorus donor fragment is believed to labilise the chloride substituent, with reversible dynamic substitution being observed when coordination of the third pendent donor is favoured (*i.e.* for **5.2-1** and **5.2-3**).

5.3.4 Addition of chloride to 5.2-1 and 5.2-3

In an effort to establish the origin of the proposed equilibrium between the bidentate [RhCl(CO){κ^2-PN(E)}] and tridentate [Rh(CO){κ^2-PN(E)}]$^+$ Cl$^-$ isomers of complexes **5.2-1** and **5.2-3**, a series of experiments were undertaken in which soluble sources of

chloride were added to solutions of these complexes and their behaviour monitored by NMR spectroscopy. It was thought that the presence of excess chloride would shift the position of equilibrium to the left, as shown in Scheme 5.4, resulting in the observation of the bidentate [RhCl(CO){κ^2-PN(E)}] complexes **5.2-1(a)/5.2-3(a)** in the $^1H/^{31}P$ $\{^1H\}$ NMR spectra of these mixtures.

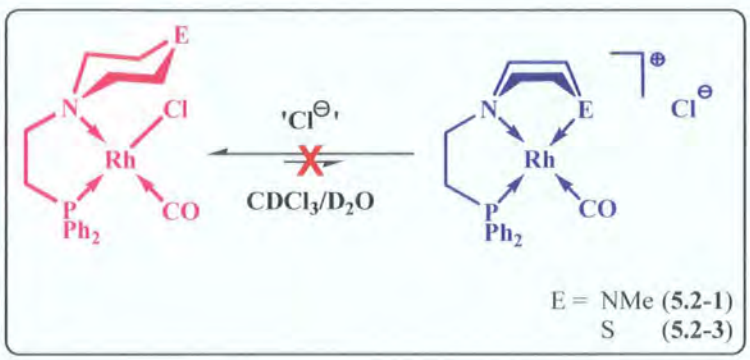

Scheme 5.4: Addition of Cl^- to **5.2-1** and **5.2-3**

Initially $CDCl_3$ solutions of complexes **5.2-1** and **5.2-3** were treated with increasing numbers of equivalents of $^tBu_4NCl$. On the addition of one equivalent of $^tBu_4NCl$, no appreciable changes were noted in their ^{31}P $\{^1H\}$ NMR spectra, as these remained substantially broadened at room temperature. Addition of further equivalents of $^tBu_4NCl$ did not result in any noticeable changes in the ^{31}P $\{^1H\}$ NMR spectra of either complex. Upon the addition of *ca.* fifteen equivalents of $^tBu_4NCl$, the solubility limit of the ammonium salt in the NMR solvent was reached with no appreciable change in the ^1H or ^{31}P $\{^1H\}$ NMR spectra of either **5.2-1** or **5.2-3** being observed, the spectra remaining identical to those of the parent solutions.

Given the limited solubility of $^tBu_4NCl$ in small volumes of $CDCl_3$, an alternative source of chloride was sought and thus these experiments were repeated using Et_3NHCl in D_2O solvent. The addition of one equivalent of Et_3NHCl to D_2O solutions of **5.2-1** and **5.2-3** again afforded no changes to their $^1H/^{31}P$ $\{^1H\}$ NMR spectra and the addition of subsequent equivalents (up to *ca.* 80 equivalents) of this ammonium salt to these samples failed to reduce the broadening of the observed doublet resonances. It is noteworthy that both complexes **5.2-1** and **5.2-3** displayed a remarkable tolerance towards D_2O with their aqueous solutions being stable for relatively long periods of time (hours) before the onset of decomposition was noted.

It is regrettable that the addition of chloride failed to limit the dynamic interconversion processes between the two isomeric forms of **5.2-1** and **5.2-3**. Given the NMR spectral evidence that supports this interconversion between [RhCl(CO){κ^2-PN(E)}] {**5.2-1(a)/5.2-3(a)**} and [Rh(CO){κ^3-PN(E)}]$^+$ Cl$^-$ {**5.2-1(b)/5.2-3(b)**} (*vide supra*), it was thought that the presence of excess chloride would limit this isomerisation and favour the existence of **5.2-1(a)/5.2-3(a)**. However, this was shown not to be the case as line broadening was observed in the room temperature of these compounds, even in the presence of large quantities of Cl$^-$.

5.3.5 NMR characterisation of 5.2-1 and 5.2-3 in methanol solution

Following the failure to establish the presence of an equilibrium between the bidentate [RhCl(CO){κ^2-PN(E)}] and tridentate [Rh(CO){κ^3-PN(E)}]$^+$ Cl$^-$ forms of **5.2-1** and **5.2-3** in solution in the presence of excess Cl$^-$, an alternative approach was sought for the characterisation of the [Rh(CO){κ^3-PN(E)}]$^+$ Cl$^-$ isomers of these compounds {**5.2-1(b)/5.2-3(b)**}.

The characterisation of ionic compounds in the solution state is assisted by solvents with high dielectric constants (such as water and alcohols) as these promote the formation of ion pairs in solution as a result of solvation of the respective ions.[20] Given the dynamic isomerisation exhibited by compounds **5.2-1** and **5.2-3** in chloroform solution at room temperature {$CHCl_3$: ε = 4.806 (20 °C)},[21] the characterisation of these compounds was undertaken in methanol. It was thought that, in a solvent with a higher dielectric constant {MeOH: ε = 32.63 (25 °C)},[21] this would shift the position of the proposed equilibrium over to the right-hand side and enable the solution state characterisation of the charged [Rh(CO){κ^3-PNE}]$^+$ Cl$^-$ isomers of these complexes {**5.2-1(b)/5.2-3(b)**}, Scheme 5.5.

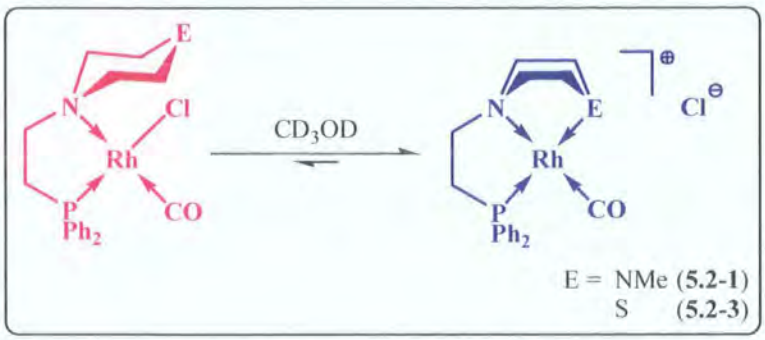

Scheme 5.5: Equilibrium of **5.2-1** and **5.2-3** in methanol solution

The ^{31}P $\{^1H\}$ NMR spectra of compounds **5.2-1** and **5.2-3** in CD_3OD were observed to be markedly different from those in $CDCl_3$ solution. For both complexes **5.2-1** and **5.2-3**, sharp doublet resonances were observed with no noticeable broadening. In both cases, there was a favourable comparison between their ^{31}P $\{^1H\}$ NMR spectra in CD_3OD solution with the low temperature ^{31}P $\{^1H\}$ NMR spectra of these complexes in chloroform solution, as shown in Table 5.4. In these spectra, a distinct similarity was noted between the resonance attributed to the charged $[Rh(CO)\{\kappa^3\text{-PNE}\}]^+ Cl^-$ complexes **5.2-1(b)/5.2-3(b)** observed at – 50 °C and signals noted in the CD_3OD spectra at room temperature. Specifically, the magnitude of the $^1J_{RhP}$ coupling exhibited in the CD_3OD spectra of compounds **5.2-1** and **5.2-3** was entirely consistent with those from the proposed charged $[Rh(CO)\{\kappa^3\text{-PNE}\}]^+ Cl^-$ structure {**5.2-1(b)/5.2-3(b)**} of these complexes.

		^{31}P $\{^1H\}$ NMR[a]		^{31}P $\{^1H\}$ NMR[b]	
		δ_P	$^1J_{RhP}$ /Hz	δ_P	$^1J_{RhP}$ /Hz
$[RhCl(CO)\{\kappa^2\text{-PNNMe}\}]$	**5.2-1(a)**	+ 61.0 (d)	171.8	+ 59.6 (d)	160.2
$[Rh(CO)\{\kappa^3\text{-PNNMe}\}]^+ Cl^-$	**5.2-1(b)**	+ 58.0 (d)	162.0		
$[RhCl(CO)\{\kappa^2\text{-PNNMe}\}]$	**5.2-3(a)**	+ 60.7 (d)	173.6	+ 54.7 (d)	164.1
$[Rh(CO)\{\kappa^3\text{-PNS}\}]^+ Cl^-$	**5.2-3(b)**	+ 53.0 (d)	162.1		

[a]202.3 MHz, $CDCl_3$, – 50 °C; [b]202.3 MHz, CD_3OD;

Table 5.4: Comparative ^{31}P $\{^1H\}$ NMR spectra of **5.2-1** and **5.2-3** ($CDCl_3/CD_3OD$ solutions)

In addition to the well-defined ^{31}P $\{^1H\}$ NMR spectra of **5.2-1** and **5.2-3** in methanol solution at 30 °C, the ^1H and ^{13}C $\{^1H\}$ NMR spectra of these compounds also

proved to be unexpectedly well-resolved at this temperature, which facilitated their solution state characterisation. In the ^{1}H NMR spectra of both **5.2-1** and **5.2-3** in CD_3OD, the signals attributed to the α- and β-bridge protons were observed as multiplet resonances although, significantly, the signals attributed to the γ- and δ-ring protons were noted to be well-resolved, thus indicating coordination of the terminal E donor to the Rh centre. The aromatic regions of these spectra were as expected and unremarkable.

The ^{13}C $\{^{1}H\}$ NMR spectra (CD_3OD) of **5.2-1** and **5.2-3** were as expected with C_α signals being observed as doublet resonances as a result of coupling to phosphorus in both spectra. All other aliphatic resonances were observed as singlet resonances with no broadening noted for the signals observed for the γ- and δ-ring carbons. Again, the aromatic regions of these spectra were unremarkable.

As the NMR spectra of **5.2-1** and **5.2-3** in $CDCl_3$ were observed to undergo significant changes upon lowering the temperature of the samples, the ^{1}H, ^{13}C $\{^{1}H\}$ and ^{31}P $\{^{1}H\}$ NMR spectra (CD_3OD) were recorded at – 50 °C. In contrast to the $CDCl_3$ spectra of these compounds, no change was noted in the CD_3OD solution spectra at low temperature, with only resonances corresponding to the $[Rh(CO)\{\kappa^3\text{-PNE}\}]^+ Cl^-$ isomers being observed.

It is interesting to note that, whilst **5.2-3** was shown to be stable in methanolic solution for long periods of time (weeks), the related complex **5.2-1** displayed limited stability in this solvent with the onset of decomposition (signified by the precipitation of a black solid from solution) being noted after approximately 48 hours.

5.3.6 Molecular structures of 5.2-1 and 5.2-2

5.3.6.1 Molecular structure of 5.2-1(a)

Due to the dynamic isomerisation exhibited by **5.2-1** in chlorinated solvent solutions, it was of interest to obtain crystals suitable for analysis by X-ray diffraction to examine its preferred configuration in the solid state. Slow diffusion of hexane into a concentrated CH_2Cl_2 solution of **5.2-1** afforded crystals whose molecular structure was shown to be consistent with the neutral $[RhCl(CO)\{\kappa^2\text{-PN(NMe)}\}]$ isomer of this complex {**5.2-1(a)**}, Figure 5.6.

Considerable disorder of both molecules was observed which did not permit further refinement, although analysis of their e.s.d. parameters revealed that the two molecules are near-identical in their extent of disorder. As a result, the following discussions of the overall structural details will centre on the least disordered of the two molecules (Molecule 1, Figure 5.6).

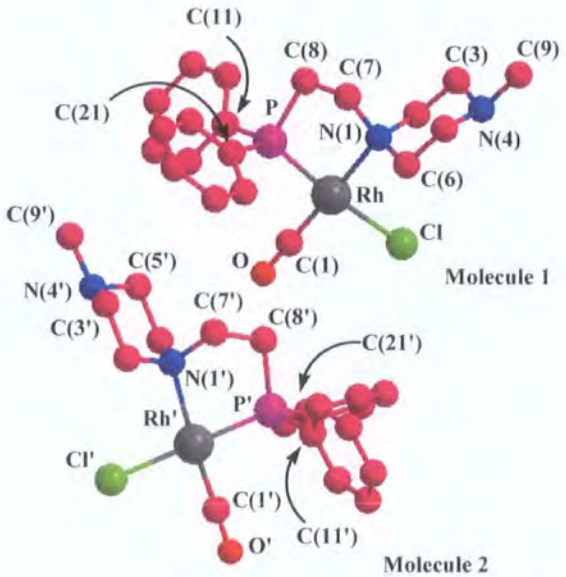

Figure 5.6: Ball and stick representation of **5.2-1(a)***

	Bond Length/Å			Bond Angle/°	
	5.2-1(a)	**2.4-1**		**5.2-1(a)**	**2.4-1**
Rh–P	2.2085(5)	-	N(1)–Rh–P	84.60(4)	-
Rh–N(1)	2.2024(14)	-	Cl–Rh–C(1)	90.56(6)	-
Rh–Cl	2.3914(5)	-	N(1)–Rh–Cl	91.97(4)	-
Rh–C(1)	1.8127(18)	-	P–Rh–C(1)	93.21(6)	-
C(1)–O	1.148(2)	-	C(11)–P–C(21)	103.41(8)	102.43(14)
P–C(8)	1.8249(17)	1.859(3)	C(2)–N(1)–C(6)	106.54(12)	109.5(2)
N(1)–C(7)	1.499(2)	1.469(4)	C(3)–N(4)–C(5)	110.67(14)	109.2(3)
P–C(Ph)	1.8164[a]	1.839[a]	$\Sigma_{\angle N(1)}$	327.29[b]	334.6[b]
			$\Sigma_{\angle N(4)}$	331.35[b]	330.7[b]
			$\Sigma_{\angle P}$	313.67[b]	301.98[b]
			P–C(8)–C(7)–N(1)	56.24(17) (Molecule 1) / –48.23(16) (Molecule 2)	–42.5(3)

[a]average; [b]angle summation; e.s.d.'s in parentheses

Table 5.5: Selected bond distances (Å) and angles (°) for **5.2-1(a)** {Molecule 1}

* Molecular structure determination performed by Dr A. S. Batsanov

The molecular structure of **5.2-1(a)** reveals the expected square planar geometry about rhodium with a mutual *trans* orientation of the amine and carbonyl donors, while the phosphine fragment is observed to lie *trans* to the chloride, as would be expected on the grounds of *trans* influence effects.[19,22] It is interesting to note that **5.2-1(a)** is racemic in the solid-state with two torsional isomers present within the unit cell. These two isomers exhibit opposite twists in their N(1)–C(7)–C(8)–P bridge relative to the Rh centre {56.24(17)° and – 48.23(16)°; Molecules 1 and 2, respectively} and hence these molecules are not related by an inversion centre. These torsional differences do not significantly affect the N(1)–Rh–P bite angles as these are observed to be 84.60(4)° and 84.53(4)° for Molecules 1 and 2 respectively, with both values being consistent for similar complexes.[9] The Cl–Rh–C(1/1′) angles are also found to be relatively unaffected by the different torsional twists, being 90.59(6)° for Molecule 1 and 89.35(6)° for Molecule 2. As a result, neither molecule is rigidly square planar with respect to the geometry about Rh. In Molecule 1, the Rh centre experiences a slight tetragonal distortion with the differences in the [N(1)–Rh–P] and [Cl–Rh–C(1)] mean planes being 8.02°. In contrast, Molecule 2 experiences a slight pyramidal distortion about Rh′ with both the Cl′ and C(1′) atoms found slightly below the [N(1′)–Rh′–P] plane. The remaining structural features of Molecules 1 and 2 are broadly comparable and thus further structural discussion will centre on Molecule 1.

The rhodium forms near-equivalent bond lengths with both the P and N(1) donors in Molecule 1 with a short Rh–C(1) bond being observed. The short nature of the Rh–P bond {1.8127(18) Å} is indicative of the strong electron donor character of the phosphine fragment, which increases π-back donation to the carbonyl, resulting in a concomitant lengthening of the C(1)–O bond distance {1.148(2) Å}.[9] In accordance with the strong *trans* influence of the phosphine donor, a long Rh–Cl distance is observed {2.3914(5) Å}.[23]

As the molecular structure for the parent ligand **2.4-1** had been obtained previously, this permitted comparison between the free phosphine and its related Rh complex with a view to assessing the geometrical perturbations taking place upon coordination. As expected, a reduction in the angles about the N(1) atom was noted upon complexation between the coordinated electron pair of **5.2-1(a)** ($\Sigma_{\angle N(1)} = 327.29°$) and the lone pair in **2.4-1** ($\Sigma_{\angle N(1)} = 334.6$). A slight narrowing of the C(2)–N(1)–C(6) angle was observed in **5.2-1(a)** upon complexation {106.54(12)°} relative to that of the

ligand **2.4-1** {109.5(2)°}, which is entirely consistent with related structures.[24] The summations of the angles about the N(4) atom in **5.2-1(a)** and **2.4-1** surprisingly were shown to be approximately equal {$\Sigma_{\angle N(1)}$ = 331.35°/330.7°; **5.2-1(a)/2.4-1**, respectively} revealing little change upon complexation. By contrast, summation of the angles about the phosphine donor in **5.2-1(a)** revealed a widening of the bonds about the phosphine donor on coordination of this donor to rhodium ($\Sigma_{\angle P}$ = 313.67°) with respect to the angle observed in the free ligand **2.4-1** ($\Sigma_{\angle P}$ = 301.98°).

5.3.6.2 Molecular structure of 5.2-2

Crystals of **5.2-2** suitable for X-ray diffraction studies were grown by slow evaporation of a CH_2Cl_2 solution, the resulting molecular structure confirming the bidentate chelation of the parent ligand (**2.4-2**) to the rhodium carbonyl chloride fragment, Figure 5.7. As predicted by NMR analysis of **5.2-2**, the morpholine oxygen donor remains unbound to the metal centre with the phosphine fragment being located *trans* to the chloride.

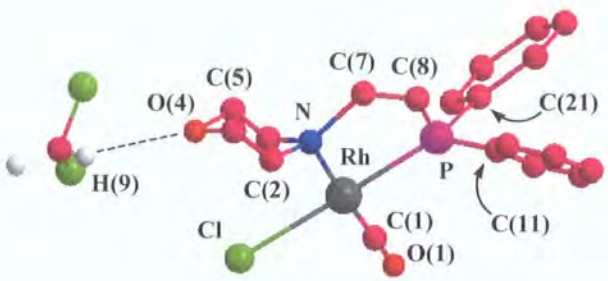

Figure 5.7: Ball and stick representation of **5.2-2**† (H–bonded CH_2Cl_2 solvent included)

	Bond Length/Å		Bond Angle/°
Rh–P	2.2007(5)	N–Rh–P	84.29(3)
Rh–N	2.2005(12)	Cl–Rh–C(1)	90.20(5)
Rh–Cl(1)	2.4012(5)	N–Rh–Cl	92.61(3)
Rh–C(1)	1.8074(15)	P–Rh–C(1)	92.76(5)
C(1)–O(1)	1.146(2)	C(11)–P–C(21)	102.84(6)
P–C(8)	1.8284(14)	C(2)–N–C(6)	107.56(11)
N–C(7)	1.5023(18)	C(3)–O(4)–C(5)	109.88(12)
P–C(Ph)	1.8179[a]	$\Sigma_{\angle N}$	328.29[b]
O(4)–H(9)	3.140(2)	$\Sigma_{\angle P}$	313.11[b]
		P–C(8)–C(7)–N	57.06(12)

[a]average; [b]angle summation

Table 5.6: Selected bond lengths (Å) and bond angles (°) for **5.2-2**

† Molecular structure determination performed by Dr A. S. Batsanov

The molecular structure of **5.2-2** revealed a slight pyramidal distortion about the rhodium centre in the solid-state with the chloride and carbonyl ligands lying slightly below the N–Rh–P plane; summation of the angles about this centre indicate that this distortion is minor nonetheless ($\Sigma_{\angle Rh}$ = 359.86°). A relatively small N–Rh–P angle is observed for **5.2-2** {84.29(3)°}, which is consistent to that observed for **5.2-1(a)** {84.60(4)°}. As a result of this small bite angle, an associated widening of the N–Rh–Cl {92.61(3)°} and P–Rh–C(1) {92.76(5)°} bond angles are noted, although the Cl–Rh–C(1) {90.20(5)°} angle remains unaffected. In contrast to **5.2-1(a)** (*vide supra*), only one geometric isomer of **5.2-2** was found in the unit cell with uniform torsion of the P–N bridge being observed {P–C(8)–C(7)–N = 57.06(12)°}.

The bond lengths about rhodium in **5.2-2** were found to be largely comparable with those of the analogous complex **5.2-1(a)**, with near-identical Rh–P {2.2007(5) Å} and Rh–N {2.2005(12) Å} bond distances being observed. As expected, as a result of the strong *trans* influence of phosphorus, a long Rh–Cl(1) {2.4012(5) Å} bond was observed.[19] Again, the strong electron donating nature of the phosphine fragment was indicated by the observation of a long C(1)–O bond {1.146(2) Å}.[9]

The monodentate N-coordinated morpholine fragment adopts the expected chair conformation with a long hydrogen bond being observed between the O(4) atom and a proton of a co-crystallised CH_2Cl_2 molecule {3.140(2) Å}. The internal morpholine ring angles {C(2)–N–C(6): 107.56(11)°; C(3)–O(4)–C(5): 109.88(12)°} were shown to be entirely consistent with similar monodentate morpholine-Rh(I) complexes in the literature.[25]

Summation of the angles about the N atom reveal the geometry about the atom to be near-tetrahedral {$\Sigma_{\angle N}$ = 328.29°}, while the angle about P was observed to be slightly smaller as expected {$\Sigma_{\angle P}$ = 313.11°}.

5.3.7 Attempted synthesis of 5.2-5

Following the successful synthesis of the [RhCl(CO){PNE}] complexes **5.2-1** – **5.2-4**, the complexation of the PNN(Ph) ligand **2.4-5** with $[Rh_2(CO)_4\{\mu\text{-}Cl\}_2]$ was undertaken, as shown in Scheme 5.6. Upon the addition of the **2.4-5** to the rhodium dimer, the evolution of gas was noted from solution, although upon stirring of the mixture at room

temperature for 2h, a distinct brown colouration of the solution was observed with the gradual formation of a brown-coloured precipitate. Upon isolation of the precipitate by filtration, analysis by $^{31}P\{^{1}H\}$ NMR spectroscopy did not indicate the presence of the target product with the spectrum being dominated by a number of presumed ligand degradation products. Subsequent analysis of the precipitate by mass spectrometry also failed to demonstrate the presence of the required complex, with a number of degradation products being observed instead.

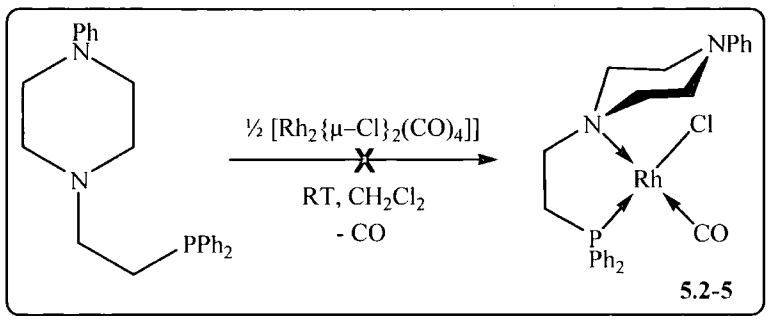

Scheme 5.6: Attempted synthesis of **5.2-5**

It is surprising that the PNN(Ph) ligand **2.4-5** failed to coordinate to the rhodium centre as it was thought that this complexation would mirror that of the related compounds **5.2-1** – **5.2-4** and afford a product with the empirical formula [RhCl(CO){PNN(Ph)}]. The origin of decomposition of the parent ligand remains unclear as similar decomposition pathways were not noted in the other related systems even under prolonged reaction times. Indeed, this situation is entirely consistent to the situation observed in the attempted complexation of **2.4-5** to $[PdCl_2(MeCN)_2]$ (Chapter 3, Section 3.2.8) where decomposition of the ligand was also observed.

5.3.8 Attempted complexation of PNNP with $[Rh_2\{\mu\text{-}Cl\}_2(CO)_4]$

Following the successful synthesis of the [RhCl(CO){PNE}] complexes **5.2-1** – **5.2-4**, the complexation of the PNNP ligand **2.4-7** with $[Rh_2\{\mu\text{-}Cl\}_2(CO)_4]$ was undertaken. As a starting point to explore the coordination of this potentially four-coordinate ligand with the 'Rh(CO)Cl' fragment, the complexation of **2.4-7** was attempted under similar

conditions to those discussed previously, *i.e.* by reaction of half a molar equivalent of the rhodium precursor with one equivalent of the ligand, as shown in Scheme 5.7, A.

Upon the addition of the ligand to $[Rh_2\{\mu\text{-}Cl\}_2(CO)_4]$, the immediate evolution of CO from the orange solution was observed, although *in situ* analysis by $^{31}P\ \{^1H\}$ NMR spectroscopy did not indicate the presence of the target product in solution, with only a number of severely broadened resonances being observed. Given the fluxional behaviour of the related [RhCl(CO){PNNMe)] complex **5.2-1** in chlorinated solutions, it was speculated that the broadened nature of the $^{31}P\ \{^1H\}$ NMR spectrum could be a result of rapid interconversion of different isomers of the target product. However, upon lowering the temperature of the sample (– 50 °C, $CDCl_3$), the appearance of numerous resonances was observed with the expected resonances corresponding to the target structure not being among these. Analysis by mass spectrometry also failed to confirm the presence of the required complex, with only a number of unassignable signals being observed.

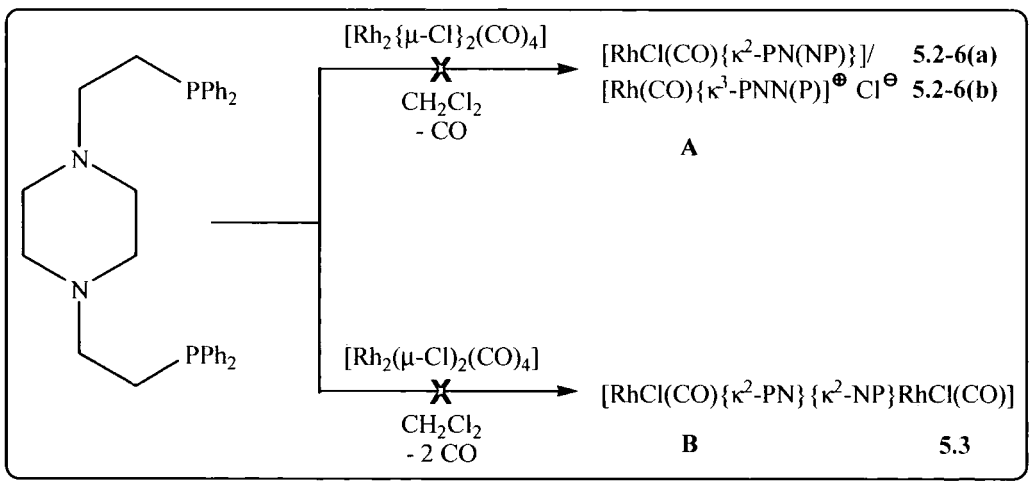

Scheme 5.7: Attempted complexation of **2.4-7** (PNNP) with $[Rh_2\{\mu\text{-}Cl\}_2(CO)_4]$

In an effort to successfully coordinate the PNNP ligand **2.4-7** to the 'RhCl(CO)' fragment, a variation of the stoichiometry of this complexation was attempted, *i.e.* by reaction of equimolar quantities of **2.4-7** to $[Rh_2(CO)_4\{\mu\text{-}Cl\}_2]$, Scheme 5.7, B. In a similar situation to that noted in the previous attempted synthesis, on addition of the ligand to the rhodium precursor, the evolution of CO gas was observed from solution, although there was a noticeable colour change of this solution from orange to dark green. Analysis of the resulting mixture by $^{31}P\ \{^1H\}$ NMR spectroscopy again afforded

a number of severely broadened resonances and lowering the temperature of the sample failed to indicate the presence of the desired bimetallic complex. Mass spectrometric analysis of the resulting green product demonstrated a number of high molecular weight products although, despite repeated attempts, these could not be assigned.

5.4 Synthesis and characterisation of $[Rh(CO)\{\kappa^3\text{-PNE}\}]^+ Cl^-$ (5.4-1 and 5.4-3)

Following the synthesis of the [RhCl(CO){PNE}] compounds (**5.2-1** – **5.2-4**), the synthesis of the $[Rh(CO)\{\kappa^3\text{-PNE}\}]^+ BF_4^-$ complexes were undertaken with complexes **5.2-1**, **5.2-2** and **5.2-3**. Given the fluxional behaviour exhibited by the [Rh(CO){PNE}] compounds **5.2-1** (E = NMe) and **5.2-3** (E = S), it was of interest to prepare 'tethered' cationic forms of these complexes by abstraction of the metal-bound chloride from the rhodium centre. Specifically, the synthesis of a range of tridentate $[Rh(CO)\{\kappa^3\text{-PNE}\}]^+ BF_4^-$ derivatives would permit ready comparison of these complexes with the $[Rh(CO)\{\kappa^3\text{-PNE}\}]^+ Cl^-$ isomers of **5.2-1** and **5.2-3** observed by NMR spectroscopy in CD_3OD solution at ambient temperature and in $CDCl_3$ solution at – 50 °C.

The syntheses of the $[Rh(CO)\{\kappa^3\text{-PNE}\}]^+ BF_4^-$ compounds proceeded according to the methodology detailed in Scheme 5.8, *i.e.* by reaction of equimolar quantities of **5.2-1** – **5.2-3** with $AgBF_4$ in CH_2Cl_2 solution. Whilst the target $[Rh(CO)\{\kappa^3\text{-PNE}\}]^+ BF_4^-$ complexes **5.4-1** (E = NMe) and **5.4-3** (E = S) were afforded in good yields, addition of $AgBF_4$ to $[RhCl(CO)\{\kappa^2\text{-PN(O)}\}]$ (**5.2-2**) resulted in the rapid precipitation of a dark brown solid from solution, which was shown to be as a result of decomposition of the parent complex through analysis by NMR spectroscopy and mass spectrometry.

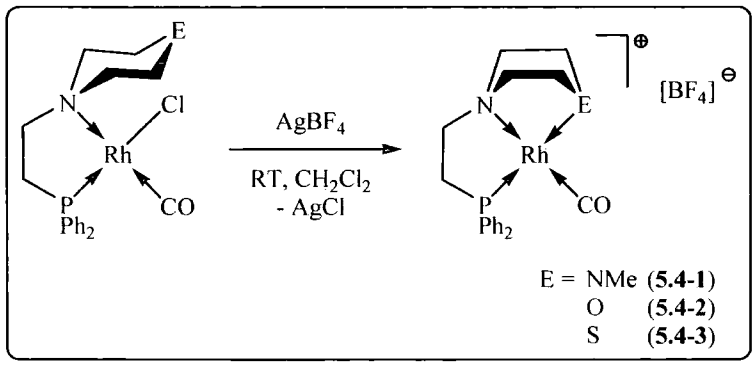

		Yield	MS (MALDI$^+$)		IR /cm^{-1}
			m/z		
[Rh(CO){κ^3-PNNMe}]$^+$ BF_4^-	**5.4-1**	66 %	443.2^a	416.6^b	2000
[Rh(CO){κ^3-PNO}]$^+$ BF_4^-	**5.4-2**	-	-	-	-
[Rh(CO){κ^3-PNS}]$^+$ BF_4^-	**5.4-3**	65 %	446.2^a	419.0^b	2011

^{a}[M]$^+$; ^{b}[M–CO]$^+$;

Scheme 5.8: Synthesis, mass spectrometric and IR spectroscopic data of **5.4-1** and **5.4-3**

Complexes **5.4-1** and **5.4-3** both afforded satisfactory CHN and mass spectrometric analyses, thus confirming the presence of the target products. However, despite repeated attempts, the BF_4^- anion could not be observed by mass spectrometry (ES^-) although its presence was unambiguously confirmed with the use of $^{19}F/^{11}B$ NMR spectroscopy. Analysis of **5.4-1** and **5.4-3** by IR spectroscopy revealed a strong carbonyl absorbance band in both cases although this was not shown to shift significantly relative to that observed for their parent [RhCl(CO){PNE}] complexes (*vide supra*).

The ^{31}P {^1H} NMR spectra of **5.4-1** and **5.4-3** both exhibited sharp, well-resolved doublet resonances at room temperature as a result of tethering of the terminal donor to the metal centre. Comparison of the both the chemical shifts and magnitude of the $^1J_{RhP}$ coupling constants observed in the ^{31}P {^1H} NMR spectra of **5.4-1** and **5.4-3** with those observed in their respective parent compounds **5.2-1** and **5.2-3** at low temperature were again indicative of dynamic isomerism between the [Rh(CO){κ^2-PN(E)}] and [Rh(CO){κ^3-PNE}]$^+$ Cl^- forms discussed previously, Table 5.7.

		$^{31}P\{^1H\}$ NMR[a,b]				$^{31}P\{^1H\}$ NMR[a,c]	
		δ_P	$^1J_{RhP}$ /Hz			δ_P	$^1J_{RhP}$ /Hz
$[Rh(CO)\{\kappa^3\text{-}PNNMe\}]^+ BF_4^-$	**5.4-1**	+ 59.9	161.8	$[RhCl(CO)\{\kappa^2\text{-}PN(NMe)\}]$	**5.2-1(a)**	+ 61.0	171.8
				$[Rh(CO)\{\kappa^3\text{-}PNNMe\}]^+ Cl^-$	**5.2-1(b)**	+ 58.0	162.0
$[Rh(CO)\{\kappa^3\text{-}PNS\}]^+ BF_4^-$	**5.4-3**	+ 54.1	162.5	$[RhCl(CO)\{\kappa^2\text{-}PN(S)\}]$	**5.2-3(a)**	+ 60.7	173.6
				$[Rh(CO)\{\kappa^3\text{-}PNS\}]^+ Cl^-$	**5.2-3(b)**	+ 53.6	162.1

[a]202.3 MHz, $CDCl_3$; [b]AT; [c]– 50 °C

Table 5.7: $^{31}P\{^1H\}$ NMR spectroscopic data for **5.4-1** and **5.4-3**
($^{31}P\{^1H\}$ NMR spectroscopic data for **5.2-1(a)/(b)** and **5.2-3(a)/(b)** included)

In contrast to the broadened ^1H and $^{13}C\{^1H\}$ NMR spectra observed for **5.2-1** and **5.2-3** at 20 °C, the corresponding spectra of complexes **5.4-1** and **5.4-3** were observed to be well-resolved at this temperature. In the ^1H NMR spectrum of **5.4-1**, the resonances associated with the γ- and δ-ring protons were observed as four multiplet resonances (each integrating to 2H), however the signals attributed to the γ- and δ-morpholine protons of **5.4-3** appeared as two resonances, integrating to 6H and 2H. In both **5.4-1** and **5.1-3**, the resonances associated with the α- and β-bridge protons were observed as discrete multiplets. The aromatic regions of both spectra were as expected and unremarkable.

The $^{13}C\{^1H\}$ NMR spectra of **5.4-1** and **5.4-3** were both as expected and consistent with the proposed structures. In the $^{13}C\{^1H\}$ NMR spectrum of **5.4-3**, the signal associated with the α-bridge carbon was surprisingly observed as a singlet, whereas this resonance in the spectrum of **5.4-1** was noted as the expected doublet. All other aliphatic resonances in both spectra were observed as singlet resonances. The aromatic region of these spectra were as expected, with coupling to phosphorus being observed for the phenyl carbon signals.

The signal attributed to the metal-bound carbonyl carbon was observed as the expected doublet of doublet resonance in the $^{13}C\{^1H\}$ NMR spectra of both complexes **5.4-1** and **5.4-3**, as a result of coupling to the ^{103}Rh and ^{31}P nuclei, Table 5.8. Surprisingly, the $^1J_{RhC}$ and $^2J_{CP}$ coupling constants exhibited by the carbonyl resonance of **5.4-3** proved markedly different in magnitude to those observed in the spectrum of

5.4-1, although the magnitudes of both of these couplings remain within the limits of those observed for cationic rhodium carbonyl centres.[26]

		^{13}C {^{1}H} NMR (Rh–CO)*		
		δ_C	$^{1}J_{RhC}$ /Hz	$^{2}J_{CP}$ /Hz
NMe	**5.4-1**	189.7	75.8	18.2
S	**5.4-3**	191.9	91.7	15.1

*125.7 MHz, $CDCl_3$

Table 5.8: Selected ^{13}C {^{1}H} NMR spectroscopic data for **5.4-1** and **5.4-3**

It is interesting to note that a direct comparison may be made between the aliphatic regions of the ^{1}H NMR spectra of **5.4-1** at 30 °C and **5.2-1** at – 50 °C as shown in Figure 5.8. Indeed, distinct similarities are noted between the spectrum observed for the $[Rh(CO)\{\kappa^3\text{-PNNMe}\}]^+ BF_4^-$ salt **5.4-1** and the resonances attributed to the $[Rh(CO)\{\kappa^3\text{-PNNMe}\}]^+ Cl^-$ isomer {**5.2-1(b)**}, with the most apparent feature of these two spectra being the similar splitting of the γ- and δ-ring resonances. Moreover, the resonances associated with the ζ-methyl protons are shown to be comparable of **5.4-1** and **5.2-1(b)**. Although not shown, the aromatic regions of these two spectra are broadly comparable with no appreciable differences being noted.

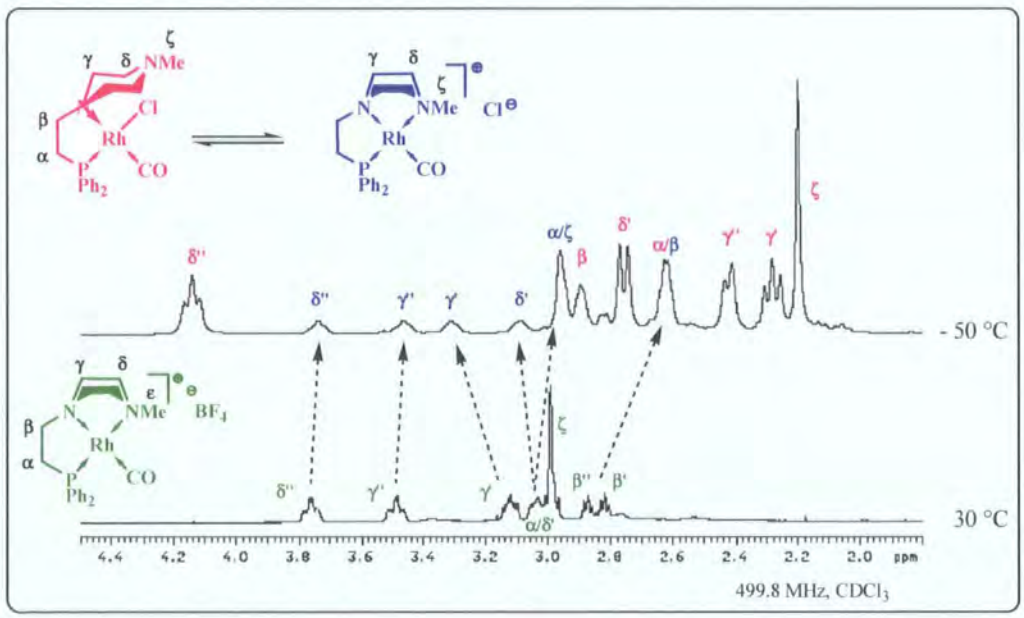

Figure 5.8: Comparison of the ^{1}H NMR spectra of **5.2-1** (– 50 °C) and **5.4-1** (30 °C) (Aromatic region omitted for clarity)

5.4.1 Molecular structure of 5.4-3

Surprisingly, the $[Rh(CO)\{\kappa^3\text{-PNS}\}]^+ BF_4^-$ complex **5.4-3** showed appreciable solubility in toluene as well as chlorinated solvents. Additionally, this complex was shown to display remarkable tolerance to atmospheric conditions for long periods of time (weeks) both in the solution- and the solid-state. Slow evaporation of a toluene solution of **5.4-3** afforded crystals suitable for study by X-ray diffraction, the gross molecular structure of these confirming the tridentate ligation of the PNS ligand (**2.4-3**) to the rhodium centre, as shown in Figure 5.9.

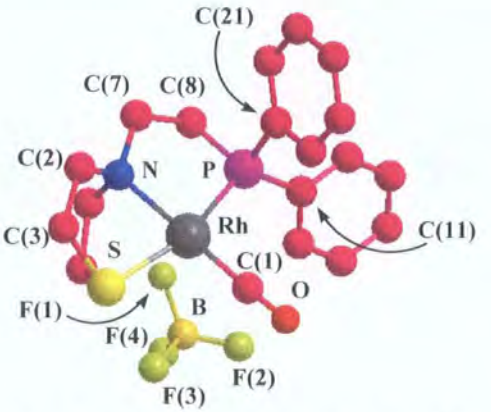

Figure 5.9: Ball and stick representation of **5.4-3**[‡]
(PhMe solvent molecule omitted for clarity)

	Bond Length/Å		Bond Angle/°
Rh–P	2.2293(6)	P–Rh–S	159.32(2)
Rh–N	2.1155(19)	N–Rh–C(1)	178.97(9)
Rh–S	2.3620(6)	P–Rh–N	85.81(6)
Rh–C(1)	1.828(2)	N–Rh–S	75.15(6)
C(1)–O	1.141(3)	S–Rh–C(1)	104.45(8)
P–C(8)	1.836(2)	P–Rh–C(1)	94.71(7)
N–C(7)	1.499(3)	C(2)–N–C(6)	109.02(19)
P–C(Ph)	1.815[a]	C(3)–S–C(5)	95.10(13)
		C(11)–P–C(21)	104.04(10)
		$\Sigma_{\angle N}$	329.11[a,b]
		$\Sigma_{\angle P}$	318.18[a,b]
		N–C(8)–C(7)–P	– 52.06

[a]average; [b]angle summation; e.s.d.'s in parentheses

Table 5.9: Selected bond lengths (Å) and bond angles (°) for **5.4-3**

[‡] Molecular structure determination performed by Dr A. S. Batsanov

The molecular structure of **5.4-3** reveals the rhodium cation to adopt a distorted square planar geometry in the solid state with the P–Rh–S bond angle {159.32(2)°} exhibiting a considerable deviation from linearity. Whilst summation of the angles of the coordinated ligands about the Rh centre indicate essentially square planar geometry ($\Sigma_{\angle Rh}$ = 360.13°), coordination of all three ligand donor atoms imposes considerable steric strain about Rh and distortion in the other angles about the metal are observed. The constraining nature of the PNS ligand results in distortion of the thiomorpholine ring, with the sulphur donor atom being located 7.90° below the P–Rh–N plane.

The small nature of the thiomorpholine fragment results in a small N–Rh–S angle {75.15(6)°}, this value is however consistent with related chelating thiomorpholine fragments.[27] The P–Rh–N angle {85.81(6)°} is found to be broadly comparable to the related [RhCl(CO){κ^2-PN(NMe)}] **5.2-1(a)** {84.60(4)°} and [RhCl(CO){κ^2-PN(O)}] **5.2-2** {84.29(3)°} (*vide supra*) with the N–C(8)–C(7)–P bridge adopting a staggered conformation as expected. As a result of this strained coordination geometry, an opening of the S–Rh–C(1) {104.45(8)°} and P–Rh–C(1) {94.71(7)°} angles is observed with the former being considerably larger.

The chelated thiomorpholine ring demonstrated an internal C(2)–N–C(6) ring angle of 109.02(19)°, which is consistent with the similar complexes **5.2-1(a)** {C(2)–N–C(6): 106.45(12)°} and **5.2-2** {C(2)–N–C(6): 107.56(11)°}. A significant narrowing of the C(3)–S–C(5) angle of **5.4-3** {95.10(13)°} was observed, a situation that is consistent with theoretical studies on metal-bound thioether donors, which note that a reduction in the R–S–R bond angle occurs upon coordination to a metal site.[28]

The Rh–P and Rh–N bond lengths {2.2293(6) Å and 2.1155(19) Å, respectively} were found to be broadly comparable, although a relatively long Rh–S bond distance was observed 2.3620(6) Å}.[29] The strongly electron donating nature of the phosphine fragment was reflected in the observation of a long C(1)–O bond {1.141(3) Å}.[9]

Summation of the angles about the N atom in **5.4-3** {$\Sigma_{\angle N}$ = 329.11°} reveal a near-tetrahedral geometry at this atom although the angle about P is noted to widen {$\Sigma_{\angle P}$ = 318.18°} in comparison to the related complexes **5.2-1(a)** {$\Sigma_{\angle P}$ = 313.67°} and **5.2-2** {$\Sigma_{\angle P}$ = 313.11°}, presumably to relieve steric strain about the phosphine donor fragment in **5.4-3**. The phenyl substituents at phosphorus display a near-perpendicular arrangement, with the intersection of their mean planes being 83.4°.

5.5 Attempted synthesis of $[RhCl(CO)(MeCN)\{\kappa^2\text{-}PN(O)\}]^+ X^-$

Following the failure of chloride abstraction from **5.2-2** by reaction with $AgBF_4$ in CH_2Cl_2, an alternative strategy for the formation of the cationic $[RhCl(CO)(MeCN)\{\kappa^2\text{-}PN(O)\}]^+$ species was sought. Nitrile donors are known to coordinate well to late transition metal centres,[30] and, specifically, coordinating solvents (*e.g.* acetonitrile) are known to block vacant sites at cationic rhodium centres.[31] With this in mind, attempts to abstract the bound chloride ligand from **5.2-2** were repeated as shown in Scheme 5.9.

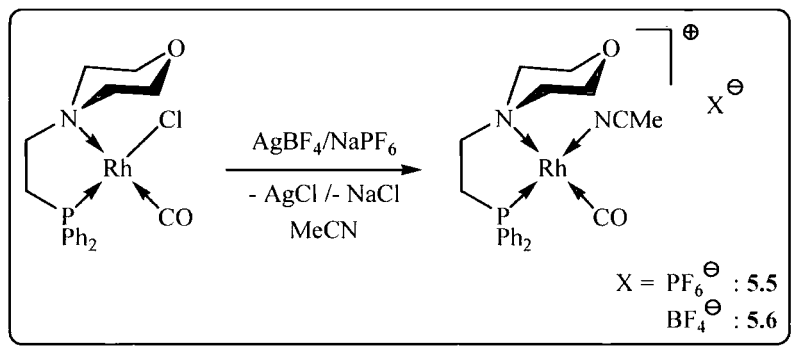

Scheme 5.9: Attempted synthesis of $[PNO\text{-}Rh(CO)(NCMe)]^+ X^-$ (**5.5/5.6**)

The abstraction of chloride from **5.2-2** was initially attempted using an excess (1.1 equivalents) of sodiumhexafluorophosphate in MeCN solution although the formation of the desired compound was not observed, even under prolonged reaction times. In an alternative effort to achieve chloride abstraction from this complex, the reaction was repeated with $AgBF_4$, but in a similar situation to the attempted synthesis of **2.4-2**, only decomposition of the parent rhodium complex was observed.

5.6 Conclusion/Summary

This chapter has described the coordination chemistry of the family of PNE ligands (**2.4-1** – **2.4-5** and **2.4-7**) with Rh(I) centres and the study of their behaviour in the solution state.

Complexation of the PNN(Me) ligand (**2.4-1**) with $[RhCl(PPh_3)_3]$ did not afford the desired $[RhCl\{\kappa^3\text{-}PNNMe\}]$ compound, but the $[RhCl(PPh_3)\{\kappa^2\text{-}PN(NMe)\}]$ complex **5.1** was obtained instead. Due to the difficulties associated with the

purification of **5.1**, this synthetic methodology was not extended to the remaining members of the PNE ligand family.

The reaction of PNE ligands **2.4-1** – **2.4-4** with $[Rh_2\{\mu\text{-}Cl\}_2(CO)_4]$ rapidly and cleanly generated a series of complexes with empirical formulae [RhCl(CO){PNE}] (**5.2-1** – **5.2-4**). While rigid κ^2-P–N ligation to the 'RhCl(CO)' fragment was noted for complexes **5.2-2** and **5.2-4**, dynamic isomerisation on the NMR time-scale in $CDCl_3$ solution was observed between the [RhCl(CO){κ^2-PN(E)}] (**a**) and [Rh(CO){κ^3-PNE}]$^+$ Cl^- (**b**) forms of complexes **5.2-1** and **5.2-3**. Low temperature multinuclear NMR spectroscopic studies of **5.2-1** clearly demonstrated the presence of the proposed isomeric forms of **5.2-1(a)** and **5.2-1(b)** in $CDCl_3$ solution at – 50 °C by $^1H/^{13}C$ $\{^1H\}$ and ^{31}P $\{^1H\}$ NMR spectroscopies. However, due to the presumed rapid interconversion between the isomeric forms of **5.2-3**, the tridentate [Rh(CO){κ^3-PNS}]$^+$ Cl^- **5.2-3(b)** could only be detected by ^{31}P $\{^1H\}$ NMR spectroscopy at low temperature. Surprisingly, the complexation of the PNN(Ph) (**2.4-5**) and PNNP (**2.4-7**) ligands to $[Rh_2\{\mu\text{-}Cl\}_2(CO)_4]$ resulted in decomposition of the parent ligands in both cases.

In an effort to definitively establish the nature of the proposed isomerisation between **5.2-1(a)/5.2-3(a)** and **5.2-1(b)/5.2-3(b)** in chloroform solution, soluble sources of chloride were added to these solutions, although this was found not to alter the position of presumed equilibrium between these two complexes. It was found, however, that **5.2-1** and **5.2-3** both exhibited NMR spectra consistent with the tridentate **5.2-1(b)** and **5.2-3(b)** structures in CD_3OD solution as a result of the high dielectric constant of methanol favouring separation of the resulting ion pairs.

X-ray diffraction studies of **5.2-1** demonstrated that this complex adopts the [RhCl(CO){κ^2-PN(NMe)}] {**5.2-1(a)**} structure in the solid state. A molecular structure was also obtained for **5.2-2** which demonstrated the expected κ^2-P–N ligation of the PNO ligand (**2.4-2**) to the Rh centre.

Abstraction of the metal-bound chloride was found to be successful for complexes **5.2-1** and **5.2-3** with the [Rh(CO){κ^3-PNE}]$^+$ BF_4^- complexes **5.4-1** and **5.4-3** (E = NMe and S, respectively) being obtained. X-ray diffraction studies of **5.4-3** demonstrated the tridentate binding of the ligand to Rh in this complex. Reaction of **5.2-2** with $AgBF_4$ under identical conditions resulted in decomposition of the parent complex. Chloride abstraction from **5.2-2** in MeCN solution with $NaPF_6$ and $AgBF_4$ both proved unsuccessful.

5.7 References

[1] "*Modern Rhodium-Catalysed Organic Reactions*", P. A. Evans (Ed.), Wiley-VCH, New York, 2005.

[2] R. S. Dickson, "*Homogeneous Catalysis with Compounds of Rhodium and Iridium*", D. Reidel Publishing Company, Dordrecht, Holland, 1985.

[3] P. S. Pregosin and R. W. Kunz, "*^{31}P and ^{13}C NMR of Transition Metal Complexes*", Springer-Verlag, Berlin, 1979.

[4] R. P. Hughes in "*Comprehensive Organometallic Chemistry; The Synthesis, Reactions and Structures of Organometallic Compounds*", G. Wilkinson, F. G. A. Stone and E. W. Abel (Eds.), Volume 5, Pergamon Press Ltd., Oxford, 1983, Chapter 35, pg. 277.

[5] H. Nagashima, K. Tatebe, T. Ishibashi, A. Nakaoka, J. Sakakibara and K. Itol, *Organometallics*, 1995, **14**, 2868 – 2879.

[6] T. Brown and P. J. Green, *J. Am. Chem. Soc.*, 1970, **92**, 2359 – 2362.

[7] I. Le Gall, P. Laurent, E. Soulier, J.-Y. Salaün and H. des Abbayes, *J. Organomet. Chem.*, 1998, **567**, 13 – 20.

[8] *NB. trans*-diphosphine 'Rh(I)Cl(CO)' complexes typically exhibit values of $^2J_{PP}$ in the order of 100 – 130 Hz. See C.H. Bushweller, C.D. Rithner and D.J. Butcher, *Inorg. Chem.*, 1986, **25**, 1610 – 1616 for examples.

[9] P. Suomalainen, S. Jääskeläinen, M. Haukka, R. H. Laitinen, J. Puriainen and T. A. Pakkenen, *Eur. J. Inorg. Chem.*, 2000, 2607 – 2613.

[10] C. E. Anderson, A. S. Batsanov, P. W. Dyer, J. Fawcett and J. A. K. Howard, *Dalton Trans.*, 2006, 5362 – 5378.

[11] M. G. L. Petrucci, A.-M. Lebuis and A. K. Kakkar, *Organometallics*, 1998, **17**, 4966 – 4975.

[12] E. Teuma, M. Loy, C. Le Berre, M. Etienne, J.-C. Daran and P. Kalck, *Organometallics*, 2003, **22**, 5261 – 5267.

[13] M. Cowie and T. Sielisch, *J. Organomet. Chem.*, 1988, **348**, 241 – 354.

[14] H. Yang, N. Lugan and R. Mattieu, *Organometallics*, 1997, **16**, 2089 – 2095.

[15] H.-J. Haupt and U. Ortmann, *Z. Anorg. Allg. Chem.*, 1993, **619**, 1209 – 1213.

[16] I. D. Kostas and C. G. Screttas, *J. Organomet. Chem.*, 1999, **585**, 1 – 6.

[17] R. K. Harris and R. A. Spragg, *J. Chem. Soc. (B)*, 1968, 684 – 691.

[18] D. H. Williams and I. Fleming, "*Spectroscopic Methods in Organic Chemistry*", 5th Edition, 1995, Cambridge, pg. 93.

[19] T. G. Appleton, H. C. Clark and L. E. Manzer, *Coord. Chem. Rev.*, 1973, **10**, 335 – 422.

[20] S. Winstein, E. Clippinger, A. H. Fainberg, R. Heck and G. C. Robinson, *J. Am. Chem. Soc.*, 1956, **78**, 328 – 335.

[21] "*CRC Handbook of Chemistry and Physics*", R. C. Weast and M. J. Astle (Ed.), CRC Press, 1982, Florida, USA.

[22] F. Basolo and R. G. Pearson, *Prog. Inorg. Chem.*, 1962, **4**, 381 – 453.

[23] T. Suzuki, K. Isobe and K. Kashiwabara, *J. Chem. Soc., Dalton Trans.*, 1995, 3609 – 3616.

[24] D. C. Clemente, A. Marzotto, G. Valle, and C. J. Visona, *Polyhedron*, 1999, **18**, 2749 – 2757.

[25] M. Beller, H. Trauthwein, M. Eichberger, C. Breindl, J. Herwig, T.E. Müller and O.R. Thiel, *Chem. A Eur. J.*, 1999, **5**, 1306 – 1319.

[26] M. J. Hanton, Ph. D. Thesis, University of Leicester, 2003.

[27] Y. Li, Y.-H. Lai, K. F. Mok and M. G. B. Drew, *Inorg. Chim. Acta*, 1999, **285**, 31 – 38.

[28] H.-B. Kraatz, H. Jacobson, T. Ziegler and P. M. Boorman, *Organometallics*, 1993, **12**, 76 – 80.

[29] J. García-Antón, R. Mathieu, N. Lugen, J. P. Picart and J. Ros, *J. Organomet. Chem.*, 2004, **689**, 1599 – 1608.

[30] P. Braunstein and F. Naud, *Angew. Chem. Int. Ed.*, 2001, **40**, 680 – 699.

[31] S. I. Pascu, K. S. Coleman, A. R. Cowley, M. L. Green and N. H. Rees, *J. Organomet. Chem.*, 2005, **690**, 1645 – 1658.

Chapter 6:

Experimental

6.1 Experimental details

All operations were performed under an atmosphere of dry nitrogen using standard Schlenk and cannula techniques, or in a nitrogen-filled glove box, unless stated otherwise. All NMR-scale reactions were conducted using Young's tap valve NMR tubes. Bulk solvents were purified and dried using an Innovative Technologies SPS facility and degassed prior to use. NMR solvents ($CDCl_3$, CD_2Cl_2, C_6D_6, d_8-PhMe) were dried over P_2O_5, distilled and degassed prior to use. Anhydrous CD_3OD was purchased from Aldrich.

Palladium and rhodium salts were used on loan from Johnson Matthey and $[RhCl(PPh_3)_3]$ was provided by Dr. E. J. Grayson. Morpholine, thiomorpholine and triphenylphosphine were purchased from Avocado, gaseous chemicals from BOC and all other chemicals from Aldrich. Where appropriate, liquid reagents were dried, distilled and deoxygenated prior to use. Gases were passed through a drying column ($CaCl_2$, P_2O_5) prior to use.

Safety spectacles and gloves were worn at all times, and all experiments conducted in an efficient fumehood, following completion of appropriate COSHH assessments. Solvents were disposed of in the appropriate waste solvent receptacles (chlorinated/non-chlorinated), metal-containing or organic waste in the appropriate residue vessels.

Routine NMR spectra were collected on a Varian Mercury 200, Mercury 400 or a Bruker Avance 400 spectrometers at ambient temperature unless stated otherwise. VT and nOe NMR experiments were conducted on a Varian Inova 500 or Unity spectrometers. Chemical shifts were referenced to residual protio impurities in the deuterated solvent (^1H), ^{13}C shift of the solvent (^{13}C) or to external aqueous 85 % H_3PO_4 (^{31}P). Solvent proton shifts (ppm): $CDCl_3$, 7.27 (s); CD_2Cl_2, 5.32 (s); C_6D_6, 128.39 (s); d_8-PhMe, 2.29 (quin), 7.09 (quin), 7.11 (s), 7.17 (m); CD_3OD, 3.34 (quin). Solvent carbon shifts (ppm): $CDCl_3$ 77.2 (t); CD_2Cl_2, 54.0 (quin); C_6D_6, 128.4 (t); d_8-PhMe, 21.7 (sept), 125.6 (t), 128.5 (t), 129.3 (t), 136.1 (s); CD_3OD: 49.8 (sept). ^1H NMR spectra were assigned with the ^1H–^1H COSY and nOeSY experiments. ^{13}C NMR spectra were assigned with the aid of DEPT 90, DEPT 135 and ^1H–^{13}C HETCOR experiments. Chemical shifts are reported in ppm and coupling constants in Hz.

Mass spectra were recorded on a Thermo Electron LTQ FT, Waters Micromass LCT or an ABI Voyager-DE STR spectrometers or at the University of Swansea by the

EPSRC Mass Spectrometry Service on a Waters Micromass ZQ4000 or a Finnigan MAT 95 XP spectrometers. The isotope distributions for all parent ion peaks for metal complexes were verified *via* comparison with a theoretical isotope pattern. CHN elemental analyses were performed on a CE-440 Elemental Analyzer ; EAI Exeter Analytical Inc. Infrared spectra were recorded on a Perkin Elmer Spectrum 100 FT-IR spectrometer. Conductimetry measurements were made at 22.5 °C using 5×10^{-3} mol dm^{-3} solutions with a Jenway 4310 dip-in probe.

6.2 Preparation of metal precursors

Preparation of *bis*-acetonitrile palladium dichloride[1] $[PdCl_2(MeCN)_2]$

Under air, a suspension of $PdCl_2$ (2.500 g, 1.410×10^{-2} mol) was allowed to stir in MeCN (150 cm^3) at room temperature for 4d to afford an orange solution and precipitate. The solid was separated by filtration, washed with petroleum ether (3×30 cm^3) and dried thoroughly *in vacuo* to afford the desired product as an orange powder (3.657 g, 93 %).

CHN: Calculated for $C_4H_6N_2PdCl_2$: C: 18.52; H: 2.33; N: 10.80. Found: 18.54; H: 2.33; N: 10.76.

Preparation of cyclooctadiene palladium dichloride[2] $[PdCl_2(cod)]$

Under air, $PdCl_2$ (2.060 g, 1.162×10^{-2} mol) was dissolved in concentrated HCl (5 cm^3) with warming. Upon cooling, the acidic solution was diluted with ethanol (150 cm^3) and filtered to afford a homogeneous solution. Cyclooctadiene (2.2 cm^3, 1.742×10^{-2} mol) was added to the stirred filtrate resulting in the immediate formation of a yellow precipitate. The solid was collected by filtration, washed with diethyl ether (3×30 cm^3) and dried *in vacuo* to afford the target product as a bright yellow solid in quantitative yield (3.280 g, 99 %).

CHN: Calculated for $C_8H_{12}PdCl_2$: C: 33.66; H: 4.24. Found: 33.72; H: 4.18.

Preparation of cyclooctadiene palladium methyl chloride[3] [PdCl(Me)(cod)]

Under nitrogen, a Schlenk flask was charged with $PdCl_2(cod)$ (0.512g, 1.793×10^{-3} mol) in CH_2Cl_2 (20 cm^3) and the flask placed in a water bath at ambient temperature. Tetramethyltin (0.25 cm^3, 1.804×10^{-3} mol) was added *via* syringe and the resulting solution allowed to stir at *ca.* 15 °C for 4d with all light excluded from the flask. Following removal of the solvent under vacuum, the resulting green solid was redissolved in CH_2Cl_2 (20 cm^3), a further equivalent of tetramethyltin (0.25 cm^3, 1.804 $\times 10^{-3}$ mol) added and the reaction allowed to stir for a further 6d at 15 °C in the absence of light. The resulting solution was filtered to remove the colloidal palladium and following removal of the volatile components *in vacuo*, the desired product was washed with diethyl ether (3×30 cm^3) and dried thoroughly under vacuum to afford a light grey solid (0.263 g, 55 %).

CHN: Calculated for $C_9H_{15}PdCl$: C: 40.78; H: 5.70. Found: C: 40.71; H: 5.87.

Preparation of (*N,N,N′,N′*-tetramethylethylenediamine) palladium dichloride[4] [$PdMe_2$(tmeda)]

Under nitrogen, a suspension of $PdCl_2$ (1.760 g, 9.926×10^{-3} mol) in MeCN (80 cm^3) was heated to reflux for 2h, affording an orange solution and precipitate. Upon cooling of the mixture, tetramethylethylenediamine (2.0 cm^3, 1.5×10^{-2} mol) was added to the flask *via* syringe resulting in the immediate formation of a bright yellow precipitate. The solid was collected by filtration and dried thoroughly under vacuum (2.634 g, 90 %).

A solution of $PdCl_2$(tmeda) (2.634 g, 8.973×10^{-3} mol) in diethyl ether (40 cm^3) was cooled to – 78 °C with stirring and MeLi (11.2 cm^3 of a 1.6 mol dm^{-3} solution in diethyl ether) added *via* syringe. The resulting solution was stirred at – 78 °C for a further 0.5h before warming slowly to room temperature. After 1h, ice-cold water (20 cm^3, degassed) was added to the main reaction vessel and the organic layer separated. Following filtration to remove the colloidal palladium, the organic fraction was dried

with $MgSO_4$, the drying agent removed by filtration and the solvent removed under vacuum to afford the target product as a white solid (1.845 g, 81 %). The product must be stored under nitrogen at low temperature to limit decomposition.

Preparation of cyclooctadiene platinum dichloride[5]
$[PtCl_2(cod)]$*

Under air, potassium tetrachloroplatinate (5.274 g, 1.270×10^{-2} mol) was dissolved in deionised water (80 cm^3) and filtered. Glacial acetic acid (120 cm^3) and cod (5.27 cm^3, 4.302×10^{-2} mol) were then added to the filtrate and the mixture stirred rapidly with heating on a steam bath for 1h. The deep red solution turned yellow with pale yellow crystals precipitating with reduction of solution volume by evaporation to approximately 60 cm^3. After cooling, the crystals were collected by filtration and washed with successive portions of water (2×50 cm^3), ethanol (2×50 cm^3) and diethyl ether (2×50 cm^3). The resulting solid was dried thoroughly *in vacuo* to afford the desired product as a white-pale yellow microcrystalline solid (4.314 g, 91 %).

NMR: ^{1}**H** (250.1 MHz, $CDCl_3$): δ 2.27 (m, 4H, C$\underline{H}_2$), 2.72 (m, 4H, C$\underline{H}_2$), 5.62 (s + Pt sats., $^2J_{PtH}$ = 66.5 Hz, C$\underline{H}$).
CHN: Calculated for $C_8H_{12}PtCl_2$: C: 25.68; H: 3.23. Found: C: 25.73; H: 3.16.

* Synthesis performed by Dr. M. J. Hanton

Preparation of di(triethylphosphine) tetrachloro-diplatinum[6]
$[PtCl(\mu\text{-}Cl)(PEt_3)]_2$[†]

Under nitrogen, a solution of $PtCl_2$ (2.091 g, 7.880×10^{-3} mol) was heated in PhCN (20 cm^3) at 100 °C for 0.5h. Following cooling of the solution to room temperature, yellow crystals of $PtCl_2(PhCN)$ precipitated from solution which were collected by filtration. The crystals were washed with petroleum ether (3×40 cm^3) and following drying under vacuum, the $PtCl_2(PhCN)_2$ precursor was obtained in excellent yield (3.021 g, 95 %).

A solution of $PtCl_2(PhCN)_2$ (2.206 g, 4.672×10^{-3} mol) in CH_2Cl_2 (15 cm^3) was treated with PEt_3 (2.86 cm^3, 9.308×10^{-3} mol) and the resulting solution allowed to stir at room temperature for 3h. The CH_2Cl_2 was then removed *in vacuo* and washed with hexane (3×50 cm^3) before drying thoroughly under vacuum. $PtCl_2(PEt_3)_2$ was afforded as a white solid in excellent yield (2.056 g, 88%).

A solution of $PtCl_2(PEt_3)_2$ (1.325 g, 2.637×10^{-3} mol) in $C_2H_2Cl_4$ (30 cm^3) was transferred *via* cannula to a $C_2H_2Cl_4$ solution (40 cm^3) of $PtCl_2$ (1.403 g, 5.274×10^{-3} mol) and the resulting solution heated to 150 °C for 2h. The solution was then allowed to cool, resulting in the precipitation of yellow crystals which were collected by filtration. Following recrystallisation from CH_2Cl_2, the target dimeric product was obtained as a dark yellow crystalline solid (1.584 g, 78 %).

NMR: $^{31}P\ \{^1H\}$ (202.3 MHz, $CDCl_3$): δ + 11.4 (s + sats., $^1J_{PtP}$ = 3843 Hz).
CHN: Calculated for $C_{12}H_{30}P_2Pt_2Cl_4$: C: 18.76; H: 3.94. Found: C: 18.62; H: 3.91.

[†] Synthesis performed by Ms P. K. Monks

Preparation of tetracarbonyl di-μ-chloro-dirhodium[7]

$[Rh_2(CO)_4\{\mu\text{-}Cl\}_2]$[‡]

The apparatus (a glass tube; 20 cm in length, 3 cm in diameter, fitted with a porous frit and CO gas feed pipe at the bottom and tubing adaptor at the top) was charged with finely ground $[RhCl_3.3H_2O]$ (13.298 g, 5.05×10^{-2} mol) and purged with CO. The bottom half of the apparatus was maintained at 98 °C whilst CO was passed slowly through the system. The tubing head was removed periodically and the condensed water removed with cotton wool. After 8h, large orange needles of the product filled the bottom half of the tube (along with a black solid). The apparatus was sealed and transferred to a glove box, where the product was dissolved in toluene and filtered to remove the black solid. Crystallisation at – 30 °C from PhMe afforded the desired product as red needle crystals (3.090 g, 31 %).

NMR: $^{13}C\ \{^1H\}$ (75.8 MHz, C_6D_6): δ 175.2 (d, $^1J_{RhC}$ = 76.8 Hz, Rh–CO);
CHN: Calculated for $C_4O_4RhCl_2$: C: 12.36. Found: 12.27.

[‡] Synthesis performed by Dr M. J. Hanton

6.3 Preparation of PNE ligands and their derivatives

6.3.1 Synthesis of Grignard reagents and chloro-/vinyl-phosphines

Preparation of *bis*-(diisopropylamino)chlorophosphine (2.1-1)[8]

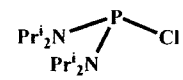

A two litre three-neck round bottom flask, fitted with a reflux condenser and a pressure-equalising dropping funnel was dried under vacuum. Then, under a flow of N_2, the flask was charged with PCl_3 (35 cm^3, 0.40 mol) and toluene (250 cm^3). The main reaction vessel was stirred and cooled to 0 °C. The dropping funnel was charged with four equivalents of $^iPr_2NH$ (225.0 cm^3, 1.60 mol) and toluene (250 cm^3), and this solution added dropwise over 1h to the cooled solution. A further aliquot of toluene (250 cm^3) was washed through the dropping funnel, before replacing it with a stopper. The reaction mixture was heated at reflux for 18h to give an orange solution with a white precipitate. The solution was separated by filtration *via* a glass frit, the precipitate washed with toluene (100 cm^3), the organic fractions combined, and the toluene removed *in vacuo* to leave an orange solid. Repeated washing with acetonitrile (5 × 80 cm^3) and drying under vacuum afforded the desired product as a crystalline white solid (76.990 g, 72 %).

NMR: ^{1}**H** (301.4 MHz, $CDCl_3$): δ 3.69 (d sept, $^3J_{HH}$ = 6.7 Hz, $^3J_{PH}$ = 5.9 Hz, 4H, $((CH_3)_2C\underline{H})_2N$), 1.24 (dd, $^3J_{HH}$ = 6.7 Hz, $^4J_{PH}$ = 2.1 Hz, 24H, $((C\underline{H}_3)_2CH)_2N$); ^{31}**P** $\{^1$**H**$\}$ (122.0 MHz, $CDCl_3$): δ + 140.6 (s).

CHN: Calculated for $C_{12}H_{28}N_2PCl$: C: 54.02; H: 10.58; N: 10.50. Found: C: 54.12; H: 10.69; N: 10.38.

Preparation of phenyl(diisopropylamino)chlorophosphine (2.1-2)

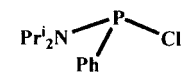

A Schlenk flask was charged with a solution of diisopropylamine (11.25cm^3, 8.025 × 10^{-2} mol) in THF (40 cm^3) and cooled to –78 °C with stirring. ^{n}BuLi (50 cm^3, 1.6 mol dm^{-3} solution in hexanes) was cautiously added *via* cannula over the course of 10 minutes and the resulting mixture maintained at – 78 °C for 0.5 h with continued stirring before being allowed to warm slowly to room temperature. Chlorodiphenylphosphine (10.9 cm^3, 8.025 × 10^{-2} mol) was added to the reaction vessel and the resulting mixture allowed to stir at room temperature for 17h. The THF was then removed under vacuum and replaced with CH_2Cl_2. The CH_2Cl_2 solution was filtered *via* a glass frit and the CH_2Cl_2 removed *in vacuo* to afford a viscous brown oil which was purified by distillation under reduced pressure to yield the target product as a yellow-orange oil (16.104 g, 82 %).

NMR: **^{1}H** (499.8 MHz, $CDCl_3$, – 20 °C): δ 0.92 (s, 3H, $((C\underline{H}_3)_2CH)_2N$), 1.20 (s, 3H, $((C\underline{H}_3)_2CH)_2N$), 1.45 (s, 3H, $((C\underline{H}_3)_2CH)_2N$), 1.55 (s, 3H, $((C\underline{H}_3)_2CH)_2N$), 3.49 (br s, $\nu_{½}$ = 40.2 Hz, 2H, $(CH_3)_2C\underline{H})_2N$), 7.38 – 7.55 (m, 3H, *m*-/*p*-Ph$\underline{H}$), 7.78 (m, 2H, *o*-Ph$\underline{H}$); **^{13}C {^{1}H}** (125.7 MHz, $CDCl_3$, – 20 °C): δ 22.0 (s, $((\underline{C}H_3)_2CH)_2N$), 25.0 (s, $((\underline{C}H_3)_2CH)_2N$), 25.2 (s, $((\underline{C}H_3)_2CH)_2N$), 27.2 (s, $((\underline{C}H_3)_2CH)_2N$), 45.5 (d, $^2J_{CP}$ = 25.4 Hz, $((CH_3)_2\underline{C}H)_2N$), 52.3 (d, $^2J_{CP}$ = 11.1 Hz, $((CH_3)_2\underline{C}H)_2N$), 128.7 (d, $^3J_{CP}$ = 3.8 Hz, *m*-Ph$\underline{C}$), 129.7 (s, *p*-Ph$\underline{C}$), 131.0 (d, $^2J_{CP}$ = *o*-Ph$\underline{C}$), 139.6 (d, $^1J_{CP}$ = 27.4 Hz, *i*-Ph$\underline{C}$); **^{31}P {^{1}H}** (162.0 MHz, $CDCl_3$): δ + 133.0 (s).

MS: Despite repeated attempts, a molecular ion could not be obtained for **2.1-2**.

Preparation of vinyl magnesium bromide (2.2-1)

An ampoule was charged with vinyl bromide (10 cm^3, 0.142 mol) by vacuum transfer and maintained at – 78 °C while a second ampoule charged with THF (90 cm^3) was prepared. The vinyl bromide was transferred from the first ampoule by vacuum transfer into the second vessel at – 196 °C and maintained at this temperature. Meanwhile, a three-neck 500 cm^3 round bottom flask fitted with a reflux condenser was charged with magnesium turnings (6.12 g, 0.252 mol), which were prepared by washing with hexane, heating to 150 °C for 1h under vacuum and allowing to cool under nitrogen. An aliquot of THF (15 cm^3, sufficient to cover the magnesium turnings) was then added to the main reaction vessel. The THF solution of vinyl bromide was allowed to warm to 0 °C and an aliquot of the solution was added *via* cannula to the main reaction vessel to initiate the reaction. Following initiation, the remaining vinyl bromide solution was added portion-wise with stirring over the course of 3h and the resulting mixture allowed to stir at room temperature for 24h. The product was filtered from the remaining magnesium *via* a glass frit and following analysis by titration, the molarity of the Grignard reagent was determined to be 1.1 mol dm^{-3}.

Preparation of allyl magnesium chloride (2.2-2)[9]

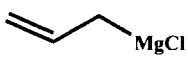

A three-neck round bottom flask fitted with a pressure-equalising dropping funnel and a double-surface reflux condenser and containing a large Teflon stirrer bar was charged with Mg turnings (14.91 g, 0.614 mol) and allowed to dry-stir vigorously for 20h. THF was then added (10 cm^3) to cover the powdered magnesium and the reaction flask cooled to 0 °C with stirring. The dropping funnel was charged with a solution of allyl chloride (10.0 cm^3, 0.123 mol) in THF (150 cm^3) and this solution added portion-wise to the main reaction vessel to initiate the reaction. Upon reaction initiation, the remaining allyl chloride solution was added drop-wise and the resulting mixture allowed to stir at room temperature for 36h. The colloidal magnesium was removed by filtration *via* a glass frit and following analysis by titration, the molarity of the Grignard reagent was found to be 0.8 mol dm^{-3}.

Preparation of diphenylvinylphosphine (2.3-1) 

A 100 cm^3 three-neck round bottom flask, fitted with a pressure-equalising dropping funnel, was charged with a solution of chlorodiphenylphosphine (7.35 cm^3, 4.01×10^{-2} mol) in THF (50 cm^3) and allowed to cool to –78 °C with stirring. The dropping funnel was charged with vinyl magnesium chloride (30 cm^3, 1.6 mol dm^{-3} solution in THF) and the Grignard reagent added dropwise to the main reaction vessel over the course of 1h. The resulting mixture was allowed to stir at – 78 °C for a further 0.5h before being allowed to warm slowly to room temperature. The THF was then removed *in vacuo*, replaced with hexane and the resulting solution filtered *via* a glass frit. The hexane was removed *in vacuo* to afford the product as a colourless oil (5.530g, 65 %).

The product is sensitive to discolouration in light, gradually changing from colourless to bright orange when allowed to stand in light for long periods although this appears to have no noticeable chemical effects.

NMR: ^{1}**H** (400.1 MHz, $CDCl_3$): δ 5.84 (m, 1H, $C\underline{H}_2$=CH–P), 6.10 (m, 1H, $C\underline{H}_2$=CH–P), 6.85 (m, 1H, CH_2=C<u>H</u>–P), 7.42 (m, 6H, *m/p*-Ph<u>H</u>), 7.54 (m, 4H, *o*-Ph<u>H</u>); ^{13}**C** {^{1}**H**} (100.6 MHz, $CDCl_3$): δ 128.6 (d, $^{3}J_{PC}$ = 6.5 Hz, *m*-Ph<u>C</u>), 128.8 (s, *p*-Ph<u>C</u>), 129.6 (d, $^{2}J_{PC}$ = 24.2 Hz, <u>C</u>H_2=CH–P), 133.3 (d, $^{2}J_{PC}$ = 19.0 Hz, *o*-Ph<u>C</u>), 136.9 (d, $^{1}J_{PC}$ = 13.9 Hz, *i*-Ph<u>C</u>), 137.7 (d, $^{1}J_{PC}$ = 9.5 Hz, CH_2=<u>C</u>H–P); ^{31}**P** {^{1}**H**} (162.0 MHz, $CDCl_3$): δ – 10.7 (s).
MS (ES^+): *m/z* = 213.1 $[MH]^+$.
CHN: Calculated for $C_{14}H_{13}P$; C: 79.22; H: 6.19; Found: C: 69.75; H: 4.86.
(Poor CHN obtained as a result of the oily nature of the compound).

Preparation of *bis*(diisopropylamino)vinylphosphine (2.3-2) 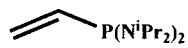

The synthesis of *bis*(diisopropylamino)vinylphosphine (**2.3-2**) was analogous to that of the related compound (**2.3-1**) employing ($^{i}Pr_2N)_2PCl$ (12.810 g, 4.48×10^{-2} mol) and vinyl magnesium chloride (30 cm^3, 1.6 mol dm^{-3} solution in THF) in THF solution (150 cm^3). Following isolation, the product was afforded as a pale yellow oil (7.577g, 61 %).

As was noted for the related diphenylvinylphosphine (**2.3-1**), the product was noted to be sensitive to decolouration in light, with the product gradually turning from pale yellow to deep orange-yellow when allowed to stand in light for long periods although this has no notable chemical effects.

NMR: ^{1}**H** (499.8 MHz, $CDCl_3$): δ 1.07 (d, $^{3}J_{HH}$ = 6.8 Hz, 12H, $N(CH(C\underline{H}_3)_2)$), 1.13 (d, $^{3}J_{HH}$ = 6.8 Hz, 12H, $N(CH(C\underline{H}_3)_2)$), 3.32 (dsept, $^{3}J_{PH}$ = 11.0 Hz, $^{3}J_{HH}$ = 6.8 Hz, 4H, $N(C\underline{H}(CH_3)_2)$), 5.49 (m, 1H, $C\underline{H}_2$=CH–P), 5.53 (m, 1H, $C\underline{H}_2$=CH–P), 6.31 (m, 1H, CH_2=C$\underline{H}$–P); ^{13}**C** {^{1}**H**} (100.6 MHz, $CDCl_3$): δ 23.1 (d, $^{3}J_{PC}$ = 6.9 Hz, $N(CH(\underline{C}H_3)_2)$), 23.6 (d, $^{3}J_{PC}$ = 6.9 Hz, $N(CH(\underline{C}H_3)_2)$), 46.5 (d, $^{2}J_{PC}$ = 11.0 Hz, $N(C\underline{H}(CH_3)_2)$), 121.4 (d, $^{2}J_{PC}$ = 23.3 Hz, $\underline{C}H_2$=CH–P), 141.3 (d, $^{1}J_{PC}$ = 3.6 Hz, CH_2=$\underline{C}$H–P); ^{31}**P** {^{1}**H**} (202.3 MHz, $CDCl_3$): δ + 54.2 (s).

MS (ES^+): *m/z* = 259.2 $[MH]^+$

CHN: Calculated for $C_{14}H_{31}N_2P$; C: 65.06; H: 12.11; N: 10.84. Found; C: 61.68; H: 11.44; N: 10.60.

(Poor CHN obtained as a result of the oily nature of the compound).

Preparation of (diisopropylamino)phenylvinylphosphine (2.3-3) 

The synthesis of (diisopropylamino)phenylvinylphosphine (**2.3-3**) was analogous to that of the related compound (**2.3-1**) employing chloro(diisopropylamino)phenylphosphine (**2.1-2**) (2.055g, 8.431×10^{-3} mol) and vinyl magnesium chloride (5.3 cm^3, 1.6 mol dm^{-3} solution in THF) in THF solution (50 cm^3). Following isolation, the product was afforded as an orange oil (1.615 g, 81 %).

NMR: ^{1}**H** (400.1 MHz, $CDCl_3$): δ 0.98 (d, $^{3}J_{HH}$ = 6.6 Hz, 6H, N(CH(C<u>H</u>$_3$)$_2$)), 1.08 (d, $^{3}J_{HH}$ = 6.6 Hz, 6H, N(CH(C<u>H</u>$_3$)$_2$)), 3.23 (dsept, $^{3}J_{PH}$ = 10.8 Hz, $^{3}J_{HH}$ = 6.6 Hz, N(C<u>H</u>(CH$_3$)$_2$)), 5.75 (m, 1H, C<u>H</u>$_2$=CH–P), 5.86 (m, 1H, C<u>H</u>$_2$=CH–P), 6.55 (m, 1H, CH$_2$=C<u>H</u>–P), 7.15 (m, 1H, *p*-Ph<u>H</u>), 7.22 (m, 2H, *m*-Ph<u>H</u>), 7.38 (m, 2H, *o*-Ph<u>H</u>); ^{13}**C** {^{1}**H**} (100.6 MHz, $CDCl_3$): δ 22.9 (d, $^{3}J_{PC}$ = 6.6 Hz, N(CH(<u>C</u>H$_3$)$_2$)), 23.2 (d, $^{3}J_{PC}$ = 6.6 Hz, N(CH(<u>C</u>H$_3$)$_2$)), 46.4 (d, $^{2}J_{PC}$ = 8.8 Hz, N(<u>C</u>H(CH$_3$)$_2$)), 126.5 (s, *p*-Ph<u>C</u>), 126.6 (d, $^{2}J_{PC}$ = 32.2 Hz, <u>C</u>H$_2$=CH–P), 126.9 (d, $^{3}J_{PC}$ = 4.4 Hz, *m*-Ph<u>C</u>), 130.0 (d, $^{2}J_{PC}$ = 18.3 Hz, *o*-Ph<u>C</u>), 138.1 (d, $^{1}J_{PC}$ = 16.1 Hz, CH$_2$=<u>C</u>H–P), 140.5 (d, $^{1}J_{PC}$ = 8.0 Hz, *i*-Ph<u>C</u>); ^{31}**P** {^{1}**H**} (81.0 MHz, $CDCl_3$): δ + 34.8 (s).

MS: Despite repeated attempts, a molecular ion peak could not be obtained for **2.3-3**

CHN: Calculated for $C_{14}H_{22}NP$; C: 71.45; H: 9.44; N: 5.95. Found; C: 68.58; H: 7.41; N: 5.70.

(Poor CHN obtained as a result of the oily nature of the compound).

Preparation of allyldiphenylphosphine (2.3-4)

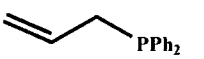

The synthesis of allyldiphenylphosphine (**2.3-4**) was analogous to that of the related compound (**2.3-1**), employing chlorodiphenylphosphine (3.7 cm^3, 2.019 × 10^{-2} mol) and allyl magnesium chloride (**2.2-2**) (30 cm^3 of 0.8 mol dm^{-3} solution in THF) in THF solution (40 cm^3). Following isolation, the product was obtained as a colourless oil (2.940g, 64 %).

NMR: ^{1}**H** (499.8 MHz, $CDCl_3$): δ 3.00 (d, $^{3}J_{HH}$ = 7.5 Hz, 2H, P–CH$_2$CH=C<u>H</u>$_2$), 5.12 (m, 2H, P–C<u>H</u>$_2$CH=CH$_2$), 5.93 (m, 1H, P–CH$_2$C<u>H</u>=CH$_2$), 7.42 (m, 6H, *m*/*p*-Ph<u>H</u>), 7.56 (m, 4H, *o*-Ph<u>H</u>); ^{13}**C** {^{1}**H**} (125.7 MHz, $CDCl_3$): δ 34.1 (d, $^{3}J_{PC}$ = 13.9 Hz, P–CH$_2$CH=<u>C</u>H$_2$), 117.8 (d, $^{1}J_{PC}$ = 10.2 Hz, P–<u>C</u>H$_2$CH=CH$_2$), 128.7 (d, $^{3}J_{PC}$ = 6.6 Hz, *m*-Ph<u>C</u>), 129.0 (s, *p*-Ph<u>C</u>), 133.2 (d, $^{2}J_{PC}$ = 18.3 Hz, *o*-Ph<u>C</u>), 133.5 (d, $^{2}J_{PC}$ = 8.8 Hz, P–CH$_2$<u>C</u>H=CH$_2$), 138.5 (d, $^{1}J_{PC}$ = 14.7 Hz, *i*-Ph<u>C</u>); ^{31}**P** {^{1}**H**} (161.9 MHz, $CDCl_3$): δ – 14.6 (s).

MS (ES$^+$): *m/z* = 277.2 [MH]$^+$

CHN: Calculated for $C_{15}H_{15}P$; C: 79.62; H: 6.70. Found; C: 80.35; H: 6.72.

(Poor CHN obtained as a result of the oily nature of the compound).

Preparation of *bis*(diisopropylamino)vinylphosphine sulphide (2.3-5)

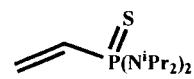

A Schlenk flask was charged with a solution of *bis*(diisopropylamino)-vinyl phosphine (**2.3-2**) (0.330 g, 1.277×10^{-3} mol) in CH_2Cl_2 at room temperature. S_8 (0.041 g, 1.277×10^{-3} mol) was added as a solid and the resulting mixture was allowed to stir at room temperature for 4h. Upon analysis by ^{31}P $\{^1H\}$ NMR spectroscopy it was shown that only 82% of the required product was present (by integration), therefore a further portion of S_8 (0.0073 g, 2.277×10^{-4} mol) was added to the reaction vessel and stirring at room temperature continued for 3h. Subsequent analysis by ^{31}P NMR spectroscopy indicated that the reaction had reached completion and therefore the solvent was removed under vacuum and the product dried thoroughly *in vacuo* to afford a yellow solid. The product was recrystallised from CH_2Cl_2/hexane to afford the product as a white solid (0.279g, 75 %).

NMR: ^{1}**H** (400.0 MHz, $CDCl_3$): δ 1.22 (d, $^3J_{HH}$ = 7.0 Hz, 12H, N(CH(C$\underline{H}_3$)$_2$)), 1.34 (d, $^3J_{HH}$ = 7.0 Hz, 12H, N(CH(C$\underline{H}_3$)$_2$)), 3.72 (dsept, $^3J_{PH}$ = 17.6 Hz, $^3J_{HH}$ = 7.0 Hz, 4H, N(C$\underline{H}$(CH$_3$)$_2$)), 6.07 (m, 1H, C$\underline{H}_2$=CH–P), 6.55 (m, 1H, CH$_2$=C$\underline{H}$–P), 6.62 (m, 1H, C$\underline{H}_2$=CH–P); ^{13}**C** $\{^1$**H**$\}$ (100.6 MHz, $CDCl_3$): δ 23.1 (d, $^3J_{PC}$ = 2.3 Hz, N(CH(C$\underline{H}_3$)$_2$)), 23.5 (d, $^3J_{PC}$ = 2.3 Hz, N(CH(C$\underline{H}_3$)$_2$)), 46.4 (d, $^2J_{PC}$ = 5.4 Hz, N(C$\underline{H}$(CH$_3$)$_2$)), 132.4 (d, $^2J_{PC}$ = 6.5 Hz, C$\underline{H}_2$=CH–P), 136.4 (d, $^1J_{PC}$ = 111.6 Hz, CH$_2$=C$\underline{H}$–P); ^{31}**P** $\{^1$**H**$\}$ (161.9 MHz, $CDCl_3$): δ + 67.1 (s).

MS (ES$^+$): *m/z* = 259.3 $[MH–S]^+$.

CHN: Calculated for $C_{14}H_{31}N_2PS$; C: 57.88; H: 10.78; N: 9.65. Found: C: 57.59; H: 10.70; N: 9.39.

6.3.2 Synthesis of PNE ligands

Synthesis of *N*-methylpiperazine-*N'*-ethylene-diphenylphosphine (2.4-1)[10]

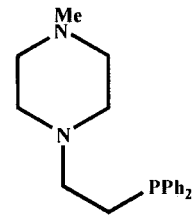

A 100 cm^3 three-neck round bottom flask fitted with a reflux condenser was charged with diphenylvinylphosphine (**2.3-1**) (1.400g, 6.600×10^{-3} mol) in THF (60 cm^3). Under a flow of nitrogen, *N*-methylpiperazine (0.75 cm^3, 6.677×10^{-3} mol) was added along with a catalytic quantity of $NaNH_2$ (1.0 cm^3 of a suspension in toluene) and the resulting mixture heated at reflux for 24h. The resulting mixture was allowed to cool to room temperature and transferred *via* cannula to an aqueous solution of NH_4Cl (50 cm^3, 10% w/v, degassed). The solution was extracted with CH_2Cl_2 (3 × 30 cm^3), the organic fractions combined and dried over $MgSO_4$. The drying agent was removed by filtration *via* a glass frit, and following removal of the CH_2Cl_2 under vacuum the desired product was afforded as a viscous yellow-orange oil (1.940 g, 94 %), which on prolonged standing (weeks) affords very pale yellow crystals suitable for X-ray diffraction studies (1.50 g, 73 %) {Full crystallographic data available in Appendix 1(a)}.

NMR: ^{1}**H** (499.8 MHz, – 50 °C, $CDCl_3$): δ 2.00 – 2.16 (m, 4H, $N(C\underline{H}_2CH_2)_2NMe$ and $N(CH_2C\underline{H}_2)_2NMe$), 2.19 – 2.34 (m, 5H, $Ph_2PC\underline{H}_2CH_2N$ and $N(CH_2CH_2)_2NC\underline{H}_3$), 2.41 (m, 2H, $Ph_2PCH_2C\underline{H}_2N$), 2.72 (m, 2H, $N(C\underline{H}_2CH_2)_2NMe$), 2.82 (m, 2H, $N(CH_2C\underline{H}_2)_2NMe$), 7.20 – 7.29 (m, 6H, *m*-/*p*-Ph$\underline{H}$), 7.37 (m, 4H, *o*-Ph$\underline{H}$); ^{13}**C {^{1}H}** (125.7 MHz, – 50 °C, $CDCl_3$) δ 24.9 (d, $^1J_{CP}$ = 12.1 Hz, $Ph_2P\underline{C}H_2CH_2N$), 45.1 (s, $N(CH_2CH_2)_2N\underline{C}H_3$), 52.0 (s, $MeN(\underline{C}H_2CH_2)_2N$), 54.1 (s, $MeN(CH_2\underline{C}H_2)_2N$), 54.3 (s, $Ph_2PCH_2\underline{C}H_2N$), 127.5 (d, $^3J_{CP}$ = 6.7 Hz, *m*-Ph$\underline{C}$), 127.7 (s, *p*-Ph$\underline{C}$), 131.8 (d, $^2J_{CP}$ = 18.7 Hz, *o*-Ph$\underline{C}$), 137.6 (d, $^1J_{CP}$ = 12.9 Hz, *i*-Ph$\underline{C}$); ^{31}**P {^{1}H}** (202.3 MHz, $CDCl_3$): δ – 19.1 (s).

MS (ES^+): *m/z* = 313.2 $[MH]^+$.

CNH: Calculated for $C_{19}H_{25}N_2P$ (solid): C, 73.04; H, 8.08; N, 8.97. Found: C, 73.00; H, 7.88; N, 8.74.

Synthesis of morpholine-*N*-ethylene-diphenylphosphine (2.4-2)

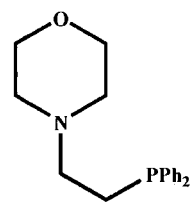

The synthesis of morpholine-*N*-ethylene-diphenylphosphine (**2.4-2**) was analogous to that of the related compound **2.4-1**, employing diphenylvinylphosphine (**2.3-1**) (2.003 g, 9.437×10^{-3} mol) and morpholine (0.83 cm^3, 9.516×10^{-3} mol) in THF solution (60 cm^3) with a catalytic quantity of $NaNH_2$ (1.0 cm^3 of a suspension in toluene). Following isolation, the desired product was afforded as a viscous yellow-orange oil (2.679 g, 95 %).

NMR: ^{1}**H** (499.8 MHz, $CDCl_3$): δ 2.18 (m, 2H, $Ph_2PC_2\underline{H}_4N$), 2.34 (br, $\nu_{½}$ = 13.9 Hz, 4H, $N(C_2\underline{H}_4)_2O$), 2.40 (m, 2H, $PC_2\underline{H}_4N$), 3.58 (m, 4H, $N(C_2\underline{H}_4)_2O$), 7.23 (m, 6H, *m*-/*p*-Ph$\underline{H}$), 7.34 (m, 4H, *o*-Ph$\underline{H}$); ^{1}**H** (499.8 MHz, $CDCl_3$ – 50 °C): δ 2.13 (m, 2H, $N(CH_2C\underline{H}_2)_2O$), 2.30 (m, 2H, $Ph_2PC\underline{H}_2CH_2N$), 2.44 (m, 2H, $Ph_2PCH_2C\underline{H}_2N$), 2.77 (m, 2H, $N(C\underline{H}_2CH_2)_2O$), 3.59 (m, 2H, $N(C\underline{H}_2CH_2)_2O$), 3.83 (m, 2H, $N(CH_2C\underline{H}_2)_2O$), 7.30 – 7.39 (m, 6H, *m*-/*p*-Ph$\underline{H}$), 7.44 (m, 4H, *o*-Ph$\underline{H}$); ^{13}**C** {^{1}**H**} (125.7 MHz, $CDCl_3$): δ 24.5 (d, $^1J_{CP}$ = 12.1 Hz, $P\underline{C}H_2CH_2N$), 52.3 (s, $N(\underline{C}H_2CH_2)_2O$), 54.5 (d, $^2J_{CP}$ = 23.0 Hz, $Ph_2PCH_2\underline{C}H_2N$), 65.8 (s, $N(CH_2\underline{C}H_2)_2O$), 127.4 (d, $^3J_{CP}$ = 6.7 Hz, *m*-Ph$\underline{C}$), 127.6 (s, *p*-Ph$\underline{C}$), 131.7 (d, $^2J_{PC}$ = 18.7 Hz, *o*-Ph$\underline{C}$), 137.3 (d, $^1J_{CP}$ = 12.6 Hz, *i*-Ph$\underline{C}$); ^{31}**P** {^{1}**H**} (202.3 MHz, $CDCl_3$): δ – 18.2 (s);

MS (ES^+): *m/z* = 300.1 $[MH]^+$.

CHN: Calculated for $C_{18}H_{22}NOP$; C: 72.21; H: 7.42; N: 4.68. Found: C: 69.86; H: 6.24; N: 4.31.

Due to the oily nature of this compound, satisfactory CHN analysis could not be obtained.

Preparation of thiomorpholine-*N*-ethylene-diphenylphosphine (2.4-3)

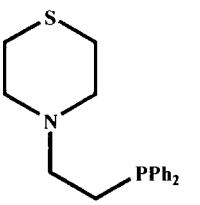

The synthesis of thiomorpholine-*N*-ethylene-diphenylphosphine (**2.4-3**) was analogous to that of the related compound **2.4-1**, employing diphenylvinylphosphine (**2.3-1**) (1.506 g, 7.096×10^{-3} mol) and thiomorpholine (0.68 cm^3, 7.155×10^{-3} mol) in THF solution (80 cm^3) with a catalytic quantity of $NaNH_2$ (1.0 cm^3 of a suspension in toluene). Following isolation, the desired product was afforded as a viscous yellow-orange oil (2.154 g, 96 %).

NMR: ^{1}**H** (499.8 MHz, $CDCl_3$): δ 2.28 (m, 2H, $Ph_2PC\underline{H}_2CH_2N$), 2.54 (m, 2H, $Ph_2PCH_2C\underline{H}_2N$), 2.63 (m, 4H, $N(CH_2C\underline{H}_2)_2S$), 2.70 (m, 4H, $N(C\underline{H}_2CH_2)_2S$), 7.28 – 7.37 (m, 6H, *m-/p*-Ph$\underline{H}$), 7.44 (m, 4H, *o*-Ph$\underline{H}$); ^{13}**C** {^{1}**H**} (125.7 MHz, $CDCl_3$): δ 25.7 (d, $^1J_{CP}$ = 12.4 Hz, $Ph_2P\underline{C}H_2CH_2N$), 28.2 (s, $N(CH_2\underline{C}H_2)_2S$), 54.9 (s, $N(\underline{C}H_2CH_2)_2S$), 56.1 (d, $^2J_{CP}$ = 23.0 Hz, $Ph_2PCH_2\underline{C}H_2N$), 128.7 (d, $^3J_{CP}$ = 6.7 Hz, *m*-Ph$\underline{C}$), 128.9 (s, *p*-Ph$\underline{C}$), 133.0 (d, $^2J_{CP}$ = 18.6 Hz, *o*-Ph$\underline{C}$), 138.7 (d, $^1J_{CP}$ = 12.9 Hz, *i*-Ph$\underline{C}$); ^{1}**H** (499.8 MHz, CD_2Cl_2, – 90 °C): δ 2.13 – 2.32 (m, 4H, $Ph_2PC\underline{H}_2CH_2N$ and $N(CH_2C\underline{H}_2)_2S$), 2.36 – 2.50 (m, 4H, $Ph_2PCH_2C\underline{H}_2N$ and $N(C\underline{H}_2CH_2)_2S$), 2.77 (m, 2H, $N(C\underline{H}_2CH_2)_2S$), 3.07 (m, 2H, $N(CH_2C\underline{H}_2)_2S$), 7.31 – 7.38 (m, 6H, *m-/p*-Ph$\underline{H}$), 7.42 (m, 4H, *o*-Ph$\underline{H}$) [*NB.* Ring proton resonance obscured by solvent]; ^{13}**C** {^{1}**H**} (125.7 MHz, CD_2Cl_2, – 90 °C): δ 24.7 (s, $Ph_2P\underline{C}H_2CH_2N$), 28.2 (s, $N(CH_2\underline{C}H_2)_2S$), 55.9 (d, $^2J_{CP}$ = 25.0 Hz, $Ph_2PCH_2\underline{C}H_2N$), 129.0 (d, $^3J_{CP}$ = 6.7 Hz, *m*-Ph$\underline{C}$), 129.2 (s, *p*-Ph$\underline{C}$), 133.0 (d, $^2J_{CP}$ = 18.2 Hz, *o*-Ph$\underline{C}$), 138.6 (d, $^1J_{CP}$ = 11.6 Hz, *i*-Ph$\underline{C}$) [*NB.* Ring proton resonance obscured by solvent]; ^{31}**P** {^{1}**H**} (202.3 MHz, $CDCl_3$): δ – 18.3 (s).

MS (ES$^+$): *m/z* = 316.1 $[MH]^+$.

CHN: Calculated for $C_{18}H_{22}NSP$; C: 68.53; H: 7.04; N: 4.44. Found: C: 67.00; H: 7.33; N: 5.12.

Due to the oily nature of this compound, satisfactory CHN analysis could not be obtained.

Preparation of piperidine-*N*-ethylene-diphenylphosphine (2.4-4)

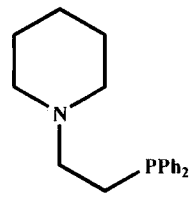

The synthesis of piperidine-*N*-ethylene-diphenylphosphine (**2.4-4**) was analogous to that of the related compound **2.4-1**, employing diphenylvinylphosphine (**2.3-1**) (1.520 g, 7.162×10^{-3} mol) and piperidine (0.7 cm^3, 7.086×10^{-3} mol) in THF solution (80 cm^3) with a catalytic quantity of $NaNH_2$ (1.0 cm^3 of a suspension in toluene). Following isolation, the product was afforded as a viscous orange oil (1.960 g, 92 %).

NMR: ^{1}**H** (499.8 MHz, $CDCl_3$): δ 1.43 (m, 2H, $N(CH_2CH_2)_2C\underline{H}_2$), 1.59 (m, 4H, $N(CH_2C\underline{H}_2)_2CH_2$), 2.28 – 2.53 (m, 8H, $Ph_2PC\underline{H}_2CH_2N$, $N(C\underline{H}_2CH_2)_2CH_2$ and $Ph_2PCH_2C\underline{H}_2N$), 7.30 – 7.35 (m, 6H, *m*-/*p*-Ph$\underline{H}$), 7.46 (m, 4H, *o*-Ph$\underline{H}$); ^{13}**C** {^{1}**H**} (125.7 MHz, $CDCl_3$): δ 24.6 (s, $N(CH_2CH_2)_2\underline{C}H_2$), 25.9 (d, $^{1}J_{CP}$ = 11.9 Hz, $Ph_2P\underline{C}H_2CH_2N$), 26.1 (s, $N(CH_2\underline{C}H_2)_2CH_2$), 54.5 (s, $N(\underline{C}H_2CH_2)_2CH_2$), 56.1 (d, $^{2}J_{CP}$ = 23.9 Hz, $Ph_2PCH_2\underline{C}H_2N$), 128.7 (d, $^{3}J_{CP}$ = 6.8 Hz, *m*-Ph$\underline{C}$), 128.8 (s, *p*-Ph$\underline{C}$), 133.0 (d, $^{2}J_{CP}$ = 18.7 Hz, *o*-Ph$\underline{C}$), 138.8 (d, $^{1}J_{CP}$ = 12.4 Hz, *i*-Ph$\underline{C}$); ^{31}**P** {^{1}**H**} (202.3 MHz, $CDCl_3$): δ – 17.8 (s).

MS (ES^+): *m/z* = 298.3 $[MH]^+$

CHN: Calculated for $C_{19}H_{24}NP$: C: 76.73; H: 8.15; N: 4.71. Found: C: 74.36; H: 7.66; N: 4.01.

Due to the oily nature of this compound, satisfactory CHN analysis could not be obtained.

Synthesis of *N*-phenylpiperazine-*N'*-ethylene-diphenylphosphine (2.4-5)

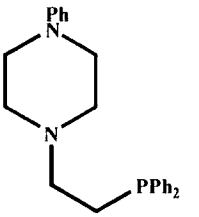

The synthesis of *N*-phenylpiperazine-*N'*-ethylene-diphenylphosphine (**2.4-5**) was analogous to that of the related compound **2.4-1**, employing diphenylvinylphosphine (**2.3-1**) (1.002 g, 7.721×10^{-3} mol) and *N*-phenylpiperazine (0.72 cm^3, 4.721×10^{-3} mol) in THF solution (60 cm^3) with a catalytic quantity of $NaNH_2$ (1.0 cm^3 of a suspension in toluene). Following isolation, the product was afforded as a viscous orange oil which was found to solidify upon repeated freeze-thaw drying cycles at – 196 °C to afford a pale orange waxy solid (1.463 g, 83 %).

NMR: ^{1}**H** (299.9 MHz, $CDCl_3$) δ 2.32 (m, 2H, $Ph_2PC\underline{H}_2CH_2N$), 2.55 (m, 2H, $Ph_2PCH_2C\underline{H}_2N$), 2.62 (pseudo t, $^3J_{HH}$ = 4.8 Hz, 4H, $PhN(CH_2C\underline{H}_2)_2N$), 3.19 (pseudo t, $^3J_{HH}$ = 4.8 Hz, 4H, $PhN(C\underline{H}_2CH_2)_2N$), 6.86 (m, 1H, *p*-Ph$\underline{H}$), 6.91 (m, 2H, *m*-Ph$\underline{H}$), 7.26 (m, 2H, *o*-Ph$\underline{H}$), 7.33 (m, 6H, *m*/*p*-$(Ph\underline{H})_2P$), 7.45 (m, 4H, *o*-$(Ph\underline{H})_2P$); ^{13}**C {^{1}H}** (100.6 MHz, $CDCl_3$): δ 26.1 (d, $^2J_{CP}$ = 12.1 Hz, $Ph_2PCH_2\underline{C}H_2N$), 48.1 (s, $PhN(\underline{C}H_2CH_2)_2N$), 51.9 (s, $PhN(CH_2\underline{C}H_2)_2N$), 54.3 (d, $^1J_{CP}$ = 23.1 Hz, $Ph_2P\underline{C}H_2CH_2N$), 115.2 (s, *m*-Ph$\underline{C}$), 118.8 (s, *p*-Ph$\underline{C}$), 127.5 (d, $^3J_{CP}$ = 6.6 Hz, *m*-$(Ph\underline{C})_2P$), 127.7 (s, *p*-$(Ph\underline{C})_2P$), 128.2 (s, *o*-Ph$\underline{C}$), 131.8 (d, $^2J_{CP}$ = 19.1 Hz, *o*-$(Ph\underline{C})_2P$), 137.4 (d, $^1J_{CP}$ = 13.2 Hz, *i*-$(Ph\underline{C})_2P$), 150.3 (s, *i*-Ph$\underline{C}$); ^{31}**P {^{1}H}** (202.3 MHz, $CDCl_3$): δ – 18.1 (s).

MS: *m/z* = 375.3 $[MH]^+$.

CHN: Calculated for $C_{24}H_{27}N_2P$: C: 76.97; H: 7.28; N: 7.48. Found: C: 76.59; H: 6.83; N: 7.00.

Due to the waxy nature of this compound, satisfactory CHN analysis could not be obtained.

Preparation of N-methylpiperazine-N′-1-methyl-ethyl-diphenyl-phosphine (2.4-6)

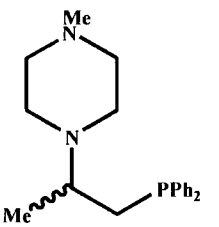

The synthesis of *N*-methylpiperazine-*N*′-1-methyl-ethyl-diphenylphosphine (**2.4-6**) was analogous to that of the related compound **2.4-1**, employing allyldiphenylphosphine (**2.3-4**) (1.513 g, 6.68×10^{-3} mol) and *N*-methylpiperazine (0.8 cm^3, 7.218×10^{-3} mol) in THF solution (80 cm^3) with a catalytic quantity of $NaNH_2$ (1.0 cm^3 of a suspension in toluene). Following isolation, the methyl-branched product was afforded as a viscous orange oil (1.960 g, 90 %).

NMR ^{1}H: (499.7 MHz, $CDCl_3$, – 50 °C): δ 1.10 (d, $^4J_{PH}$ = 6.0 Hz, 3H, $CH_2CH(C\underline{H}_3)N$, 1.97 (m, 2H, $N(CH_2C\underline{H}_2)_2NMe$), 2.11 (m, 1H, $Ph_2PC\underline{H}_2CH(CH_3)N$), 2.26 (s, 3H, $C\underline{H}_3N(C_4H_8)N$), 2.36 (m, 1H, $Ph_2PC\underline{H}_2CH(CH_3)N$), 2.45 (m, 2H, $N(C\underline{H}_2CH_2)_2NMe$), 2.55 (overlapping m, 3H, $N(C\underline{H}_2CH_2)_2NMe$ and $Ph_2PCH_2C\underline{H}(CH_3)N$), 2.72 (m, 2H, $N(CH_2C\underline{H}_2)_2NMe$), 7.25 – 7.35 (m, 6H, *m*-/*p*-Ph$\underline{H}$), 7.40 (m, 2H *o*-Ph$\underline{H}$), 7.45 (m, 2H, *o*-Ph$\underline{H}$); **^{13}C{^{1}H}** (100.6 MHz, $CDCl_3$, – 50 °C): δ 14.6 (d, $^3J_{CP}$ = 7.5 Hz, $CH_2CH(\underline{C}H_3)N$), 31.8 (d, $^1J_{CP}$ = 13.0 Hz, $Ph_2P\underline{C}H_2CH(CH_3)N$), 44.9 (s, $\underline{C}H_3N(C_4H_8)N$), 46.5 (br s, $\nu_{½}$ = 49.2 Hz, $CH_3N(\underline{C}H_2CH_2)_2N$), 54.1 (s, $CH_3N(CH_2\underline{C}H_2)_2N$), 55.8 (d, $^2J_{CP}$ = 16.0 Hz, $Ph_2PCH_2\underline{C}H(CH_3)N$), 127.2 (d, $^3J_{CP}$ = 7.0 Hz, *m*-Ph$\underline{C}$), 127.3 (d, $^3J_{CP}$ = 7.0 Hz, *m*-Ph$\underline{C}$), 127.4 (s, *p*-Ph$\underline{C}$), 127.5 (s, *p*-Ph$\underline{C}$), 131.8 (d, $^2J_{CP}$ = 15.0 Hz, *o*-Ph$\underline{C}$), 131.8 (d, $^2J_{CP}$ = 15.1 Hz, *o*-Ph$\underline{C}$), 138.1 (d, $^1J_{CP}$ = 14.0 Hz, *i*-Ph$\underline{C}$), 138.4 (d, $^1J_{CP}$ = 14.0 Hz, *i*-Ph$\underline{C}$); **^{31}P {^{1}H}** (121.4 MHz, $CDCl_3$): δ – 18.6 (s).

MS (ES^+): *m/z* = 327.2 $[MH]^+$.

CHN: Calculated for $C_{20}H_{28}N_2P$: C: 73.35; H: 8.64; N: 8.56. Found: C: 71.07; H: 7.95; N: 8.42.

Due to the oily nature of this compound, satisfactory CHN analysis could not be obtained.

Preparation of piperazine-N,N′-diethylene-tetraphenyldiphosphine (2.4-7)

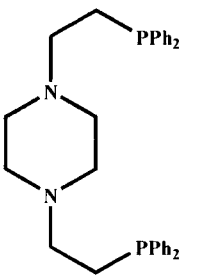

A 100 cm^3 three-neck round bottom flask fitted with a reflux condenser was charged with piperazine (0.494 g, 5.739×10^{-3} mol) and two equivalents of diphenylvinylphosphine (**2.3-1**) (2.436 g, 1.148×10^{-2} mol) in THF (70 cm^3). Under a flow of nitrogen, a catalytic quantity of $NaNH_2$ (1.0 cm^3 of a suspension in toluene) and the resulting mixture heated to reflux for 20h. The resulting mixture was allowed to cool to room temperature and transferred *via* cannula to an aqueous solution of NH_4Cl (50 cm^3, 10% w/v, degassed). The solution was extracted with CH_2Cl_2 (3 × 30 cm^3), the organic fractions combined and dried over $MgSO_4$. The drying agent was removed by filtration *via* a glass frit, and following removal of the CH_2Cl_2 under vacuum, the product was obtained as a waxy beige solid (2.260 g, 77 %).

NMR: ^{1}**H** (499.8 MHz, $CDCl_3$, – 50 °C): δ 2.11 (pseudo d, $^2J_{HH}$ = 7.8 Hz, 4H, N($C_4\underline{H}_8$)N), 2.29 (m, 4H, $Ph_2C\underline{H}_2CH_2N$), 2.46 (m, 4H, $Ph_2PCH_2C\underline{H}_2N$), 2.90 (pseudo d, $^2J_{HH}$ = 7.8 Hz, 4H, N($C_4\underline{H}_8$)N), 7.31 – 7.39 (m, 12H, *m-/p*-Ph$\underline{H}$), 7.44 (m, 8H, *o*-Ph$\underline{H}$); ^{13}**C {^{1}H}** (125.7 MHz, $CDCl_3$, – 50 °C): δ 25.8 (d, $^1J_{CP}$ = 10.6 Hz, $Ph_2P\underline{C}H_2CH_2N$), 53.1 (s, N($\underline{C}_4H_8$)N), 55.3 (d, $^2J_{CP}$ = 24.4 Hz, $Ph_2PCH_2\underline{C}H_2N$), 129.0 (d, $^3J_{CP}$ = 6.7 Hz, *m*-Ph$\underline{C}$), 129.2 (s, *p*-Ph$\underline{C}$), 133.5 (d, $^2J_{CP}$ = 18.2 Hz, *o*-Ph$\underline{C}$), 138.0 (d, $^1J_{CP}$ = 11.1 Hz, *i*-Ph$\underline{C}$); ^{31}**P {^{1}H}** (161.9 MHz, $CDCl_3$, – 50 °C): δ – 19.1 (s).

MS (ES^+): *m/z* = 511.1 $[MH]^+$.

CHN: Calculated for $C_{32}H_{36}N_2P_2$: C: 75.26; H: 7.12; N: 5.49. Found: C: 74.76; H: 6.52; N: 4.99.

6.3.3 Synthesis of PNE hydrochloride salts

Synthesis of *N*-methylpiperazine-*N'*-ethylene-diphenyl-phosphine dihydrochloride (2.5-1)

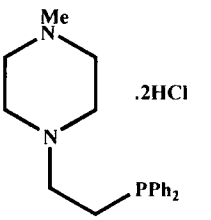

A solution of *N*-methylpiperazine-*N'*-ethylene-diphenylphosphine (2.4-1) (0.473 g, 1.514×10^{-3} mol) in Et_2O (50 cm^3) was treated with excess gaseous HCl resulting in the immediate formation of a white solid. The solid was collected by filtration and following purification by recrystallisation from $CHCl_3/Et_2O$, the product was afforded in near-quantitative yield as a white solid (0.583 g, 95 %).

NMR: ^{1}**H** (499.8 MHz, $CDCl_3$): δ 2.63 (m, 2H, $Ph_2PC\underline{H}_2CH_2N$), 2.89 (s, 3H, $C\underline{H}_3N(CH_2CH_2)_2N$), 3.12 (m, 2H, $Ph_2PCH_2C\underline{H}_2N$), 3.54 – 3.62 (m, 4H, $MeN(C\underline{H}_2CH_2)_2N$ and $MeN(CH_2C\underline{H}_2)_2N$), 3.85 (m, 2H, $MeN(CH_2C\underline{H}_2)_2N$), 4.04 (m, 2H, $MeN(C\underline{H}_2CH_2)_2N$), 7.37 – 7.40 (m, 6H, *m-/p*-Ph$\underline{H}$), 7.44 (m, 4H, *o*-Ph$\underline{H}$), 13.66 (br s, $\nu_{½}$ = 34.4 Hz, 1H, $MeN^+\underline{H}(CH_2CH_2)_2N^+H$), 13.75 (br s, $\nu_{½}$ = 46.9 Hz, 1H, $MeN^+H(CH_2CH_2)_2N^+\underline{H}$); ^{13}**C {^{1}H}** (125.7 MHz, $CDCl_3$): δ 27.7 (d, $^1J_{CP}$ = 17.7 Hz, $Ph_2P\underline{C}H_2CH_2N$), 43.2 (s, $\underline{C}H_3N(CH_2CH_2)_2N$), 48.3 (s, $MeN(CH_2\underline{C}H_2)_2N$), 50.0 (s, $MeN(\underline{C}H_2CH_2)_2N$), 55.1 (d, $^2J_{CP}$ = 29.3 Hz, $Ph_2PCH_2\underline{C}H_2N$), 129.3 (d, $^3J_{CP}$ = 6.7 Hz, *m*-Ph$\underline{C}$), 129.9 (s, *p*-Ph$\underline{C}$), 132.9 (d, $^2J_{CP}$ = 19.6 Hz, *o*-Ph$\underline{C}$), 135.4 (d, $^1J_{CP}$ = 11.9 Hz, *i*-Ph$\underline{C}$); ^{31}**P {^{1}H}** (121.4 MHz, $CDCl_3$) δ – 20.0 (s).

MS (ES^+): *m/z* = 313.2 $[MH]^+$.

CHN: Calculated for $C_{19}H_{27}N_2PCl_2$: C: 59.22; H: 7.08; N: 7.27. Found: C: 59.58; H: 7.11; N: 7.54.

Preparation of morpholine-*N*-ethylene-diphenylphosphine hydrochloride (2.5-2)

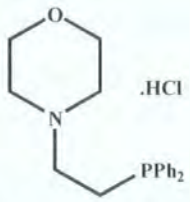

A solution of morpholine-*N*-ethylene-diphenylphosphine (**2.4-2**) (0.356 g, 1.189×10^{-3} mol) in Et_2O (50 cm^3) was treated with excess gaseous HCl resulting in the immediate formation of a white solid. The solid was collected by filtration and following purification by recrystallisation from $CHCl_3/Et_2O$, the desired product was afforded in near-quantitative yield (0.399 g, 91 %). Slow diffusion of Et_2O into a saturated $CHCl_3$ solution of **2.5-2** afforded single crystals suitable for study by X-ray diffraction {Full crystallographic data available in Appendix 1(a)}.

NMR: ^{1}**H** (499.8 MHz, $CDCl_3$): δ 2.67 (m, 2H, $Ph_2PC\underline{H}_2CH_2N$), 2.78 (m, 2H, $N(C\underline{H}_2CH_2)_2O$), 2.99 (m, 2H, $Ph_2PCH_2C\underline{H}_2N$), 3.41 (m, 2H, $N(C\underline{H}_2CH_2)_2O$), 3.90 (m, 2H, $N(CH_2C\underline{H}_2)_2O$), 4.23 (m, 2H, $N(CH_2C\underline{H}_2)_2O$), 7.31 – 7.36 (m, 6H, *m*-/*p*-Ph$\underline{H}$), 7.44 (m, 4H, *o*-Ph$\underline{H}$), 13.19 (br s, $\nu_{½}$ = 25.2 Hz, 1H, NH^+); ^{13}**C** {^{1}**H**} (125.7 MHz, $CDCl_3$): δ 22.1 (d, $^1J_{CP}$ = 16.5 Hz, $Ph_2P\underline{C}H_2CH_2N$), 51.9 (s, $N(\underline{C}H_2CH_2)_2O$), 55.7 (d, $^2J_{CP}$ = 28.7 Hz, $Ph_2PCH_2\underline{C}H_2N$), 63.7 (s, $N(CH_2\underline{C}H_2)_2O$), 129.2 (d, $^3J_{CP}$ = 7.2 Hz, *m*-Ph$\underline{C}$), 129.7 (s, *p*-Ph$\underline{C}$), 132.9 (d, $^3J_{CP}$ = 19.5 Hz, *o*-Ph$\underline{C}$), 135.8 (d, $^1J_{CP}$ = 11.6 Hz, *i*-Ph$\underline{C}$); ^{31}**P** {^{1}**H**} (80.9 MHz, $CDCl_3$): δ – 19.6 (s).

MS (ES^+): *m/z* = 300.2 $[MH - HCl]^+$

CHN: Calculated for $C_{18}H_{23}NOPCl$: C: 64.37; H: 6.92; N: 4.17. Found: C: 64.29; H: 6.87; N: 3.98.

Attempted preparation of thiomorpholine-*N*-ethylene-diphenylphosphine hydrochloride (2.5-3)

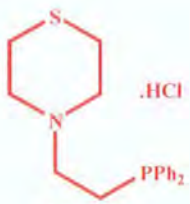

A solution of thiomorpholine-*N*-ethylene-diphenylphosphine (**2.4-3**) (0.182 g, 5.770×10^{-4} mol) in Et_2O (60 cm^3) was treated with excess gaseous HCl resulting in the formation of a white precipitate. The solid was collected by filtration and recrystallised from $CHCl_3/Et_2O$ however, upon analysis, by NMR spectroscopy and mass spectrometry, the presence of the required product was not detected.

Preparation of piperidine-*N*-ethylene-diphenylphosphine hydrochloride (2.5-4)

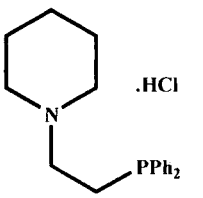

A solution of piperidine-*N*-ethylene-diphenylphosphine (**2.4-4**) (0.220 g, 7.397×10^{-4} mol) in Et_2O (50 cm^3) was treated with excess gaseous HCl resulting in the immediate formation of a white solid. The precipitate was collected by filtration and following recrystallisation from $CHCl_3/Et_2O$, the product was afforded as a white solid (0.230g, 93 %).

NMR: ^{1}**H** (499.8 MHz, $CDCl_3$): δ 1.29 (m, 1H, $N(CH_2CH_2)_2C\underline{H}_2$), 1.64 – 1.77 (m, 3H, $N(CH_2C\underline{H}_2)_2CH_2$ and $N(CH_2CH_2)_2C\underline{H}_2$), 2.11 (m, 2H, $N(CH_2C\underline{H}_2)_2CH_2$), 2.54 (m, 2H, $N(C\underline{H}_2CH_2)_2CH_2$), 2.64 (m, 2H, $Ph_2PC\underline{H}_2CH_2N$), 2.89 (m, 2H, $Ph_2PCH_2C\underline{H}_2N$), 3.38 (m, 2H, $N(C\underline{H}_2CH_2)_2CH_2$), 7.22 – 7.28 (m, 6H, *m-/p*-Ph$\underline{H}$), 7.37 (m, 4H, *o*-Ph$\underline{H}$), 11.95 (br s, $\nu_{½}$ = 23.0 Hz, 1H, $N^+\underline{H}(CH_2CH_2)_2CH_2$); ^{13}**C {^{1}H}** (125.7 MHz, $CDCl_3$): δ 22.2 (s, $N(CH_2CH_2)_2\underline{C}H_2$), 22.4 (d, $^1J_{CP}$ = 12.1 Hz, $Ph_2P\underline{C}H_2CH_2N$), 22.8 (s, $N(CH_2\underline{C}H_2)_2CH_2$), 53.1 (s, $N(\underline{C}H_2CH_2)_2CH_2$), 55.0 (d, $^2J_{CP}$ = 27.3 Hz, $Ph_2PCH_2\underline{C}H_2N$), 129.1 (s, *p*-Ph$\underline{C}$), 129.6 (s, *m*-Ph$\underline{C}$), 132.9 (d, $^2J_{CP}$ = 17.2 Hz, *o*-Ph$\underline{C}$), 135.8 (s, *i*-Ph$\underline{C}$); ^{31}**P {^{1}H}** (81.0 MHz, $CDCl_3$): δ – 19.3 (s).

MS (ES$^+$): *m/z* = 298.3 $[MH–HCl]^+$

CHN: Calculated for $C_{19}H_{25}NPCl$: C: 68.35; H: 7.56; N: 4.20. Found: C: 68.42; H: 7.45; N: 4.37.

Preparation of *N*-methylpiperazine-*N'*-1-methly-ethyl-diphenylphosphine hydrochloride (2.5-5)

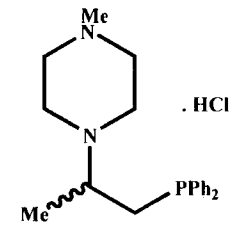

A solution of N-methylpiperazine-N'-1-methyl-ethyl-diphenylphosphine (2.4-6) (0.853 g, 2.60×10^{-3} mol) in diethyl ether was treated with excess gaseous HCl resulting in the immediate formation of a solid. The solid was collected by filtration, and following recrystallisation, the desired product was afforded as a white solid (0.930 g, 98 %). Slow diffusion of Et_2O into a concentrated $CHCl_3$ solution of 2.5-5 afforded crystals suitable for study by X-ray diffraction {Full crystallographic data available in Appendix 1(a)}.

NMR: ^{1}**H** (499.7 MHz, $CDCl_3$): δ 1.05 (d, $^{4}J_{PH}$ = 6.4 Hz, 3H, $Ph_2PCH_2CH(C\underline{H}_3)N$), 1.90 (m, 1H, $N(C_4\underline{H}_8)N$), 2.10 – 2.35 (m, 2H, $N(C_4\underline{H}_8)N$), 2.45 – 2.85 (m, 6H, $N(C_4\underline{H}_8)N$, $Ph_2PC\underline{H}_2CH(CH_3)N$), 2.95 – 3.34 (m, 5H, $N(C_4\underline{H}_8)N$, $C\underline{H}_3N(C_4H_8)N$, and $Ph_2PCH_2C\underline{H}(CH_3)N$), 7.18 – 7.32 (m, 8H, *o*-/*m*-Ph$\underline{H}$), 7.41 (s, 2H, *p*-Ph$\underline{H}$), 12.27 (br s, $\nu_{½}$ = 37.5 Hz, 1H, N$\underline{H}^{+}$); ^{1}**H** (499.7 MHz, $CDCl_3$, –50 °C): δ 1.08 (s, 3H, $CH_2CH(C\underline{H}_3)N$), 1.86 – 2.09 (m, 2H, $Ph_2PC\underline{H}_2CH(CH_3)N$ and $N(C_4\underline{H}_8)N$), 2.32 – 2.88 (m, 8H, $Ph_2PC\underline{H}_2CH(CH_3)N$, $N(C_4\underline{H}_8)N$, $N(C_4H_8)NC\underline{H}_3$, and $Ph_2PCH_2C\underline{H}(CH_3)N$), 3.07 (m, 3H, $N(C_4\underline{H}_8)N$), 3.34 (m, 1H, $N(C_4\underline{H}_8)N$), 7.26 – 7.41 (m, 8H, *o*-/*m*-Ph$\underline{H}$), 7.50 (s, 2H, *p*-Ph$\underline{H}$), 11.72 (br s, $\nu_{½}$ = 33.3 Hz, 1H, N$\underline{H}^{+}$); ^{13}**C {^{1}H}** (100.6 MHz, $CDCl_3$): δ 14.4 (d, $^{3}J_{CP}$ = 8.0 Hz, $CH_2CH(\underline{C}H_3)N$), 31.9 (s, $Ph_2P\underline{C}H_2CH(CH_3)N$), 42.7 (s, $N(C_4H_8)N\underline{C}H_3$), 46.3 (s, $N(\underline{C}H_2CH_2)_2NCH_3$), 52.0 (s, $N(CH_2\underline{C}H_2)_2NCH_3$), 56.9 (s, $Ph_2PCH_2\underline{C}H(CH_3)N$), 127.4 (d, $^{3}J_{CP}$ = 7.5 Hz, *m*-Ph$\underline{C}$), 127.6 (d, $^{3}J_{CP}$ = 7.5 Hz, *m*-Ph$\underline{C}$), 127.7 (s, *p*-Ph$\underline{C}$), 127.9 (s, *p*-Ph$\underline{C}$), 131.5 (d, $^{2}J_{CP}$ = 19.5 Hz, *o*-Ph$\underline{C}$), 132.1 (d, $^{2}J_{CP}$ = 19.5 Hz, *o*-Ph$\underline{C}$), 137.5 (s, *i*-Ph$\underline{C}$); ^{31}**P {^{1}H}** (121.4 MHz, $CDCl_3$): δ – 17.3 (s);
MS (ES^{+}, MeOH): *m/z* = 343.4 $[M–Cl + Me]^{+}$.
CHN: Calculated for $C_{20}H_{28}N_2PCl$ C: 66.19; H: 7.79; N: 7.72. Found: C: 66.36; H: 7.76; N: 7.92).

Preparation of piperazine-*N,N'*-diethylene-tetraphenyldiphosphine dihydrochloride (2.5-6)

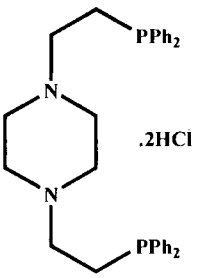

A solution of piperazine-*N,N'*-diethyltetraphenyldiphosphine (**2.4-7**) (0.159 g, 3.114×10^{-4} mol) in Et_2O (100 cm^3) was treated with excess gaseous HCl resulting in the immediate formation of a white solid. The precipitate was collected by filtration and following recrystallisation from $CHCl_3/Et_2O$, the target product was afforded as a white solid in near-quantitative yield (0.160 g, 88 %).

NMR: ^{1}**H** (299.9 MHz, $CDCl_3$): δ 2.63 (m, 4H, $N(C_4\underline{H}_8)N$); 3.09 (m, 4H, $Ph_2PC\underline{H}_2CH_2N$), 3.55 (m, 4H, $Ph_2PCH_2C\underline{H}_2N$), 3.83 (m, 4H, $N(C_4\underline{H}_8)N$), 7.30 – 7.65 (*o-/m-/p*-Ph$\underline{H}$), 7.77 (br s, $\nu_{½}$ = 29.4 Hz, $N\underline{H}^+$) ; ^{13}**C {^{1}H}** (125.67 MHz, $CDCl_3$): δ 23.0 (d, $^1J_{CP}$ = 17.3 Hz, $Ph_2P\underline{C}H_2CH_2N$), 48.7 (s, $N(\underline{C}_4H_8)N$), 55.0 (d, $^2J_{CP}$ = 28.4 Hz, $Ph_2PCH_2\underline{C}H_2N$), 129.2 (d, $^3J_{CP}$ = 6.7, *m*-Ph$\underline{C}$), 129.8 (s, *p*-Ph$\underline{C}$), 132.9 (d, $^2J_{CP}$ = 19.1 Hz, *o*-Ph$\underline{C}$), 135.8 (d, $^1J_{CP}$ = 12.9 Hz, *i*-Ph$\underline{C}$); ^{31}**P {^{1}H}** (80.9 MHz, $CDCl_3$): δ – 19.9 (br s, $\nu_{½}$ = 20.9 Hz).

MS (ES^+): *m/z* = 511.3 $[MH–2HCl]^+$.

CHN: Calculated for $C_{32}H_{38}N_2P_2Cl_2$: C: 65.86; H: 6.58; N: 4.80. Found: C: 63.98; H: 6.32; N: 4.09.

6.3.4 Synthesis of S=PNE ligand derivatives

Synthesis of *N*-methylpiperazine-*N'*-ethylene-diphenyl-phosphine sulphide (2.6-1)

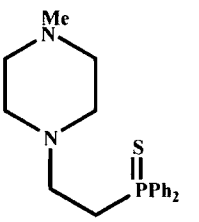

To a solution of *N*-methylpiperazine-*N'*-ethylene-diphenylphosphine (**2.4-1**) (0.219 g, 7.010×10^{-4} mol) in CH_2Cl_2 (10cm^3) was added S_8 (0.022 g, 7.010×10^{-4} mol) as a solid under a flow of N_2 and the resulting solution allowed to stir at room temperature for 2h. Subsequent *in situ* analysis by ^{31}P NMR spectroscopy showed only partial conversion to the required product with 32% (by integration) of the free phosphine present. In order to achieve complete oxidation of the phosphine, a further portion of S_8 (0.007 g, 2.183×10^{-4} mol) was added to the reaction vessel and the mixture allowed to stir at room temperature for 2h when analysis by ^{31}P NMR spectroscopy revealed complete conversion to the target species. The CH_2Cl_2 was removed under vacuum and crystallisation from CH_2Cl_2/hexane afforded the desired product as a pale yellow solid (0.203 g, 84 %).

NMR: ^{1}**H** ($CDCl_3$, 499.8 MHz, – 50 °C): δ 2.02 (m, 2H, MeN($CH_2\underline{CH_2}$)$_2$N), 2.16 (m, 2H, MeN($\underline{CH_2}CH_2$)$_2$N), 2.27 (s, 3H, $\underline{CH_3}$N(CH_2CH_2)$_2$N), 2.64 – 2.70 (m, 4H, $Ph_2PCH_2\underline{CH_2}N$ and MeN($\underline{CH_2}CH_2$)$_2$N), 2.74 – 2.83 (m, 4H, $Ph_2PCH_2\underline{CH_2}N$ and MeN($CH_2\underline{CH_2}$)$_2$N), 7.40 – 7.49 (m, 6H, *m-/p*-Ph$\underline{H}$), 7.79 (m, 4H, *o*-Ph$\underline{H}$); ^{13}**C {^{1}H}** ($CDCl_3$, 125.7 MHz): δ 29.0 (d, $^1J_{CP}$ = 57.0 Hz, $Ph_2P\underline{C}H_2CH_2N$), 44.8 (s, $\underline{C}H_3N(C_4H_8)N$), 50.5 (s, $Ph_2PCH_2\underline{C}H_2N$), 51.5 (s, MeN($\underline{C}H_2CH_2$)$_2$N), 53.8 (s, MeN($CH_2\underline{C}H_2$)$_2$N), 127.6 (d, $^3J_{CP}$ = 12.5 Hz, *m*-Ph$\underline{C}$), 130.0 (d, $^2J_{CP}$ = 10.3 Hz, *o*-Ph$\underline{C}$), 130.4 (d, $^4J_{CP}$ = 2.9 Hz, *p*-Ph$\underline{C}$), 132.0 (d, $^1J_{CP}$ = 81.2 Hz, *i*-Ph$\underline{C}$); ^{31}**P {^{1}H}** ($CDCl_3$, 161.9 MHz): δ + 41.4 (s).

MS (ES$^+$): *m/z* = 345.2 $[MH]^+$.

CHN: Calculated for $C_{19}H_{25}N_2PS$: C: 66.24; H: 7.33; N: 8.13. Found: C: 66.17; H: 7.15; N: 8.21.

Preparation of morpholine-*N*-ethylene-diphenylphosphine sulphide (2.6-2)

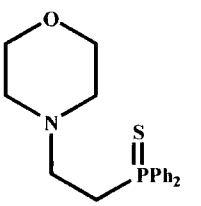

To a solution of morpholine-*N*-ethylene-diphenylphosphine (**2.4-2**) (0.188 g, 6.280×10^{-4} mol) in CH_2Cl_2 (10 cm^3) was added S_8 (0.020 g, 6.280×10^{-4} mol) and the resulting mixture allowed to stir at room temperature for 4h. Following *in situ* analysis by ^{31}P NMR spectroscopy it was shown that only 55% of the required product was present, therefore a further portion of S_8 (0.009 g, 2.806×10^{-4} mol) was added under a flow of N_2 and the stirring continued for 2h when analysis by ^{31}P NMR spectroscopy revealed complete conversion to the target compound. The CH_2Cl_2 was removed under vacuum and crystallisation from CH_2Cl_2/hexane afforded the desired product as a pale yellow solid (0.169 g, 81 %).

NMR: ^{1}**H** (499.8 MHz, $CDCl_3$): δ 2.42 (m, 4H, $N(C\underline{H}_2CH_2)_2O$), 2.68 (m, 2H, $Ph_2PC\underline{H}_2CH_2N$), 2.75 (m, 2H, $Ph_2PCH_2C\underline{H}_2N$), 3.58 (m, 4H, $N(CH_2C\underline{H}_2)_2O$), 7.43 – 7.53 (m, 6H, *m*-/*p*-Ph<u>H</u>), 7.84 (m, 4H, *o*-Ph<u>H</u>); ^{13}**C** $\{^{1}$**H**$\}$ (125.7 MHz, $CDCl_3$): δ 30.0 (d, $^{1}J_{CP}$ = 56.6 Hz, $Ph_2P\underline{C}H_2CH_2N$), 52.3 (s, $Ph_2PCH_2\underline{C}H_2N$), 53.5 (s, $N(\underline{C}H_2CH_2)_2O$), 67.0 (s, $N(CH_2\underline{C}H_2)_2O$), 128.9 (d, $^{3}J_{CP}$ = 11.9 Hz, *m*-Ph<u>C</u>), 131.2 (d, $^{2}J_{CP}$ = 10.1 Hz, *o*-Ph<u>C</u>), 131.8 (d, $^{4}J_{CP}$ = 2.9 Hz, *p*-Ph<u>C</u>), 133.1 (d, $^{1}J_{CP}$ = 81.1 Hz, *i*-Ph<u>C</u>); ^{31}**P** $\{^{1}$**H**$\}$ (161.9 MHz, $CDCl_3$): δ + 41.5 (s).

MS (ES^+): *m/z* = 332.2 $[MH]^+$.

CHN: Calculated for $C_{18}H_{22}NOPS$: C: 65.22; H: 6.70; N: 4.23. Found: C: 65.06; H: 6.75; N: 4.22.

Preparation of thiomorpholine-*N*-ethylene-diphenylphosphine sulphide (2.6-3)

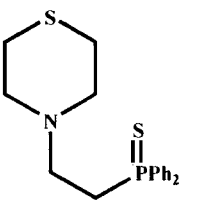

To a solution of thiomorpholine-*N*-ethylene-diphenylphosphine (**2.4-3**) (0.180 g, 5.706×10^{-4} mol) in CH_2Cl_2 (10 cm^3) was added S_8 (0.018 g, 5.706×10^{-4} mol) under a flow of N_2 and the resulting mixture allowed to stir at room temperature for 4h. Analysis by ^{31}P NMR spectroscopy showed complete conversion to the required product without the need for a second portion of S_8 therefore the solvent was removed under vacuum and crystallisation from CH_2Cl_2/hexane afforded the desired product as a pale yellow solid (0.163 g, 82 %).

NMR: ^{1}**H** (499.8 MHz, $CDCl_3$): δ 2.51 (m, 4H, $N(CH_2C\underline{H}_2)_2S$), 2.62 – 2.70 (m, 6H, $Ph_2PC\underline{H}_2CH_2N$ and $N(C\underline{H}_2CH_2)_2S$), 2.79 (m, 2H, $Ph_2PCH_2C\underline{H}_2N$), 7.42 – 7.52 (m, 6H, *m*-/*p*-Ph<u>H</u>), 7.83 (m, 4H, *o*-Ph<u>H</u>); ^{13}**C {^{1}H}** (125.7 MHz, $CDCl_3$): δ 28.0 (s, $N(CH_2\underline{C}H_2)_2S$), 29.7 (d, $^{1}J_{CP}$ = 56.0 Hz, $Ph_2P\underline{C}H_2CH_2N$), 52.7 (s, $Ph_2PCH_2\underline{C}H_2N$), 54.9 (s, $N(\underline{C}H_2CH_2)_2S$), 128.9 (d, $^{3}J_{CP}$ = 12.1 Hz, *m*-Ph<u>C</u>), 131.2 (d, $^{2}J_{CP}$ = 10.2 Hz, *o*-Ph<u>C</u>), 131.7 (d, $^{4}J_{CP}$ = 2.9 Hz, *p*-Ph<u>C</u>), 133.2 (d, $^{1}J_{CP}$ = 80.9 Hz, *i*-Ph<u>C</u>); ^{31}**P {^{1}H}** (161.9 MHz, $CDCl_3$): δ + 41.6 (s).

MS (ES^+): *m/z* = 348.1 $[MH]^+$.

CHN: Calculated for $C_{18}H_{22}NS_2P$: C: 62.21; H: 6.39; N: 4.03. Found: C: 62.29; H: 6.48; N: 3.91.

Preparation of piperidine-*N*-ethylene-diphenylphosphine sulphide (2.6-4)

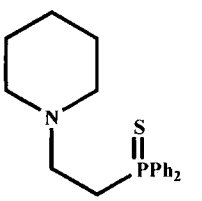

To a solution of piperidine-*N*-ethylene-diphenylphosphine (**2.4-4**) (0.106 g, 3.564×10^{-4} mol) in CH_2Cl_2 (10 cm^3) was added S_8 (0.011 g, 3.564×10^{-4} mol) as a solid and the resulting mixture allowed to stir at room temperature for 2h. Following *in situ* analysis by ^{31}P NMR spectroscopy, it was found that the required product was only present in 91% relative to the parent phosphine (by integration). A further portion of S_8 (0.002 g, 6.236×10^{-5} mol) was added under a flow of nitrogen and the stirring continued for a further 2h when analysis by ^{31}P NMR spectroscopy revealed complete conversion to the required product. The CH_2Cl_2 was removed under vacuum and crystallisation from CH_2Cl_2/hexane afforded the product as a light orange solid (0.092 g, 79 %).

NMR: ^{1}**H** (499.8 MHz, $CDCl_3$): δ 1.37 (m, 2H, $N(CH_2CH_2)_2C\underline{H}_2$), 1.49 (m, 2H, $N(CH_2C\underline{H}_2)_2CH_2$), 2.37 (m, 2H, $N(C\underline{H}_2CH_2)_2CH_2$), 2.63 – 2.74 (m, 4H, $Ph_2PC\underline{H}_2CH_2N$ and $Ph_2PCH_2C\underline{H}_2N$), 7.39 – 7.51 (m, 6H, *m*-/*p*-PhH), 7.83 (m, 4H, *o*-PhH); ^{13}**C {^{1}H}** (125.7 MHz, $CDCl_3$): δ 24.4 (s, $N(CH_2CH_2)_2\underline{C}H_2$), 26.0 (s, $N(CH_2\underline{C}H_2)_2CH_2$), 30.1 (d, $^{1}J_{CP}$ = 56.2 Hz, $Ph_2P\underline{C}H_2CH_2N$), 52.6 (s, $Ph_2PCH_2\underline{C}H_2N$), 54.5 (s, $N(\underline{C}H_2CH_2)_2CH_2$), 128.9 (d, $^{3}J_{CP}$ = 11.9 Hz, *m*-Ph<u>C</u>), 131.2 (d, $^{2}J_{CP}$ = 10.1 Hz, *o*-Ph<u>C</u>), 131.7 (d, $^{4}J_{CP}$ = 2.9 Hz, *p*-Ph<u>C</u>), 133.1 (d, $^{1}J_{CP}$ = 80.6 Hz, *i*-Ph<u>C</u>); ^{31}**P {^{1}H}** (161.9 MHz, $CDCl_3$): δ + 41.5 (s).

MS (ES^+): *m/z* = 330.1 $[MH]^+$.

CHN: Calculated for $C_{19}H_{24}NSP$: C: 69.26; H: 7.36; N: 4.25. Found: C: 69.36; H: 7.47; N: 4.06.

6.3.5 Attempted synthesis of aminophosphine-containing PNE ligands

Attempted preparation of *N*-methylpiperazine-*N'*-ethylene-*bis*(diisopropylamino)phosphine (2.7-1)

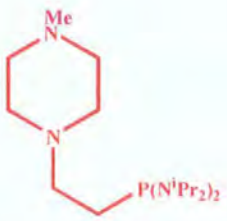

A 100 cm^3 three-neck round bottom flask fitted with a reflux condenser was charged with *bis*(diisopropylamino)vinylphosphine (**2.3-2**) (0.327 g, 1.265×10^{-3} mol) in THF (60 cm^3). Under a flow of nitrogen, *N*-methylpiperazine (0.15 cm^3, 1.353×10^{-3} mol) and a catalytic quantity of $NaNH_2$ (1.0 cm^3 of a suspension in toluene) were added to the main reaction vessel and the resulting mixture heated at reflux for 14h. Following cooling of the reaction mixture to room temperature, the $NaNH_2$ was quenched by the addition of an aqueous solution of NH_4Cl (50 cm^3, 10% w/v, degassed) and the resulting solution extracted with CH_2Cl_2 (3×30 cm^3). The organic fractions were combined, dried over $MgSO_4$ and following removal of the drying agent by filtration, the solvent was removed *in vacuo* to afford a light orange oil. However subsequent analyses of the product by multinuclear NMR spectroscopy and mass spectrometry failed to demonstrate the presence of the expected product.

Attempted preparation of *N*-methylpiperazine-*N'*-ethylene-*bis*(diisopropylamino)phosphine sulphide (2.7-2)

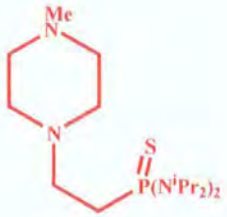

The attempted preparation of *N*-methylpiperazine-*N'*-ethylene-*bis*(diisopropylamino)phosphine sulphide (**2.7-2**) was analogous to that of (**2.7-1**) employing *bis*(diisopropylamino)vinylphosphine sulphide (**2.3-5**) (0.100 g, 3.442×10^{-4} mol) and *N*-methylpiperazine (0.04 cm^3, 3.442×10^{-4} mol) in THF solution (30 cm^3). Isolation of the reaction product afforded an orange oil, however this was shown by multinuclear NMR spectroscopy and mass spectrometry not to be the desired species.

Attempted preparation of *N*-methylpiperazine-*N'*-ethylene-phenyl(diisopropylamino)phosphine (2.7-3)

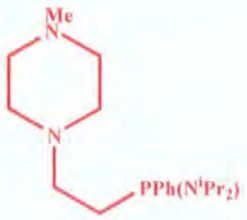

The attempted preparation of *N*-methylpiperazine-*N'*-ethylene-phenyl(diisopropylamino)phosphine (**2.7-3**) was analogous to that of (**2.7-1**) employing diisopropylaminophenylvinylphosphine **(2.3-3)** (0.132 g, 5.609×10^{-4} mol) and *N*-methylpiperazine (0.07 cm^3, 6.316×10^{-4} mol) in THF solution (40 cm^3). Isolation of the reaction product afforded a colourless oil, however this was shown by multinuclear NMR spectroscopy and mass spectrometry not to be the desired species.

6.3.6 Synthesis of Se=PNE ligand derivatives

Synthesis of *N*-methylpiperazine-*N'*-ethylene-diphenylphosphine selenide (2.8-1)

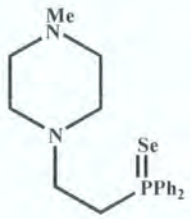

In a glove box, a Young's tap NMR tube was charged with *N*-methylpiperazine-*N'*-ethylene-diphenylphosphine (**2.4-1**) (0.162 g, 5.185×10^{-4} mol) and grey Se (0.410 g, 5.193×10^{-3} mol) and the tube sealed transferred to a Schlenk line. $CDCl_3$ (0.6 cm^3) was added, the tube sealed and the mixture heated gently to 50 °C for 0.5h, when analysis by ^{31}P NMR spectroscopy showed complete conversion to the required product. The excess unreacted selenium was removed by filtration under air and the $CDCl_3$ removed *in vacuo*. The product was recrystallised by CH_2Cl_2/hexane affording a waxy orange solid (0.189 g, 93 %).

NMR: ^{1}H ($CDCl_3$, 499.8 MHz, – 50 °C): δ 1.90 (m, 2H, MeN($C_4\underline{H}_8$)N), 2.04 (m, 2H, MeN($C_4\underline{H}_8$)N), 2.15 (s, 3H, $C\underline{H}_3N(C_4H_8)N$), 2.15 – 2.78 (m, 8H, $Ph_2PC\underline{H}_2CH_2N$, $Ph_2PCH_2C\underline{H}_2N$ and MeN($C_4\underline{H}_8$)N), 7.28 – 7.42 (m, 6H, *m*-/*p*-Ph$\underline{H}$), 7.69 (m, 4H, *o*-Ph$\underline{H}$); **^{13}C {^{1}H}** ($CDCl_3$, 100.6 MHz): δ 28.8 (d, $^1J_{CP}$ = 49.8 Hz, $Ph_2P\underline{C}H_2CH_2N$), 44.9 (s, $\underline{C}H_3N(C_4H_8)N$), 51.3 (s, $Ph_2PCH_2\underline{C}H_2N$), 51.7 (s, MeN($\underline{C}_4H_8$)N), 53.9 (s, MeN($\underline{C}_4H_8$)N), 127.6 (d, $^3J_{CP}$ = 12.4 Hz, *m*-Ph$\underline{C}$), 130.4 (s, *p*-Ph$\underline{C}$), 130.5 (d, $^2J_{CP}$ = 10.3 Hz, *o*-Ph$\underline{C}$), 130.7 (d, $^1J_{CP}$ = 73.1 Hz, *i*-Ph$\underline{C}$); **^{31}P {^{1}H}** ($CDCl_3$, 121.4 MHz): δ + 32.3 (s + sat., $^1J_{PSe}$ = 726 Hz).

MS (ES$^+$): *m/z* = 392.2 $[MH]^+$.

Preparation of morpholine-*N*-ethylene-diphenylphosphine selenide (2.8-2)

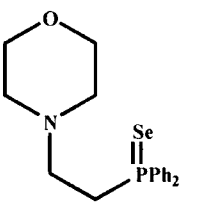

The synthesis of morpholine-*N*-ethylene-diphenylphosphine selenide (**2.8-2**) was analogous to that of **2.8-1** and employed morpholine-*N*-ethylene-diphenylphosphine (**2.4-2**) (0.145 g, 4.844×10^{-4} mol) and grey Se (0.385 g, 4.876×10^{-3} mol) in $CDCl_3$. Following recrystallisation from CH_2Cl_2/hexane, the product was afforded as an orange waxy solid (0.174 g, 95 %).

NMR: ^{1}**H** (499.8 MHz, $CDCl_3$): δ 2.40 (m, 4H, $N(C\underline{H}_2CH_2)_2O$), 2.69 – 2.84 (m, 4H, $Ph_2PC\underline{H}_2CH_2N$ and $Ph_2PCH_2C\underline{H}_2N$), 3.54 (m, 4H, $N(CH_2C\underline{H}_2)_2O$), 7.41 – 7.50 (m, 6H, *m*-/*p*-Ph<u>H</u>), 7.83 (m, 4H, *o*-Ph<u>H</u>); ^{13}**C** $\{^{1}$**H**$\}$ (125.7 MHz, $CDCl_3$): δ 29.8 (d, $^{1}J_{CP}$ = 49.9 Hz, $Ph_2P\underline{C}H_2CH_2N$), 53.1 (s, $Ph_2PCH_2\underline{C}H_2N$), 53.6 (s, $N(\underline{C}H_2CH_2)_2O$), 67.0 (s, $N(CH_2\underline{C}H_2)_2O$), 128.9 (d, $^{3}J_{CP}$ = 11.9 Hz, *m*-Ph<u>C</u>), 131.7 (d, $^{1}J_{CP}$ = 10.6 Hz, *o*-Ph<u>C</u>), 131.8 (d, $^{4}J_{CP}$ = 2.9 Hz, *p*-Ph<u>C</u>), 131.9 (d, $^{1}J_{CP}$ = 72.9 Hz, *i*-Ph<u>C</u>); ^{31}**P** $\{^{1}$**H**$\}$ (121.4 MHz, $CDCl_3$): δ + 32.4 (s, Se satellites, $^{1}J_{PSe}$ = 727 Hz).
MS (ES^+): *m/z* = 380.0 $[MH]^+$.

Preparation of thiomorpholine-*N*-ethylene-diphenylphosphine selenide (2.8-3)

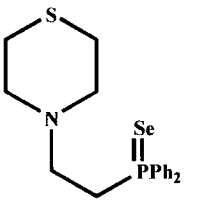

The synthesis of thiomorpholine-*N*-ethylene-diphenylphosphine selenide (**2.8-3**) was analogous to that of **2.8-1** and employed thiomorpholine-*N*-ethylene-diphenylphosphine (**2.4-3**) (0.172 g, 5.453×10^{-4} mol) and grey Se (0.440 g, 5.572×10^{-3} mol) in $CDCl_3$. Following recrystallisation from CH_2Cl_2/hexane, the product was afforded as an orange waxy solid (0.123 g, 93 %).

NMR: ^{1}**H** (499.8 MHz, $CDCl_3$): δ 2.45 (m, 4H, $N(CH_2C\underline{H}_2)_2S$), 2.64 (m, 4H, $N(C\underline{H}_2CH_2)_2S$), 2.72 – 2.83 (m, 4H, $Ph_2PC\underline{H}_2CH_2N$ and $Ph_2PCH_2C\underline{H}_2N$), 7.36 – 7.48 (m, 6H, *m*-/*p*-Ph<u>H</u>), 7.80 (m, 4H, *o*-Ph<u>H</u>); ^{13}**C** $\{^{1}$**H**$\}$ (125.7 MHz, $CDCl_3$): δ 27.9 (s, $N(CH_2\underline{C}H_2)_2S$), 29.4 (d, $^{1}J_{CP}$ = 48.9 Hz, $Ph_2\underline{C}H_2CH_2N$), 53.5 (s, $Ph_2PCH_2\underline{C}H_2N$), 54.9 (s, $N(\underline{C}H_2CH_2)_2S$), 128.9 (d, $^{3}J_{CP}$ = 11.9 Hz, *m*-Ph<u>C</u>), 131.7 (d, $^{2}J_{CP}$ = 10.5 Hz, *o*-Ph<u>C</u>),

131.8 (d, $^4J_{CP}$ = 2.9 Hz, *p*-PhC), 131.9 (d, $^1J_{CP}$ = 72.8 Hz, *i*-PhC); **^{31}P {^{1}H}** (121.4 MHz, $CDCl_3$): δ + 32.8 (s + Se satellites, $^1J_{PSe}$ = 726 Hz).

MS (ES$^+$): *m/z* = 395.9 $[MH]^+$.

Preparation of piperidine-*N*-ethylene-diphenylphosphine selenide (2.8-4)

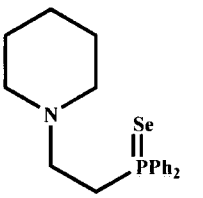

The synthesis of piperidine-*N*-ethylene-diphenylphosphine selenide (**2.8-4**) was analogous to that of **2.8-1** and employed piperidine-*N*-ethylene-diphenylphosphine (**2.4-4**) (0.104 g, 3.497×10^{-4} mol) and grey Se (0.290 g, 3.673×10^{-3} mol) in $CDCl_3$. Following recrystallisation from CH_2Cl_2/hexane, the product was afforded as an orange waxy solid (0.123 g, 93 %).

NMR: ^{1}H (499.8 MHz, $CDCl_3$): δ 1.36 (m, 2H, $N(CH_2CH_2)_2CH_2$), 1.47 (m, 4H, $N(CH_2CH_2)_2CH_2$), 2.35 (m, 4H, $N(CH_2CH_2)_2CH_2$), 2.67 (m, 2H, $Ph_2PCH_2CH_2N$), 2.79 (m, 2H, $Ph_2PCH_2CH_2N$), 7.38 – 7.47 (m, 6H, *m*-/*p*-PhH), 7.82 (m, 4H, *o*-PhH); **^{13}C {^{1}H}** (125.7 MHz, $CDCl_3$): δ 24.4 (s, $N(CH_2CH_2)_2CH_2$), 26.0 (s, $N(CH_2CH_2)_2CH_2$), 29.9 (d, $^1J_{CP}$ = 49.4 Hz, $Ph_2PCH_2CH_2N$), 53.3 (s, $Ph_2PCH_2CH_2N$), 54.5 (s, $N(CH_2CH_2)_2CH_2$), 128.8 (d, $^3J_{CP}$ = 12.1 Hz, *m*-PhC), 131.7 (d, $^2J_{CP}$ = 10.6 Hz, *o*-PhC), 131.8 (s, *p*-PhC), 131.9 (d, $^1J_{CP}$ = 72.4 Hz, *i*-PhC); **^{31}P {^{1}H}** (121.4 MHz, $CDCl_3$): δ + 32.2 (s + Se satellites, $^1J_{PSe}$ = 725 Hz).

MS (ES$^+$): *m/z* = 378.2 $[MH]^+$.

Preparation of *N*-phenylpiperazine-*N'*-ethylene-diphenyl-phosphine selenide (2.8-5)

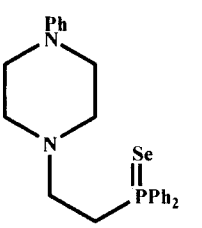

The synthesis of *N*-phenylpiperazine-*N'*-ethylene-diphenylphosphine selenide (**2.8-5**) was analogous to that of **2.8-1** and employed *N*-phenylpiperazine-*N'*-ethylene-diphenylphosphine (**2.4-5**) (0.166 g, 4.433×10^{-4} mol) and grey Se (0.352 g, 4.458×10^{-3} mol) in $CDCl_3$. Following recrystallisation from CH_2Cl_2/hexane, the product was afforded as an orange waxy solid (0.180 g, 90 %).

NMR: ^{1}**H:** (499.8 MHz, $CDCl_3$): δ 2.60 (pseudo t, $^{3}J_{HH}$ = 5.0 Hz, 4H, $N(C\underline{H}_2CH_2)_2NPh$), 2.81 – 2.87 (m, 4H, $Ph_2PC\underline{H}_2CH_2N$ and $Ph_2PCH_2C\underline{H}_2N$), 3.09 (pseudo t, $^{3}J_{HH}$ = 5.0 Hz, 4H, $N(CH_2C\underline{H}_2)_2NPh$), 6.86 (m, 1H, *p*-Ph$\underline{H}$), 6.89 (m, 2H, *m*-Ph$\underline{H}$), 7.26 (m, 2H, *o*-Ph$\underline{H}$), 7.44 – 7.52 (m, 6H, *m*-/*p*-Ph$\underline{H}${P}), 7.87 (m, 4H, *o*-Ph$\underline{H}${P}); **^{13}C {^{1}H}** (125.7 MHz, $CDCl_3$): δ 30.0 (d, $^{1}J_{CP}$ = 49.4 Hz, $Ph_2P\underline{C}H_2CH_2N$), 49.2 (s, $N(CH_2\underline{C}H_2)_2NPh$), 52.7 (s, $Ph_2PCH_2\underline{C}H_2N$), 53.2 (s, $N(\underline{C}H_2CH_2)_2NPh$), 116.3 (s, *m*-Ph$\underline{C}$), 120.0 (s, *p*-Ph$\underline{C}$), 128.9 (d, $^{3}J_{CP}$ = 11.9 Hz, *m*-Ph$\underline{C}${P}), 129.3 (s, *o*-Ph$\underline{C}$), 131.7 (d, $^{2}J_{CP}$ = 10.6 Hz, *o*-Ph$\underline{C}${P}), 131.8 (d, $^{1}J_{CP}$ = 72.6 Hz, *i*-PhC{$\underline{P}$}), 131.9 (d, $^{4}J_{CP}$ = 3.4 Hz, *p*-Ph$\underline{C}${P}), 151.4 (s, *i*-Ph$\underline{C}$); **^{31}P {^{1}H}** (121.4 MHz, $CDCl_3$): δ 32.6 (s + Se satellites, $^{1}J_{PSe}$ = 725 Hz).

MS (ES^{+}): *m/z* = 455.2 $[MH]^{+}$.

Preparation of *N*-methylpiperazine-*N'*-1-methyl-ethyl-diphenyl-phosphine selenide (2.8-6)

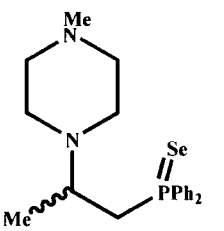

The synthesis of *N*-methylpiperazine-*N'*-1-methyl-ethyl-diphenylphosphine selenide (**2.8-6**) was analogous to that of **2.8-1** and employed *N*-methylpiperazine-*N'*-1-methyl-ethyl-diphenylphosphine (**2.4-6**) (0.110 g, 3.359×10^{-4} mol) and grey Se (0.263 g, 3.331×10^{-3} mol) in $CDCl_3$. Following recrystallisation from CH_2Cl_2/hexane, the product was afforded as an orange waxy solid (0.124 g, 91 %).

NMR: ^{1}**H** (499.8 MHz, $CDCl_3$, – 50 °C): δ 0.66 – 0.78 (m, 1H, $N(C_4\underline{H}_8)NMe$), 0.90 (d, $^{4}J_{PH}$ = 5.5 Hz, 3H, $Ph_2PCH_2CH(C\underline{H}_3)N$), 1.64 – 1.74 (m, 1H, $N(C_4\underline{H}_8)NMe$), 1.99 (s, 3H, $N(C_4H_8)NC\underline{H}_3$), 2.04 – 2.18 (m, 2H, $N(C_4\underline{H}_8)NMe$), 2.22 – 2.41 (m, 3H, $Ph_2PC\underline{H}_2CH(Me)N$ and $N(C_4\underline{H}_8)NMe$), 2.43 – 2.62 (m, 2H, $N(C_4\underline{H}_8)NMe$), 2.92 (m, 1H, $Ph_2PC\underline{H}_2CH(Me)N$), 3.49 (m, 1H, $Ph_2PCH_2C\underline{H}(Me)N$), 7.28 – 7.43 (m, 6H, *m*-/*p*-Ph$\underline{H}$), 7.68 (m, 2H, *o*-Ph$\underline{H}$), 7.78 (m, 2H, *o*-Ph$\underline{H}$); **^{13}C {^{1}H}** (125.7 MHz, $CDCl_3$, – 50 °C): δ 15.2 (d, $^{3}J_{CP}$ = 10.6 Hz, $Ph_2PCH_2CH(\underline{C}H_3)N$), 34.6 (d, $^{1}J_{CP}$ = 50.1 Hz, $Ph_2P\underline{C}H_2CH(Me)N$), 45.0 (s, $N(\underline{C}_4H_8)NMe$), 50.2 ($N(\underline{C}_4H_8)NMe$), 53.9 (s, $N(\underline{C}_4H_8)NMe$), 54.8 (s, $N(\underline{C}_4H_8)NMe$), 55.2 (s, $Ph_2PCH_2\underline{C}H(Me)N$), 128.7 (d, $^{3}J_{CP}$ =

11.7 Hz, *m*-PhC), 129.0 (d, $^{3}J_{CP}$ = 11.7 Hz, *m*-PhC), 131.4 (d, $^{2}J_{CP}$ = 10.6 Hz, *o*-PhC), 131.5 (d, $^{1}J_{CP}$ = 74.4 Hz, *i*-PhC), 131.6 (s, *p*-PhC), 131.8 (s, *p*-PhC), 132.0 (d, $^{2}J_{CP}$ = 10.6 Hz, *o*-PhC), 133.4 (d, $^{1}J_{CP}$ = 74.4 Hz, *i*-PhC); **^{31}P {^{1}H}** (121.4 MHz, $CDCl_3$): δ + 34.3 (s + sats., $^{1}J_{PSe}$ = 727 Hz).

MS (ES$^+$): *m/z* = 407.3 $[MH]^+$.

Preparation of piperazine-*N,N′*-diethylene- tetraphenyldiphosphine diselenide (2.8-7)

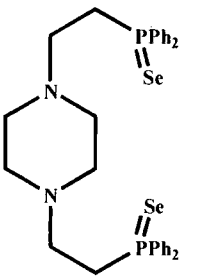

The synthesis of piperazine-*N,N′*-diethylene-tetraphenyldiphosphine diselenide **(2.8-7)** was analogous to that of **2.8-1** and employed piperazine-*N,N′*-diethylene-tetraphenyldiphosphine (**2.4-7**) (0.145 g, 2.840×10^{-4} mol) and grey Se (0.450 g, 5.699×10^{-3} mol) in $CDCl_3$. Following recrystallisation from CH_2Cl_2/hexane, the product was afforded as an orange waxy solid (0.169 g, 89 %).

NMR: ^{1}H (499.8 MHz, $CDCl_3$): δ 2.22 – 2.46 (m, 8H, N(C_4H_8)N), 2.65 – 2.79 (m, 8H, $Ph_2PCH_2CH_2N$ and $Ph_2PCH_2CH_2N$), 7.39 – 7.50 (m, 12H, *m*-/*p*-PhH), 7.81 (m, 8H, *o*-PhH); **^{13}C {^{1}H}** (125.7 MHz, $CDCl_3$): δ 29.9 (d, $^{1}J_{CP}$ = 49.8 Hz, $Ph_2PCH_2CH_2N$), 52.5 (s, $Ph_2PCH_2CH_2N$), 52.8 (s, N(C_4H_8)N), 128.9 (d, $^{3}J_{CP}$ = 12.1 Hz, *m*-PhC), 131.7 (d, $^{2}J_{CP}$ = 10.6 Hz, *o*-PhC), 131.8 (d, $^{1}J_{CP}$ = 72.9 Hz, *i*-PhC), 131.9 (d, $^{4}J_{CP}$ = 2.9 Hz, *p*-PhC); **^{31}P {^{1}H}** (121.4 MHz, $CDCl_3$): δ + 32.3 (s + Se satellite, $^{1}J_{PSe}$ = 726 Hz).

MS (ES$^+$): *m/z* = 669.2 $[MH]^+$

6.4 Preparation of PNE-Pd complexes

6.4.1 Synthesis of [$PdCl_2${PNE}] complexes and derivatives

Preparation of *N*-methylpiperazine-*N'*-ethylene-diphenylphosphine palladium dichloride (3.1-1)

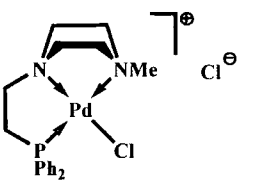

To a Schlenk charged with $[PdCl_2(MeCN)_2]$ (0.110 g, 4.240×10^{-4} mol) was added *N*-methylpiperazine-*N'*-ethylene-diphenylphosphine (**2.4-1**) (0.132 g, 4.225×10^{-4} mol) and CH_2Cl_2 (20 cm^3). The mixture was stirred at room temperature for 12 h, which resulted in the formation of a fine yellow solid. The precipitate was isolated by cannula filtration, washed repeatedly with hexane and diethyl ether and dried *in vacuo* to afford the product as a bright yellow powder (0.141 g, 68%). Slow evaporation of a dilute CH_2Cl_2 solution of **3.1-1** afforded crystals suitable for study by X-ray diffraction {Full crystallographic data available in Appendix 1(b)}.

NMR: ^{1}**H** (400.1 MHz, D_2O): δ 2.78 (d, $^4J_{PH}$ = 5.1 Hz, 3H, $N(CH_2CH_2)_2C\underline{H}_3$), 3.05 (m, 2H, $N(CH_2C\underline{H}_2)_2NMe$), 3.12 (m, 2H, $Ph_2PC\underline{H}_2CH_2N$), 3.19 (m, 2H, $N(C\underline{H}_2CH_2)_2NMe$), 3.37 (m, 2H, $Ph_2PCH_2C\underline{H}_2N$), 3.95 (m, 2H, $N(CH_2C\underline{H}_2)_2NMe$, 4.07 (m, 2H, $N(C\underline{H}_2CH_2)_2NMe$), 7.58 (m, 4H, *m*-Ph$\underline{H}$), 7.64 (m, 2H, *p*-Ph$\underline{H}$), 7.96 (m, 4H, *o*-Ph$\underline{H}$); ^{13}**C {^{1}H}** (100.6 MHz, D_2O): δ 35.0 (d, $^1J_{PC}$ = 32.0 Hz, $Ph_2P\underline{C}H_2CH_2N$), 45.9 (s, $\underline{C}H_3N(CH_2CH_2)_2N$), 57.0 (s, $MeN(\underline{C}H_2CH_2)_2N$), 57.6 (s, $MeN(CH_2\underline{C}H_2)_2N$), 58.0 (s, $Ph_2PCH_2\underline{C}H_2N$), 126.0 (d, $^1J_{PC}$ = 52.5 Hz, *i*-Ph$\underline{C}$), 130.3 (d, $^3J_{PC}$ = 11.5 Hz, *m*-Ph$\underline{C}$), 133.8 (d, $^4J_{PC}$ = 7.0 Hz, *p*-Ph$\underline{C}$), 134.0 (d, $^2J_{PC}$ = 12.0 Hz, *o*-Ph$\underline{C}$); ^{31}**P {^{1}H}** (121.4 MHz, D_2O): δ + 45.7 (s); ^{31}**P {^{1}H}** (121.4 MHz, CD_3OD): δ + 46.5 (s);

MS (MALDI$^+$, dithranol matrix): *m/z* = 455.0 $[M–Cl]^+$.

CHN: Calculated for $C_{19}H_{25}N_2PPdCl_2$: C: 46.59; H: 5.16; N: 5.72. Found: C: 46.17; H: 5.15; N: 5.82).

Λ_M (MeOH, 5×10^{-3} mol, 22.5°C): 68 Ω cm^2 mol^{-1}.

Preparation of morpholine-*N*-ethylene-diphenylphosphine palladium dichloride (3.1-2)

$[PdCl\text{-}\{\kappa^3\text{-}PNO\}]^+ Cl^-$

The synthesis of **3.1-2** was analogous to that of **3.1-1**, *i.e.* employing morpholine-*N*-ethylene-diphenylphosphine (**2.4-2**) (0.200 g, 6.680×10^{-4} mol) and $[PdCl_2(MeCN)_2]$ (0.171 g, 6.591×10^{-4} mol) in CH_2Cl_2 (20 cm^3). Following isolation and purification, the product was afforded as a dark yellow powder (0.21 g, 67%).

NMR: $^1H/^{13}C$ $\{^1H\}$ (d_6-DMSO): the poor solubility of **3.1-2** precluded data acquisition.
^{31}P $\{^1H\}$ (121.4 MHz, d_6-DMSO): δ + 50.4 (br s, $\nu_{½}$ = 24 Hz);
MS (ES^+): *m/z* = 441.9 $[M–Cl]^+$.
CHN: Calculated for $C_{18}H_{22}NOPPdCl_2$: C: 45.35; H: 4.66; N: 2.94. Found: C: 45.18; H: 4.57; N: 2.78).

Preparation of thiomorpholine-*N'*-ethylene-diphenylphosphine palladium dichloride (3.1-3)

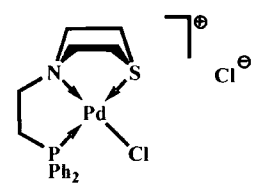

The synthesis of **3.1-3** was analogous to that of **3.1-1**, *i.e.* employing thiomorpholine-*N*-ethylene-diphenylphosphine (**2.4-3**) (0.200 g, 6.341×10^{-4} mol) and $[PdCl_2(MeCN)_2]$ (0.165 g, 6.341×10^{-4} mol) in CH_2Cl_2 (20 cm^3). Following isolation and purification, the product was afforded as a yellow powder (0.254 g, 80%).

NMR: ^1H (299.9 MHz, d_6-DMSO): δ 2.80-3.45 (m, 8H, C<u>H</u>$_2$), 3.82 (m, 2H, C<u>H</u>$_2$), 4.34 (m, 2H, C<u>H</u>$_2$), 7.51 (m, 6H, *m-/p*-Ph<u>H</u>), 7.89 (m, 4H, *o*-Ph<u>H</u>); **^{13}C $\{^1H\}$** (d_6-DMSO): the low solubility of this compound precluded data acquisition; **^{31}P $\{^1H\}$** (121.4 MHz, d_6-DMSO): δ + 49.8 (br s, $\nu_{½}$ = 27 Hz);
MS (ES^+): *m/z* = 457.9 $[M–Cl]^+$.
CHN: Calculated for $C_{18}H_{22}NSPPdCl_2$: C: 43.87; H: 4.51; N: 2.84. Found: C: 43.93; H: 4.62; N: 2.82.

Preparation of piperidine-*N*-ethylene-diphenylphosphine palladium dichloride (3.1-4)

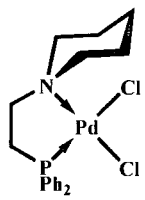

The synthesis of **3.1-3** was analogous to that of **3.1-1**, *i.e.* employing piperidine-*N*-ethylene-diphenylphosphine (**2.4-4**) (0.202 g, 6.792×10^{-4} mol) and $[PdCl_2(MeCN)_2]$ (0.176 g, 6.792×10^{-4} mol) in CH_2Cl_2 (20 cm^3). Following isolation and purification, the product was afforded as a yellow powder (0.185 g, 57 %). Slow evaporation of a chloroform solution of **3.1-4** afforded crystals suitable for study by X-ray diffraction.

NMR: ^{1}**H** (499.8 MHz, d_6-DMSO): δ 1.30 (m, 2H, $N(CH_2C\underline{H}_2)_2CH_2$), 1.38 (m, 2H, *exo*-$N(CH_2CH_2)_2C\underline{H}_2$), 1.66 (m, 1H, *endo*-$N(CH_2CH_2)_2C\underline{H}_2$), 1.77 (m, 2H, $N(CH_2C\underline{H}_2)_2CH_2$), 2.83 – 3.12 (m, 4H, $Ph_2PC\underline{H}_2CH_2N$ and $Ph_2PCH_2C\underline{H}_2N$), 3.28 (m, 2H, $N(C\underline{H}_2CH_2)_2CH_2$), 4.12 (m, 2H, $N(C\underline{H}_2CH_2)_2CH_2$), 7.56 (m, 4H, *m*-Ph$\underline{H}$), 7.65 (m, 2H, *p*-Ph$\underline{H}$), 7.91 (*o*-Ph$\underline{H}$); ^{13}**C {^{1}H}** (125.7 MHz, d_6-DMSO): δ 20.7 (s, $N(CH_2\underline{C}H_2)_2CH_2$), 23.9 (s, $N(CH_2CH_2)_2\underline{C}H_2$), 29.7 (d, $^{1}J_{CP}$ = 29.8 Hz, $Ph_2P\underline{C}H_2CH_2N$), 53.8 (s, $Ph_2PCH_2\underline{C}H_2N$), 57.8 (s, $N(\underline{C}H_2CH_2)_2CH_2$), 128.0 (d, $^{1}J_{CP}$ = 56.1 Hz, *i*-Ph$\underline{C}$), 129.6 (d, $^{3}J_{CP}$ = 11.4 Hz, *m*-Ph$\underline{C}$), 132.7 (d, $^{4}J_{CP}$ = 2.8 Hz, *p*-Ph$\underline{C}$), 134.2 (d, $^{2}J_{CP}$ = 11.1 Hz, *o*-Ph$\underline{C}$); ^{31}**P {^{1}H}** (161.9 MHz, d_6-DMSO): δ + 49.9 (s).

MS (MALDI^{+}, dithranol matrix): *m/z* = 438.1 $[M–Cl]^{+}$.

CHN: Calculated for $C_{19}H_{24}NPPdCl_2$: C: 48.07; H: 5.11; N: 2.95. Found: C: 47.89; N: 4.92; N: 2.81.

Preparation of *N*-phenylpiperazine-*N′*-ethylene-diphenylphosphine palladium dichloride (3.1-5)

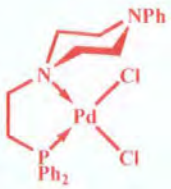

The attempted synthesis of **3.1-5** used an analogous methodology to that used for the synthesis of **3.1-1** (*vide supra*), *i.e.* employing *N*-phenylpiperazine-*N′*-ethylene-diphenylphosphine (**2.4-5**) (0.129 g, 3.445×10^{-4} mol) and $[PdCl_2(MeCN)_2]$ (0.129 g, 3.445×10^{-4} mol) in CH_2Cl_2 (25 cm^3). The resulting mixture was allowed to stir at room temperature for 15h, upon which time the formation of a brown precipitate was noted, although analysis of both the precipitate and the supernatant solution by $^{31}P\{^1H\}$ NMR spectroscopy failed to establish the presence of the target product.

Attempted preparation of piperazine-*N,N′*-diethylene-tetraphenyldiphosphine palladium dichloride (3.1-6)
$[PdCl_2\{PNNP\}]$

The attempted synthesis of **3.1-6** used an analogous methodology to that used for the synthesis of **3.1-1** (*vide supra*), *i.e.* employing piperazine-*N,N′*-diethylene-tetraphenyldiphosphine (0.237 g, 4.641×10^{-4} mol) (**2.4-7**) and $[PdCl_2(MeCN)_2]$ (0.120 g, 4.641×10^{-4} mol). Upon removal of the solvent under vacuum, washing with hexane and thorough drying *in vacuo*, a red-brown powder was afforded, however the target product was not identified by either NMR spectroscopic or mass spectrometric analyses.

Preparation of tetraaquamagnesium-*bis*-sulphato-*N*-methylpiperazine-*N'*-ethylene-diphenylphosphine palladium chloride {3.1-1(b)}

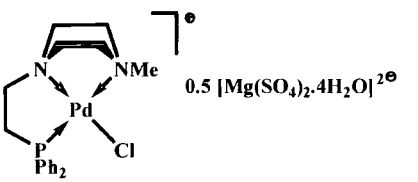

Under air, *N*-methylpiperazine-*N'*-ethylene-diphenylphosphine palladium dichloride (**2.4-1**) (0.100 g, 2.08×10^{-4} mol) was treated with $MgSO_4$ (1.010 g, 8.352×10^{-3} mol) in methanol (10 cm^3) and the resulting mixture allowed to stir at room temperature for 36h. The excess unreacted $MgSO_4$ and $MgCl_2$ by-product were removed by filtration and solvent removed *in vacuo* to afford the product as a vivid yellow powder (0.220 g, 89%). Slow evaporation of a methanolic solution of **3.1-1(b)** in air afforded crystals suitable for study by X-ray diffraction {Full crystallographic data available in Appendix 1(b)}.

NMR: ^{1}**H** (299.9 MHz, CD_3OD): δ 2.67 (d, $^4J_{PH}$ = 5.0 Hz, 3H, $N(CH_2CH_2)_2NC\underline{H}_3$), 2.95 (m, 4H, $MeN(C\underline{H}_2CH_2)_2N$), 3.08 (m, 4H, $MeN(CH_2C\underline{H}_2)_2N$), 3.83 (m, 2H, $Ph_2PCH_2C\underline{H}_2N$), 3.96 (m, 2H, $Ph_2PC\underline{H}_2CH_2N$), 7.58 (m, 4H, *m*-Ph$\underline{H}$), 7.60 (m, 6H, *p*-Ph$\underline{H}$), 7.96 (m, 4H, *o*-Ph$\underline{H}$) {*NB.* the resonance due to the solvent obscures a 2H multiplet}; ^{13}**C {^{1}H}** (100.6 MHz, CD_3OD): δ 34.4 (d, $^1J_{CP}$ = 12.0 Hz, $Ph_2P\underline{C}H_2CH_2N$), 44.9 (d, $^2J_{CP}$ = 2.5 Hz, $N(CH_2CH_2)_2N\underline{C}H_3$), 56.5 (s, $MeN(\underline{C}H_2CH_2)_2N$), 57.0 (s, $MeN(CH_2\underline{C}H_2)_2N$), 57.5 (d, $^2J_{CP}$ = 4.0 Hz, $Ph_2PCH_2\underline{C}H_2N$), 126.5 (d, $^1J_{CP}$ = 53.0 Hz, *i*-Ph$\underline{C}$), 129.4 (d, $^3J_{CP}$ = 12.0 Hz, *m*-Ph$\underline{C}$), 132.6 (d, $^4J_{CP}$ = 2.5 Hz, *p*-Ph$\underline{C}$), 133.2 (d, $^2J_{CP}$ = 11.5 Hz, *o*-Ph$\underline{C}$); ^{31}**P {^{1}H}** (121.4 MHz, CD_3OD): δ + 46.5 (s);

MS (ES^+, MeOH): *m/z* = 455.0 $[M–Cl]^+$; **(ES^-, MeOH):** *m/z* = 97.0 $[HSO_4]^-$;

Λ_M (MeOH, 5×10^{-3} mol, 22.5 °C): 360 Ω cm^2 mol^{-1}.

CHN: Analyses proved unreliable as a result of desolvation and decomposition.

Preparation of *N*-methylpiperazine-*N'*-ethylene-diphenylphosphine dicyclohexylphosphino-ethylene-dimethylammonium palladium dichloride (3.2)

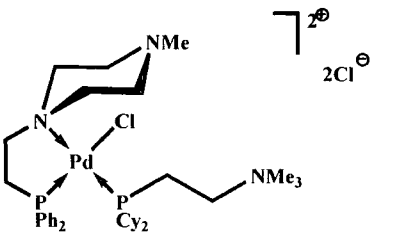

A solution of *N*-methylpiperazine-*N'*-ethylene-diphenylphosphine palladium dichloride (**3.1-1**) (0.018 g, 3.68×10^{-5} mol) in D_2O was treated with $Cy_2PC_2H_4NMe_3Cl$ (0.012 g, 3.680×10^{-5} mol) and the resultant mixture allowed to stir at RT for 12h which was subsequently analysed by NMR spectroscopy.

NMR: $^{1}H/^{13}C$ $\{^{1}H\}$ (D_2O): Satisfactory data could not be obtained for this species; ^{31}P $\{^{1}H\}$ (121.4 MHz, D_2O): δ + 54.8 (d, $^{2}J_{PP}$ = 12.0 Hz, $Cy_2\underline{P}CH_2CH_2NMe_3$), + 44.1 (d, $^{2}J_{PP}$ = 12.0 Hz, $Ph_2\underline{P}CH_2CH_2N$).

Attempted preparation of *bis*-palladium [piperazine-*N,N'*-diethylene-tetraphenyldiphosphine] tetrachloride
$[PdCl_2\{\kappa^2\text{-PN}\}\{\kappa^2\text{-NP}\}PdCl_2]$
(3.2)

A solution of *N*-phenylpiperazine-*N'*-ethylene-diphenylphosphine (**2.4-7**) (0.102 g, 2.004×10^{-4} mol) in CH_2Cl_2 (20 cm^3) was transferred *via* cannula to a CH_2Cl_2 solution (30 cm^3) of $PdCl_2(MeCN)_2$ (0.104 g, 4.009×10^{-4} mol) and the resulting mixture allowed to stir at room temperature for 17h. Upon removal of the solvent under vacuum and washing with hexane, an orange solid was afforded however the target product was not identified by either NMR spectroscopic or mass spectrometric analyses.

Preparation of *N,N'*-methylpiperazine palladium dichloride (3.4)[11]

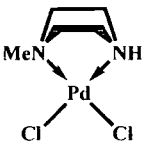

Initially, $[K_2PdCl_4]$ was prepared by treating an aqueous suspension of $PdCl_2$ (0.32 g, 1.80×10^{-3} mol) with KCl (0.27 g, 3.62×10^{-3} mol) in water (*ca.* 10 cm^3) under air. The resulting orange-brown solution was filtered and neat *N*-methylpiperazine (0.20 cm^3, 1.80×10^{-3} mol) added dropwise, under air, which resulted in the immediate precipitation of an orange solid. The product was isolated by filtration and subsequent washing with ice-cold water (2×1 cm^3), ethanol (2×10 cm^3), methanol (2×10 cm^3), diethyl ether (3×10 cm^3) and drying *in vacuo*, afforded the product as an orange solid (0.47 g, 94 %).

Slow cooling of a hot aqueous solution of **3.4** to 5 °C afforded crystals suitable for study by X-ray diffraction.

NMR: ^{1}**H** (400.1 MHz, D_2O): δ 2.49 (s, 3H, $HN(CH_2CH_2)_2NC\underline{H}_3$), 2.55 (pseudo d, J_{HH} = 7.6 Hz, 4H, $HN(CH_2C\underline{H}_2)_2NMe$), 3.80 (pseudo d, J_{HH} = 7.6 Hz, 4H, $HN(C\underline{H}_2CH_2)_2NMe$); ^{13}**C** {^{1}**H**} (100.6 MHz, d_6-DMSO): δ 46.0 (s, $HN(CH_2CH_2)_2N\underline{C}H_3$), 50.0 (s, $HN(\underline{C}H_2CH_2)_2NMe$), 54.8 (s, $HN(CH_2\underline{C}H_2)_2NMe$).
MS (ES$^+$, MeCN/DMSO): *m/z* = 283.2 $[M–Cl + MeCN]^+$, 316.2 $[M–Cl + DMSO]^+$.
CHN: Calculated for $C_5H_{12}Cl_2N_2Pd$: C: 21.64; H: 4.37; N: 10.10. Found: C: 21.33; H: 4.37; N: 9.82).

6.4.2 Synthesis of [PdCl(Me){PNE}] complexes

Preparation of *N*-methylpiperazine-*N'*-ethylene-diphenylphosphine palladium methyl chloride (3.5-1)

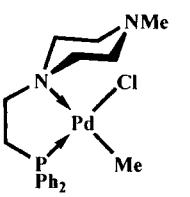

To a Schlenk flask charged with [PdCl(Me)(cod)] (0.084 g, 3.201×10^{-4} mol) was added *N*-methylpiperazine-*N'*-ethylene-diphenylphosphine (**2.4-1**) (0.100 g, 3.201×10^{-4} mol) in CH_2Cl_2 (10 cm^3). The resulting mixture was allowed to stir at room temperature for 18h with all light excluded from the flask. The solvent was then removed under vacuum, the product washed with hexane and dried thoroughly *in vacuo* to afford an orange-yellow powder (0.110 g, 76 %).

NMR: ^{1}**H** (499.8 MHz, $CDCl_3$, – 50 °C): δ 0.51 (s, 3H, Pd–C$\underline{H}_3$), 2.16 – 2.43 (m, 5H, C$\underline{H}_3$N(C_4H_8)N and $Ph_2PCH_2C\underline{H}_2N$), 2.48 – 2.69 (m, 4H, $Ph_2PC\underline{H}_2CH_2N$ and N($C\underline{H}_2CH_2$)$_2$NMe), 2.71 – 2.88 (m, 4H, N($CH_2C\underline{H}_2$)$_2$NMe), 4.12 (m, 2H, N($C\underline{H}_2CH_2$)$_2$NMe), 7.41 – 7.56 (m, 6H, *m*-/*p*-Ph$\underline{H}$), 7.64 (m, 4H, *o*-Ph$\underline{H}$); **^{13}C {^{1}H}** (125.7 MHz, $CDCl_3$): δ – 5.4 (s, Pd–CH_3), 30.8 (d, $^{1}J_{CP}$ = 27.5 Hz, $Ph_2P\underline{C}H_2CH_2N$), 46.5 (s, $\underline{C}H_3N(CH_2CH_2)_2N$), 49.3 (s, N($\underline{C}H_2CH_2$)$_2$NMe), 50.6 (s, $Ph_2PCH_2\underline{C}H_2N$), 53.9 (s, N($CH_2\underline{C}H_2$)$_2$NMe), 129.3 (d, $^{3}J_{CP}$ = 11.0 Hz, *m*-Ph$\underline{C}$), 129.9 (s, *i*-Ph$\underline{C}$), 131.6 (s, *p*-Ph$\underline{C}$), 133.6 (d, $^{2}J_{CP}$ = 12.5 Hz, *o*-Ph$\underline{C}$); **^{31}P {^{1}H}** (161.9 MHz, $CDCl_3$): δ + 45.7 (s); **MS (ES$^+$):** *m/z* = 433.0 $[M\text{-}Cl]^+$; **MS** (EI): *m/z* = 433.0 $[M\text{-}Cl]^+$; 454.3 $[M–CH_3]^+$. **CHN:** Calculated for $C_{20}H_{28}N_2PPdCl$: C: 51.18; H: 6.03; N: 5.97. Found C: 51.17; H: 6.09; N: 5.80.

Preparation of morpholine-*N*-ethylene-diphenylphosphine palladium methyl chloride (3.5-2)

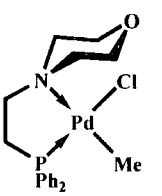

The synthesis of 3.5-2 was analogous to that of 3.5-1 (*vide supra*) and employed morpholine-*N*-ethylene-diphenylphosphine (2.4-2) (0.079 g, 2.640×10^{-4} mol) and [PdCl(Me)(cod)] (0.070 g, 2.640×10^{-4} mol) in CH_2Cl_2 (20 cm^3) with the exclusion of light from the flask. Following isolation and purification, the product was afforded as a pale-yellow powder (0.083 g, 69 %).

NMR: ^{1}**H** (499.8 MHz, $CDCl_3$): δ 0.67 (d, $^{3}J_{PH}$ = 3.0 Hz, 3H, Pd–C$\underline{H}_3$), 2.54 – 2.68 (m, 4H, $Ph_2PC\underline{H}_2CH_2N$ and N($C_4\underline{H}_8$)$_2$O), 2.90 (m, 2H, $Ph_2CH_2C\underline{H}_2N$), 3.89 (m, 2H, N($C_4\underline{H}_8$)O), 3.98 (m, 6H, N($C_4\underline{H}_8$)O), 7.48 (m, 4H, *m*-Ph$\underline{H}$), 7.52 (m, 2H, *p*-Ph$\underline{H}$), 7.66 (m, 4H, *o*-Ph$\underline{H}$); **^{13}C {^{1}H}** (125.7 MHz, $CDCl_3$): δ – 4.2 (s, Pd–$\underline{C}H_3$), 30.6 (d, $^{1}J_{CP}$ = 27.9 Hz, $Ph_2P\underline{C}H_2CH_2N$), 52.6 (s, $Ph_2PCH_2\underline{C}H_2N$), 54.7 (s, N($\underline{C}_4H_8$)O), 61.8 (s, N($\underline{C}_4H_8$)O), 129.3 (d, $^{3}J_{CP}$ = 11.1 Hz, *m*-Ph$\underline{C}$), 129.8 (s, *i*-Ph$\underline{C}$), 131.7 (d, $^{4}J_{CP}$ = 2.4 Hz, *p*-Ph$\underline{C}$), 133.5 (d, $^{2}J_{CP}$ = 11.9 Hz, *o*-Ph$\underline{C}$); **^{31}P {^{1}H}** (161.9 MHz, $CDCl_3$): δ + 43.1 (s). **MS (MALDI+, dithranol matrix):** *m/z* = 440.1 $[M–Me]^+$; 420.1 $[M–Cl]^+$. **CHN**: Calculated for $C_{19}H_{25}NOPPdCl$: C: 50.01; H: 5.53; N: 3.07. Found: C: 49.95, H: 5.32; N: 2.91.

Preparation of thiomorpholine-*N*-ethylene-diphenylphosphine palladium methyl chloride (3.5-3)

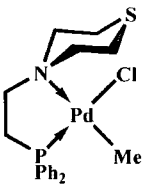

The synthesis of **3.5-3** was analogous to that of **3.5-1** (*vide supra*) and employed thiomorpholine-*N*-ethylene-diphenylphosphine (**2.4-3**) (0.103 g, 3.265×10^{-4} mol) and [PdCl(Me)(cod)] (0.087 g, 3.265×10^{-4} mol) in CH_2Cl_2 (25 cm^3) with the exclusion of light from the flask. Following isolation and purification, the product was afforded as a pale-yellow powder (0.102 g, 66 %).

NMR: ^{1}**H** (499.8 MHz, $CDCl_3$): δ 0.64 (d, $^3J_{PH}$ = 3.0 Hz, Pd–C$\underline{H}_3$), 2.24 (m, 2H, N($CH_2C\underline{H}_2$)$_2$S), 2.57 (m, 2H, $Ph_2PC\underline{H}_2CH_2N$), 2.86 (m, 2H, $Ph_2PCH_2C\underline{H}_2N$), 3.07 – 3.21 (m, 4H, N($C\underline{H}_2CH_2$)$_2$S and N($CH_2C\underline{H}_2$)$_2$S), 4.26 (m, 2H, N($C\underline{H}_2CH_2$)$_2$S), 7.46 (m, 4H, *m*-Ph$\underline{H}$), 7.51 (m, 2H, *p*-Ph$\underline{H}$), 7.65 (m, 4H, *o*-Ph$\underline{H}$); ^{13}**C {^{1}H}** (125.7 MHz, $CDCl_3$): δ – 5.1 (s, Pd–$\underline{C}H_3$), 20.3 (s, N($CH_2\underline{C}H_2$)$_2$S), 30.7 (d, $^1J_{CP}$ = 28.3 Hz, $Ph_2P\underline{C}H_2CH_2N$), 49.1 (s, $Ph_2PCH_2\underline{C}H_2N$), 54.3 (s, N($\underline{C}H_2CH_2$)$_2$S), 129.3 (d, $^3J_{CP}$ = 11.1 Hz, *m*-Ph$\underline{C}$), 129.4 (d, $^1J_{CP}$ = 50.3 Hz, *i*-Ph$\underline{C}$), 131.7 (d, $^4J_{CP}$ = 2.4 Hz, *p*-Ph$\underline{C}$), 133.5 (d, $^2J_{CP}$ = 12.1 Hz, *o*-Ph$\underline{C}$); ^{31}**P {^{1}H}** (161.9 MHz, $CDCl_3$): δ + 43.5 (s).

MS (MALDI$^+$, dithranol matrix): *m/z* = 458.0 $[M–Me]^+$; 436.0 $[M–Cl]^+$;

CHN: Calculated for $C_{19}H_{25}NPSPdCl$: C: 48.31; H: 5.35; N: 2.97. Found: C: 48.21; H: 5.17; N: 3.15.

Preparation of piperidine-*N*-ethylene-diphenylphosphine palladium methyl chloride (3.5-4)

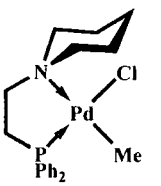

The synthesis of **3.5-4** was analogous to that of **3.5-1** (*vide supra*) and employed piperidine-*N*-ethylene-diphenylphosphine (**2.4-4**) (0.091 g, 3.060×10^{-4} mol) and [PdCl(Me)(cod)] (0.081 g, 3.060×10^{-4} mol) in CH_2Cl_2 (20 cm^3) with the exclusion of light from the flask. Following isolation and purification, the product was afforded as a pale-yellow powder (0.095 g, 68 %).

NMR: ^{1}**H** (499.8 MHz, $CDCl_3$): δ 0.56 (d, $^3J_{PH}$ = 3.0 Hz, 3H, Pd–C$\underline{H}_3$), 1.36 (m, 2H, N($CH_2C\underline{H}_2$)$_2CH_2$), 1.56 – 1.72 (m, 4H, N($CH_2C\underline{H}_2$)$_2CH_2$ and N(CH_2CH_2)$_2C\underline{H}_2$), 2.51 (m, 2H, $Ph_2PC\underline{H}_2CH_2N$), 2.80 (m, 2H, $Ph_2PCH_2C\underline{H}_2N$), 2.86 (m, 2H, N($C\underline{H}_2CH_2$)$_2CH_2$), 3.89 (m, 2H, N($C\underline{H}_2CH_2$)$_2CH_2$), 7.45 (m, 4H, *m*-Ph$\underline{H}$), 7.50 (m, 2H, *p*-Ph$\underline{H}$), 7.65 (m, 4H, *o*-Ph$\underline{H}$); ^{13}**C {^{1}H}** (125.7 MHz, $CDCl_3$): δ – 6.4 (d, $^2J_{CP}$ = 3.4 Hz, Pd–$\underline{C}H_3$), 19.9 (s, N($CH_2\underline{C}H_2$)$_2CH_2$), 24.1 (s, N(CH_2CH_2)$_2\underline{C}H_2$), 31.3 (d, $^1J_{CP}$ = 28.3 Hz, $Ph_2P\underline{C}H_2CH_2N$), 49.3 (d, $^2J_{CP}$ = 4.3 Hz, $Ph_2PCH_2\underline{C}H_2N$), 54.1 (s, N($\underline{C}H_2CH_2$)$_2CH_2$), 129.2 (d, $^3J_{CP}$ = 11.1 Hz, *m*-Ph$\underline{C}$), 129.7 (d, $^1J_{CP}$ = 50.3 Hz, *i*-Ph$\underline{C}$), 131.6 (d, $^4J_{CP}$ = 2.4 Hz, *p*-Ph$\underline{C}$), 133.6 (d, $^2J_{CP}$ = 11.9 Hz, *o*-Ph$\underline{C}$); ^{31}**P {^{1}H}** (161.9 MHz, $CDCl_3$): δ + 44.6 (s).

MS (MALDI$^+$, dithranol matrix): *m/z* = 438.0 $[M–Me]^+$; 418.1 $[M–Cl]^+$;

CHN: Calculated for $C_{20}H_{27}NPPdCl$: C: 52.87; H: 6.00; N: 3.08. Found: C: 52.87; H: 6.09; N: 3.14.

6.4.3 Synthesis of [$PdMe_2${PNE}] complexes

Preparation of *N*-methylpiperazine-*N'*-ethylene-diphenylphosphine dimethyl palladium (3.6-1)

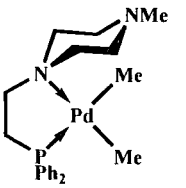

To a Schlenk flask charged with [$PdMe_2$(tmeda)] (0.152 g, 5.950×10^{-4} mol) in toluene (10 cm^3) was added a toluene solution (10 cm^3) of *N*-methylpiperazine-*N'*-ethylene-diphenylphosphine (**2.4-1**) (0.194 g, 5.950×10^{-4} mol). The resulting mixture was stirred at – 20 °C with light excluded from the reaction vessel for 45 mins by which time analysis by ^{31}P NMR spectroscopy indicated ligand coordination to Pd. The solvent was then removed under vacuum affording the product as a yellow-orange solid, which was stored at – 30 °C in an effort to minimise complex decomposition. NMR analysis was undertaken by addition of d_8-PhMe to a sample of the product held at – 196 °C in the absence of light.

NMR: ^{1}H (499.8 MHz, d_8-PhMe, – 20 °C): δ 0.55 (s, 3H, Pd–C$\underline{H}_3$), 1.05 (s, 3H, Pd–C$\underline{H}_3$), 2.15 (m, 4H, MeN($C_4\underline{H}_8$)N), 2.21 – 2.28 (m, 5H, $Ph_2PC_2\underline{H}_4N$ and C$\underline{H}_3$N(C_4H_8)N), 2.62 (m, 4H, MeN($C_4\underline{H}_8$)N), 2.90 (m, 2H, $Ph_2PC_2\underline{H}_4N$), 7.22 – 7.27 (m, 8H, *o*-/*m*-Ph$\underline{H}$), 7.79 (m, 2H, *p*-Ph$\underline{H}$); ^{13}C {^{1}H} (125.7 MHz, d_8-PhMe, – 50 °C): δ – 2.3 (s, Pd–$\underline{C}H_3$), 15.4 (s, Pd–$\underline{C}H_3$), 26.6 (s, $Ph_2P\underline{C}H_2CH_2N$), 51.4 (s, $\underline{C}H_3N(CH_2CH_2)_2N$), 58.2 (s, MeN($\underline{C}H_2CH_2)_2N$), 60.5 (s, MeN($CH_2\underline{C}H_2)_2N$), 63.8 (s, $PCH_2\underline{C}H_2N$), 133.4 (s, *m*-Ph$\underline{C}$), 133.6 (s, *p*-Ph$\underline{C}$), 134.4 (s, *o*-Ph$\underline{C}$), 138.6 (s, *i*-Ph$\underline{C}$) {*NB.* aryl J_{CP} couplings obscured by solvent}; ^{31}P {^{1}H} (202.3 MHz, d_8-PhMe, – 50 °C): δ + 16.5 (s).
MS/CHN: The thermally sensitive nature of **3.5-1** precluded the acquisition of satisfactory data.

Preparation of morpholine-*N*-ethylene-diphenylphosphine dimethyl palladium (3.6-2)

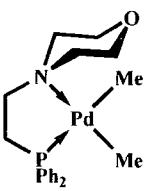

The preparation of **3.6-2** was analogous to that of **3.6-1** (*vide supra*), employing morpholine-*N*-ethylene-diphenylphosphine (**2.4-2**) (0.097 g, 3.240×10^{-4} mol) and [$PdMe_2$(tmeda)] (0.082 g, 3.240×10^{-4} mol) in toluene (10 cm^3) at – 78 °C in the absence of light. *In situ* analysis by ^{31}P {^1H} NMR spectroscopy after 20 minutes indicated coordination of the ligand to Pd and the solvent was therefore removed *in vacuo* to afford a grey-white solid. The product **3.5-2** displayed a greater tolerance towards higher temperatures (approx. 1h at 0 °C before the onset of decomposition), thus permitting purification of the product by washing with hexane before thorough drying under vacuum. The product was afforded as a white powder (0.064 g, 44 %).

NMR: ^1H (499.8 MHz, d_8-PhMe, – 60 °C): δ 1.18 (s, 3H, Pd–C$\underline{H}_3$), 1.97 (m, 2H, $Ph_2PC\underline{H}_2CH_2N$), 2.18 (m, 4H, $N(C_4\underline{H}_8)O$), 2.77 (m, 2H, $Ph_2PCH_2C\underline{H}_2N$), 3.53 (m, 2H, $N(C_4\underline{H}_8)O$), 3.72 (m, 2H, $N(C_4\underline{H}_8)O$), 7.12 (m, 4H, *m*-Ph$\underline{H}$), 7.19 (m, 2H, *p*-Ph$\underline{H}$), 7.27 (m, 4H, *o*-Ph$\underline{H}$) {*NB.* Pd–C$\underline{H}_3$ resonance absent from spectrum}; **^{13}C {^1H}** (125.7 MHz, d_8-PhMe, – 60 °C): δ 6.5 (s, Pd–$\underline{C}H_3$), 15.4 (dd, $^5J_{CP}$ = 14.5 Hz, $^2J_{CP}$ = 105.9 Hz, Pd–$\underline{C}H_3$), 30.5 (s, $Ph_2P\underline{C}H_2CH_2N$), 58.5 (s, $N(\underline{C}H_2CH_2)_2O$), 60.6 (s, $Ph_2PCH_2\underline{C}H_2N$), 72.0 (s, $N(CH_2\underline{C}H_2)_2O$), 130.6 (s, *m*-Ph$\underline{C}$), 133.4 (s, *o*-Ph$\underline{C}$), 134.3 (s, *p*-Ph$\underline{C}$), 138.6 (s, *i*-Ph$\underline{C}$) {*NB.* aryl J_{CP} couplings obscured by solvent}; **^{31}P {^1H}** (202.3 MHz, d_8-PhMe, – 60 °C): δ + 16.0 (s).

MS (MALDI$^+$, dithranol matrix): *m/z* = 420.1 $[M–CH_3]^+$.

CHN: The thermally sensitive nature of **3.6-2** precluded the acquisition of CHN data.

Preparation of thiomorpholine-*N*-ethylene-diphenylphosphine dimethyl palladium (3.6-3)

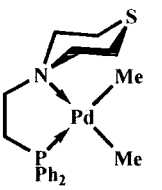

The preparation of **3.6-3** was analogous to that of **3.6-1** (*vide supra*), employing thiomorpholine-*N*-ethylene-diphenylphosphine (**2.4-3**) (0.106 g, 3.363×10^{-4} mol) and [$PdMe_2$(tmeda)] (0.085 g, 3.363×10^{-4} mol) in toluene (10 cm^3) at – 78 °C in the absence of light. *In situ* analysis by ^{31}P NMR spectroscopy indicated the coordination of the ligand to Pd after 20 minutes and thus the solvent was removed under vacuum. The highly unstable nature of **3.6-3** precluded the full characterisation of this compound by multinuclear NMR spectroscopy as rapid decomposition was noted (even at – 30 °C).

$^1H/^{13}C$ {^1H} NMR/MS/CHN: The extremely thermally sensitive nature of **3.6-3** precluded the acquisition of satisfactory data due to rapid decomposition.
NMR: ^{31}P {^1H} (202.3 MHz, d_8-PhMe, – 30 °C): δ + 16.2 (s).

Preparation of piperidine-*N*-ethylene-diphenylphosphine dimethyl palladium (3.6-4)

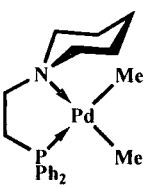

The preparation of **3.6-4** was analogous to that of **3.6-1** (*vide supra*), employing piperidine-*N*-ethylene-diphenylphosphine (**2.4-4**) (0.151 g, 5.077×10^{-4} mol) and [$PdMe_2$(tmeda)] (0.128 g, 5.077×10^{-4} mol) in toluene (10 cm^3) at – 78 °C in the absence of light. *In situ* analysis by ^{31}P NMR spectroscopy indicated the coordination of the ligand to Pd after 15 minutes and thus the solvent was removed under vacuum. The highly unstable nature of **3.6-4** precluded the full characterisation of this compound by multinuclear NMR spectroscopy as rapid decomposition was noted (even at – 30 °C).

$^1H/^{13}C$ {^1H} NMR/MS/CHN: The extremely thermally sensitive nature of **3.5-4** precluded the acquisition of satisfactory data due to rapid decomposition.
NMR: ^{31}P {^1H} (202.3 MHz, d_8-PhMe, – 30 °C): δ + 16.5 (s).

6.5 Preparation of PNE-Pt complexes

6.5.1 Synthesis of $[PtCl\{\kappa^2\text{-PN(E)}\}\{\kappa^1\text{-P(NE)}\}]^+ Cl^-$ complexes

Preparation of (κ^2-PN-*N*-methylpiperazine-*N'*-ethylene-diphenyl-phosphine)(κ^1-P-*N*-methylpiperazine-*N'*-ethylene-diphenyl-phosphine) platinum chloride (4.1-1) ($[PtCl\{\kappa^2\text{-PN(NMe)}\}\{\kappa^1\text{-P(NNMe)}\}]^+ Cl^-$)

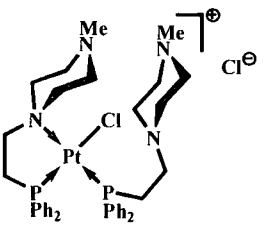

A solution of *N*-methylpiperazine-*N'*-ethylene-diphenylphosphine (**2.4-1**) (0.125 g, 4.001×10^{-4} mol) in CH_2Cl_2 (20 cm^3) was transferred *via* cannula to a CH_2Cl_2 solution (15 cm^3) of $PtCl_2$(cod) (0.150g, 4.001×10^{-4} mol) and the resulting solution allowed to stir at room temperature for 16h. The solvent was removed under vacuum and following washing with hexane and thorough drying *in vacuo*, a white powder was obtained (0.120 g).

Analysis of the product revealed the presence of approximately 0.5 equivalents of unreacted $PtCl_2$(cod). Attempts to remove this impurity by repeated recrystallisation from CH_2Cl_2/hexane proved unsuccessful and thus the crude yield is reported.

NMR: $^1H/^{13}C\{^1H\}$: spectra were too broad for reliable assignment of resonances.
$^{31}P\{^1H\}$ (121.4 MHz, $CDCl_3$): δ + 1.6 (br s + sats., $^1J_{PtP}$ = 3186 Hz, $\nu_{½}$ = 66 Hz, κ^1-P(NNMe)), + 35.7 (br s + sats., $^1J_{PtP}$ = 3748 Hz, $\nu_{½}$ = 78 Hz, κ^2-PN(NMe)).
MS (MALDI$^+$, dithranol matrix): *m/z* = 855 $[M–Cl]^+$; 543 $[M–(PNN + Cl)]^+$.

Preparation of (κ^2-PN-morpholine-*N*-ethylene-diphenyl-phosphine)(κ^1-P-morpholine-*N*-ethylene-diphenylphosphine) platinum chloride (4.1-2)
($[PtCl\{\kappa^2$-PN(O)$\}\{\kappa^1$-P(NO)$\}]^+$ Cl^-)

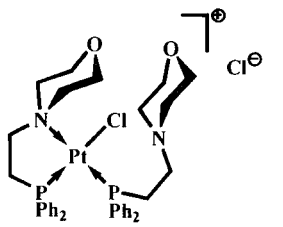

The synthesis of **4.1-2** was analogous to that of **4.1-1** (*vide supra*), employing morpholine-*N*-ethylene-diphenylphosphine (**2.4-2**) (0.160 g, 5.345×10^{-4} mol) and $PtCl_2$(cod) (0.200 g, 5.345×10^{-4} mol) in CH_2Cl_2 (35 cm^3). Following isolation, a white powder was obtained (0.145 g).

Analysis of the product revealed the presence of 0.5 equivalents of unreacted $PtCl_2$(cod). Attempts to remove this impurity by repeated recrystallisation from CH_2Cl_2/hexane proved unsuccessful and thus the crude yield is reported. Slow diffusion of hexane into a concentrated CH_2Cl_2 solution of the product mixture afforded colourless crystals of **4.1-2** which were suitable for analysis by X-ray diffraction studies and shown to be a derivative of the product depicted.

NMR: $^1H/^{13}C$ $\{^1H\}$: spectra were too broad for reliable assignment of resonances.
^{31}P $\{^1H\}$ (121.4 MHz, $CDCl_3$): δ + 0.8 (br s + sats., $^1J_{PtP}$ = 3241 Hz, $\nu_{½}$ = 77 Hz, κ^1-P(NO)), + 35.9 (br s + sats., $^1J_{PtP}$ = 3767 Hz, $\nu_{½}$ = 80 Hz, κ^2-PN(O)).
MS (MALDI$^+$, dithranol matrix): *m/z* = 829 $[M–Cl]^+$; 529 $[M–(PNO + Cl)]^+$.

Preparation of (κ^2-PN-thiomorpholine-*N*-ethylene-diphenyl-phosphine)(κ^1-P-thiomorpholine-*N*-ethylene-diphenyl-phosphine) platinum chloride (4.1-3)
([PtCl{κ^2-PN(O)}{κ^1-P(NO)}]$^+$ Cl$^-$)

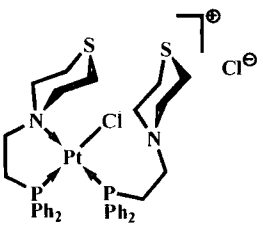

The synthesis of **4.1-3** was analogous to that of **4.1-1** (*vide supra*), employing thiomorpholine-*N*-ethylene-diphenylphosphine (**2.4-3**) (0.115 g, 3.646×10^{-4} mol) and $PtCl_2$(cod) (0.130 g, 3.474×10^{-4} mol) in CH_2Cl_2 (30 cm^3). Following isolation, a white powder was obtained (0.126 g).

Analysis of the product revealed the presence of 0.5 equivalents of unreacted $PtCl_2$(cod). Attempts to remove this impurity by repeated recrystallisation from CH_2Cl_2/hexane proved unsuccessful and thus the crude yield is reported.

NMR: ^{1}H/^{13}C {^{1}H}: spectra were too broad for reliable assignment of resonances.
^{31}P {^{1}H} (121.4 MHz, $CDCl_3$): δ + 0.9 (br s + sats., $^1J_{PtP}$ = 3208 Hz, $\nu_{½}$ = 55 Hz, κ^1-P(NS)), + 35.8 (br s + sats., $^1J_{PtP}$ = 3771, $\nu_{½}$ = 72 Hz, κ^2-PN(S)).
MS (MALDI$^+$, dithranol matrix): *m/z* = 861 [M–Cl]$^+$; 546 [M–(PNS + Cl)]$^+$.

Direct preparation of (κ^2-PN-*N*-methylpiperazine-*N'*-ethylene-diphenylphosphine)(κ^1-P-*N*-methylpiperazine-*N'*-ethylene-diphenylphosphine) platinum dichloride (4.1-1)
([PtCl{κ^2-PN(NMe)}{κ^1-P(NNMe)}]$^+$ Cl$^-$)

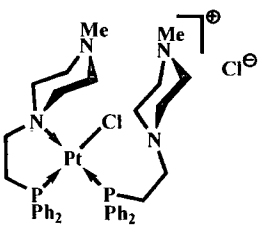

A solution of *N*-methylpiperazine-*N'*-ethylene-diphenyl-phosphine (**2.4-1**) (0.159 g, 5.089×10^{-4} mol) in CH_2Cl_2 (15 cm^3) was transferred *via* cannula to a CH_2Cl_2 (20 cm^3) solution of $PtCl_2$(cod) (0.095 g, 2.545×10^{-4} mol) and the resulting solution allowed to stir at room temperature for 12h. The solvent was subsequently removed under vacuum and following extraction with hexane and thorough drying *in vacuo*, the product was afforded as a white solid (0.118 g, 52 %).

NMR: ^{1}H/^{13}C {^{1}H}: spectra were too broad for reliable assignment of resonances.

^{31}P {^{1}H} (121.4 MHz, $CDCl_3$): δ + 1.6 (br s + sats., $^{1}J_{PtP}$ = 3168 Hz, $\nu_{½}$ = 83 Hz, κ^{1}-P(NNMe)), + 35.6 (br s + sats., $^{1}J_{PtP}$ = 3760 Hz, $\nu_{½}$ = 78 Hz, κ^{2}-PN(NMe)).
MS (MALDI^{+}, dithranol matrix): *m/z* = 855 $[M–Cl]^{+}$; 543 $[M–(PNNMe + Cl)]^{+}$.

Direct preparation of (κ^{2}-PN-morpholine-*N*-ethylene-diphenyl-phosphine)(κ^{1}-P-morpholine-*N*-ethylene-diphenylphosphine) platinum dichloride (4.1-2) ([PtCl{κ^{2}-PN(O)}{κ^{1}-P(NO)}]$^{+}$ Cl^{-})

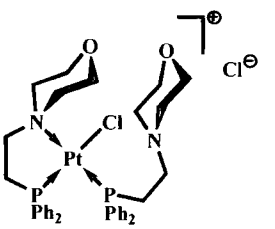

The direct preparation of **4.1-2** was analogous to that of the direct preparation of **4.1-1** (*vide supra*) employing morpholine-*N*-ethylene-diphenylphosphine (**2.4-2**) (0.145 g, 4.844×10^{-4} mol) and $PtCl_2$(cod) (0.091 g, 2.422×10^{-4} mol) in CH_2Cl_2 (20 cm^3). Following isolation and purification, the product was afforded as a white solid (0.118 g, 56 %).

NMR: ^{1}H/^{13}C {^{1}H}: spectra were too broad for reliable assignment of resonances.
^{31}P {^{1}H} (121.4 MHz, $CDCl_3$): δ + 1.3 (br s + sats., $^{1}J_{PtP}$ = 3151 Hz, $\nu_{½}$ = 56 Hz, κ^{1}-P(NO)), + 36.1 (br s + sats., $^{1}J_{PtP}$ = 3716 Hz, $\nu_{½}$ = 71 Hz, κ^{2}-PN(O)).
MS (MALDI^{+}, dithranol matrix): *m/z* = 829 $[M–Cl]^{+}$; 529 $[M–(PNO + Cl)]^{+}$.

Direct preparation of (κ^2-PN-thiomorpholine-*N*-ethylene-diphenyl-phosphine)(κ^1-P-thiomorpholine-*N*-ethylene-diphenyl-phosphine) platinum dichloride (4.1-3) ($[PtCl\{\kappa^2\text{-}PN(O)\}\{\kappa^1\text{-}P(NO)\}]^+ Cl^-$)

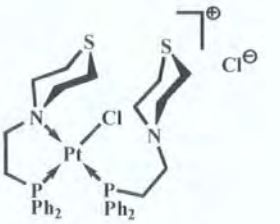

The direct preparation of **4.1-3** was analogous to that of the direct preparation of **4.1-1** (*vide supra*) employing thiomorpholine-*N*-ethylene-diphenylphosphine (**2.4-3**) (0.151 g, 4.787×10^{-4} mol) and $PtCl_2(cod)$ (0.090 g, 2.393×10^{-4} mol) in CH_2Cl_2 (20 cm^3). Following isolation and purification, the product was afforded as a white solid (0.139 g, 64 %).

NMR: $^1H/^{13}C\{^1H\}$: spectra were too broad for reliable assignment of resonances.
$^{31}P\{^1H\}$ (121.4 MHz, $CDCl_3$): δ + 1.4 (br s + sats., $^1J_{PtP}$ = 3146 Hz, $\nu_{½}$ = 60 Hz, κ^1-P(NS)), + 35.9 (br s + sats., $^1J_{PtP}$ = 3771 Hz, $\nu_{½}$ = 72 Hz, κ^2-PN(S)).
MS (MALDI$^+$, dithranol matrix): *m/z* = 861 $[M–Cl]^+$; 546 $[M–(PNS + Cl)]^+$.

6.5.2 Attempted synthesis of $[PtCl\{\kappa^2\text{-}PN(E)\}\{\kappa^1\text{-}P(NE)\}]^+ Cl^-$ derivatives

Attempted preparation of *bis*(κ^2-PN-*N*-methylpiperazine-*N'*-ethylene-diphenylphosphine) platinum dihexafluorophosphate (4.2-1) ($[PtCl\{\kappa^2\text{-}PN(NMe)\}_2]^{2+}$ $2PF_6^-$)

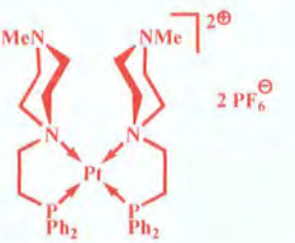

A solution of $[PtCl\{\kappa^2\text{-}PN(NMe)\}\{\kappa^1\text{-}P(NNMe)\}]^+ Cl^-$ (**4.1-1**)) (0.143 g, 1.605×10^{-4} mol) in CH_2Cl_2 (10 cm^3) was added *via* cannula to a suspension of $NaPF_6$ (0.054 g, 3.210×10^{-4} mol) in CH_2Cl_2 (25 cm^3) and the resulting mixture allowed to stir at room temperature for 48h. Analysis of the product mixture by $^{31}P\{^1H\}$ NMR spectroscopy indicated that the required reaction had not taken place, presumably due to the limited solubility of $NaPF_6$ in CH_2Cl_2. A small volume of MeOH (10 cm^3) was therefore added to the reaction vessel in an effort to solubilise the $NaPF_6$ and the stirring was allowed to continue for a further 150h. Following separation of the undissolved precipitate by filtration and removal of the volatile components under vacuum, analysis of the

obtained product by multinuclear NMR spectroscopy and mass spectrometry indicated that the required product had not formed and only unreacted $NaPF_6$ could be identified in the product mixture.

Attempted Preparation of *bis*(κ^2-PN-morpholine-*N*-ethylene-diphenylphosphine) platinum dihexafluorophosphate (4.2-2) ($[PtCl\{\kappa^2\text{-}PN(O)\}_2]^{2+}$ $2PF_6^-$)

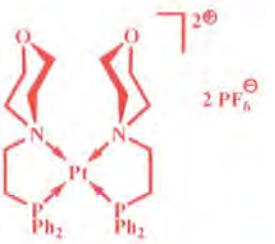

The attempted synthesis of the dihexafluorophosphate salt **4.2-2** was analogous to that of **4.2-1** (*vide supra*), employing $[PtCl\{\kappa^2\text{-}PN(O)\}\{\kappa^1\text{-}P(NO)\}]^+$ Cl^- (**4.1-2**) (0.140 g, 1.619×10^{-4} mol) and $NaPF_6$ (0.054 g, 3.238×10^{-4} mol) in CH_2Cl_2 at room temperature. As was observed in the synthesis of **4.2-1**, no reaction had occurred after 40h and therefore an aliquot of MeOH (10 cm^3) was added to the reaction mixture although this failed to solubilise the $NaPF_6$ salt and did not promote the required transformation.

Attempted Preparation of *bis*(κ^2-PN-thiomorpholine-*N*-ethylene-diphenylphosphine) platinum dihexafluorophosphate (4.2-3) ($[PtCl\{\kappa^2\text{-}PN(S)\}_2]^{2+}$ $2PF_6^-$)

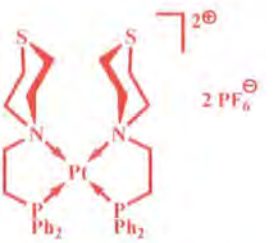

The attempted synthesis of the dihexafluorophosphate salt **4.2-3** was analogous to that of **4.2-1** (*vide supra*) employing $[PtCl\{\kappa^2\text{-}PN(O)\}\{\kappa^1\text{-}P(NO)\}]^+$ Cl^- (**4.1-3**) (0.126 g, 1.405×10^{-4} mol) and $NaPF_6$ (0.047 g, 2.810×10^{-4} mol) in CH_2Cl_2 at room temperature. As was observed in the synthesis of **4.2-1**, no reaction had occurred after 60h and therefore an aliquot of MeOH (10 cm^3) was added to the reaction mixture although this failed to solubilise the $NaPF_6$ salt and did not promote the required transformation.

Attempted Preparation of (κ^2-PN-*N*-methylpiperazine-*N'*-ethylene-diphenylphosphine) platinum triphenylphosphine dichloride (4.3-1)
($[PtCl\{\kappa^2\text{-}PN(NMe)\}(PPh_3)]^+ Cl^-$)

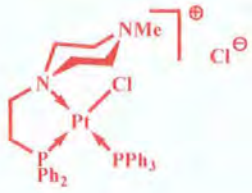

To a solution of $[PtCl\{\kappa^2\text{-}PN(NMe)\}\{\kappa^1\text{-}P(NNMe)\}]^+ Cl^-$ (**4.1-1**) (0.095 g, 1.066×10^{-4} mol) in CH_2Cl_2 (10 cm^3) was added an equimolar quanitiy of triphenylphosphine (0.028 g, 1.066×10^{-4} mol) as a solid and the resulting solution allowed to stir at room temperature for 18h. *In situ* analysis of the reaction by $^{31}P\{^1H\}$ NMR spectroscopy did not demonstrate the presence of the required product with only extemely broadened resonances being observed.

In an effort to generate the required product **4.3-1**, the obtained product was redissolved in CH_2Cl_2 (30 cm^3), another equivalent of PPh_3 (0.028 g, 1.066×10^{-4} mol) was added to the reaction vessel as a solid and the resulting mixture allowed to stir at room temperature for a further 18h. Following removal of the solvent *in vacuo*, analysis of the obtained product by multinuclear NMR spectroscopy again did not indicate the formation of the required product with only unreacted PPh_3 being observed in the $^{31}P\{^1H\}$ spectrum. Mass spectrometric analysis also failed to confirm the presence of the product.

Attempted Preparation of (κ^2-*PN*-morpholine-*N*-ethylene-diphenylphosphine) platinum triphenylphosphine dichloride (4.3-2)
($[PtCl(PPh_3)\{\kappa^2\text{-}PN(O)\}]^+ Cl^-$)

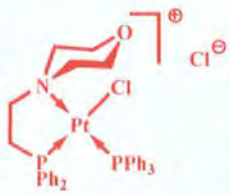

The attempted synthesis of **4.3-2** was analogous to that detailed for **4.3-1** (*vide supra*), employing $[PtCl\{\kappa^2\text{-}PN(O)\}\{\kappa^1\text{-}P(NO)\}]^+ Cl^-$ (**4.1-2**) (0.107 g, 1.237×10^{-4} mol) and PPh_3 (0.032 g, 1.237×10^{-4} mol) in CH_2Cl_2 for 15h. As was noted in the synthesis of **4.3-1**, analysis of the obtained product by $^{31}P\{^1H\}$ NMR spectroscopy did not demonstrate the presence of the required species and thus the obtained product was treated with a second equivalent of PPh_3 (0.032 g, 1.237×10^{-4} mol). However, following isolation, the required product was not detected by NMR spectroscopic and

mass spectrometric analyses with only unreacted PPh_3 being observed by ^{31}P $\{^1H\}$ NMR spectroscopy.

Attempted Preparation of (κ^2-PN-thiomorpholine-*N*-ethylene-diphenylphosphine) platinum triphenylphosphine dichloride (4.3-3)

($[PtCl\{\kappa^2\text{-}PN(S)\}(PPh_3)]^+$ Cl^-)

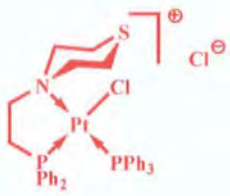

The attempted synthesis of **4.3-3** was analogous to that detailed for **4.3-1** (*vide supra*), employing $[PtCl\{\kappa^2\text{-}PN(S)\}\{\kappa^1\text{-}P(NS)\}]^+$ Cl^- (**4.1-3**) (0.112 g, 1.249×10^{-4} mol) and PPh_3 (0.033 g, 1.249×10^{-4} mol) in CH_2Cl_2 for 21h. As was noted in the synthesis of **4.3-1**, analysis of the obtained product by ^{31}P $\{^1H\}$ NMR spectroscopy did not demonstrate the presence of the required species and thus the obtained product was treated with a second equivalent of PPh_3 (0.033 g, 1.249×10^{-4} mol). However, following isolation, the required product was not detected by NMR spectroscopic and mass spectrometric analyses with only unreacted PPh_3 being observed by ^{31}P $\{^1H\}$ NMR spectroscopy.

6.5.3 Synthesis of [PtCl(PEt$_3$){PN(E)}] complexes

Preparation of *N*-methylpiperazine-*N'*-ethylene-diphenylphosphine platinum triethylphosphine dichloride (4.4-1) ([PtCl{κ^2-PN(NMe)}PEt$_3$]$^+$Cl$^-$)

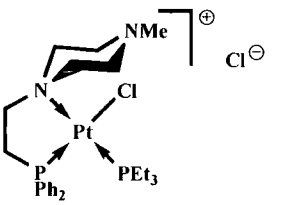

In a glove box, a Young's tap NMR tube was charged with *N*-methylpiperazine-*N'*-ethylene-diphenylphosphine (**2.4-1**) (0.062 g, 1.984×10^{-4} mol) and [PtCl(μ-Cl)(PEt$_3$)]$_2$ (0.076 g, 9.922×10^{-5} mol) and transferred to a Schlenk line. $CDCl_3$ (0.6 cm^3) was added to the tube and the sample shaken well to dissolve to platinum dimer. Following removal of the solvent under vacuum and washing with hexane, the air-stable solid was purified by recrystallisation from CH_2Cl_2/hexane which afforded the required product as a white microcrystalline solid (0.112 g, 81%).

NMR: ^{1}**H** (499.8 MHz, $CDCl_3$): δ 0.82 (dt, $^3J_{PH}$ = 18.0 Hz, $^3J_{HH}$ = 7.5 Hz, 9H, P($CH_2C\underline{H}_3$)$_3$), 1.52 (dq, $^2J_{PH}$ = 18.0 Hz, $^3J_{HH}$ = 7.5 Hz, 6H, P($C\underline{H}_2CH_3$)$_3$), 2.16 (s, 3H, N(CH_2CH_2)$_2$N$C\underline{H}_3$), 2.47 (m, 4H, N($CH_2C\underline{H}_2$)$_2$NMe), 2.92 (m, 2H, $Ph_2PCH_2C\underline{H}_2N$), 3.01 – 3.12 (m, 4H, $Ph_2PC\underline{H}_2CH_2N$ and $Ph_2PCH_2C\underline{H}_2N$), 4.33 (m, 2H, N($C\underline{H}_2CH_2$)$_2$NMe), 7.49 (m, 4H, *m*-Ph$\underline{H}$), 7.54 (m, 2H, *p*-Ph$\underline{H}$), 7.77 (m, 4H, *o*-Ph$\underline{H}$); ^{13}**C {^{1}H}** (125.7 MHz, $CDCl_3$): δ 8.6 (d, $^2J_{CP}$ = 3.9 Hz, P($CH_2\underline{C}H_3$)$_3$), 16.1 (d, $^1J_{CP}$ = 39.3 Hz, P($\underline{C}H_2CH_3$)$_3$), 35.1 (d, $^1J_{CP}$ = 36.9 Hz, $Ph_2P\underline{C}H_2CH_2N$), 46.2 (s, N($CH_2CH_2$)$_2N\underline{C}H_3$), 49.3 (s, N($CH_2\underline{C}H_2$)$_2$NMe), 52.3 (s, $Ph_2PCH_2\underline{C}H_2N$), 55.3 (s, N($\underline{C}H_2CH_2$)$_2$NMe), 124.7 (d, $^1J_{CP}$ = 62.8 Hz, *i*-Ph$\underline{C}$), 130.0 (d, $^3J_{CP}$ = 11.9 Hz, *m*-Ph$\underline{C}$), 133.7 (d, $^4J_{CP}$ = 2.4 Hz, *p*-Ph$\underline{C}$), 134.2 (d, $^2J_{CP}$ = 11.6 Hz, *o*-Ph$\underline{C}$); ^{31}**P {^{1}H}** (161.9 MHz, $CDCl_3$): δ + 6.4 (d + sats., $^1J_{PtP}$ = 3020 Hz, $^2J_{PP}$ = 17.2 Hz, P–$\underline{P}Et_3$), + 34.4 (d + sats., $^1J_{PtP}$ = 3822 Hz, $^2J_{PP}$ = 17.2 Hz, $Ph_2\underline{P}CH_2CH_2N$).

MS (MALDI$^+$, dithranol matrix): *m/z* = 660.3 [M]$^+$.

CHN: Calculated for $C_{25}H_{40}N_2P_2PtCl_2$: C: 43.10; H: 5.80; N: 4.02. Found: C: 43.01; H: 5.62; N: 4.06.

Preparation of morpholine-*N*-ethylene-diphenyl-phosphine platinum triethylphosphine dichloride (4.4-2) ($[PtCl\{\kappa^2\text{-}PN(O)\}PEt_3]^+Cl^-$)

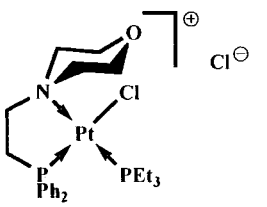

The synthesis of **4.4-2** was analogous to that of **4.4-1** (*vide supra*), employing morpholine-N-ethylene-diphenylphosphine (**2.4-2**) (0.048 g, 1.603×10^{-4} mol) with $[PtCl(\mu\text{-}Cl)(PEt_3)]_2$ (0.062 g, 8.017×10^{-5} mol) in $CDCl_3$ (0.6 cm^3). Following isolation and purification, **4.4-2** was afforded as a white microcrystalline solid (0.091 g, 83 %).

NMR: ^{1}**H** (499.8 MHz, $CDCl_3$): δ 0.82 (dt, $^3J_{PH}$ = 18.0 Hz, $^3J_{HH}$ = 7.5 Hz, 9H, $P(CH_2C\underline{H}_3)_3$), 1.52 (dq, $^2J_{PH}$ = 18.0 Hz, $^3J_{HH}$ = 7.5 Hz, 6H, $P(C\underline{H}_2CH_3)_3$), 3.02 (m, 2H, $N(C\underline{H}_2CH_2)_2O$), 3.07 – 3.24 (m, 4H, $Ph_2PC\underline{H}_2CH_2N$ and $Ph_2PCH_2C\underline{H}_2N$), 3.50 (m, 2H, $N(CH_2C\underline{H}_2)_2O$), 4.00 (m, 2H, $N(CH_2C\underline{H}_2)_2O$), 4.45 (m, 2H, $N(C\underline{H}_2CH_2)_2O$), 7.49 (m, 4H, *m*-Ph$\underline{H}$), 7.56 (m, 2H, *p*-Ph$\underline{H}$), 7.77 (m, 4H, *o*-Ph$\underline{H}$); ^{13}**C** $\{^1$**H**$\}$ (125.7 MHz, $CDCl_3$): δ 8.6 (d, $^2J_{CP}$ = 3.9 Hz, $P(CH_2\underline{C}H_3)_3$), 16.1 (d, $^1J_{CP}$ = 39.3 Hz, $P(\underline{C}H_2CH_3)_2$), 35.4 (d, $^1J_{CP}$ = 40.7, $Ph_2P\underline{C}H_2CH_2N$), 52.6 (s, $Ph_2PCH_2\underline{C}H_2N$), 55.6 (s, $N(\underline{C}H_2CH_2)_2O$), 61.6 (s, $N(CH_2\underline{C}H_2)_2O$), 124.6 (d, $^1J_{CP}$ = 60.8 Hz, *i*-Ph$\underline{C}$), 130.6 (d, $^3J_{CP}$ = 11.6 Hz, *m*-Ph$\underline{C}$), 133.8 (s, *p*-Ph$\underline{C}$), 134.1 (d, $^2J_{CP}$ = 11.4 Hz, *o*-Ph$\underline{C}$); ^{31}**P** $\{^1$**H**$\}$ (161.9 MHz, $CDCl_3$): δ + 6.6 (d + sats., $^1J_{PtP}$ = 3027 Hz, $^2J_{PP}$ = 17.6 Hz, Pt–$\underline{P}Et_3$), + 34.2 (d + sats., $^1J_{PtP}$ = 3803 Hz, $^2J_{HH}$ = 17.6 Hz, $Ph_2\underline{P}CH_2CH_2N$).

MS (MALDI$^+$, dithranol matrix): *m/z* = 664.1 $[M–OH_2]^+$.

CHN: Calculated for $C_{24}H_{37}NOP_2PtCl_2$: C: 42.17; H: 5.47; N: 2.05. Found: C: 42.11; H: 5.27; N: 2.00.

Preparation of thiomorpholine-*N*-ethylene-diphenylphosphine platinum triethylphosphine dichloride (4.4-3)

($[PtCl\{\kappa^2\text{-}PN(S)\}PEt_3]^+Cl^-$)

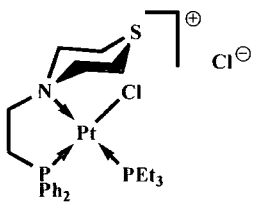

The synthesis of **4.4-3** was analogous to that of **4.4-1** (*vide supra*), employing thiomorpholine-*N*-ethylene-diphenylphosphine (**2.4-3**) (0.070 g, 2.219×10^{-4} mol) with $[PtCl(\mu\text{-}Cl)(PEt_3)]_2$ (0.085 g, 1.109×10^{-5} mol) in $CDCl_3$ (0.6 cm^3). Following isolation and purification, **4.4-3** was afforded as a white microcrystalline solid (0.121 g, 78 %).

NMR: ^{1}**H** (499.8 MHz, $CDCl_3$, 10 °C): δ 0.83 (dt, $^3J_{PH}$ = 18.0 Hz, $^3J_{HH}$ = 7.5 Hz, 9H, $P(CH_2C\underline{H}_3)_3$), 1.53 (dq, $^2J_{PH}$ = 17.5 Hz, $^3J_{HH}$ = 8.2 Hz, 6H, $P(C\underline{H}_2CH_3)_3$), 2.10 (m, 2H, $N(CH_2C\underline{H}_2)_2S$), 3.00 (m, 2H, $Ph_2PCH_2C\underline{H}_2N$), 3.14 (m, 2H, $Ph_2PC\underline{H}_2CH_2N$), 3.30 (m, 2H, $N(CH_2C\underline{H}_2)_2S$), 3.43 (m, 2H, $N(C\underline{H}_2CH_2)_2S$), 4.45 (m, 2H, $N(C\underline{H}_2CH_2)_2S$), 7.52 (m, 4H, *m*-Ph$\underline{H}$), 7.58 (m, 2H, *p*-Ph$\underline{H}$), 7.78 (m, 4H, *o*-Ph$\underline{H}$); ^{13}**C** $\{^1$**H**$\}$ (125.7 MHz, $CDCl_3$, 10 °C): δ 8.7 (d, $^2J_{CP}$ = 3.8 Hz, $P(CH_2\underline{C}H_3)_3$), 16.0 (d, $^1J_{CP}$ = 39.3 Hz, $P(\underline{C}H_2CH_3)_3$), 21.0 (s, $N(CH_2\underline{C}H_2)_2S$), 35.2 (d, $^1J_{CP}$ = 37.8 Hz, $Ph_2P\underline{C}H_2CH_2N$), 51.9 (s, $Ph_2PCH_2\underline{C}H_2N$), 56.7 (s, $N(\underline{C}H_2CH_2)_2S$), 124.5 (d, $^1J_{CP}$ = 62.7 Hz, *i*-Ph$\underline{C}$), 130.1 (d, $^3J_{CP}$ = 11.6 Hz, *m*-Ph$\underline{C}$), 133.9 (s, *p*-Ph$\underline{C}$), 134.2 (*o*-Ph$\underline{C}$); ^{31}**P** $\{^1$**H**$\}$ (161.9 MHz, $CDCl_3$): δ + 6.5 (d + sats., $^1J_{PtP}$ = 3037 Hz, $^2J_{PP}$ = 17.2 Hz, Pt–$\underline{P}Et_3$), + 34.1 (d + sats., $^1J_{PtP}$ = 3792 Hz, $^2J_{PP}$ = 17.4 Hz, $Ph_2\underline{P}CH_2CH_2N$).

MS (MALDI$^+$, dithranol matrix): *m/z* = 545.0 $[M–PEt_3]^+$

CHN: Calculated for $C_{24}H_{37}NSP_2PtCl_2$: C: 41.20; H: 5.34; N: 2.00. Found: C: 41.29; H: 5.30; N: 2.17.

Preparation of piperidine-*N*-ethylene-diphenylphosphine platinum triethylphosphine dichloride (4.4-4) ($[PtCl\{\kappa^2\text{-}PN(C)\}PEt_3]^+Cl^-$)

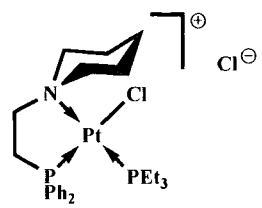

The synthesis of **4.4-4** was analogous to that of **4.4-1** (*vide supra*), employing piperdine-*N*-ethylene-diphenylphosphine (**2.4-3**) (0.046 g, 1.547×10^{-4} mol) with $[PtCl(\mu\text{-}Cl)(PEt_3)]_2$ (0.059 g, 7.733×10^{-5} mol) in $CDCl_3$ (0.6 cm^3). Following isolation and purification, **4.4-4** was afforded as a white microcrystalline solid (0.081 g, 77 %). Slow diffusion of hexane into a concentrated solution of **4.4-4** in CH_2Cl_2 afforded colourless crystals suitable for analysis for X-ray diffraction studies.

NMR: ^{1}**H** (499.8 MHz, $CDCl_3$): δ 0.82 (dt, $^3J_{PH}$ = 18.0 Hz, $^3J_{HH}$ = 7.5 Hz, 9H, $P(CH_2C\underline{H}_3)_3$), 1.38 (m, 2H, $N(CH_2C\underline{H}_2)_2CH_2$), 1.46 (m, 1H, $N(CH_2CH_2)_2C\underline{H}_2$), 1.52 (dq, $^2J_{PH}$ = 17.5 Hz, $^3J_{HH}$ = 8.0 Hz, 6H, $P(C\underline{H}_2CH_3)_3$), 1.63 (m, 1H, $N(CH_2CH_2)_2C\underline{H}_2$), 1.86 (m, 2H, $N(CH_2C\underline{H}_2)_2CH_2$), 2.89 – 3.04 (m, 6H, $Ph_2PC\underline{H}_2CH_2N$, $Ph_2PCH_2C\underline{H}_2N$ and $N(C\underline{H}_2CH_2)_2CH_2$), 4.08 (m, 2H, $N(C\underline{H}_2CH_2)_2CH_2$), 7.51 (m, 4H, *m*-Ph$\underline{H}$), 7.57 (m, 2H, *p*-Ph$\underline{H}$), 7.75 (m, 4H, *o*-Ph$\underline{H}$); ^{13}**C** $\{^1$**H**$\}$ (125.7 MHz, $CDCl_3$): δ 8.6 (d, $^2J_{CP}$ = 3.7 Hz, $P(CH_2\underline{C}H_3)_3$), 16.1 (d, $^1J_{CP}$ = 39.3 Hz, $P(\underline{C}H_2CH_3)_3$), 20.6 (s, $N(CH_2\underline{C}H_2)_2CH_2$), 23.5 (s, $N(CH_2CH_2)_2\underline{C}H_2$), 35.5 (d, $^1J_{CP}$ = 38.3 Hz, $Ph_2P\underline{C}H_2CH_2N$), 52.6 (d, $^2J_{CP}$ = 2.4 Hz, $Ph_2PCH_2\underline{C}H_2N$), 56.3 (s, $N(\underline{C}H_2CH_2)_2CH_2$), 124.6 (d, $^1J_{CP}$ = 62.8 Hz, *i*-Ph$\underline{C}$), 130.0 (d, $^3J_{CP}$ = 11.9 Hz, *m*-Ph$\underline{C}$), 133.8 (d, $^4J_{CP}$ = 2.9 Hz, *p*-Ph$\underline{C}$), 134.1 (d, $^2J_{CP}$ = 11.6 Hz, *o*-Ph$\underline{C}$); ^{31}**P** $\{^1$**H**$\}$ (161.9 MHz, $CDCl_3$): δ + 5.9 (d + sats., $^1J_{PtP}$ = 2971 Hz, $^2J_{PP}$ = 17.2 Hz, Pt–$\underline{P}Et_3$), + 34.2 (d + sats., $^1J_{PtP}$ = 3834 Hz, $^2J_{PP}$ = 17.5 Hz, $Ph_2\underline{P}CH_2CH_2N$).

MS (MALDI$^+$, dithranol matrix): *m/z* = 646.2 $[M]^+$.

CHN: Calculated for $C_{25}H_{39}NP_2PtCl_2$: C: 44.02; H: 5.78; N: 2.06. Found: C: 44.02; H: 5.80; N: 2.11.

6.6 Preparation of [RhCl(CO){PNE}] complexes

6.6.1 Synthesis of [RhCl(CO){PNE}] complexes

Preparation of *N*-methylpiperazine-*N'*-ethylene-diphenylphosphine rhodium triphenylphosphine carbonyl chloride (5.1)

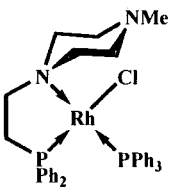

A solution of *N*-methylpiperazine-*N'*-ethylene-diphenylphosphine (**2.4-1**) (0.068 g, 2.176×10^{-4} mol) in CH_2Cl_2 (20 cm^3) was transferred *via* cannula to a CH_2Cl_2 solution (30 cm^3) of $[RhCl(PPh_3)_3]$ (0.200 g, 2.162×10^{-4} mol) and the resulting solution allowed to stir at room temperature for 16h. The solvent was removed *in vacuo* and the resulting solid extracted repeatedly with hexane. Following thorough drying under vacuum, the product was afforded as an orange solid (0.082 g, 53 %).

NMR: $^1H/^{13}C$ $\{^1H\}$: Spectra too broad for reliable assignment.
^{31}P $\{^1H\}$ (121.4 MHz, C_6D_6): δ + 36.8 (dd, $^1J_{RhP}$ = 125.9 Hz, $^2J_{PP}$ = 32.2 Hz, $\underline{P}Ph_3$), + 62.6 (dd, $^1J_{RhP}$ = 173.6 Hz, $^2J_{PP}$ = 32.2 Hz, $Ph_2\underline{P}CH_2CH_2N$).

Preparation of *N*-methylpiperazine-*N'*-ethylene-diphenyl-phosphine rhodium carbonyl chloride (5.2-1)

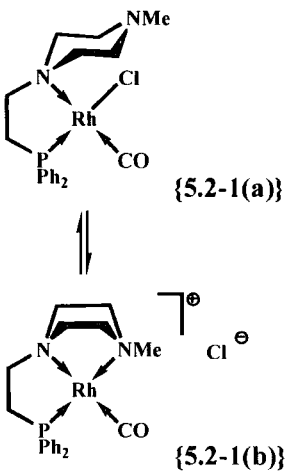

A solution of *N*-methylpiperazine-*N'*-ethylene-diphenyl-phosphine (**2.4-1**) (0.188 g, 6.017×10^{-4} mol) in CH_2Cl_2 (10 cm^3) was transferred *via* cannula to a CH_2Cl_2 solution (10 cm^3) of $[Rh_2\{\mu\text{-}Cl\}_2(CO)_4]$ (0.117 g, 3.009×10^{-4} mol) and the resulting solution allowed to stir at room temperature for 2h. The solvent was then removed under vacuum and following extraction with hexane and thorough drying *in vacuo*, the product was afforded as a dark yellow solid (0.204 g, 71 %). Slow diffusion of hexane into a concentrated CH_2Cl_2 solution of **5.2-1** afforded crystals suitable for study by X-ray diffraction, the structure of which was shown to be consistent with that of **5.2-1(a)**.

Due to the fluxionality exhibited by **5.2-1** in chlorinated solution, NMR spectroscopic analyses were performed at low temperatures. At – 50 °C, two discrete structures were observed in the ^{1}H, ^{13}C $\{^{1}H\}$ and ^{31}P $\{^{1}H\}$ NMR spectra. Integration of both the ^{1}H and ^{31}P $\{^{1}H\}$ NMR spectra revealed the ratio of **5.2-1(a)**:**5.2-1(b)** as 4:1.

NMR: ^{1}H (499.8 MHz, $CDCl_3$, – 50 °C):

	5.2-1(a)	**5.2-1(b)**
δ	2.22 (s, 3H, $N(CH_2CH_2)_2NC\underline{H}_3$)	
	2.29 (m, 2H, $N(C\underline{H}_2CH_2)_2NMe$)	
	2.44 (m, 2H, $N(C\underline{H}_2CH_2)_2NMe$)	
	2.58 – (m, 2.4H:	
	2.65 2H, $Ph_2PC\underline{H}_2CH_2N$	0.4H, $Ph_2PCH_2C\underline{H}_2N$)
	2.77 (m, 2H, $N(CH_2C\underline{H}_2)_2NMe$)	
	2.88 – (m, 3H:	
	3.13 2H, $Ph_2PCH_2C\underline{H}_2N$	0.4H, $Ph_2PC\underline{H}_2CH_2N$, and $N(CH_2CH_2)_2NC\underline{H}_3$)
		3.12 (m, 0.4H, $N(CH_2C\underline{H}_2)_2NMe$)
		3.37 (m, 0.4H, $N(C\underline{H}_2CH_2)_2NMe$)
		3.46 (m, 0.4H, $N(C\underline{H}_2CH_2)_2NMe$)
		3.75 (m, 0.4H, $N(CH_2C\underline{H}_2)_2NMe$)
	4.17 (m, 2H, $N(CH_2C\underline{H}_2)_2NMe$)	
	7.41 – (m, 4.8H:	
	7.58 4H, *m*-/*p*-Ph$\underline{H}$	0.8H, *m*-/*p*-Ph$\underline{H}$)
	7.62 – (m, 7.2H:	
	7.77 6H, *o*-Ph$\underline{H}$	1.2H, *o*-Ph$\underline{H}$).

^{13}C {^{1}H} (125.7 MHz, $CDCl_3$, – 50 °C):

	5.2-1(a)		**5.2-1(b)**	
δ	30.1	(d, $^{1}J_{CP}$ = 27.3 Hz, $Ph_2P\underline{C}H_2CH_2N$)	35.1	(d, $^{1}J_{CP}$ = 28.8 Hz, $Ph_2P\underline{C}H_2CH_2N$)
	46.9	(s, $N(CH_2CH_2)_2N\underline{C}H_3$)	50.6	(s, $Ph_2PCH_2\underline{C}H_2N$)
	48.4	(s, $N(\underline{C}H_2CH_2)_2NMe$)	50.9	(s, $N(CH_2CH_2)_2N\underline{C}H_3$)
	53.0	(s, $N(CH_2\underline{C}H_2)_2NMe$)	53.6	(s, $N(\underline{C}H_2CH_2)_2NMe$)
	54.2	(s, $Ph_2PCH_2\underline{C}H_2N$)	57.3	(s, $N(CH_2\underline{C}H_2)_2NMe$)
	129.3	(d, $^{3}J_{CP}$ = 11.1 Hz, *m*-Ph$\underline{C}$)	129.7	(d, $^{3}J_{CP}$ = 11.1 Hz, *m*-Ph$\underline{C}$)
	131.3	(s, *i*-Ph$\underline{C}$)	130.2	(s, *i*-Ph$\underline{C}$)
	131.7	(s, *p*-Ph$\underline{C}$)	130.9	(d, $^{2}J_{CP}$ = 9.6 Hz, *o*-Ph$\underline{C}$)
	133.3	(d, $^{2}J_{CP}$ = 12.1 Hz, *o*-Ph$\underline{C}$)	132.4	(s, *p*-Ph$\underline{C}$)
	188.0	(dd, $^{1}J_{RhC}$ = 72.6 Hz, $^{2}J_{CP}$ = 17.9 Hz, Rh–$\underline{C}$O)	181.4	(d, $^{1}J_{RhC}$ = 72.4 Hz, Rh–$\underline{C}$O)

^{31}P {^{1}H} (202.3 MHz, $CDCl_3$, – 50 °C):

	5.2-1(a)			**5.2-1(b)**		
δ	+ 61.0	(d, $^{1}J_{RhP}$ = 171.8 Hz)	80 %	+ 58.0	(d, $^{1}J_{RhP}$ = 162.0 Hz)	20 %

As discussed in Chapter 5, Section 5.3, the $^{1}H/^{13}C$ {^{1}H}/^{31}P {^{1}H} NMR spectra of **5.2-1** in CD_3OD were shown to be consistent with the charged $[RhCl(CO)\{\kappa^3\text{-}PNNMe\}]^+ Cl^-$ structure **5.2-1(b)**.

NMR: ^{1}H (299.9 MHz, CD_3OD, AT): δ 2.58 – 3.20 (m, 11H, $Ph_2PC\underline{H}_2CH_2N$, $Ph_2PCH_2C\underline{H}_2N$, $N(C_4\underline{H}_8)NMe$, $N(C_4H_8)NC\underline{H}_3$), 3.62 (m, 2H, $N(C_4\underline{H}_8)NMe$), 3.84 (m, 2H, $N(C_4\underline{H}_8)NMe$), 7.25 – 7.36 (*m*-/*p*-Ph$\underline{H}$), 7.78 (m, 4H, *o*-Ph$\underline{H}$); **^{13}C {^{1}H}** (125.7 MHz, CD_3OD, AT): δ 34.5 (d, $^{1}J_{CP}$ = 30.7 Hz, $Ph_2P\underline{C}H_2CH_2N$), 49.5 (s, $N(CH_2CH_2)_2N\underline{C}H_3$), 53.2 (s, $N(CH_2\underline{C}H_2)_2NMe$), 54.1 (s, $Ph_2PCH_2\underline{C}H_2N$), 56.8 (s, $N(\underline{C}H_2CH_2)_2NMe$), 129.1 (d, $^{1}J_{CP}$ = 11.1 Hz, *m*-Ph$\underline{C}$), 130.6 (d, $^{1}J_{CP}$ = 9.7 Hz, *i*-Ph$\underline{C}$),

131.6 (s, *p*-PhC), 132.9 (d, $^2J_{CP}$ = 11.9 Hz, *o*-PhC), 190.7 (dd, $^1J_{RhC}$ = 79.7 Hz, $^2J_{CP}$ = 16.8 Hz, Rh–CO); **^{31}P {^{1}H}** (202.3 MHz, CD_3OD, AT): δ + 59.6 (d, $^1J_{RhP}$ = 160.2 Hz).

MS (MALDI$^+$, dithranol matrix): *m/z* = 443.0 $[M–Cl]^+$.

CHN: Calculated for $C_{20}H_{25}N_2PORhCl$: C: 50.17; H: 5.27; N: 5.85. Found: C: 50.23; H: 5.16; N: 5.80.

IR ($CHCl_3$ solution): 1998 cm^{-1} (ν_{CO}).

Preparation of morpholine-*N*-ethylene-diphenylphosphine rhodium carbonyl chloride (5.2-2)

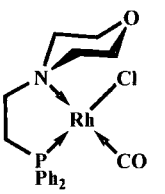

The synthesis of **5.2-2** was analogous to that detailed for the related compound **5.2-1** (*vide supra*), *i.e.* employing morpholine-*N*-ethylene-diphenylphosphine (**2.4-2**) (0.200 g, 6.681×10^{-4} mol) with $[Rh_2\{\mu\text{-}Cl\}_2(CO)_4]$ (0.130 g, 3.340×10^{-4} mol) in CH_2Cl_2 (20 cm^3). Following isolation and purification, the target product **5.2-2** was afforded as a bright yellow powder (0.232 g, 75 %). Slow evaporation of a CH_2Cl_2 solution of **5.2-2** afforded crystals suitable for analysis by X-ray diffraction.

NMR: ^{1}H (499.8 MHz, $CDCl_3$, – 10 °C): δ 2.58 – 2.70 (m, 4H, $Ph_2PCH_2CH_2N$ and $N(CH_2CH_2)_2O$), 3.12 (m, 2H, $Ph_2PCH_2CH_2N$), 3.54 (m, 2H, $N(CH_2CH_2)_2O$), 3.85 (m, 2H, $N(CH_2CH_2)_2O$), 4.33 (m, 2H, $N(CH_2CH_2)_2O$), 7.46 (m, 4H, *m*-PhH), 7.51 (m, 2H, *p*-PhH), 7.74 (m, 4H, *o*-PhH); **^{13}C {^{1}H}** (125.7 MHz, $CDCl_3$, – 50 °C): δ 30.2 (d, $^1J_{CP}$ = 27.8 Hz, $Ph_2PCH_2CH_2N$), 50.7 (br s, $\nu_{½}$ = 35.9 Hz, $Ph_2PCH_2CH_2N$), 53.3 (s, $N(CH_2CH_2)_2O$), 60.3 (s, $N(CH_2CH_2)_2O$), 129.3 (d, $^3J_{CP}$ = 10.6 Hz, *m*-PhC), 131.0 (s, *i*-PhC), 131.8 (s, *p*-PhC), 133.3 (d, $^2J_{CP}$ = 11.9 Hz, *o*-PhC), 187.8 (dd, $^1J_{RhP}$ = 73.1 Hz, $^2J_{CP}$ = 18.9 Hz, Rh–CO); **^{31}P {^{1}H}** (202.3 MHz, $CDCl_3$,– 50 °C): δ + 60.8 (d, $^1J_{RhP}$ = 172.6 Hz);

MS (MALDI$^+$, dithranol matrix): *m/z* = 430.0 $[M–Cl]^+$

CHN: Calculated for $C_{19}H_{22}NO_2PRhCl$: C: 49.00; H: 4.77; N: 3.01. Found: C: 48.87; H: 4.56; N: 2.71.

IR ($CHCl_3$ solution): 2001 cm^{-1} (ν_{CO}).

Preparation of thiomorpholine-N-ethylene-diphenylphosphine rhodium carbonyl chloride (5.2-3)

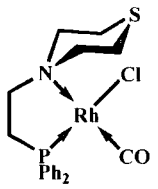

{5.2-3(a)}

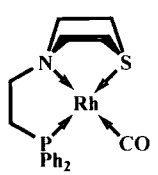

{5.2-3(b)}

The synthesis of **5.2-3** was analogous to that detailed for the related compound **5.2-1** (*vide supra*), *i.e.* employing thiomorpholine-*N*-ethylene-diphenylphosphine (**2.4-3**) (0.400 g, 1.268×10^{-3} mol) with $[Rh_2\{\mu\text{-}Cl\}_2(CO)_4]$ (0.246 g, 6.340×10^{-4} mol) in CH_2Cl_2 (20 cm^3). Following isolation and purification, the target product **5.2-3** was afforded as a bright yellow powder (0.527 g, 86 %).

Due to the fluxionality exhibited by **5.2-3**, NMR spectroscopic analysis was performed at low temperatures. At – 50 °C, two discrete structures were observed in the ^{31}P $\{^1H\}$ NMR spectrum. Integration of the ^{31}P $\{^1H\}$ spectrum revealed the ratio of **5.2-3(a)**:**5.2-3(b)** as 4:1 (– 50 °C). The severely broadened nature of the ^1H and ^{13}C $\{^1H\}$ NMR spectra in $CDCl_3$, even at low temperatures, precluded solution characterisation of **5.2-3** by these nuclei.

^{31}P $\{^1H\}$ (202.3 MHz, $CDCl_3$, – 50 °C):

	5.2-3(a)		**5.2-3(b)**	
δ	+ 60.7 (d, $^1J_{RhP}$ = 173.6 Hz)	80 %	+ 53.6 (d, $^1J_{RhP}$ = 162.1 Hz)	20%

As discussed in Chapter 5, Section 5.3, the $^1H/^{13}C$ $\{^1H\}/^{31}P$ $\{^1H\}$ NMR spectra of **5.2-3** in CD_3OD were shown to be consistent with the charged $[RhCl(CO)\{\kappa^3\text{-}PNS\}]^+ Cl^-$ structure **5.2-3(b)**.

NMR: ^1H (499.8 MHz, CD_3OD, AT): δ 2.81 – 2.94 (m, 4H, $Ph_2PCH_2C\underline{H}_2N$ and $N(C_4\underline{H}_8)S$), 3.19 (m, 2H, $Ph_2PC\underline{H}_2CH_2N$), 3.35 – 3.46 (m, 2H, $N(C_4\underline{H}_8)S$), 3.53 – 3.66 (m, 4H, $N(C_4\underline{H}_8)S$), 7.55 – 7.64 (m, 6H, *m*-/*p*-Ph$\underline{H}$), 7.82 (m, 4H, *o*-Ph$\underline{H}$); **^{13}C $\{^1H\}$** (125.7 MHz, CD_3OD, AT): δ 33.0 (d, $^1J_{CP}$ = 30.2 Hz, $Ph_2P\underline{C}H_2CH_2N$), 55.2 (s,

N($\underline{C}_4H_8$)S), 55.7 (s, $Ph_2PCH_2\underline{C}H_2N$), 129.3 (d, $^3J_{CP}$ = 11.1 Hz, *m*-Ph$\underline{C}$), 130.2 (d, $^1J_{CP}$ = 50.4 Hz, *i*-Ph$\underline{C}$), 131.9 (d, $^4J_{CP}$ = 2.4 Hz, *p*-Ph$\underline{C}$), 133.1 (d, $^2J_{CP}$ = 12.4 Hz, *o*-Ph$\underline{C}$). *NB*. N($\underline{C}_4H_8$)S resonance obscured by solvent signal and Rh–$\underline{C}$O signal not observed due to high signal to noise ratio of dilute sample.

^{31}P {^{1}H} (202.3 MHz, CD_3OD, AT): δ + 54.7 (d, $^1J_{RhP}$ = 164.1 Hz).

MS (MALDI+, dithranol matrix): *m/z* = 446.1 $[M–Cl]^+$.

CHN: Calculated for $C_{19}H_{22}NPSORhCl$: C: 47.36; H: 4.61; N: 2.91. Found: C: 47.04; H: 4.33; N: 2.83.

IR ($CHCl_3$ solution): 2000 cm^{-1} (ν_{CO}).

Preparation of piperidine-N-ethylene-diphenylphosphine rhodium carbonyl chloride (5.2-4)

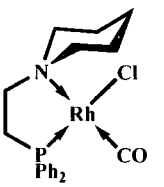

The synthesis of **5.2-4** was analogous to that detailed for the relatedcompound **5.2-1** (*vide supra*), *i.e.* employing piperidine-*N*-ethylene-diphenylphosphine (**2.4-4**) (0.141 g, 4.741×10^{-4} mol) with $[Rh_2\{\mu\text{-}Cl\}_2(CO)_4]$ (0.092 g, 2.370×10^{-4} mol) in CH_2Cl_2 (15 cm^3). Following isolation and purification, the target product **5.2-3** was afforded as a yellow-brown powder (0.174 g, 79 %).

NMR: ^{1}H (499.8 MHz, $CDCl_3$): δ 1.33 (m, 2H, $N(CH_2C\underline{H}_2)_2CH_2$), 1.53 – 1.75 (m, 4H, $N(CH_2C\underline{H}_2)_2CH_2$ and $N(CH_2CH_2)_2C\underline{H}_2$), 2.59 (m, 2H, $Ph_2PC\underline{H}_2CH_2N$), 2.81 (m, 2H, $N(C\underline{H}_2CH_2)_2CH_2$), 2.93 (m, 2H, $Ph_2PCH_2C\underline{H}_2N$), 3.95 (m, 2H, $N(C\underline{H}_2CH_2)_2CH_2$), 7.42 – 7.51 (m, 6H, *m-/p*-Ph$\underline{H}$), 7.75 (m, 4H, *o*-Ph$\underline{H}$); **^{13}C {^{1}H}** (125.7 MHz, $CDCl_3$): δ 19.4 (s, $N(CH_2\underline{C}H_2)_2CH_2$), 23.9 (s, $N(CH_2CH_2)_2\underline{C}H_2$), 30.4 (d, $^2J_{CP}$ = 27.4 Hz, $Ph_2P\underline{C}H_2CH_2N$), 50.7 (d, $^2J_{CP}$ = 5.3 Hz, $Ph_2PCH_2\underline{C}H_2N$), 53.8 (s, $N(\underline{C}H_2CH_2)_2CH_2$), 129.1 (d, $^3J_{CP}$ = 10.3 Hz, *m*-Ph$\underline{C}$), 131.3 (d, $^4J_{CP}$ = 2.4 Hz, *p*-Ph$\underline{C}$), 132.2 (d, $^1J_{CP}$ = 51.3 Hz, *i*-Ph$\underline{C}$), 133.1 (d, $^2J_{CP}$ = 12.4 Hz, *o*-Ph$\underline{C}$), 188.1 (dd, $^1J_{RhC}$ = 72.0 Hz, $^2J_{CP}$ = 18.2 Hz, Rh–$\underline{C}$O); **^{31}P {^{1}H}** (202.3 MHz, $CDCl_3$): δ + 60.8 ($^1J_{RhP}$ = 175.5 Hz);

MS (ES^+): *m/z* = 428.1 $[M–Cl]^+$

CHN: Calculated for $C_{20}H_{24}PNORhCl$: C: 51.79; H: 5.23; N: 3.02. Found: C: 51.61; H: 5.11; N: 2.84.

IR ($CHCl_3$ solution): 1998 cm^{-1} (ν_{CO}).

Attempted preparation of *N*-phenylpiperazine-*N'*-ethylene-diphenylphosphine rhodium carbonyl chloride (5.2-5)

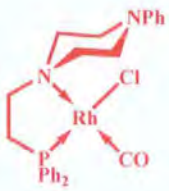

The attempted synthesis of 5.2-5 was analogous to that detailed for the related compound 5.2-1 (*vide supra*), *i.e.* employing *N*-phenylpiperazine-*N'*-ethylene-diphenylphosphine (2.4-5) (0.173 g, 4.631×10^{-4} mol) with $[Rh_2\{\mu\text{-}Cl\}_2(CO)_4]$ (0.090 g, 2.315×10^{-4} mol) in CH_2Cl_2 (30 cm^3). Upon stirring of the reaction mixture at room temperature for 2h, the formation of a brown precipitate was observed. However, analysis by NMR spectroscopy and mass spectrometry did not demonstrate the presence of the target product.

Attempted preparation of piperazine-*N,N'*-diethylene-tetraphenyldiphosphine rhodium carbonyl chloride (5.2-6)
[RhCl(CO){PNNP}]

The attempted synthesis of 5.2-6 was analogous to that detailed for the related compound 5.2-1 (*vide supra*), *i.e.* employing piperazine-*N,N'*-diethylene-tetraphenyldiphosphine (2.4-7) (0.307 g, 6.020×10^{-4} mol) with $[Rh_2\{\mu\text{-}Cl\}_2(CO)_4]$ (0.117 g, 3.010×10^{-4} mol) in CH_2Cl_2 (35 cm^3). However, upon isolation of the obtained product, analysis by NMR spectroscopy and mass spectroscopy did not demonstrate the presence of the target product.

Attempted preparation of piperazine-*N,N'*-diethylene-tetraphenyldiphosphine *bis*(rhodium carbonyl chloride) (5.3)
$[Rh_2Cl_2(CO)_2\{PNNP\}]$

A solution of piperazine-*N,N'*-diethylene-tetraphenyldiphosphine (**2.4-7**) (0.131 g, 2.573×10^{-4} mol) in CH_2Cl_2 (10 cm^3) was transferred *via* cannula to a CH_2Cl_2 solution (10 cm^3) of $[Rh_2\{\mu\text{-}Cl\}_2(CO)_4]$ (0.100 g, 2.573×10^{-4} mol). On addition of **2.4-7** to the rhodium precursor, the solution was noted to undergo a rapid colour change from dark orange to green. The resulting mixture was allowed to stir at room temperature for 2h

before removal of the solvent under vacuum. Following washing with hexane and thorough drying under vacuum, a dark green-brown solid was obtained, however analysis by NMR spectroscopy and mass spectrometry did not demonstrate the presence of the target bimetallic product.

6.6.2 Synthesis of $[RhCl(CO)\{\kappa^3\text{-PNE}\}]^+ BF_4^-$ complexes

Preparation of *N*-methylpiperazine-*N'*-ethylene-diphenyl-phosphine rhodium carbonyl tetrafluoroborate (5.4-1)

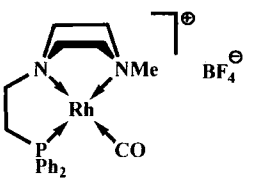

In a glove box, a Schlenk flask was charged with *N*-methylpiperazine-*N'*-ethylene-diphenylphosphine rhodium carbonyl chloride (**5.4-1**) (0.202 g, 4.219×10^{-4} mol) and silver tetrafluoroborate (0.082 g, 4.219×10^{-4} mol) and the flask transferred to a vacuum line. CH_2Cl_2 (15 cm^3) was added *via* cannula to the flask and the resulting mixture allowed to stir at room temperature for 15h by which time the formation of a dark grey-brown suspension was evident. The solution was filtered to removed the precipitated salt and the product dried under vacuum. Following extraction with hexane and drying *in vacuo*, the product was afforded as a light brown powder (0.148 g, 66 %).

NMR: ^{1}**H** (499.8 MHz, $CDCl_3$): δ 2.84 (m, 2H, $Ph_2PCH_2C\underline{H}_2N$), 2.96 – 3.07 (m, 7H, $Ph_2PC\underline{H}_2CH_2N$; $N(CH_2C\underline{H}_2)_2NMe$ and $N(CH_2CH_2)_2NC\underline{H}_3$), 3.12 (m, 2H, $N(C\underline{H}_2CH_2)_2NMe$), 3.49 (m, 2H, $N(C\underline{H}_2CH_2)_2NMe$), 3.76 (m, 2H, $N(CH_2C\underline{H}_2)_2NMe$), 7.46 – 7.55 (m, 6H, *m-/p*-Ph<u>H</u>), 7.67 (m, 4H, *o*-Ph<u>H</u>); ^{13}**C** {^{1}**H**} (125.7 MHz, $CDCl_3$): δ 33.8 (d, $^2J_{PC}$ = 29.7 Hz, $Ph_2P\underline{C}H_2CH_2N$), 49.4 (s, $N(CH_2CH_2)_2N\underline{C}H_3$), 52.2 (s, $N(\underline{C}H_2CH_2)_2NMe$), 53.0 (s, $Ph_2PCH_2\underline{C}H_2N$), 56.0 (s, $N(CH_2\underline{C}H_2)_2NMe$), 128.3 (d, $^3J_{CP}$ = 11.1 Hz, *m*-Ph<u>C</u>), 128.9 (d, $^1J_{PC}$ = 2.0 Hz, *i*-Ph<u>C</u>), 130.7 (d, $^4J_{CP}$ = 2.4 Hz, *p*-Ph<u>C</u>), 131.7 (d, $^2J_{CP}$ = 12.4 Hz, *o*-Ph<u>C</u>), 189.1 (dd, $^1J_{RhC}$ = 75.8 Hz, $^2J_{CP}$ = 18.2 Hz, Rh–<u>C</u>O); ^{31}**P** {^{1}**H**} (202.3 MHz, $CDCl_3$): δ + 59.0 (d, $^1J_{RhP}$ = 161.8 Hz); ^{19}**F** (282.2 MHz, $CDCl_3$): δ – 151.7 (s); ^{11}**B** (128.4 MHz, $CDCl_3$): δ – 0.94 (s).

MS (MALDI$^+$, dithranol matrix): *m/z* = 443.2 $[M]^+$; 416.6 $[M–CO]^+$

CHN: Calculated for $C_{20}H_{25}N_2OPRhBF_4$: C: 45.31; H: 4.76; N: 5.29. Found: C: 45.49; H: 4.80; N: 5.40.

IR ($CHCl_3$ solution): 2000 cm^{-1} (ν_{CO}).

Attempted preparation of morpholine-N-ethylene-diphenyl-phosphine rhodium carbonyl tetrafluoroborate (5.4-2)

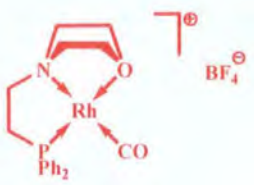

The attempted synthesis of **5.4-2** was analogous to that of the related complex **5.4-1** (*vide supra*), *i.e.* employing morpholine-*N*-ethylene-diphenylphosphine rhodium carbonyl chloride (**5.2-1**) (0.105 g, 2.255×10^{-4} mol) and $AgBF_4$ (0.044 g, 2.255×10^{-4} mol) in CH_2Cl_2 (20 cm^3). Upon allowing the resulting mixture to stir at room temperature for 14h, the formation of a black precipitate was noted which was separated from the orange supernatant solution by filtration. Removal of the solvent from the orange filtrate afforded a dark orange solid which was shown by $^{31}P\{^1H\}$ NMR spectroscopy to comprise a number of presumed ligand degradation products whilst analysis of the precipitate by NMR spectroscopy and mass spectrometry did not indicate the presence of the target product.

Preparation of thiomorpholine-*N*-ethylene-diphenylphosphine rhodium carbonyl tetrafluoroborate

(5.4-3)

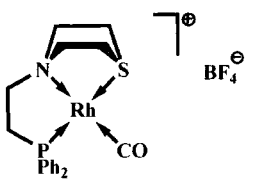

The attempted synthesis of **5.4-3** was analogous to that of the related complex **5.4-1** (*vide supra*), *i.e.* employing thiomorpholine-*N*-ethylene-diphenylphosphine rhodium carbonyl chloride (**5.2-3**) (0.125 g, 2.594×10^{-4} mol) and $AgBF_4$ (0.051 g, 2.594×10^{-4} mol) in CH_2Cl_2 (20 cm^3). Following isolation and purification, the product was afforded as a dark yellow-brown powder (0.090 g, 65 %).

5.4-3 was shown to demonstrate a unexpected tolerance to atmospheric conditions and proved to be soluble in toluene. Upon slow evaporation of a PhMe solution of **5.4-3** under air, crystals suitable for analysis by X-ray diffraction were obtained.

NMR: ^{1}**H** (400.1 MHz, $CDCl_3$): δ 2.85 (m, 2H, $Ph_2PC_2\underline{H}_4N$), 2.94 (m, 2H, $Ph_2NC_2\underline{H}_4N$), 3.09 (m, 2H, $NC_4\underline{H}_8S$), 3.38 (m, 6H, $NC_4\underline{H}_8S$), 7.42 – 7.51 (m, 6H, *m-/p*-Ph<u>H</u>), 7.62 (m, 4H, *o*-Ph<u>H</u>); ^{13}**C {^{1}H}** (125.7 MHz, $CDCl_3$): δ 29.9 (s, $Ph_2P\underline{C}H_2CH_2N$); 33.8 (s, $N(\underline{C}H_2CH_2)_2S$), 55.4 (s, $N(CH_2\underline{C}H_2)_2S$), 56.0 (s, $Ph_2PCH_2\underline{C}H_2N$), 129.8 (d, $^{3}J_{CP}$ = 10.9 Hz, *m*-Ph<u>C</u>), 132.3 (s, *p*-Ph<u>C</u>), 133.1 (d, $^{2}J_{CP}$ = 12.4 Hz, *o*-Ph<u>C</u>), 138.2 (s, *i*-Ph<u>C</u>), 191.9 (dd, $^{1}J_{RhC}$ = 91.7 Hz, $^{1}J_{CP}$ = 15.1 Hz, Rh–<u>C</u>O); ^{31}**P {^{1}H}** (202.3 MHz, $CDCl_3$): δ + 54.1 (d, $^{1}J_{RhP}$ = 162.5 Hz); ^{19}**F** (188.2 MHz, $CDCl_3$): δ – 151.8 (s); ^{11}**B** (128.4 MHz, $CDCl_3$): δ – 0.92 (s).

MS (MALDI^{+}, dithranol matrix): *m/z* = 446.2 $[M]^{+}$; 419.0 $[M–CO]^{+}$.

CHN: Calculated for $C_{19}H_{22}NSPORhBF_4$: C: 42.80; H: 4.17; N: 2.63. Found: C: 43.09; H: 4.66; N: 2.86.

IR ($CHCl_3$ solution): 2011 cm^{-1} (ν_{CO}).

6.6.3 Attempted Synthesis of [RhCl(CO){PNO}] derivatives

Attempted preparation of morpholine-*N*-ethylene-diphenylphosphine rhodium acetonitrile carbonyl hexafluorophosphate (5.5)

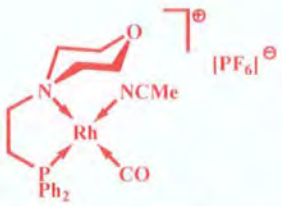

Under a flow of nitrogen, $NaPF_6$ (0.029 g, 1.727×10^{-4} mol) was added as a solid to a MeCN solution (50 cm^3) of morpholine-*N*-ethylene-diphenylphosphine rhodium carbonyl chloride (**5.2-2**) (0.072 g, 1.546×10^{-4} mol). Upon stirring of the mixture for 24h, the formation of a black precipitate was noted which was separated from the solution by filtration, although upon analysis of both the solid and solution by $^{31}P\ \{^1H\}$ NMR spectroscopy, no reaction was observed to have occurred.

Attempted preparation of morpholine-*N*-ethylene-diphenylphosphine rhodium acetonitrile carbonyl tetrafluoroborate (5.6)

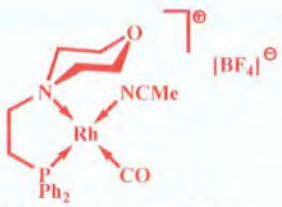

The attempted synthesis of **5.6** was analogous to that detailed for **5.5** (*vide supra*), *i.e.* by reaction of morpholine-*N*-ethylene-diphenylphosphine rhodium carbonyl chloride (**5.2-2**) with $AgBF_4$ in MeCN (45 cm^3). Upon stirring of the mixture for 14h at room temperature, the formation of a black precipitate was noted, which was separated from solution by filtration. However, the presence of the target product was not noted in either the solid or solution fractions by $^{31}P\ \{^1H\}$ NMR spectroscopy with only a number of presumed degradation products being observed instead.

6.7 References

[1] S. Komiya, "*Synthesis of Organometallic Compounds – A Practical Guide*", Wiley-Interscience, New York, 1998.

[2] J. R. Doyle and D. Drew, *Inorg. Synth.*, 1990, **28**, 346 – 349.

[3] An adaptation of the preparation by R. E. Rülke, J. M. Ernsting, A. L. Spek, C. J. Elsevier, P. W. N. M. van Leeuwen and K. Vrieze, *Inorg. Chem.*, 1993, 5769 – 5778 was used for the preparation of this compound.

[4] W. de Graaf, J. Boersma, W. J. J. Smeets, A. L. Spek and G. van Koten, *Organometallics*, 1989, **8**, 2907 – 2917.

[5] J. X. McDermott, J. F. White, G. M. Whitesides, *J. Am. Chem. Soc.*, 1976, **98**, 6521 – 6528.

[6] An adaptation of the syntheses reported by J. Chatt and L. M. Venanzi, *J. Chem. Soc.*, 1955, 2787 – 2793 and W. Baratta and P. S. Pregosin, *Inorg. Chim. Acta*, 1993, **1993**, 85 – 87 were employed in the synthesis of this compound.

[7] J. A. Cleverty and G. Wilkinson, *Inorg. Synth.*, 1966, **8**, 211 – 214.

[8] J. R. Doyle and D. Drew, *Inorg. Synth.*, 1990, **28**, 346 – 349.

[9] K. V. Barker, J. M. Brown, N. Hughes, A. J. Skarnulis and A. Sexton, *J. Org. Chem.*, 1991, **56**, 698 – 703.

[10] M. Bassett, D. L. Davies, J. Neild, L. J. S. Prouse and D. R. Russell, *Polyhedron*, 1991, **10**, 501 – 507.

[11] An adaptation of the preparation by R. R. Fenton, F. Huq and T. W. Hambley, *Polyhedron*, 1999, **18**, 2149 – 2156.

Appendix

Appendix 1: Data collection and refinement parameters for molecular structures detailed in text

Chapter 2: Synthesis and derivatisation of PNE ligands

Compound number	**2.4-1**	**2.5-2**	**2.5-5**
Empirical formula	$C_{19}H_{25}N_2P$	$C_{18}H_{23}NOPCl$	$C_{20}H_{28}N_2PCl$
Formula weight	312.38	335.79	362.86
T / K	120	120	120
Crystal system	Monoclinic	Monoclinic	Orthorhombic
Space group	$P2_1/c$	$P2_1/n^*$	F$dd2$
a / Å	7.1829(14)	15.4226(19)	20.016(2)
b / Å	7.3477(14)	6.9489(9)	68.506(9)
c / Å	33.014(6)	18.487(2)	5.9460(7)
α / °	90	90	90
β / °	90.10(1)	114.37	90
γ / °	90	90	90
V / Å^3	1742.4(6)	1804.7(4)	8153.3(17)
Z	4	4	16
ρ / g cm^{-3}	1.191	1.236	1.182
μ(Mo Kα), mm^{-1}	0.157	0.302	0.270
Reflections: collected	16022	20659	16540
Unique	4000	4796	3952
with $I > 2\sigma(I)$	3059	4054	3234
R_{int} (%)	8.2	2.6	5.2
Refined variables	200	291	225
R_1 and wR_2 (%)[§]	7.5, 20.1	2.9, 7.7	7.1, 15.5

*Non-standard setting; § $R_1 = \Sigma||F_c|-|F_o||/\Sigma|F_o|$ for reflections with $I>2\sigma(I)$, $wR_2 = [\Sigma w(F_o^2-F_c^2)^2/\Sigma w(F_o^2)^2]^{1/2}$ for all data.

Chapter 3: Complexation of PNE ligands with Pd

Compound number	**3.1-1(a)**	**3.1-1(c)**	**3.1-4**	**3.4**
Empirical formula	$C_{19}H_{25}N_2PPdCl_2$	$[C_{19}H_{25}ClN_2PPd^+]_2[Mg(SO_4)_2(H_2O)_4]^{2-}\cdot 6H_2O$	$C_{20}H_{25}NPPdCl_5$	$C_5H_{12}N_2PdCl_2$
Formula weight	489.68	1305.05	594.03	277.47
T / K	120	120	120	120
Crystal system	Triclinic	Monoclinic	Monoclinic	Orthorhombic
Space group	$P\bar{1}$	$P2_1/c$	$P2_1/n$	$Pnma$
a / Å	7.938(1)	16.9252(17)	7.9121(14)	11.0551
b / Å	9.597(1)	8.6573(9)	50.039(9)	8.1413
c / Å	13.675(1)	18.0774(18)	12.512(2)	9.3990
α / °	75.08(1)	90	90	90
β / °	80.52(1)	92.94(1)	106.55(1)	90
γ / °	88.71(1)	90	90	90
V / Å^3	992.7(2)	2645.3(5)	4748.4(14)	845.94(14)
Z	2	2	8	4
ρ / g cm^{-3}	1.638	1.638	1.662	2.179
μ(Mo Kα), mm^{-1}	1.289	1.003	1.419	2.752
Reflections: collected	16957	30538	23491	11409
Unique	5768	7011	8349	1316
with $I >$ $2\sigma(I)$	4813	6194	2143	1233
R_{int} (%)	4.7	3.4	49.4	2.2
Refined variables	228	355	306	81
R_1 and wR_2 (%)[§]	2.7, 5.9	2.5, 5.4	11.7, 26.1	1.9, 4.7

[§] $R_1 = \Sigma||F_c|-|F_o||/\Sigma|F_o|$ for reflections with $I>2\sigma(I)$, $wR_2 = [\Sigma w(F_o^2-F_c^2)^2/\Sigma w(F_o^2)^2]^{½}$ for all data.

Chapter 4: Complexation of PNE ligands with Pt

Compound number	**4.1-1.HCl**	**4.4-4**
Empirical formula	$C_{36}H_{57}N_2P_2O_6PtCl_6$	$C_{25}H_{39}NP_2PtCl$, CH_2Cl_2, H_2O
Formula weight	1083.57	784.44
T / K	120	120
Crystal system	Monoclinic	Monoclinic
Space group	$C2$	$P2_1/n^*$
a / Å	27.8386(13)	10.175(1)
b / Å	16.3038(7)	29.744(3)
c / Å	9.5155(4)	10.500(1)
α / °	90	90
β / °	90.343(1)	90.21(1)
γ / °	90	90
V / Å^3	4318.8(3)	3177.8(5)
Z	4	4
ρ / g cm^{-3}	1.666	1.640
μ(Mo Kα), mm^{-1}	3.739	4.873
Reflections: collected	23375	55403
Unique	9919	13429
with $I > 2\sigma(I)$	8017	11848
R_{int} (%)	6.8	2.8
Refined variables	485	331
R_1 and wR_2 (%)[§]	5.7, 11.2	2.7, 5.0

*Non-standard setting; § $R_1 = \Sigma||F_c|-|F_o||/\Sigma|F_o|$ for reflections with $I>2\sigma(I)$, $wR_2 = [\Sigma w(F_o^2-F_c^2)^2/\Sigma w(F_o^2)^2]^{1/2}$ for all data.

Chapter 5: Complexation of PNE ligands with Rh

Compound number	**5.2-1(a)**	**5.2-2**	**5.4-3**
Empirical formula	$C_{20}H_{25}N_2OPRhCl$	$C_{19}H_{22}NPRhCl$, CH_2Cl_2	$C_{19}H_{22}NOPSRh$, BF_4, 0.5 C_7H_8
Formula weight	478.75	550.63	579.19
T / K	120	120	120
Crystal system	Monoclinic	Monoclinic	Triclinic
Space group	*Pn*	$P2_1/c$	$P\bar{1}$
a / Å	10.369(1)	16.0321(12)	9.564(1)
b / Å	12.481(1)	9.8374(8)	10.307(1)
c / Å	15.662(1)	15.9824(11)	12.651(1)
α / °	90	90	75.02(1)
β / °	96.85(1)	119.84(1)	87.81(1)
γ / °	90	90	83.47(1)
V / Å^3	2012.4(3)	2186.5(3)	1196.8(2)
Z	4	4	2
ρ / g cm^{-3}	1.580	1.673	1.607
μ(Mo Kα), mm^{-1}	1.072	1.237	0.914
Reflections: collected	28606	52358	21622
Unique	11555	9619	6981
with $I > 2\sigma(I)$	11428	8272	5925
R_{int} (%)	1.7	3.2	4.8
Refined variables	476	257	335
R_1 and wR_2 (%)[§]	1.8, 4.5	2.9, 7.0	3.3, 8.2

[§] $R_1 = \Sigma||F_c|-|F_o||/\ \Sigma|F_o|$ for reflections with $I>2\sigma(I)$, $wR_2 = [\Sigma w(F_o^2-F_c^2)^2/\Sigma w(F_o^2)^2]^{1/2}$ for all data.